# CHARACTERISATION OF THE ROLE OF DIFFERENT REGULATORY T CELLS IN BYSTANDER SUPPRESSION

By KONSTANTINA PETKOU

A thesis submitted to the University of Birmingham for the degree of Doctor of Philosophy




UNIVERSITY OF BIRMINGHAM

Institute of Immunology and Immunotherapy

College of Medical and Dental Sciences

University of Birmingham

February 2023

UNIVERSITY OF
BIRMINGHAM

## University of Birmingham Research Archive

### e-theses repository

This unpublished thesis/dissertation is copyright of the author and/or third parties. The intellectual property rights of the author or third parties in respect of this work are as defined by The Copyright Designs and Patents Act 1988 or as modified by any successor legislation.

Any use made of information contained in this thesis/dissertation must be in accordance with that legislation and must be properly acknowledged. Further distribution or reproduction in any format is prohibited without the permission of the copyright holder.

## Abstract

Current treatments for autoimmune diseases do not provide a cure and heavily rely on broad-range immunosuppressive drugs that can compromise the ability of the host to fight infections or cancers. In recent years, **antigen-specific immunotherapies** have shown promising results in establishing protective immunity towards autoreactive T cells by administrating disease-relevant antigen(s) in a tolerogenic delivery platform. Using a peptide treatment protocol that induces immune tolerance by giving rise to **anergic CD4$^+$IL-10$^+$ T cells**, we were keen to characterise the role of **TIGIT**, a co-inhibitory receptor, in the development, stability and capacity of these cells to maintain central and peripheral tolerance. Importantly, in multi-antigen diseases, such as multiple sclerosis, inducing tolerance to the immunodominant antigen only can provide protection against other antigens that are found within the same tissue, due to the process of **bystander suppression**. In this thesis, we aimed to dissect the mechanisms underpinning bystander suppression and investigate the role of different peptide-treated regulatory T cell (Treg) populations. Tregs from the transgenic **Tg4 mouse model**, with a TCR specific for $MBP_{Ac1-9}$, were tested for suppression of 2D2 responder cells, specific for a different myelin epitope, $MOG_{35-55}$ both *in vitro* and *in vivo*. Finally, we were interested to investigate the impact of peptide immunotherapy on **FoxP3$^+$ Tregs** by studying their phenotypic and functional properties. By using **RNA sequencing** approaches, we characterised the transcriptional signatures that are differentially expressed in peptide-treated Tregs and are essential for the licensing of these cells to acquire a highly tolerogenic phenotype. The work presented here clarifies the **mechanism of action** of peptide immunotherapy and paves the way for the application of this platform for the effective treatment of autoimmune diseases.

## Acknowledgements

Firstly, I would like to take this opportunity to thank my primary supervisor, Prof David Wraith, for sharing his inspiring knowledge and experience, academic guidance, and advice throughout my PhD. I would like to express my gratitude to him for his endless help, which was invaluable for my development, not only as a scientist, but also as a person and for always believing in me and encouraging me to reach my full potential. The emotional support during challenging times, such as the unprecedented situation with the COVID-19 pandemic, was of paramount importance when I needed it the most.

All members of the Wraith group (past and present) have been invaluable in providing continued support, advice, and fun times, so many thanks to my wonderful colleagues: Dr Heather Streeter, Dr Naomi Richardson, Lora Lucas, Dr San Pyae Phyo, Joe Clarke, Dr Sky Ng, and Dr Mike Price. Furthermore, I would like to thank my second supervisor, Prof Graham Anderson, and his entire group for always being more than happy to offer help me with the setup of the experiments as well as interpreting the results.

I would like to also thank Dr Ethan Shevach for accepting me in his lab at the National Institutes of Health (NIH) in the US for 3 months and for providing me with all the necessary resources for the scRNAseq results presented in this thesis and for always being up for a chat. The whole experience in the US was one of the major highlights of my PhD and I will be forever grateful for getting to experience this environment. Moreover, another collaboration was formed with the lab of Prof Shimon Sakaguchi at Osaka University in Japan. I would like to thank Prof Sakaguchi and in particular Prof Naganari Ohkura from his group for offering some help with the demethylation analysis of my samples.

I would also like to thank my friends and family from Greece for always trying to motivate me from far away and make sure that I am enjoying my life in the UK! Special thanks to my grandmother who has been with me from my very first day, next to me in every step of the way, through ups and downs and who even learned how to use a tablet at the age of 84 just to be able to see me and check up on me every day. Importantly, I want to thank Simon, my greatest supporter, for always being there for me, willing to listen and cheer me up when the stress was getting overwhelming. His infectious positivity and optimism were something to look forward to since he was always able to make me smile and encourage me to carry on with confidence!

Finally, it needs to be acknowledged that the majority of this PhD was done during the COVID-19 pandemic and my work was severely delayed, during the first lockdown when we had to trim the mouse colonies down to the minimum. Despite all the efforts to adjust my research to mitigate the delays I had due to COVID-19 disruptions, my project was still impacted to a great extent, and I wish to acknowledge that this inevitably prevented me from completing some of my experimental aims.

# Table of Contents

CHAPTER 1: INTRODUCTION ..... 1
1.1 Introduction to the immune system ..... 2
1.1.1 The innate immune system ..... 3
1.1.2 The adaptive immune system ..... 5
1.2 Antigen processing, T cell activation and regulation ..... 11
1.3 Immune regulation by co-inhibitory receptors ..... 16
1.3.1 The CD226/TIGIT/CD155 pathway ..... 17
1.3.2 The CTLA-4/CD28/CD80/CD86 pathway ..... 22
1.4 Thymic T cell development and central tolerance ..... 23
1.5 Peripheral tolerance ..... 27
1.5.1 FoxP3$^{+}$ regulatory T cells ..... 28
1.5.2 IL-10$^{+}$FoxP3$^{-}$ Tr1 cells ..... 37
1.6 Autoimmune Diseases ..... 39
1.7 Antigen-specific immunotherapy for the treatment of autoimmune diseases ..... 41
1.7.1 Platforms used for immunotherapy – the importance of peptide immunotherapy ..... 42
1.8 Bystander suppression: proposed mechanisms and relevance to peptide immunotherapy ..... 49
1.9 Thesis aims ..... 53
CHAPTER 2: MATERIALS & METHODS ..... 55
2.1 Experimental animals ..... 56
2.1.1 Tg4 mice ..... 56
2.1.2 Tg4.TIGIT Crispr knockout mice ..... 57
2.1.3 2D2 mice ..... 63
2.1.4 B10.PL mice ..... 64

2.1.5 C57BL/6 mice ..... 64
2.1.6 (B10.PL x C57BL/6) F1 and (Tg4 x C57BL/6) F1 mice ..... 64
2.2 Reagents for cell preparations and cell cultures ..... 65

2.2.1 RPMI-1640 ..... 65
2.2.2 Cell isolation and staining buffers ..... 65
2.2.3 Peptide antigens ..... 66
2.3 *In vitro* methods ..... 66

2.3.1 Isolation of mouse splenocytes for analysis ..... 66
2.3.2 Cell counting using a glass haemocytometer ..... 67
2.3.3 Live/dead separation ..... 68
2.3.4 Isolation of mouse thymocytes for analysis ..... 68
2.3.5 Cell culture of naïve T cells ..... 69
2.3.6 Th1/Th2-polarised cell culture ..... 69
2.3.7 Generation of iTregs ..... 70
2.3.8 Establishment of a CD4tol primary cell line ..... 70
2.3.9 Mouse cell isolation from splenocytes ..... 71
2.3.10 Staining of $CD4^+$ T cells with Cell Trace Violet (CTV) ..... 73
2.3.11 *In vitro* bystander suppression assays ..... 73
2.3.12 T cell: DC co-cultures ..... 74
2.3.13 Transwell assay ..... 74
2.3.14 Neutralisation of IL-10R/CTLA-4 using blocking antibodies ..... 75
2.3.15 Assessment of cell proliferation by $^3$H-TdR incorporation ..... 75
2.3.16 Assessment of cytokine secretion by ELISA ..... 76
2.3.17 Gene expression analysis ..... 77
2.3.18 Flow cytometry ..... 78
2.4 *In situ* immunofluorescent staining ..... 83

2.5 *In vivo* methods ..... 84

2.5.1 Antigen administration/Dose escalation protocol ..... 84
2.5.2 Bromodeoxyuridine Proliferation analysis ..... 84
2.5.3 Preparation of CFA adjuvant ..... 85

2.5.4 Adoptive cell transfers in Tg4 x C57BL/6 recipients ..... 85
2.5.5 Adoptive cell co-transfers in B10.PL x C57BL/6 or B10.PL recipients..... 86
2.6 Bioinformatic analysis ..... 86
2.6.1 Bulk RNA sequencing..... 86
2.6.2 Single-cell RNA sequencing (scRNAseq) ..... 87
2.7 Statistical analysis..... 88
CHAPTER 3: THE ROLE OF TIGIT IN IMMUNE REGULATION ..... 89
3.1 Introduction..... 90
3.2 TIGIT expression is enhanced on thymic and peripheral Tregs ..... 94
3.3 Phenotypic characterisation of the TIGIT KO mice ..... 98
3.3.1 Tg4 mice lacking TIGIT display increased frequencies of FoxP3$^{+}$ Tregs... 100
3.3.2 Investigation of the proliferative capacity of Tregs from TIGIT KO and Tg4 mice ..... 103
3.3.3 Localisation of TIGIT$^{-/-}$ Tregs in the thymus ..... 105
3.4 Development of protocol for *in vitro* expansion of CD4$^{+}$ T cells from 4Y-treated mice (CD4$^{+}$tol)..... 108
3.4.1 Assessment of the cytokine profile of CD4$^{+}$tol from TIGIT$^{-/-}$ and Tg4 mice after *in vitro* re-challenge with MBP$_{Ac1-9}$ analogues..... 113
3.5 The role of TIGIT in the generation of iTregs..... 119
3.6 TIGIT is dispensable for the suppressive capacity of different regulatory T cells ..... 122
3.6.1 Evaluation of the suppressive capacity of TIGIT$^{-/-}$ iTregs, CD4tol and 4Y-treated FoxP3$^{+}$ Tregs..... 123
3.6.2 Impact of TIGIT on the ability of responder cells to produce pro- or anti-inflammatory cytokines *in vitro* ..... 128
3.7 The role of TIGIT in the T-cell mediated inhibition of dendritic cell maturation ..... 130

3.8 Discussion ..... 134

CHAPTER 4: CHARACTERISATION OF THE ROLE OF DIFFERENT REGULATORY T CELLS IN BYSTANDER SUPPRESSION ..... 140

4.1 Introduction ..... 141

4.2 Introduction to the *in vitro* model of bystander suppression: co-cultures of putative suppressive Tg4 T cell populations and 2D2 $CD4^+$ T responder cells ..... 144

4.3 CD4tol cells are potent mediators of bystander suppression *in vitro* ..... 149

4.4 Requirement for cell-contact for bystander suppression mediated by CD4tol cells *in vitro* ..... 153

4.4.1 Antigen presentation by a central APC versus separate APCs ..... 153

4.4.2 Co-cultures of CD4tol suppressor cells and 2D2 responders in a transwell setting ..... 159

4.4.3 A role for CTLA-4 and IL-10 in bystander suppression mediated by CD4tol cells *in vitro* ..... 164

4.5 Evidence of bystander suppression *in vivo* ..... 166

4.5.1 (Tg4 x C57BL/6) F1 model ..... 166

4.5.2 Adoptive co-transfers of 2D2 responder cells with Tg4 CD4tol cells into (B10.PL x C57BL/6) F1 recipient mice ..... 170

4.5.3 Adoptive co-transfers of Tg4 responder cells with Tg4 CD4tol cells into B10.PL recipient mice ..... 172

4.5.4 Dendritic cells are modulated by tolerance induction *in vivo* ..... 175

4.6 Peptide immunotherapy licenses $FoxP3^+$ Tregs to acquire a highly suppressive phenotype *in vitro* ..... 177

4.7 Naïve antigen-presenting cells are modulated by co-culture with different regulatory T cells *in vitro* ..... 186

4.7.1 Dendritic cell modulation by co-culture with different regulatory T cells *in vitro* ..... 186

4.7.2 Production of IL-10 and IL-12 by DC co-culture with regulatory T cells *in vitro* ..... 191

4.7.3 Requirement for cell-contact for inhibition of DC maturation by regulatory T cells..... 194

4.7.4 Role of CTLA and IL-10 in the suppressive effect of regulatory T cells on DCs ..... 196

4.8 Discussion..... 198

CHAPTER 5: IMPACT OF PEPTIDE IMMUNOTHERAPY ON THE TRANCRIPTIONAL RE-PROGRAMMING OF REGULATORY T CELLS..... 205

5.1 Introduction..... 206

5.2 Characterisation of the phenotype of tolerised $CD4^+$ T cells ..... 208

5.2.1 Expansion of IL-$10^+$FoxP$3^-$ Tr1 cells and FoxP$3^+$ Tregs following peptide treatment..... 208

5.2.2 The expression of co-inhibitory receptors is upregulated both in Tr1 and Tregs following tolerance induction..... 214

5.3 Optimisation of the *in vitro* conditions for stimulation of regulatory T cells..... 217

5.4 Bulk RNA sequencing ..... 223

5.4.1 Hierarchical clustering and pathway analysis ..... 223

5.5 Single-cell RNA sequencing..... 228

5.5.1 Expression of selected genes..... 228

5.6 Analysis of differentially expressed genes (DEGs) by bulk and single-cell RNAseq ..... 233

5.7 Correlation of IL-10 with other genes associated with immune tolerance using scRNAseq ..... 244

5.8 Validation of selected DEGs by RT-PCR..... 249

5.9 Demethylation analysis of FoxP3 CNS2 region ..... 251

5.10 Discussion..... 254

CHAPTER 6: GENERAL DISCUSSION ..... 259
6.1 Future directions ..... 271

REFERENCES ..... 274

## List of figures

### Chapter 1: Introduction

1.1 MHC Class I and Class II antigen processing and presentation pathways……...14

1.2 The proposed mechanisms of action for TIGIT……21

1.3 T cell development in the thymus ……....26

1.4 Mechanisms of Treg-mediated suppression …….31

1.5 Transcriptional Regulation of Differentiation and Functions of Effector T Regulatory Cells ……33

1.6 Differentiation of effector $CD4^+$ T cells and Tregs ….…….36

1.7 Summary of antigen-specific immunotherapy approaches in preclinical/clinical development ……47

1.8 Mechanism of action of peptide immunotherapy using soluble peptides ……51

### Chapter 3: The role of TIGIT in immune regulation

3.1 TIGIT expression is enhanced on Tregs in the thymus and spleen ……. 96

3.2 Phenotypic characterisation of T cell subsets in the thymus of TIGIT KO mice and Tg4 controls ……... 98

3.3 TIGIT-/- mice display higher frequencies of FoxP3+ Tregs both in the thymus and spleen …… 100

3.4 Assessment of Treg proliferation with BrdU ……..103

3.5 The absence of TIGIT does not interfere with the localisation of Tregs in the thymus……... 105

3.6 Protocol for tolerance induction and establishment of anergy ……...110

3.7 IL-10 levels of CD4tol cells deriving from either $TIGIT^{-/-}$ or Tg4 mice after *in vitro* re-challenge with MBP analogues of different affinity ……113

3.8 IFN-γ levels of CD4tol cells deriving from either TIGIT$^{-/-}$ or Tg4 mice after *in vitro* re-challenge with MBP analogues of different affinity ……115

3.9 Cytokine profile of tolerant cells deriving from either TIGIT$^{-/-}$ or Tg4 mice after stimulation with PMA/Ionomycin ……116

3.10 TIGIT is dispensable for the generation of iTregs ……119

3.11 TIGIT is dispensable for the suppressive capacity of CD4tol and iTregs …….123

3.12 TIGIT does not play a role in the suppressive capacity of tolerised FoxP3$^{+}$ Tregs……..126

3.13 The absence of TIGIT does not interfere with the ability of responder cells to produce pro- or anti-inflammatory cytokines ……128

3.14 The absence of TIGIT does not interfere with the ability of CD4tol cells or iTregs to modulate DC maturation …….. 130

3.15 The absence of TIGIT does not interfere with cytokine production from CD4tol cells or iTregs in co-cultures with dendritic cells ……..132

Chapter 4: Characterisation of the role of different regulatory T cells in bystander suppression

4.1 Proliferation of $MOG_{35-55}$ specific CD4$^{+}$ T cells from 2D2 mice can be monitored by Cell Trace Violet *in vitro* ……...139

4.2 Tg4 cells are $MBP_{Ac1-9}$-specific, while 2D2 cells are $MOG_{35-55}$-specific and can respond to both linked $MBP_{Ac1-9}$-$MOG_{35-55}$ and $MOG_{35-55}$ at 100μg/ml ……...141

4.3 Both separate $MOG_{35-55}$ + $MBP_{Ac1-9}$ and linked peptides can stimulate CD4tol and 2D2 cells ……142

4.4 CD4tol cells are potent mediators of bystander suppression …….. 145

4.5 (B10.PL x C57BL/6) F1 splenocytes can present both $MBP_{Ac1-9}$ and $MOG_{35-55}$ on the same APC and facilitate the establishment of bystander suppression in a more effective way compared to the combination of B10.PL + C57BL/6 ……150

4.6 Antigen-presentation in the context of (B10.PL x C57BL/6) F1 splenocytes can lead to downregulation of activation markers on 2D2 cells in the presence of CD4tol cells ……...152

4.7 Cell contact is required for the suppressive function of CD4tol cells ……154

4.8 Soluble factors secreted in culture supernatants of CD4tol cells are not able to mediate bystander suppression ……...157

4.9 Simultaneous neutralisation of CTLA-4 and IL-10 reverses the suppression mediated by CD4tol cells ……159

4.10 Peptide treatment establishes a tolerogenic environment that prevents the proliferation of adoptively transferred naïve T cells ……. 162

4.11 Peptide treatment establishes a tolerogenic environment that prevents the activation of adoptively transferred naïve T cells ……...163

4.12 CD4tol cells are able to mediate bystander suppression *in vivo* ……165

4.13 CD4tol cells are able to mediate antigen-specific suppression *in vivo* ……168

4.14 Tolerance induction has an impact on DCs *in vivo*, making them downregulate CD80 and CD86 ……..170

4.15 FoxP3$^+$ Tregs from peptide-treated Tg4 mice are able to suppress responder 2D2 cells even at low ratios, while naïve FoxP3$^+$ Tregs are not suppressive …….. 175

4.16 FoxP3$^+$ Tregs from peptide-treated Tg4 mice are able to completely switch off IFN-γ production and promote IL-10 production ……. 177

4.17 The full course of tolerance induction is required for the complete licensing of Tregs ……...179

4.18 FoxP3$^+$ Tregs from peptide-treated Tg4 mice are the most potent suppressors of CD80 and CD86 expression on dendritic cells, followed by CD4tol cells ……..183

4.19 In the presence of 4Y-treated FoxP3$^+$ Tregs and FoxP3$^-$ CD4tol cells, the secretion of IL-10 was enhanced, while IL-12 was downregulated ……187

4.20 Soluble factors secreted in CD4tol culture supernatants were not sufficient to downregulate CD80 and CD86 on dendritic cells ……189

4.21 Neutralisation of IL-10R but not CTLA-4 reversed the downregulation of CD80 and CD86 on DCs mediated by CD4tol cells ……..191

Chapter 5: Impact of peptide immunotherapy on the transcriptional re-programming of regulatory T cells

5.1 Evaluation of the purity of the isolated fractions and correlation between FoxP3 and IL-10 ……....203

5.2 Tg4 mice undergo IL-10$^+$ cell expansion of both CD4$^+$FoxP3$^+$ Tregs and CD4$^+$FoxP3$^-$ Tr1 cells following tolerance induction with $MBP_{Ac1-9}$ [4Y] peptide ……..205

5.3 Tg4 mice after tolerance induction with $MBP_{Ac1-9}$ [4Y] peptide undergo expansion of inhibitory receptors, which correlates with IL-10 expression ……....209

5.4 CD25 expression 2h after *in vivo* treatment with a single dose of 80μg 4Y ……...214

5.5 The optimal *in vitro* re-stimulation regime for Tregs is with soluble anti-CD3/anti-CD28 monoclonal antibodies for 4 hours …….215

5.6 PCA plot and hierarchical clustering tree showing the clustering of the 12 samples based on similarity ……...219

5.7 Selected gene expression across the UMAP with feature plots …….224

5.8 IL-10, c-Maf and Blimp-1 are highly expressed on Tregs following peptide immunotherapy …….225

5.9 Peptide immunotherapy induces the upregulation of tolerance-associated genes in FoxP3$^+$ Tregs with a concomitant downregulation of effector genes ……...231

5.10 Peptide treatment has an impact on 4Y-treated Tconv cells by inducing some tolerance-associated genes that are also found in 4Y-treated Tregs …….232

5.11 Combined bulk and scRNA-seq data ……235

5.12 IL-10 expression is associated with upregulation of other regulatory genes such as CTLA-4, Maf, Icos, Ccr2 and Ccr5 on FoxP3$^+$ Tregs ……..237

5.13 Co-expression plots of chosen target genes in PBS- and 4Y-treated Tregs …….239

5.14 Co-expression plots of chosen target genes in naïve and treated T conventional cells ……...240

5.15 Expression of genes associated with the differentiation and function of both Tconv and Tregs following tolerance induction …….242

5.16 Demethylation status of FoxP3 CNS2 region ……..245

Chapter 6: General Discussion

6.1 Timeline of major breakthroughs in the field of antigen-driven bystander suppression ……. 259

6.2 Life cycle of regulatory and conventional CD4$^+$ T cells ……265

## List of tables

2.1 Initial PCR reaction ……..79

2.2 Sequencing reaction …….…….79

2.3 Recombinant cytokines …….87

2.4 Antibodies used for surface staining ……96

2.5 Antibodies used for intracellular staining …….98

5.1 Summary of differentially expressed genes between PBS-treated and 4Y-treated Tregs……. 237

5.2 Summary of differentially expressed genes between PBS-treated and 4Y-treated Tconv…… 238

## List of abbreviations

| | |
|---|---|
| APC | Antigen-presenting cell |
| ASI | Antigen-specific immunotherapy |
| BCR | B cell receptor |
| BrdU | Bromodeoxyuridine |
| BMSU | Biomedical Services Unit |
| Breg | B regulatory cell |
| BSA | Bovine Serum Albumin |
| Ccpm | Corrected counts per minute |
| CDR | Complementarity Determining Regions |
| CFA | Complete Freud's Adjuvant |
| CNS | Central Nervous System |
| CNS2 | Conserved non-coding region 2 |
| cTEC | Cortical Thymic Epithelial Cells |
| CTLs | Cytotoxic T lymphocytes |
| CTV | Cell Trace Violet |
| DC | Dendritic Cell |
| DEG | Differentially Expressed Gene |
| DN | Double negative ($CD4^-CD8^-$) |

| | |
|---|---|
| DP | Double positive ($CD4^+CD8^+$) |
| EAE | Experimental Autoimmune Encephalomyelitis |
| ER | Endoplasmic Reticulum |
| eTreg | Effector Treg |
| ELISA | Enzyme-Linked Immunosorbent Assay |
| FACS | Fluorescence-activated Cell Sorting |
| FMO | Fluorescence Minus One |
| FoxP3 | Forkhead box P3 |
| Ig | Immunoglobulin |
| IL | Interleukin |
| INF | Interferon |
| iTreg | *in vitro*-induced Treg |
| KC | Kupffer cells |
| LCMV | Lymphocytic Choriomeningitis Virus |
| LPS | Lipopolysaccharide |
| MBP | Myelin Basic Protein |
| MFI | Mean Fluorescent Intensity |
| MHC | Major Histocompatibility Complex |
| MoA | Mechanism of Action |
| MOG | Myelin Oligodendrocyte Protein |
| MRI | Magnetic Resonance Imaging |
| mTEC | Medullary Thymic Epithelial Cells |
| MS | Multiple Sclerosis |
| nTreg | Natural T regulatory |
| PAMPs | Pathogen Associated Molecular Patterns |
| PFR | Peptide flanking regions |
| PMA | Phorbol 12-myristate 13-acetate |
| pMHC | Peptide loaded major histocompatibility complex |

| | |
|---|---|
| PRRs | Pattern Recognition Receptors |
| RA | Rheumatoid Arthritis |
| RAG | Recombinase Activating Gene |
| RBC | Red Blood Cells |
| RRMS | Relapsing-remitting multiple sclerosis |
| SLE | Systemic Lupus Erythematosus |
| SP | Single positive ($CD4^+$ or $CD8^+$) |
| ssDC | Steady-state dendritic cell |
| T1D | Type 1 Diabetes |
| TAP | Transport Associated with Antigen Processing |
| TCR | T cell receptor |
| TGF-β | Transforming Growth Factor β |
| Th | T helper |
| TIGIT | T cell immunoreceptor with Ig and ITIM domains |
| TILs | Tumour Infiltrating Lymphocytes |
| TLRs | Toll-like Receptors |
| TME | Tumour Microenvironment |
| TNFRSF | Tumour Necrosis Factor Receptor Superfamily |
| TRA | Tissue restricted antigens |
| Treg | T regulatory cell |
| TSDR | Treg-specific demethylation region |
| VDJ | Variable, Diverse, Joining segments |

# CHAPTER 1: INTRODUCTION

## 1.1 Introduction to the immune system

The immune system has evolved over the years to provide the host with protection against potentially harmful foreign pathogens through mechanisms that prevent damage caused by the infection. Comprising a wide variety of cells, tissues, and organs, the immune system is responsible for the detection and clearance of invading microorganisms such as bacteria, fungi, viruses, and parasites that are found in the environment. Its instrumental role in the maintenance of tissue homeostasis is highlighted in individuals where the immune homeostasis is perturbed, as in the cases of either **immunodeficiency** with suboptimal immune responses rendering the individuals susceptible to disease development, or **autoimmune and allergic responses**, that are characterised by the inability to distinguish between self, non-self, and overactive immune activation, respectively (Okada et al., 2010; Ean -F Rançois and Ach, 2002; Brodin and Davis, 2017). Therefore, the regulation of the immune system is of critical importance for its proper functioning and protection of the host.

Furthermore, the immune system consists of two main branches: the **innate** and the **adaptive**. The cells of the innate immune system comprise the first line of defense against infection, and they provide a **rapid, non-antigen-specific response** to microorganisms. The innate immune cells are characterised by receptor commonality and have shared expression of recognition molecules that detect a vast array of common pathogenic molecular patterns (Brubaker et al., 2015). However, the specificity of the adaptive immune system, which derives from the expression of a unique and diverse repertoire of receptors, allows a more efficient way of dealing with pathogens. During immune cell development, the process of gene rearrangement takes place and gives rise

to a wide range of receptors, which facilitates the recognition of specific pathogenic features, therefore acting as a more targeted immune response (Arstila et al., 1999).

Despite their different contribution to the functional outcome of the immune response, the innate and adaptive arms of the immune system have supplementary roles, with the initial activation of the adaptive immune response being heavily dependent on preliminary triggering from the innate counterpart. Upon entry of pathogens through the skin and mucous membranes, innate immunity acts as the **frontline for host defence** (Turvey and Broide, 2010). The innate immune cells express on their surface receptors that recognise structures shared between many pathogens. Upon engagement of these receptors, an immediate immune response is mounted and cells become activated to supply the molecules that are required for the initiation of the adaptive immune response (Gasteiger and Rudensky, 2014; Thornton and Morgan, 2009).

In the steady state, adaptive immune cells are maintained at lower antigen-specific clonal numbers, and subsequently, upon activation, these selected cells undergo **clonal expansion** (Burnet, 1959). Through this process, cells proliferate and increase in numbers to support an efficient response. Due to the time required for proliferation and differentiation to effector cells, the initiation of the adaptive immune response is **delayed**, but it provides the host with **memory cells** and long-lived immunity, allowing rapid responses upon re-challenge with the same antigen (MacLeod et al., 2010).

### 1.1.1 The innate immune system

The innate immune system consists of both **cellular** and **humoral** components. Regarding the cellular part, it comprises cells such as mast cells, eosinophils, basophils, natural killer cells, and phagocytes such as neutrophils and macrophages. These cells

express various **Pattern Recognition Receptors** (PRRs), including **Toll-Like Receptors** (TLRs) that recognise common pathogenic structures known as **Pathogen Associated Molecular Patterns** (PAMPs), which include cell wall components, metabolic products, and nucleic acids (Fischer and Deindl, 2022). Different TLRs recognise different surface-expressed pathogenic features (i.e., TLR-5 recognises flagellin on bacterial cells, TLR-4 has an affinity for endotoxin lipopolysaccharide (LPS), and TLR-3 can bind non-host, double-stranded DNA within endosomes, indicative of pathogenic invasion) (O'Neill et al., 2013). In all the different types of TLRs, receptor engagement results in the initiation of an immune response targeted towards the elimination of the pathogen and the restoration of immune homeostasis.

Regarding the humoral part, it consists of a variety of soluble, plasma PPRs, including pentraxins and collectins that bind to foreign PAMPs and coat the surface of target cells (Mantovani and Garlanda, 2023). This process, also known as **opsonisation**, essentially facilitates the targeting of the invading pathogens that are subsequently processed and cleared by other innate immune cells, such as macrophages via **phagocytosis** (Appelberg, 2007). **Neutrophils** and **macrophages** also play a critical role in pathogen clearance, since they express Fc or complement receptors that enable them to recognise and target opsonised bacteria (Parkin and Cohen, 2001).

Although it provides a rapid response, the innate immune response is not able to clear all pathogens, due to the limited number of motifs being recognised. Following the initial innate response, the recognition of PAMPs through PRRs ultimately triggers a cascade of downstream signalling pathways associated with the induction of inflammation to facilitate the secretion of cytokines for enhanced cell recruitment to the

inflamed area, which is essential for prolonged detection of foreign antigens and sustained clearance of invading pathogens.

Therefore, on the one hand, the innate immune system orchestrates the initial immune response to clear the pathogen and on the other hand, induces the activation of the adaptive arm via the secretion of inflammatory cytokines and chemokines by innate cells and through the recruitment of dendritic cells (DCs) for subsequent antigen processing and presentation (Iwasaki and Medzhitov, 2010). Upon encounter of inflammatory stimuli, DCs become activated and upregulate the costimulatory molecules CD80 and CD86, which in turn support the increased activation of adaptive immune cells as DCs circulate through secondary lymphoid organs such as spleen and lymph nodes (Delves and Roitt, 2000).

### 1.1.2 The adaptive immune system

The evolutionary emergence of vertebrates was accompanied by the invention of adaptive immunity, which emerged twice during early vertebrate evolution. The first instance was reported in the lineage that gave rise to jawless fish (i.e., lamprey and hagfish), and the second occurrence was evidenced in the lineage of jawed vertebrates, ranging from cartilaginous fish to mammals (Flajnik and Kasahara, 2010). Only vertebrates that are characterised by a higher degree of complexity have this additional, more sophisticated system of defense mechanisms, which armours them with a broad genetic diversity in immunity **(evolutionary advantage),** which enables them to adapt and survive in an environment full of diverse pathogens (Cooper and Alder, 2006).

The adaptive immune system is characterised by two remarkable features that distinguish it from the innate immune system. The first one is the ability to remember

previous pathogen encounters and can either repel a second invasion or quickly eliminate the recurrent invader by mounting a faster and more efficient secondary immune response. This important feature, also known as **immunological memory,** forms the basis for effective immunisations against infectious diseases, which provide long-lasting protective immunity **(anamnestic response)**. Protective immunity against reinfection is one of the most important consequences of adaptive immunity and results from the establishment of populations of long-lived memory B and T cells.

The second important feature is **antigen specificity**. The adaptive immune system consists of T lymphocytes (T cells) and B lymphocytes (B cells) and the specificity of the adaptive immune response stems from the fact that naïve T and B cells display multiple copies of a unique T- or B- cell receptor on their surface that is responsible for the recognition of antigenic configurations of specific pathogenic epitopes. This antigen recognition subsequently leads to clonal amplification, cellular differentiation and production of antibodies with the same antigen-binding specificity (Burnet, 1959).

In the next paragraphs, B cells are discussed briefly, followed by T cells, and in particular, $CD4^+$ T cells, which are described more extensively since they are the central theme of this thesis.

#### *1.1.2.1 B cells*

The generation of B cells is initiated from a group of pluripotent hematopoietic stem cells in the foetal liver and subsequently, this process is maintained in the bone marrow and continues there throughout adult life. At the early stages of development, B cells express the endonuclease recombinase activating gene 1/2 (RAG 1/2) that is pivotal for the successful gene rearrangement of Variable, Diverse and Joining (VDJ) segments

of the immunoglobulin genes that are expressed on the cell surface (Jung and Alt, 2004). These gene rearrangements are critical for the reconfiguration of cell surface immunoglobulin (Ig) genes to establish a cell surface receptor able to recognise pathogens effectively (Bassing et al., 2002).

During gene rearrangement, B cells are screened against self-antigens, in order to prevent the potential release of self-reactive B cells. During the screening process, autoreactive B cells are identified and subsequently undergo either **clonal deletion** or **receptor editing** to convert their receptor to a non-autoreactive variant, or **clonal anergy** so that their receptor is unable to be activated by cognate antigen in the periphery (Goodnow et al., 2005).

B cells can enter germinal centre reactions through interaction with activated T cells, in order to initiate **somatic hypermutation** and **class switch recombination** to become IgG, IgA, or IgE. Once again, the interaction with the antigen during this process is necessary for the selection of higher affinity B cell clones. Furthermore, B cells undergo the process of gene rearrangement that gives rise to a highly diverse B cell receptor (BCR) repertoire that allows a B cell response to a wide range of antigens to take place. B cells can subsequently differentiate into either **long-lived memory cells** or **plasma cells** that produce **high-affinity antibody** following germinal centre reactions (Zhang et al., 2016).

#### *1.1.2.2 T cells*

T cells are characterised as either conventional αβ-T cells, that express a T cell receptor (TCR) that consists of alpha (α) or beta (β) chains, or γδ-T cells that express a TCR with gamma (γ) and delta (δ) chains. Both T cell subsets are generated in the thymus from bone marrow precursors, and they exit the thymus with a pre-determined

commitment and disseminate into the periphery as mature T cells. Functions of γδ-T cells are less investigated; however, a functional difference between these populations is their localisation. αβ-T cells are found in secondary lymphoid organs such as the spleen and lymph nodes, whereas γδ-T cells reside in epithelial layers of the tissue, including the skin and intestinal epithelium (Allison and Havran, 1991).

αβ-T cells can be classified as either $CD4^+$ or $CD8^+$ depending upon their surface expression of these molecules and they both have T cell receptors that tend to recognise pathogenic material that is presented to them in a processed manner, rather than directly. These αβ-T cells are more likely to encounter antigen-presenting cells (APCs) for activation while they reside or migrate through secondary lymphoid organs. APCs can present antigens to T cells as it is presented in the context of the major histocompatibility complex (MHC) on the APC surface which can be recognised by cognate αβTCR. Interaction between αβ T cells and APCs allows αβ T cells to differentiate into distinct effector subsets with a $CD4^+$ having a "helper" role and $CD8^+$ T cells having a cytotoxic role. For the purposes of this thesis, the focus will be on αβ T cells only, and not γδ T cells.

In the next paragraphs, the role of $CD8^+$ T cells in adaptive immunity will be covered briefly, followed by an extensive description of the different subsets of $CD4^+$ T cells, since the focus of this thesis is the study of the role and impact of $CD4^+$ T cells in the immune regulation of autoimmune disease.

#### 1.1.2.2.1 CD8+ T cells

$CD8^+$ T cells respond to antigens that are presented in the context of MHC class I, which is expressed on all nucleated cells. Once the antigen is processed and broken

down by proteasomes that are found inside the cell, it can be subsequently presented via MHC class I to the surface of antigen presenting cells, initiating the activation of $CD8^+$ T cells (Blum et al., 2013). Activated $CD8^+$ T cells are responsible for the uptake and destruction of viruses and tumours via the production of perforin and granzyme molecules that promote apoptotic cell death via ligation of Fas with FasL (Bannard et al., 2009).

#### 1.1.2.2.2 CD4+ T cells

$CD4^+$ T cells exit the thymus as naïve conventional cells or natural regulatory Tregs **(nTreg)** also known as thymic Tregs **(tTregs)**. The latter are fully functional upon release from the thymus, and they are capable of being activated in the periphery to suppress self-reactive T cells that have escaped negative selection (see section 1.4). On the other hand, conventional T cells (Tconv) develop within the thymus based upon their medium binding affinity to self-antigens presented on the medulla. This has been illustrated using the Nur77GFP model, where GFP levels correlate with the TCR signal strength (Ashouri and Weiss, 2017). Furthermore, higher TCR signal strength was found to correlate with Treg induction rather than the lower level of GFP and signal strength that was required for Tconv (Moran et al., 2011).

The successful development of $CD4^+$ T cells in the thymus depends on thymic antigen presenting cells (APCs) including cortical thymic epithelial cells (cTECs), medullary thymic epithelial cells (mTECs) and thymic dendritic cells (DCs). cTECs are involved in the positive selection that takes place in the thymic cortex, but they can be involved in the negative selection of thymocytes with strong self-reactivity, and they can also facilitate Treg differentiation (Goldman et al., 2005). Similarly, mTECs can negatively select thymocytes with high affinity to self-antigens, and mediate positive selection of Tregs (Williams et al., 2014). Finally, thymic DCs consist of three distinct

subsets: $CD8^+$ conventional DCs (cDCs) that occupy almost half of the thymic DC pool, $Sirp\alpha^+$ cDCs that consist 20% of the total DC population in the thymus and, plasmacytoid DCs (pDCs) (Wu and Shortman, 2005). All three populations of APCs are critical players for the generation of Tconv and Tregs in the thymus.

Unlike nTreg, naïve $CD4^+$ T cells need to undergo further maturation in the periphery to be fully functional. This maturation begins with the TCR activation by professional APCs, such as DCs, presenting antigen in an MHC class II-restricted manner (signal I). Furthermore, the interaction between CD28 on T cells and CD80/CD86 on APCs provides a supportive co-stimulatory signal required for efficient T cell activation (signal II). Finally, the determining factor for the destiny of naïve T cells depends on the exposure to the lineage-inducing cytokines released by the APCs (signal III) (Kaiko et al., 2008; Zhu and Paul, 2010). This enables naïve $CD4^+$ T cells to differentiate into a specific T helper (Th) subset.

Exposure to IL-2 and IFN-γ induces the transcription factor Tbet which determines the Th1 lineage (Szabo et al., 2000). These cells produce IL-2 and IFN-γ, which in turn drives the clearance of intracellular pathogens (Zhu and Paul, 2008). Furthermore, a Th2 phenotype is established upon exposure of naïve T cells to IL-4 that induces the expression of the transcription factor GATA-3. These cells subsequently produce IL-4 and IL-5 to support B cell class switching, in addition to the removal of extracellular parasites (Zheng and Flavell, 1997). Finally, a Th17 lineage occurs through exposure to Transforming Growth Factor β (TGF-β) together with IL-6. These cells express the transcription factors RORγt and RORα and produce IL-6 and IL-17 to mediate the clearance of extracellular bacteria and fungi (Harrington et al., 2005; Ivanov et al., 2006).

All T cell populations can become dysregulated and initiate a destructive response against self in the case of Th1 and Th17 responses being closely linked to autoimmunity, while Th2 responses have been associated with allergy (Zhu and Paul, 2008). In addition to the nTreg lineage that is in charge of the surveillance of autoreactive cells in the periphery, naïve T cells can also be induced to acquire a regulatory phenotype in peripheral tissues upon exposure to TGF-β that in turn induces expression of forkhead box P3 (**FoxP3**) (Chen et al., 2003). The requirement for Treg was clearly demonstrated in mice, which had a mutation in the FoxP3 gene (**scurfy mice**) that ultimately died at an early age due to severe lymphoproliferative disorder (Chang et al., 2005). Similarly in man, **I**mmune Dysregulation, **P**olyendocrinopathy, **E**nteropathy, **X**-linked syndrome (IPEX) has been shown to develop as a result of mutations in the FoxP3 transcription factor that can subsequently lead to disruption of Treg function and resultant multiorgan autoimmune disease (Barzaghi et al., 2012). Therefore, the requirement for immune regulation by Tregs is important to ensure homeostasis and prevention of T cell-mediated autoreactive immune responses.

$FoxP3^+$ Tregs and $FoxP3^-IL\text{-}10^+$ Tr1 cells are subsets of $CD4^+$ T cells and will be discussed in further detail under 'Peripheral tolerance', in sections 1.5.1 and 1.5.2, respectively.

## 1.2 Antigen processing, T cell activation and regulation

Evolutionary pressure has led the adaptive immune response to develop two distinct arms, which are defined by the **site of infection**. MHC class I molecules can present endogenous pathogens and initiate an immune response by $CD8^+$ T cells, while MHC class II molecules present exogenous pathogens and initiate an immune response mediated by $CD4^+$ T cells.

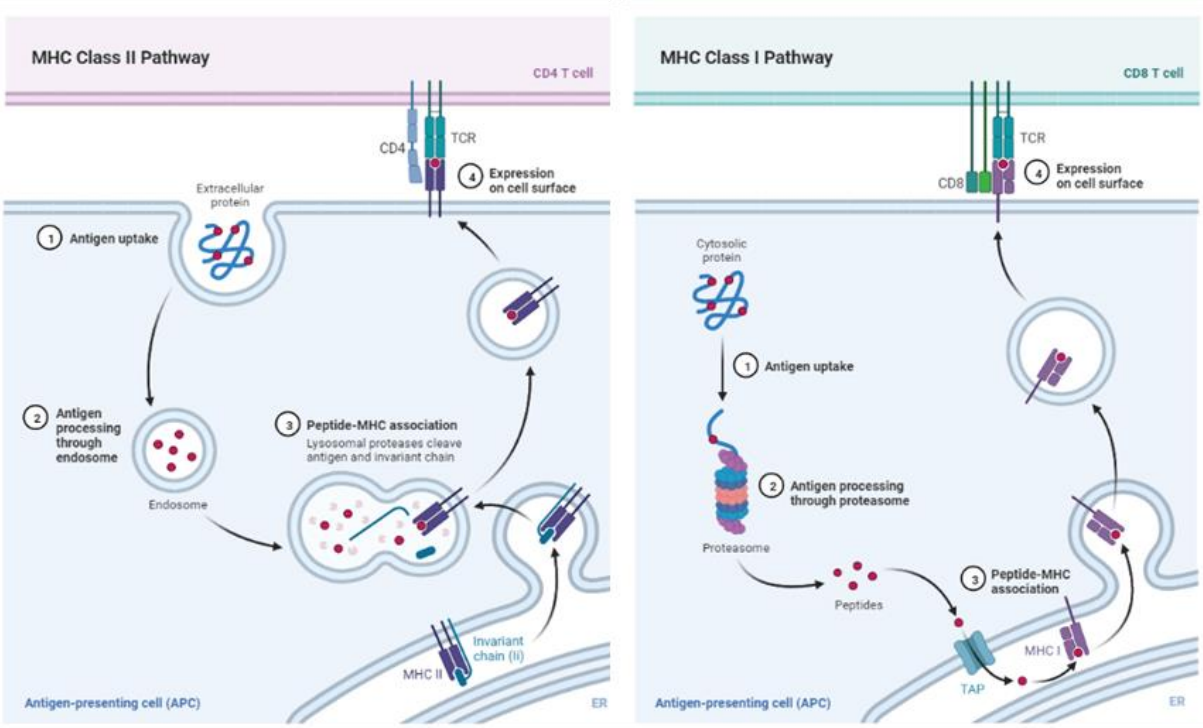
The function of MHC molecules is to bind peptide fragments derived from pathogens and display them on the cell surface of antigen-presenting cells for recognition by the appropriate T cells. $CD4^+$ and $CD8^+$ T cells become activated upon recognition of their cognate antigen that is presented in the context of MHC class II and I molecules, respectively. This phenomenon is known as **MHC restriction** because the MHC genotype 'restricts' the antigen specificity of T cells since the binding specificity of an individual TCR is not only for its peptide antigen but also for the complex of peptide and MHC molecule. The MHC locus is characterised by a high degree of **polygenicity** since it contains several different MHC I and II genes so that every individual can possess a set of MHC molecules with distinct ranges of peptide-binding specificities. Furthermore, the MHC locus is amongst the most highly **polymorphic** regions of the mammalian genome, with multiple variants or alleles of each gene within the population as a whole (Flajnik and Kasahara, 2001). These properties ensure the diversity of haplotypes and enable each haplotype to bind a vast range of self- and pathogen-derived antigens that will subsequently be recognised by TCRs on T cells.

MHC I and II differ in both their structure and their expression pattern in the tissues of the body. MHC class I molecules are expressed almost on all nucleated cells, which therefore can present endogenous peptides from within the host cell. Cells use this mechanism to present intracellularly-derived viral peptides in MHC I molecules and target infected cells for destruction by $CD8^+$ T cells (Vyas et al., 2008). Endogenous peptides are targeted for loading onto the MHC I through the recognition of the transport associated with antigen processing (TAP) molecule, which is part of the peptide loading complex that also contains chaperone proteins that are responsible for the transfer of cytosolic peptides from the endoplasmic reticulum to the MHC I molecules (Blum et al.,

2013). MHC I molecules can subsequently be expressed on the surface of cells and when infected, antigen presentation will take place, which in turn will trigger the $CD8^+$ T cell lineage and initiate an immune response (Fig. 1.1 – right).

On the other hand, expression of MHC II is restricted to either the surface of professional APCs, which are found in environmentally exposed sites, or on other cells, such as astrocytes that can upregulate MHC II upon exposure to IFN-γ (Vardjan et al., 2012). In the first instance, these locations are the place where the capturing of extracellular sources via receptor-mediated phagocytosis, endocytosis, or autophagy occurs, before enzymatic antigen processing within the endosomal compartments and loading onto the MHC II molecule (Roche and Furuta, 2015; Dengjel et al., 2005). Following antigen processing, MHC II can be loaded with the processed peptide and expressed on the surface of the antigen-presenting cells that are responsible for antigen presentation to $CD4^+$ T cells (Fig. 1.1 – left).

It should be noted that professional APCs include DCs, macrophages, and B cells, with DCs being the most potent activators of T cells. These cells can prime naïve T cells through the surface expression of peptide-loaded MHC-II, expression of co-stimulatory molecules, as well as through the secretion of polarising cytokines (Matzinger and Guerder, 1989). On the other hand, non-professional APCs describe non-conventional cells (such as epithelial cells and fibroblasts) bearing MHC-II that can modulate immune responses that were already initiated by DCs, rather than driving primary antigen presentation to naïve T cells (Schuijs et al., 2019).




MHC II peptide binding groove:

- α and β chain
- open-end loops
- peptides usually longer than 11 aa
- highly polymorphic β chain

MHC I peptide binding groove:

- α chain only
- closed-end loops
- peptides usually between 7-9 aa
- highly polymorphic

**Figure 1.1 MHC Class I and Class II antigen processing and presentation pathways.** MHC class II pathway: APCs take up extracellular proteins into early endosomes where proteases (cathepsins, aminopeptidases etc.) generate peptides for loading of MHC II in late endosomes. The structure of the MHC II peptide cleft is open-ended and can fit peptides that contain at least 11 amino acids. Usually, the core binding region is around 9 amino acids, however, the surrounding peptide flanking regions (PFR) contribute significantly to the binding affinity of MHC II. MHC class I pathway: Cytosolic proteins undergo proteasomal cleavage to generate short peptides for loading onto MHC I molecules within the endoplasmic reticulum (ER). The closed structure of the MHC I peptide cleft is made up by the MHC I α chain and normally accommodates shorter peptides, between 7-9 amino acids long. Figure generated using Biorender.

**T cell activation** is initiated by the ligation of the TCR with peptide-loaded MHC molecules (pMHC) induces an intracellular signalling cascade that involves recruitment of transcription factors and re-arrangement of the cytoskeleton, which eventually results in the activation of T cells that subsequently respond with cytokine production, proliferation, cell survival and differentiation (Hwang et al., 2020; Huang and August, 2015). Depending on the magnitude, context and duration of the interaction between the TCR and pMHC, as well as co-stimulatory signal from molecules such as CD28, ICOS, OX40 and cytokines, naïve T cells differentiate into fully functional effector populations (Zikherman and Au-Yeung, 2015).

**Immune regulation** is of pivotal importance for the maintenance of homeostasis and effective immune response upon antigenic challenge. A recent publication shows that major infections, such as the plague, have driven broad genetic diversity in adaptive immunity to deal with a broad range of pathogens (Klunk et al., 2022). Even though the vast repertoire of TCRs gives the host the ability to fight against a wide variety of infections, sometimes it can mistakenly recognise and attack self-antigens or innocuous, environmental antigens. In the first instance, a Th1/Th17 immune response is mounted, which would normally deal with bacteria and fungi, but when perturbated can lead to **autoimmunity**, while in the second instance, a Th2 immune response is initiated which would otherwise deal with parasites, but in that case can lead to **allergy**. These immune pathologies highlight the need for immune regulation that would prevent the development of autoimmune or allergic reactions.

There are different mechanisms of immune regulation. For example, if the interaction of TCR with pMHC takes place in the absence of any co-stimulatory signals, cells enter a state of unresponsiveness known as **anergy** (Fathman and Lineberry, 2007).

Furthermore, the expression of **co-inhibitory receptors** such as CTLA-4, TIGIT, LAG-3, TIM-3 and PD-1, provides an active mechanism of immune regulation by exerting suppressive signals that dampen the immune response (Joller and Kuchroo, 2017).

In the next paragraph, the focus will be on two inhibitory pathways, TIGIT and CTLA-4. The TIGIT pathway is central to the work described in this thesis, while previous work from our lab has also focused on the role of CTLA-4 in immune regulation. The two pathways share some features, such as **ligand promiscuity** and it is worth studying them in parallel to take advantage of the knowledge obtained from the more well-characterised CTLA-4 pathway.

## 1.3 Immune regulation by co-inhibitory receptors

In addition to antigen-specific stimulation of the TCR by a peptide-MHC complex, the functional outcome of TCR engagement is further regulated by antigen-independent signals, which are provided by a set of activating and inhibitory receptors expressed on T cells and their cognate ligands on APCs and tumour cells. Many of these receptors are members of the CD28 family that either positively or negatively contribute to TCR signalling, thus fine-tuning the threshold for T cell activation (Chen and Flies, 2013).

Positive co-stimulatory molecules promote T cell proliferation, with the most prominent example being CD28, which allows effective T cell activation upon engagement of its ligands CD80/CD86 on mature APCs (Esensten et al., 2016; Riley and June, 2005). Signalling via co-inhibitory receptor pathways competes against TCR-driven T cell activation and promotes functional inactivation that results in anergy and a state of tolerance. This counterbalance of co-stimulatory signals is pivotal for the prevention of

excessive effector T cell activation, thereby providing a negative feedback mechanism to inhibit excessive and potentially harmful immune responses (Waterhouse et al., 1995; Allison and Krummel, 1995). The importance of co-inhibitory pathways becomes clear especially in the context of autoimmunity, where genetic polymorphisms in the genes of various co-inhibitory receptors have been associated with autoimmune diseases in humans (Fife and Bluestone, 2008; Qu et al., 2009; Song et al., 2011; Wang et al., 2014).

### 1.3.1 The CD226/TIGIT/CD155 pathway

T cell Ig and ITIM domain (TIGIT) is an inhibitory receptor expressed on lymphocytes that binds to CD155 on professional APCs, such as dendritic cells, making them produce the immunomodulatory cytokine, IL-10, and therefore driving a tolerogenic phenotype. TIGIT has been mainly studied in the context of anti-tumour immunity (Sanchez-Correa et al., 2019a; Dougall et al., 2017; Stamm et al., 2018) and anti-viral immunity (Schorer et al., 2020; Johnston et al., 2014b); however, recent data suggest that loss of TIGIT can also result in susceptibility to autoimmune disease (Yue et al., 2022; Li et al., 2021). In both mice and humans, activated $CD4^+$ and $CD8^+$ T cells, Tregs and NK cells express TIGIT. The levels of TIGIT are low in naïve cells and they gradually go up after activation, while the highest expression of TIGIT can be found in Tregs, memory and activated T cells, and NK cells, indicating a potential functional role in these cells (Kurtulus et al., 2015a; Joller et al., 2014b). In addition to CD155, TIGIT also binds to CD112 and CD113, yet with lower affinity. CD155 is predominantly expressed by DCs, T cells, B cells and macrophages but also in the kidney, nervous system, and intestines. On the other hand, CD112 can be found both in hematopoietic and non-hematopoietic tissues including the bone marrow, pancreas, kidneys and lungs, whereas

CD113 has a more tissue-specific expression as it is restricted in non-hematopoietic tissues such as the placenta, kidneys and lungs (Stanietsky, Noa; Tihana, 2014; Tahara-Hanaoka et al., 2004).

Initially, it was proposed that the inhibitory effects of TIGIT could be mediated indirectly, through the triggering of CD155 on dendritic cells (DCs) (Harjunpää and Guillerey, 2019). This interaction was responsible for the attenuation of immune responses *in vivo*, predominantly through tyrosine phosphorylation of the ITIM domain of CD155, which in turn recruits the Src kinases and SHP-2 (SH2-domain-containing tyrosine phosphatase-2), and induces the production of the immunosuppressive cytokines, IL-10 and TGF-β by DCs, rendering them tolerogenic (Fig. 1.2).

These DCs are characterised by decreased antigen presentation, low levels of co-stimulatory molecules, such as CD80, CD86 and CD40 and finally decreased secretion of proinflammatory cytokines, such as IL-12. It was later shown that TIGIT can also have **T cell intrinsic effects**, as agonistic anti-TIGIT antibodies were able to inhibit T cell proliferation, even in the absence of any other cell type. TIGIT can also disrupt the activating signals in **a cell-extrinsic manner**, by interfering with CD226 co-stimulation (Joller et al., 2011c; Dixon et al., 2018). TIGIT, together with DNAM-1 (CD226) and Tactile (CD96) binds the Nectin/Nectin-like (Necl) family member poliovirus receptor (PVR, NecI-5, CD155), whereas CD226 also recognises PVRL2 (Nectin-2, CD112). Nectins belong to the Ig superfamily (IgSF) of cell surface receptors that play a critical role in cell adhesion, movement, and tissue organisation. They can function as both ligands and receptors, thus allowing bidirectional signalling in neighbouring cells. TIGIT binds CD155 with the highest affinity followed by CD96 and then CD226. In particular, engagement of TIGIT to CD155 leads to an anti-inflammatory response, while ligation

of CD155 with the lower affinity activating receptor, CD226, on T and NK cells facilitates immune activation (Fig. 1.2) (Fuhrman et al., 2015a; Pauken and Wherry, 2014; Harjunpää and Guillerey, 2019).

This difference seen in **binding affinity**, where the inhibitory receptor displays a high affinity, whereas the co-stimulatory receptor has a lower affinity for the same ligand, indicates that the activating receptor needs to outcompete the inhibiting interaction to deliver a stimulatory signal. In such systems, where some paired receptors recognise a set of shared ligands, changes in the expression of one molecule can have an impact on the overall balance of the receptor-ligand interactions, therefore providing several layers of immune regulation, which fine-tune the course, duration and strength of T cell responses (Schnell et al., 2020). Having said this, a disruption of the balance between activating and inhibitory signals results in perturbation of the immune homeostasis, as witnessed by the fact that homozygous deletion of TIGIT in mice leads to hyper-proliferative T cell responses and increased susceptibility to autoimmune diseases (Joller et al., 2011) .

One of the questions that remains unanswered is why T cells would require three different receptors for CD155. This ligand promiscuity is reminiscent of T cells, in which the co-inhibitory receptor CTLA-4 binds the same ligands (B7-1 and B7-2) as the co-activating receptor CD28. This ligand competition is resolved partly because CTLA-4 is upregulated upon T cell activation and also binds the shared ligand with higher affinity compared to CD28, therefore resulting in the inhibition of T cell activation (Sansom, 2000). The case of redundancy seen in both pathways, could indicate that each pathway orchestrates distinct aspects of the immune response, potentially triggering different signalling pathways, or even regulating different functional outcomes based on the

expression in each compartment, ensuring a more time- and tissue-restricted regulation during T cell activation.

However, the CD226/TIGIT/CD155 pathway appears to be more complex, given that TIGIT and CD226 also share CD112 as a ligand and CD112R (PVRIG), a newly identified checkpoint receptor expressed on T cells and NK cells, which also competes with CD226 and TIGIT for the binding of CD112 (Negishi et al., 2018; Lozano et al., 2012b). Furthermore, CD96, which contains both activating and inhibitory motifs in its cytoplasmic tail, was initially considered stimulatory in humans, since it was inducing the cytotoxicity of NK cells (Liu et al., 2013; Zhang et al., 2018); however, it was later found that murine CD96 also has an inhibitory potential that competes against CD226 stimulatory activity. Even though, these nectin receptors differ in terms of affinity and specificity for their cognate ligands, the molecular basis for these differences remains elusive. Even though TIGIT has been studied primarily in the context of anti-tumour immunity, there is ever-growing evidence to support its role in the regulation of autoimmunity via its expression on Tregs (Joller et al., 2014). Therefore, a part of this thesis aims to elucidate the role of TIGIT on the establishment of central and peripheral tolerance and its potential involvement in bystander suppression (see Chapter 3 – Results).

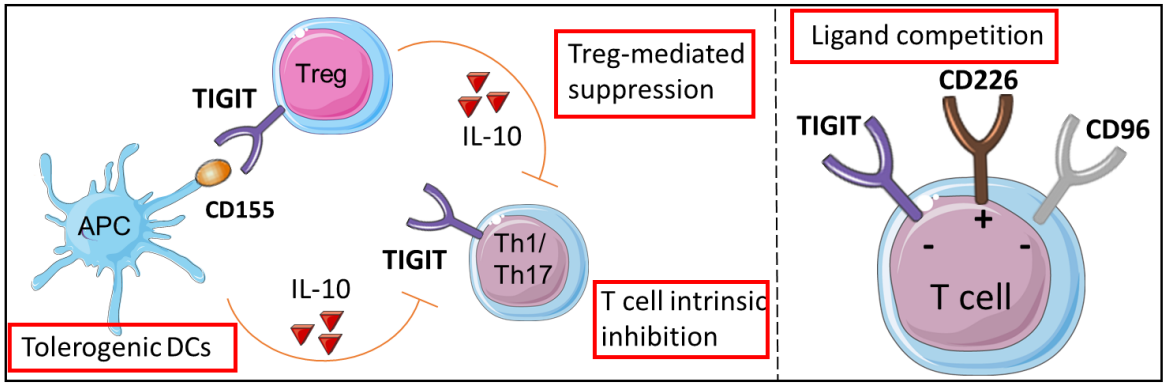



**Figure 1.2 The proposed mechanisms of action for TIGIT.** TIGIT can bind CD155 and trigger direct inhibitory signals in T cells via its cytoplasmic tail (T cell intrinsic inhibition). TIGIT and its activating receptor counterpart CD226 compete for binding of two known ligands CD112 and CD155, with TIGIT being able to disrupt the homodimerization of CD226 on the cell surface and prevent its interaction with CD155. TIGIT ligation with CD155 induces IL-10 production by APCs, which negatively regulates inflammatory processes (induction of tolerogenic DCs). TIGIT is often upregulated in Tregs marking a highly suppressive phenotype (Treg-mediated suppression). Parts of the figure were drawn by using pictures from Servier Medical Art. Servier Medical Art by Servier is licensed under a Creative Commons Attribution 3.0 Unported License (https://creativecommons.org/licenses/by/3.0/).

### 1.3.2 The CTLA-4/CD28/CD80/CD86 pathway

CTLA-4 belongs to the immunoglobulin Ig superfamily and is constitutively expressed on Tregs and upon activation on Tconv cells. CTLA-4 competes with CD28 for binding to the same ligands, CD80 (B7-1) and CD86 (B7-2); however, it binds with approximately 20-fold greater affinity and avidity than CD28, transmitting a T cell intrinsic inhibitory signal (Krummel and Allison, 1995; Linsley et al., 1991; Walunas et al., 1996). Ligation of CD80 and CD86 with CD28 leads to an induction of a positive activation signal and competition between CD28 and CTLA-4 essentially attenuates T cell activation by limiting the number of available ligands for CD28.

The downstream signalling pathway of CTLA-4 is predominantly mediated by PI3K and AKT and provides a robust signal that is directly proportional to the TCR signal strength (Pagès et al., 1994; Kane et al., 2001). CTLA-4 knock out mice suffer from severe lymphoproliferative disorders and tissue destruction of multiple organs (Tivol et al., 1995). Interestingly, Treg-specific CTLA-4 ablation induced severe lymphoproliferation in mice by the age of 3-4 weeks, suggesting that CTLA-4 is instrumental for the maintenance of immunological tolerance mediated via Tregs (Friedline et al., 2009; Read et al., 2006; Wing et al., 2008).

The CTLA-4 pathway has been exploited in the context of cancer immunotherapy, particularly for the treatment of melanoma patients. Similar to T cell exhaustion seen during chronic infections, tumour infiltrating T cells (TILs) express increased levels of inhibitory receptors that limit their function and can be targeted with blocking antibodies (Ahmadzadeh et al., 2009). CTLA-4 blockade can induce tumour rejection by either favouring CD28-mediated positive co-stimulation at sites of T cell activation (Ramagopal et al., 2017), or by ripping off CD80 and/or CD86 from the surface of APCs , thereby

inhibiting the activation of other naïve or effector T cells since they are not able to receive a co-stimulatory signal via the CD28-CD80/CD86 pathway (Qureshi et al., 2011). Finally, it has also been suggested that tumour rejection via CTLA-4 blockade can occur by depleting Tregs in the tumour microenvironment, therefore removing the burden for effective tumour clearance (Simpson et al., 2013; Selby et al., 2013).

## 1.4 Thymic T cell development and central tolerance

The thymus produces multiple T cell types that play instrumental roles in both the innate and the adaptive branch of the immune system. In particular, in this primary lymphoid organ, T cell receptors (TCR) are generated by gene rearrangement that takes place during early T cell development and gives rise to a wide range of antigen receptors that target non-self (αβTCR repertoire) (Inglesfield et al., 2019). During TCR gene rearrangement, T cell progenitors first undergo somatic rearrangement of the TCR α and β loci with insertions of non-coded nucleotides into the hyper-variable regions to produce novel TCR genes.

Pairing of the resulting proteins gives rise to a wide range of TCR sequences with novel amino-acid sequences in the complementarity determining regions (CDR) that are responsible for the interaction with the antigen (Marrack et al., 2008). It is estimated that in humans, each individual possesses approximately $10^{15}$ different αβ TCR permutations, creating a highly diverse naïve repertoire, which is a critical feature of a functional immune system that is capable of controlling a vast range of viral infections and other pathogens (Arstila et al., 1999; Keşmir et al., 2000; Fuschiotti et al., 2007). This process is of pivotal importance as it ensures that only conventional T cells that both 1) recognise self-MHC proteins and at the same time, 2) are tolerant to self-antigens will escape the thymus and enter the periphery. The first requirement is achieved during the process of

**positive selection**, where immature thymocytes, which express a TCR with intermediate affinity for self-peptide-MHC complexes (MHC restriction), are induced to differentiate into mature, single positive, either $CD4^+$ or $CD8^+$ thymocytes according to their affinity for MHC class II and I, respectively (Takada and Takahama, 2015). This process takes place in the thymic cortex and heavily relies on sustained rather than transient interactions between developing thymocytes and thymic stromal cells (cortical thymic epithelial cells, cTECs) (Anderson and Takahama, 2012; Anderson et al., 1994; Wilkinson et al., 1995).

The second requirement is achieved via **negative selection**, during which process, double-positive ($CD4^+CD8^+$) or single-positive thymocytes that express TCRs with high affinity for self-antigens are eliminated in the thymus before they enter the periphery (Klein et al., 2009; Takaba and Takayanagi, 2017). This is achieved when positively selected $CD4^+$ or $CD8^+$ T cells express the chemokine receptor CCR7 that allows them to migrate into the medulla, where the CCR7 ligands, CCL19 and CCL21 are highly expressed by the medullary thymic epithelial cells (mTECs) (Förster et al., 2008).

In the medulla, $CD4^+$ or $CD8^+$ T cells interact with APCs such as mTECs or dendritic cells (DCs) and that interaction results in the deletion of autoreactive T cells **(clonal deletion)**. Given that certain antigens are only expressed in specific tissues, it is important that mTECs can present tissue-restricted antigens (TRAs), which in turn enables the deletion of cells specific for antigens that would normally be found only in peripheral tissues (Derbinski et al., 2001). TRA expression is controlled by transcriptional regulators such as Aire and Fezf2 in the mTECs (St-Pierre et al., 2015) (Fig. 1.3).

Most of the T cells that recognise self-antigen-MHC complexes are deleted by mTECs and thymic DCs via apoptosis (negative selection), but a fraction of $CD4^+$ single

positive thymocytes differentiates into the regulatory T cell lineage, which express FoxP3 and specialise in the control of immune tolerance (agonistic selection) (Sakaguchi, 2000). Similar to negative selection, both mTECs and thymic DCs play an instrumental role in $FoxP3^+$ thymic Treg (tTreg) development (Cowan et al., 2013; Perry et al., 2014). tTregs are mainly distributed in the thymic medulla prior to their migration into secondary lymphoid organs, where they limit autoreactive responses initiated by T cells that escaped central tolerance (Li and Zheng, 2015).

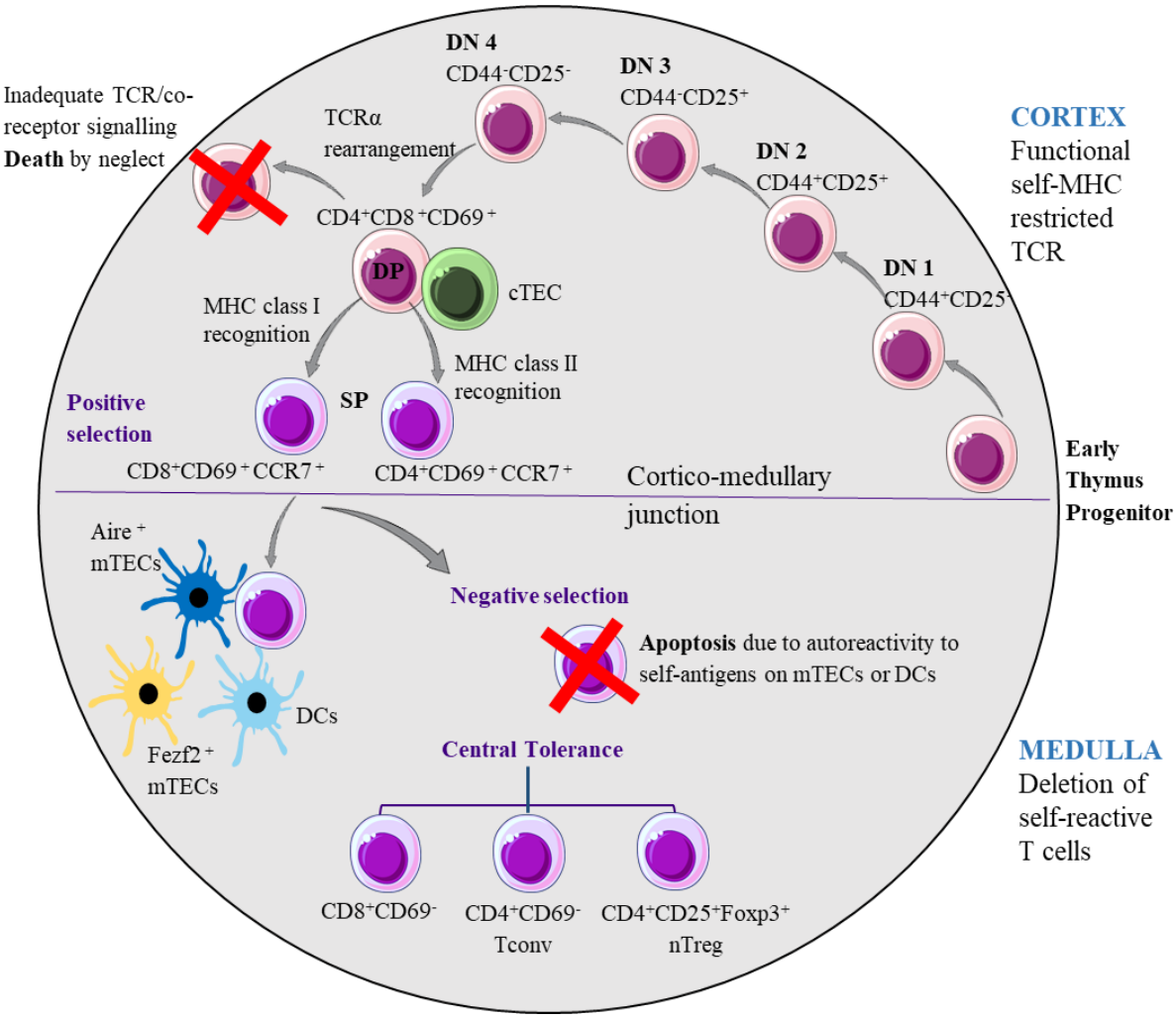



**Figure 1.3 T cell development in the thymus.** Initially, a population of early thymus progenitor cells enters the corticomedullary junction in the thymus. At this stage, the cells migrate into the cortex, rearrange their TCR genes and undergo multiple stages of development as double negative (DN) cells. A TCR is then presented on the surface of the cells, which differentiate into a double positive (DP) population, that expresses both CD4 and CD8. Subsequently, developing thymocytes interact with cTECs, in a process known as positive selection, giving rise to single positive (SP), either $CD4^+$ or $CD8^+$ T cells. SP cells can then upregulate CCR7 that allows their migration to the medulla, where negative selection takes place. In the medulla, SP cells interact with dendritic cells (DCs) or $Aire^+$ and $Fezf2^+$ mTECs that express tissue-restricted antigens (TRA). During negative selection, cells that are autoreactive undergo apoptosis, while the rest of the cells can successfully pass through the central tolerance screening, fully mature and egress from the thymus into the periphery as naïve T cells.

There are two alternative mechanisms that give rise to tTregs. The first suggests that once the TCR is engaged with its cognate antigen with medium affinity, there is an upregulation of the α chain of the IL-2 receptor, also known as CD25, that causes cells to become $CD25^{+}FoxP3^{-}$ precursors, which can subsequently mature via IL-2 recognition, which drives STAT5 to support FoxP3 expression and development into $CD25^{+}FoxP3^{+}$ fully mature nTreg (Lio and Hsieh, 2008). Alternatively, nTreg can also develop from a $CD25^{-}FoxP3^{+}$ precursor population. FoxP3 is initially acquired via TCR engagement, which in turn leads to the phosphorylation of the proapoptotic molecule Bim. Furthermore, exposure to the common cytokine receptor γ chain family of cytokines (IL-7, IL-2, IL-15 etc.) promotes Bcl-2 pro-survival factors, which rescue cells via CD25 upregulation as they mature into $CD25^{+}FoxP3^{+}$ nTreg (Tai et al., 2013).

## 1.5 Peripheral tolerance

The primary mechanism that leads to self-tolerance is thymic deletion of autoreactive T cells (Kappler et al., 1987). However, thymic deletion can be imperfect and as a result, autoreactive T cells that recognise self-antigens, such as myelin basic protein (MBP), may escape to the periphery (Burns et al., 1983; Ponsford et al., 2001; Zhang et al., 1994), despite expression of such proteins in the thymus (Pribyl et al., 1993; Heath et al., 1998). The question that arises is how these autoreactive cells appear in the T cell repertoire of healthy individuals without triggering autoimmune responses. The answer can be found in the fact that these cells recognise their antigens with low avidity (Anderton and Wraith, 2002), and more importantly, these cells are subject to mechanisms of peripheral tolerance that include **T cell anergy** (Schwartz, 1990) and **T cell ignorance** (Schietinger and Greenberg, 2014) or active mechanism of tolerance induction, which is mediated by distinct subset of regulatory T cells. In healthy

individuals, these mechanisms suppress the activation and expansion of autoreactive T cells that have escaped central tolerance in the thymus (Shevach, 2002).

### 1.5.1 FoxP3$^+$ regulatory T cells

FoxP3$^+$ regulatory T cells (Tregs) were first described by Sakaguchi and co-workers as a potent CD4$^+$ immunomodulatory T cell population that can be defined by the expression of the IL-2R α chain (Sakaguchi, 1995). The initial doubts about their existence were dissipated in 2003 by the discovery of the lineage-specific transcription factor FoxP3 (Hori et al., 2003; Fontenot et al., 2003; Khattri et al., 2003). Tregs are a subset of CD4$^+$ T cells that are pivotal for the maintenance of tolerance and tissue homeostasis and are primarily generated in the thymus **(tTregs)**, but can also be generated extrathymically at peripheral sites from naïve T cells **(pTregs)** or *in vitro*-induced **(iTregs)** in the presence of TGF-β (Shevach and Thornton, 2015).

tTregs differentiate from CD4$^+$CD8$^+$ DP or CD4$^+$ SP thymocytes depending on the expression of tissue-restricted self-antigens expressed in medullary thymic epithelial cells (Fontenot et al., 2005; Abbas et al., 2013; Hsieh et al., 2012; Klein et al., 2019). pTregs differentiate from naïve CD4$^+$ T cells in secondary lymphoid tissue upon antigen recognition in the presence of TGF-β (Chen et al., 2003). Helios and neuropilin-1 (Nrp-1) are the most commonly used markers to distinguish tTregs (Helios$^+$Nrp-1$^+$) from pTregs (Helios$^-$Nrp1$^-$) (Yadav et al., 2012; Weiss et al., 2012; Thornton et al., 2019).

Many of the concepts developed in Treg biology over the last 20 years are based on *in vitro* studies that were aiming to measure the suppressive function of Tregs by co-culturing them with different ratios of non-Treg cells (responder CD4$^+$ or CD8$^+$ T cells) that were triggered by TCR signalling in the presence of APCs (Thornton and Shevach,

2000, 1998; Sakaguchi, 1995; Takahashi et al., 1998). Tregs can suppress a wide range of immune cells, but primarily they exert their suppressive function by inhibiting the activation and expansion of naïve and memory Tconv cells (Levings et al., 2001).

Several mechanisms have been proposed for the Treg-mediated suppression that can have either a direct effect on effector T cells (Piccirillo et al., 2002) or an indirect effect by altering the ability of APCs to present antigen or provide co-stimulatory signals. In particular, some of the mechanisms include the **production of tolerogenic molecules** (Shevach, 2009; Andersson et al., 2008; Collison et al., 2008; Borsellino et al., 2007), **consumption of IL-2**, since they express the high affinity IL-2R, CD25, thereby acting as IL-2 sinks to inhibit Tconv proliferation (Pandiyan et al., 2007), CTLA-4-mediated inhibition of co-stimulation **(trogocytosis)** (Wing et al., 2008; Qureshi et al., 2011) or **depletion of peptide-MHC II** complex of DCs (Akkaya et al., 2019) and contact-dependant killing of antigen-presentation through **granzyme B and perforin** (Cao et al., 2007) (Fig. 1.4). In addition to CTLA-4, the specific functions of other inhibitory receptors expressed at high levels by Tregs such as TIGIT, LAG-3, TIM-3 and PD-1 can also be involved in cell-contact-dependent suppression by specialised mechanisms (Anderson et al., 2016).

FoxP3$^+$ Tregs are not a uniform population of cells, but rather comprise several sub-phenotypes with differences in their differentiation stage and expression of effector molecules of suppression (Hori, 2014; Liston and Piccirillo, 2013). Depending on the inflammatory cues, co-stimulatory signals and tissue localisation, there is a network of Tregs, which ensures that the timely and efficient T cell immunoregulation will occur (Stephens et al., 2007; Shevach, 2006). This high degree of **heterogeneity** within the Treg pool potentially reflects distinct physiological roles that are required throughout the

course of an immune response that allow a partial shift towards an effector phenotype while maintaining core suppressive functions (Cretney et al., 2013).

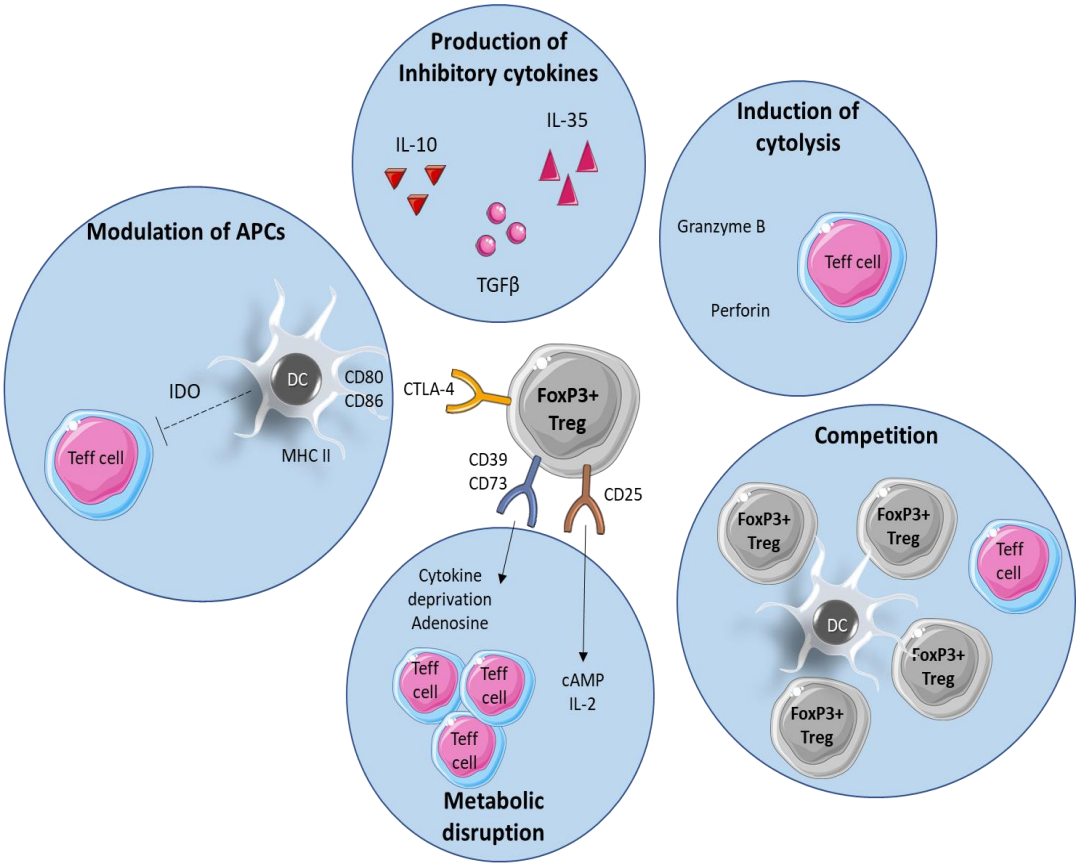



**Figure 1.4 Mechanisms of Treg-mediated suppression.** (1) Targeting DCs – modulation of APC activity through Treg engagement of co-stimulatory molecules such as CD80 and CD86 on the DC surface, leading to weak or abrogated signals to naïve/effector T cells; (2) Metabolic disruption includes cytokine deprivation, cyclic AMP-mediated inhibition, and adenosine receptor (A2A)-mediated immunosuppression; (3) Tregs can compete against effector T cells for critical cytokines such as IL-2 and even directly disrupt effector T cell engagement with APCs; (4) Cytolysis of effector T cells or APCs via the production of granzyme B and perforin that leads to apoptosis; (5) Secretion of anti-inflammatory cytokines such as IL-10, IL-35 and TGF-β.

In recent years, a new classification system of Treg cells was used based on their activation status. tTregs can be subdivided into naïve-like, resting, central Tregs **(cTregs)**, versus activated, effector-like Tregs **(eTregs)** (Hayatsu et al., 2017; Luo et al., 2016; Liston and Piccirillo, 2013). In the presence of TCR, CD28 and IL-2 signalling, cTregs differentiate into eTregs, which are defined by $CD62L^{low}CD44^{hi}$ or $CCR7^{lo}CD44^{hi}$ (Smigiel et al., 2014; Levine et al., 2014; Li and Rudensky, 2016). eTregs express high levels of CTLA-4, TIGIT, ICOS, GITR, IL-10 compared to cTregs, which likely contributes to the enhanced suppressive capacity of these cells (Koizumi et al., 2018; Wei et al., 2017; Dias et al., 2017).

A central driver of eTreg differentiation is a transcriptional program driven by IRF4, which is activated by TCR. Together with BATF, JunB and other AP-1 transcription factors, IRF4 regulates the majority of eTreg genes such as Blimp-1, which in turn promotes the expression of IL-10 (Cretney et al., 2011; Ogawa et al., 2018; Iwasaki et al., 2013). Even though eTregs bear a lot of similarities with antigen-experienced Tconv, it is not clear whether TCR engagement alone is sufficient to drive eTreg differentiation or whether there is a requirement for additional stimuli *in vivo*, such as IL-2, inflammatory signals, or co-stimulation (Fig. 1.5).

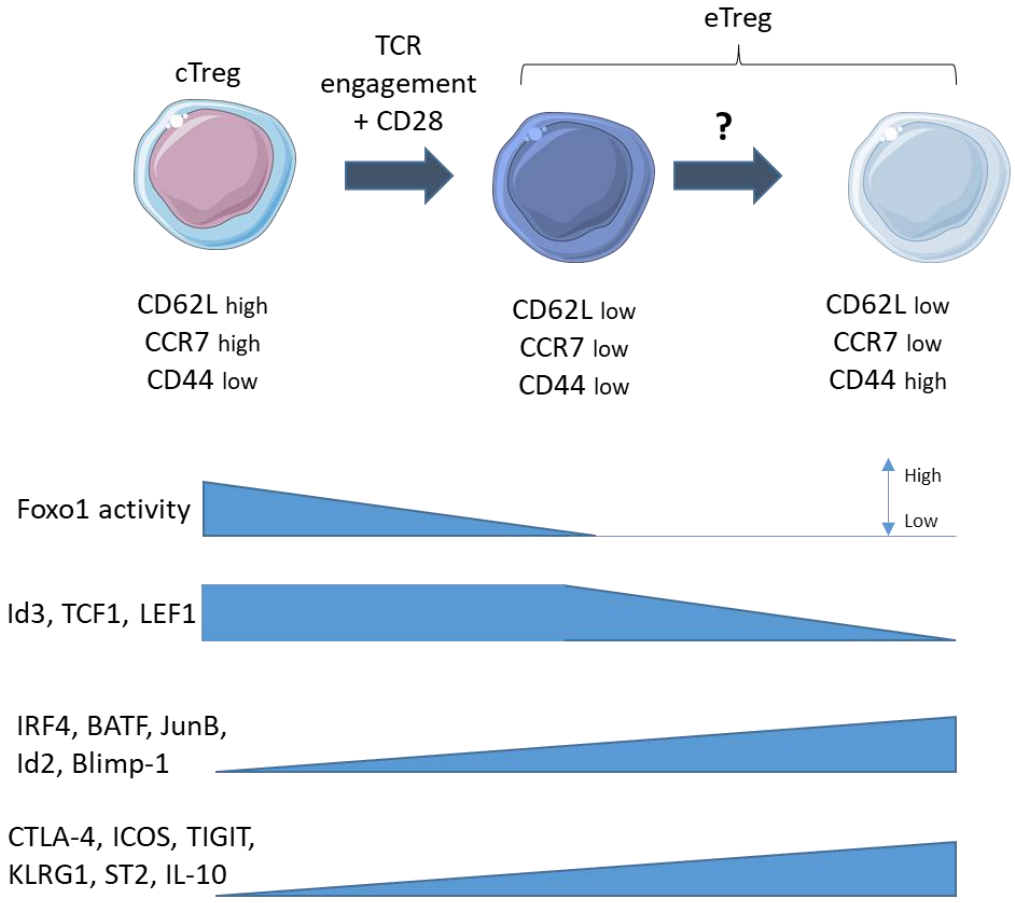



**Figure 1.5 Transcriptional Regulation of Differentiation and Functions of Effector T Regulatory Cells.** Upon antigen stimulation, central Treg (cTregs) cells ($CD62L^{hi}$ $CCR7^{hi}$ $CD44^{lo}$) differentiate into effector Treg (eTreg) cells ($CD62L^{lo}CCR7^{lo}CD44^{hi}$), depending on TCR and CD28 signalling. After activation, TCR-dependent transcription factors, such as interferon regulatory factor 4 (IRF4), are induced and regulate the eTreg transcriptional program. In contrast, Foxo1 is inactivated by Akt-signalling, which downregulates expression of cTreg-related molecules. Loss of Id2, transcription factor 1 (TCF1), and lymphoid enhancer binding factor 1 (LEF1) expression is a signature of mature eTreg cells. Mature eTreg cells highly express immune suppressive molecules, such as cytotoxic T cell antigen 4 (CTLA-4), B-lymphocyte-induced maturation protein 1 (Blimp-1), IL-10 and inducible T cell co-stimulator (ICOS). Adapted from: Koizumi, S., & Ishikawa, H. (2019). Transcriptional Regulation of Differentiation and Functions of Effector T Regulatory Cells.

eTregs can undergo further stimulus-specific differentiation that is regulated by transcription factors typically associated with the differentiation of conventional T-helper ($T_H$) cells. In particular, naïve $CD4^+$ T cells can differentiate into functionally distinct subsets of effector T cells (T helper 1 (Th1), Th2 and Th17) defined by the expression of the transcription factors Tbet, GATA3, RORγt, respectively (Zhu et al., 2012). Surprisingly, recent findings show that the cytokine signals that polarise Tconv cells, not only have an impact on $T_H$ cell differentiation, but also on the functional specialisation of eTregs under these conditions **(model of parallel differentiation)** (Fig. 1.6) (Levine et al., 2017; Sefik et al., 2016; Koch et al., 2009; Ohnmacht et al., 2015).

Furthermore, Th2-like Tregs expressing GATA3 and IRF4 have been proposed to play a role in controlling all eTregs and not just mirror the Th2 phenotype specifically (Wohlfert et al., 2011). It has been proposed that each Th-like phenotype of Tregs may enable them to migrate to the inflamed tissue site and suppress the corresponding Tconv subgroup (Wing and Sakaguchi, 2012). This division of labour among Tregs, witnessed both at immune homeostasis and during inflammatory conditions, may regulate specialised regulation of specific T helper cell responses without giving rise to any undesired bystander effect (Chaudhry and Rudensky, 2013; Josefowicz et al., 2012). Whether expression of these factors indicates the heterogeneity of functionally distinct subsets, with stable, terminally differentiated states, or maybe readily reversible, remains to be determined (Liston and Gray, 2014).

In addition to transcription factors, **epigenetic modifications** are also associated with eTreg differentiation (Nakatsukasa et al., 2019; Yue et al., 2019; Obata et al., 2014). However, the molecular associations between the transcriptional programming and epigenetic modifications of eTregs are not well-defined. Further elucidation of the role of

eTreg-related transcription factors in gene expression, chromatin accessibility and histone modifications will pave the way towards understanding the crosstalk between transcriptional signatures and epigenetic regulators in eTreg biology.

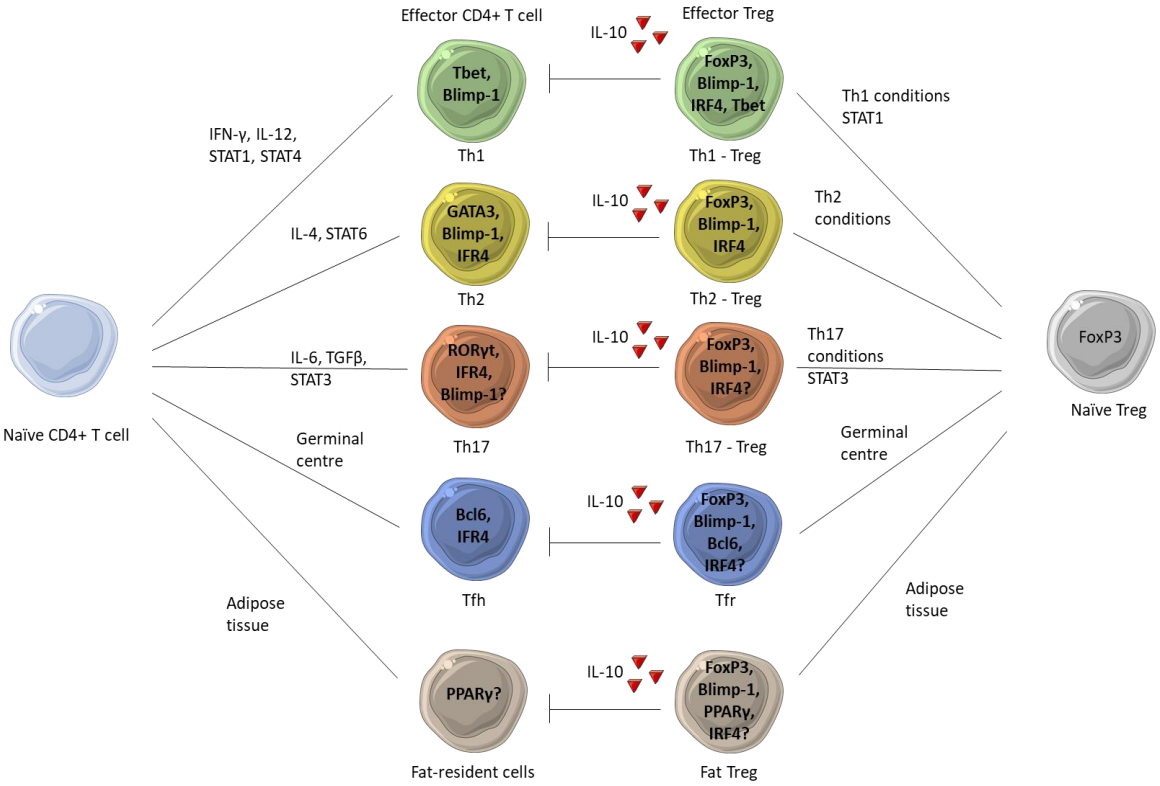



**Figure 1.6 Differentiation of effector CD4$^+$ T cells and Tregs.** Following TCR engagement, naïve CD4$^+$ T cells can functionally differentiate into different effector cell lineages (Th1, Th2, Th17). The differentiation pathway relies both on the inflammatory signals found in the microenvironment of the cells, as well as on transcriptional factors (TF) including Tbet (Th1), GATA3 and IRF4 (Th2) and RORγt (Th17). Similarly, upon repeated exposure to antigen, naïve Tregs can also differentiate into distinct effector Treg (eTreg) lineages, by expressing TFs that were previously thought to be expressed only by conventional T cells. Even though eTregs demonstrate a high degree of heterogeneity, depending on the tissue they are found in, and the polarising conditions, IL-10 and Blimp-1 appear to be among the most stably expressed markers.

### 1.5.2 IL-10$^{+}$FoxP3$^{-}$ Tr1 cells

In addition to thymically derived Foxp3$^{+}$ Tregs, there are other types of regulatory T cells that can differentiate from naive T cells upon repeated exposure to antigen in the presence of anti-inflammatory cytokines. For instance, IL-10-secreting cells that lack the expression of FoxP3, also known as Tr1 cells, can be induced *in vitro* from naïve T cells that were stimulated repeatedly via their TCR in the presence of IL-10 (Groux et al., 1997; Barrat et al., 2002). Furthermore, Tr1 cells can also be induced *in vivo* by repeated administration of superantigens (Sundstedt et al., 1997; Miller et al., 1999) or soluble peptides via a tolerogenic route (Burkhart et al., 1999). These cells are predominantly CD25$^{-}$ (Sundstedt et al., 2003), although they can transiently upregulate CD25 upon antigen exposure (Anderson et al., 2005). They primarily exert their immunosuppressive phenotype via secretion of the immunomodulatory cytokine, IL-10, which dampens the function of both antigen-presenting cells, giving rise to tolerogenic dendritic cells (tolDCs) and antigen-specific effector T cells (Chihara et al., 2016).

tolDCs can also produce lower levels of the pro-inflammatory cytokine, IL-12, which in turn potentiates naïve T cells to acquire a Th1 effector phenotype (Gabrysova et al., 2009). Furthermore, like FoxP3$^{+}$ Tregs, Tr1 cells can kill effector and myeloid cells through the perforin-granzyme B pathway (Roncarolo et al., 2014). The existence of antigen-specific Tr1 cells makes them a very appealing target for antigen-specific immunotherapies to treat a wide range of autoimmune diseases in a more effective way, by circumventing the side effects associated with immunosuppressive drugs.

Despite the fact that Tr1 cells lack FoxP3 expression, they exert a similar *in vitro* phenotype to those of Foxp3$^{+}$ Tregs. In particular, they remain unresponsive in terms of proliferation upon antigen recognition, they can mediate suppression that is driven by cell

contact, they secrete very low levels of IL-2, and they express activation markers on their surface (Vieira et al., 2004). We speculate that FoxP3$^-$ Tr1 and Foxp3$^+$ Tregs potentially share some suppressive mechanisms *in vitro*; however, their long-term stability *in vivo* is yet to be determined.

Previous work by the Wraith lab has shown that presentation of peptide antigens on steady state dendritic cells increases the proportion of Foxp3$^+$ T cells *in vivo;* however, the major impact of treatment with tolerogenic peptides, is to convert potentially pathogenic T cells that derive from a Th1-skewed murine model, into regulatory Tr1 cells (Burton et al., 2014; Burkhart et al., 1999; Sundstedt et al., 2003). In a recent publication, Shepard et al., has shown that for effective tolerance induction, peptides must be designed to bind the MHC class II molecule on immature, steady-state dendritic cells (ssDCs) in a conformation that mimics the naturally processed epitope (antigen-processing independent epitopes/apitopes. ssDCs express low levels of MHC II and co-stimulatory molecules (CD80, CD86, CD40), therefore the presentation of T cell epitopes by them is tolerogenic, leading to T cell death, anergy or the adoption of a regulatory phenotype (Steinman et al., 2003). A critical requirement for that is **peptide solubility** since peptides should be in soluble form in order to be **tolerogenic rather than immunogenic** and distribute throughout the body to bind to their MHC restriction element on ssDCs in lymphoid organs (Shepard et al., 2021).

These Tr1 cells that are generated in response to soluble peptides presented by ssDCs are anergic, they produce high levels of IL-10, and lack expression of Foxp3, but express a similar tolerance associated gene signature to the IL-10-producing cells that control immune pathology in chronic infection (Sundstedt et al., 2003). In particular, they express the IL-10 promoting transcription factors c-Maf and NFIL3 and upregulate

inhibitory receptors CTLA-4, LAG-3, TIM-3 and TIGIT (Burton et al., 2014). Recent publication from our lab has shown that tolerance induction is responsible for the preferential epigenetic priming of tolerance-associated genes, rendering them more responsive by allowing them to be induced at a lower threshold of TCR/CD28 signalling than that required for immune response genes (Bevington et al., 2020).

In particular, Tr1 cells were less inducible at immune response gene sites, such as *Nr4a3, Il2, Tnf, Cfs2, Cd40Ig, Nfkb1*, while becoming more inducible for tolerance-associated genes, including inhibitory receptors, such as *Ctla4, Tigit, Lag3, Havcr2* (TIM-3), *Pdcd1* (PD-1), transcription factors *Nfil3* and *Maf*, and the immunoregulatory cytokine genes *Il10* and *Il21* (Bevington et al., 2020). Even though it has been suggested that Tr1 cells bear a lot of phenotypic similarities with exhausted T cells found in the tumour microenvironment (Chaudhary and Elkord, 2016), in our system, Tr1 cells are highly functional upon antigen encounter, which promotes IL-10 production and expression of co-inhibitory receptors and their state of anergy is reversible with addition of external IL-2 (Anderson et al., 2005).

## 1.6 Autoimmune Diseases

Even through there are several levels of immune regulation in place to ensure a state of non-responsiveness to specific antigens, immune responses are still raised to innocuous antigens from host tissue, the environment, commensal bacteria, or food particles due to a loss or dysfunction of tolerance mechanisms. In these cases, detrimental chronic inflammation is mounted, and disorders occur, including allergic reactions, such as asthma and autoimmune diseases, such as rheumatoid arthritis (RA), systemic lupus erythematosus (SLE), type I diabetes (T1D) and multiple sclerosis (MS). In these autoimmune diseases, the immune system attacks the host, because the immune cells of

the affected individuals are insufficiently tolerant towards certain 'self' proteins, and they attack them as foreign.

Most autoimmune diseases are **polygenic disorders** reflecting the complex interface between disease susceptibility and resistance genes and they have been strongly associated with genetic, infectious, and environmental predisposing factors. They comprise multiple disorders with a wide range of symptoms from **organ-specific** (e.g., Graves' diseases – thyroid gland, Hashimoto's – thyroid gland, Goodpasture's – lungs and kidneys, T1D – beta cells of the endocrine pancreas), in which antibodies and T cells react to self-antigens localised in a specific tissue, to **systemic** (SLE, RA), which are characterised by reactivity against a specific antigen(s) spread throughout various tissues in the body. The aetiology remains largely unknown with more than ¾ of those affected being women (Jacobson et al., 1997). Although the underlying mechanisms for this predisposition are not well understood, it is known that females produce much higher levels of oestrogen and reduced levels of testosterone, and it is well documented that these hormones may modify the outcome of the immune response (Cutolo et al., 2004).

There are a few different mechanisms of tolerance breakdown that lead to autoimmunity including, **molecular mimicry**, **bystander activation**, and exposure of **cryptic antigens**. In the case of molecular mimicry, exposure to foreign antigens induces excessive inflammation due to cross-reactive epitopes that are essentially shared immunological epitopes between the pathogen and the host (Fujinami et al., 1983). This high degree of homology in sequence or structure between foreign and self-antigens epitopes (cross-reactivity) can lead to a persistent proinflammatory cytokine release against host tissue and eventually in undesired immune pathology (Cusick et al., 2012). Furthermore, bystander activation is characterised by autoreactive T and B cells that

undergo activation in the absence of antigen recognition. In that case, self-reactive T cells can be activated by a combination of co-signalling ligands and interactions with adjacent cells, which spread the inflammatory cues to bystander cells that are found in close proximity; this results in additional immunopathology at sites of infection (Pacheco et al., 2019). Finally, it has been proposed that anatomically sequestered epitopes that are found in tissues or cellular locations that are less accessible, such as the immune privileged sites (i.e., CNS), are not readily presented for recognition by T cells. These epitopes are termed cryptic, and when they become visible to the immune system they can elicit a sustained pathogenic response that can propagate autoimmunity (Warnock and Goodacre, 1997).

There is no cure for autoimmune diseases and the traditional therapeutic strategies aim at long-lasting remission with reduction of the symptoms and improvement of the quality of life. There is a pressing need to better understand the mechanisms underpinning the autoimmune conditions and develop more targeted approaches for their successful treatment. In the next paragraph, there is a description of novel approaches in the field of immunotherapy that are currently being developed and some of them are already tested in the clinic.

## 1.7 Antigen-specific immunotherapy for the treatment of autoimmune diseases

Allergen immunotherapy (AIT) has been practised in the field of allergy for over a century now (Noon, 1911). In the initial studies, it was shown for the first time that repeated inoculation with grass pollen extract using increasing subcutaneous doses led to amelioration of the disease symptoms setting the foundations of the allergic desensitisation protocols practised today (Patel et al., 2013). Allergic reactions have a lot

in common with autoimmune responses, because in both settings there is a population of over-active antigen-specific T and B cells that drives the disease development. Therefore, the development of antigen-specific immunotherapy (ASI) approaches for the treatment of autoimmune diseases has benefited from substantial knowledge transfer between the two fields.

Furthermore, over the past decades, the prevalence of autoimmune diseases has risen, with recent estimations reporting that these conditions can impact up to 10% of individuals at some point in their life, highlighting the unmet need for a safe, effective and long-lasting treatment regime (Lerner et al., 2015). Current immunotherapies use **non-specific immunotherapeutic drugs** that cause systemic immunosuppression and have both short- and long-term adverse effects by rendering the patient susceptible to infections and cancer. Furthermore, these drugs fail to resolve the underlying cause of the immunopathology and the breach in tolerance to self-antigens. Novel approaches in antigen-specific immunotherapy aim to **reinstate the state of immune tolerance to self-antigens** exclusively in the autoreactive cells that are responsible for the disease progression, while leaving the rest of the immune cells intact and capable of fighting infectious agents and tumour cells. In that way, the function of disease-causing cells would be targeted specifically to become disease-regulating, without compromising the entirety of the immune system (Wraith, 2016).

### 1.7.1 Platforms used for immunotherapy – the importance of peptide immunotherapy

There are currently several different approaches used for immunotherapies based on four central themes: i) targeting the DC:T cell interaction and generating tolerogenic DCs using immunosuppressive agents, ii) administrating self-antigens with peptide MHC

II nanoparticles (pMHC-NP), iii) delivering peptide conjugated erythrocytes iv) administrating self-antigen derived T cell epitopes optimised for solubility and MHC binding, injected directly without carrier or adjuvant (Fig. 1.7) (Wraith, 2018).

#### *1.7.1.1 Autologous tolerogenic DCs*

Previous studies have shown that it is possible to modify autoimmune phenomena *in vivo* by targeting autoantigens to tolerogenic DCs or by the simultaneous delivery of autoantigens with drugs designed to sustain the immature phenotype of DCs *in vivo* (Bell et al., 2017; Martin et al., 2007; Benham et al., 2015). Immature steady-state DCs (ssDCs) are tolerogenic since they have low expression of MHC II and low levels of the co-stimulatory molecules CD80, CD86, CD40, which are upregulated upon encounter with inflammatory signals via PAMPs. If antigens are presented by ssDCs, T cells are not sufficiently stimulated and either die by apoptosis or divert into an anergic or a regulatory phenotype (Perona-Wright et al., 2007).

Several groups have developed methods to generate monocyte-derived DC populations (moDC), which can be treated with vitamin D3 or rapamycin to enhance their capacity for tolerance induction. Normally, tolerogenic DCs are pre-loaded with antigen prior to re-infusion to direct their function towards specific antigens. In recent studies for the treatment of RA, tolerogenic DCs were induced either by using dexamethasone, vitamin D3 and monophosphoryl lipid A or by inhibiting the NF-κB pathway. In the first case, the resulting cells were anergic and capable of suppressing T cell proliferation and production of pro-inflammatory cytokines such as IFN-γ and IL-17 (Harry et al., 2010). In the second case, DCs were treated with NF-κB inhibitor, Bay11-7082, and subsequently suppressed RA in an antigen-specific manner in mice (Martin et al., 2007). Notably, these treatments rendered tolerogenic DCs incapable of responding to any

inflammatory signals *in vitro*, indicating that the effect of the treatment was not readily reversible and that the tolerogenic phenotype was well established.

#### *1.7.1.2 Peptide MHC II – Nanoparticles (pMHC-NP)*

This approach utilises a system where nanoparticles are coated with MHC class II and antigenic peptide creating an artificial APC (Clemente-Casares et al., 2016). The principle behind this system is very similar to the peptide immunotherapy protocol (see section 1.5.2 about IL-10$^{+}$FoxP3$^{-}$ Tr1 cells) as they both establish immune tolerance by the induction of IL-10-producing CD4$^{+}$ T cells through a negative feedback mechanism (Gabrysova et al., 2009; Gabryšová and Wraith, 2010; Metzler and Wraith, 1993). However, with this approach the generated Tr1 cells not only express IL-10 and co-inhibitory molecules, but also express low levels of pro-inflammatory cytokines such as TNF-α, IL-5 and GM-CSF (Singha et al., 2017). In two recent studies, it was demonstrated that the administration of these nanoparticles to the liver can reinstate immune tolerance towards liver autoantigens and interestingly, mediate a strong bystander suppression effect between distinct liver autoantigens (Umeshappa et al., 2019, 2020).

However, it should be noted that MHC-Ag bearing nanoparticles will suppress only ongoing autoimmune diseases, but will not serve as a prophylactic measure to prevent disease onset, since they are not able to interact with naïve T cells, which require at least low levels of co-stimulatory signals.

#### *1.7.1.3 Peptide conjugated erythrocytes*

It has been shown that red blood cells (RBC) that are pre-coated with tolerogenic peptides bind macrophages in the spleen and Kupffer cells (KC) in the liver, to induce the

expansion of FoxP3$^{+}$ Treg cells (Grimm et al., 2015; Carambia et al., 2015). RBC and larger liposomes that target the liver as a site for tolerance induction utilise the ability of this organ to establish and maintain a tolerogenic environment despite the constant supply of antigens deriving from the blood or gut that even though innocuous, they could potentially initiate an undesired immune response. Furthermore, KC can also induce localised tolerance since they were the predominant population within the liver to internalise labelled particles and promoted the expansion of OVA-specific FoxP3$^{+}$ Tregs *in vivo* as shown by tracking OVA-loaded liposomes using intravital microscopy (Heymann et al., 2015).

#### *1.7.1.4 Soluble peptides/Apitopes*

Previous work from the Wraith group has shed light in some of the mechanisms of peptide immunotherapy using the Tg4 mouse model, in which approximately 95% of CD4$^{+}$ T cells are specific to the immunodominant peptide of myelin basic protein $MBP_{Ac1-9}$ (Liu et al., 1995). The dose escalation regime that was developed, in which increasing doses of the high affinity $MBP_{Ac1-9}$ [4Y] were administered in saline via a tolerogenic route over the course of 4 weeks was able to induce IL-10-producing Tr1 cells *in vivo*, which in turn were able to orchestrate IL-10-dependant negative feedback pathways that ameliorated EAE pathology driven by MBP (Liu and Wraith, 1995; Sundstedt et al., 2003; Gabrysova et al., 2009; Burkhart et al., 1999; Nicolson et al., 2006). The gradual increase in the antigen concentration is a prerequisite that ensures both the safety and efficacy of peptide immunotherapy, and it circumvents adverse events (i.e., cytokine storm) that could potentially occur with direct administration of high dose and affinity antigen (Sabatos-Peyton et al., 2010; Gabryšová and Wraith, 2010).

ASI may form the basis of future therapies in autoimmune disease because it has proven efficacious in disease progression as evidenced by induction of long term remission in two clinical trials (Streeter et al., 2015; Chataway et al., 2018). A better understanding of the mechanistic basis for the use of tolerogenic peptides for the generation of Tr1 cells *in vivo* as well as their functional and phenotypic properties of these cells will be of great benefit for the treatment of human autoimmune conditions. From a logistical point of view, short peptides can be manufactured in a standardised manner with low production costs and are relatively stable in a lyophilised form at room temperature (Moldaver and Larché, 2011). Also, cost of production of peptide-based therapies is low since mass production of high purity product is achievable making this approach the most straightforward and inexpensive for the treatment of autoimmune diseases.

The challenge with each one of these approaches will be to find the optimal dose and route of administration for treating patients in a safe and effective manner. As these options progress towards clinical trials, it is vital that their mechanisms of action are thoroughly investigated so that affected individuals can benefit fully from antigen-specific immunotherapy for autoimmune disease. At this time, only the soluble peptide approach has undergone extensive clinical testing in the field of allergy (Campbell et al., 2009; Ellis et al., 2017), hypersensitivity (Goel et al., 2017), and autoimmunity, both in T1D (Thrower et al., 2009; Ali et al., 2017) and MS (Walczak et al., 2013) and this, the most simple and straightforward of the approaches described, has proven safe and well tolerated.

In particular, for the treatment of MS, a phase I clinical trial with ATX-MS-1467, a cocktail of 4 MBP epitopes, showed that this treatment is safe and well-tolerated in a

group of 6 patients with secondary progressive MS (Streeter et al., 2015). The same treatment regime was used in patients with relapsing MS in a phase II clinical trial that assessed the efficacy by evaluating MRI parameters and clinical variables. In this study, the T1 gadolinium enhancing lesions that are associated with active inflammation in MS were significantly reduced in 37 participants upon treatment compared to baseline and remained reduced until the completion of the study. Interestingly, a longer dose escalation treatment had a more favourable effect on efficacy, since it provided long-lasting protection during off-treatment follow-up (Chataway et al., 2018). The data from these studies demonstrate that the treatment with increasing doses of MBP epitopes (dose escalation) is safe, well-tolerated and effective, and further trials are warranted.

Furthermore, it was shown that treatment of HLA-DR transgenic mice with epitopes of the thyrotropin receptor (TSHR) was sufficient to suppress both the T cell and antibody response to TSHR that can lead to the development of Graves' disease (GD); therefore, this study provided the rationale for using antigen-specific immunotherapy for treatment of GD (Jansson et al., 2018). In a phase I clinical trial for GD, 12 participants with previously untreated mild to moderate Graves' hyperthyroidism were administered intradermally with ATX-GD-59, a combination of two TSHR peptides over an 18-week period. Results from this study showed that this treatment was safe and well-tolerated, with improvement in free thyroid hormones in 70% of the participants suggesting the potential efficacy of this approach (Pearce et al., 2019). Taken together, the clinical trials in both MS and GD provide evidence on the clinical relevance and application of peptide immunotherapy for the treatment of autoimmunity.

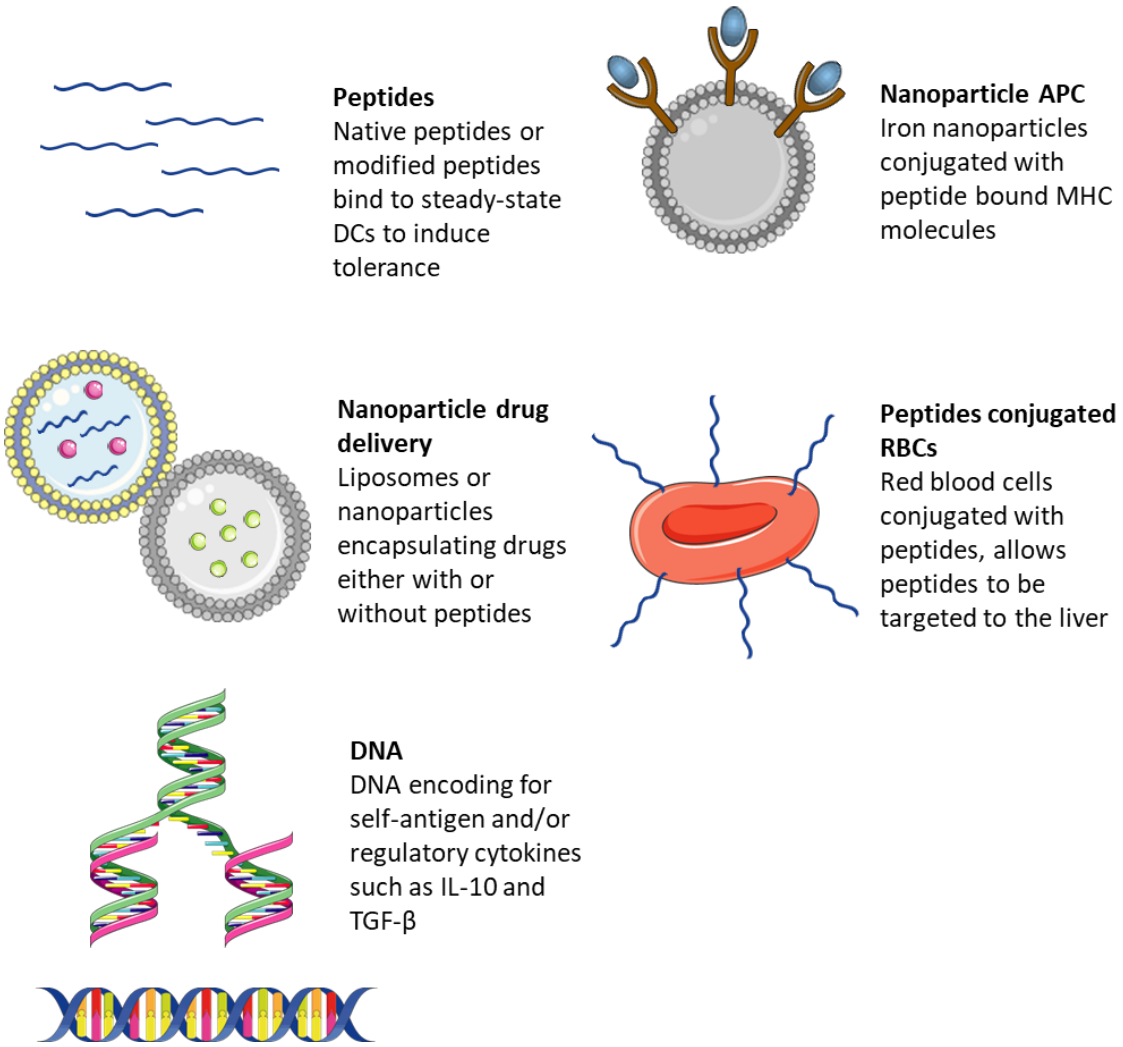



**Figure 1.7 Summary of antigen-specific immunotherapy approaches in preclinical/clinical development.** Antigen-specific immunotherapies can vary from the simple administration of soluble peptides that bind ssDCs to more complex approaches that utilise carrier systems to ensure antigen delivery to the target tissue. A brief description of each one of the current approaches is presented with their main principles.

## 1.8 Bystander suppression: proposed mechanisms and relevance to peptide immunotherapy

The complex and multifactorial nature of autoimmune diseases makes the identification of disease-initiating autoantigens a significant challenge especially if we consider the high degree of variability among the immune responses of patients and at different stages throughout the course of disease progression (Mazza et al., 2002; Ponsford et al., 2001). For example, for diseases like Graves' disease, the target antigen is well-defined. However, for most autoimmune diseases it is not fully understood which antigen is targeted by the immune system to initiate the disease. For many others, antibodies specific for self-antigens are associated with disease, but it's not clear whether they play a role in immune pathology.

Furthermore, the phenomenon of **epitope spreading**, where the initial immune response towards the dominant epitope is extended to secondary epitopes over the time, adds another layer of complexity (Chan et al., 1998). Despite these obstacles, a series of studies for different autoimmune disease has led to the design of clinical trials, where peptides were tested for the treatment of MS, T1D, SLE and Graves' disease (Ali et al., 2017; Chataway et al., 2018; Pearce et al., 2019; Zimmer et al., 2013).

The outstanding question that arises is how we can tolerise T cells against all (known and unknown) epitopes involved in disease progression. The answer may lie in the induction of **linked** or **bystander** suppression. In particular, if the autoantigen that is initiating the autoimmune response is not well-defined or when the disease is triggered by multiple autoantigens, it is possible to modulate the course of the response by targeting only one antigen if it is found withing close physical proximity via linked or bystander

suppression. Linked and bystander suppression were two terms first coined 30 years ago by Miller and colleagues during their studies of oral tolerance induction and initially they were used interchangeably to describe the same phenomenon (Miller et al., 1992). However, there are some fine differences between the two types, because linked suppression refers to the phenomenon where antigen-specific T cells towards antigen A can dampen immune responses against antigen B by either inhibiting APCs or adjacent T cells if both antigens are presented on the surface of the same APC, while in bystander suppression, antigens can be presented on different APCs. Both linked (Hoyne et al., 1993, 1999) and bystander suppression (Anderton and Wraith, 1998) have been reported to be outcomes of ASI in allergic and autoimmune settings.

The processes by which this antigen-independent type of suppression occurs remain largely obscure, however it has been shown to play a role in murine models of peptide tolerance seen in EAE and allergic contexts (Anderton and Wraith, 1998; Miller et al., 1991). Anderton and colleagues have demonstrated that there is a certain degree of hierarchy in terms of tolerogenicity between three encephalitogenic peptides that were associated with EAE and derived from myelin, $MBP_{Ac1-9}$, $MBP_{89-101}$ and proteolipid protein $PLP_{139-151}$. These three myelin epitopes showed differential abilities to induce antigen-specific tolerance as well as bystander suppression to multiple antigens. Administration of $MBP_{Ac1-9}$ could induce tolerance in $MBP_{Ac1-9}$-specific T cells and to $MBP_{89-101}$-specific T cells, hence demonstrating linked suppression (Anderton et al., 2002).

Conversely, tolerisation with $PLP_{139-151}$ peptide could control T cell-mediated immune responses both towards $PLP_{139-151}$, and also towards $MBP_{89-101}$ and $MBP_{Ac1-9}$ due to the bystander effect. Tolerance to $PLP_{139-151}$ peptide could be extended to include the

MBP epitopes, only if the $PLP_{139-151}$-treated mice were immunised with the whole MBP antigen, rather than the separate MBP epitopes. This requirement implies that the antigenic epitopes of MBP need to be presented within the draining lymph node simultaneously as the tolerogenic PLP peptide for the bystander suppression to take place.

Similarly, another study showed that Treg-derived TGF-β can prevent EAE both when disease is initiated via MBP or PLP, indicating a bystander regulation of multiple antigen specificities in complex disease (Chen et al., 1994). This phenomenon is also seen in the field of allergy, and in particular cat allergy, where tolerance induction using 12 Fel d1 peptides not only suppressed patient responses to these 12 peptides, but also to peptides that were not included in the tolerogenic mixture (Campbell et al., 2009).

Antigen-specific immunotherapies based on single antigen specificities are not very promising when it comes to tackling complex and dynamic multi-antigen diseases such as type I diabetes (T1D) and rheumatoid arthritis (RA), unless they are able to mediate a strong bystander effect that will be able to control pathogenic T cells of various antigen specificities. At present, we know little about the mechanism of action (MoA) of novel ASI approaches that are being tested in clinical trials. There is a pressing need to define the optimal conditions for induction of tolerance, defining the means of establishing efficient desensitisation and duration of the disease suppression while also elucidating the molecular basis of effective immunotherapies. Therefore, understanding the MoA of bystander suppression and how to incorporate it into current peptide immunotherapies in the most effective way will open new avenues of treatment of autoimmune disease without the need to target a specific antigen.

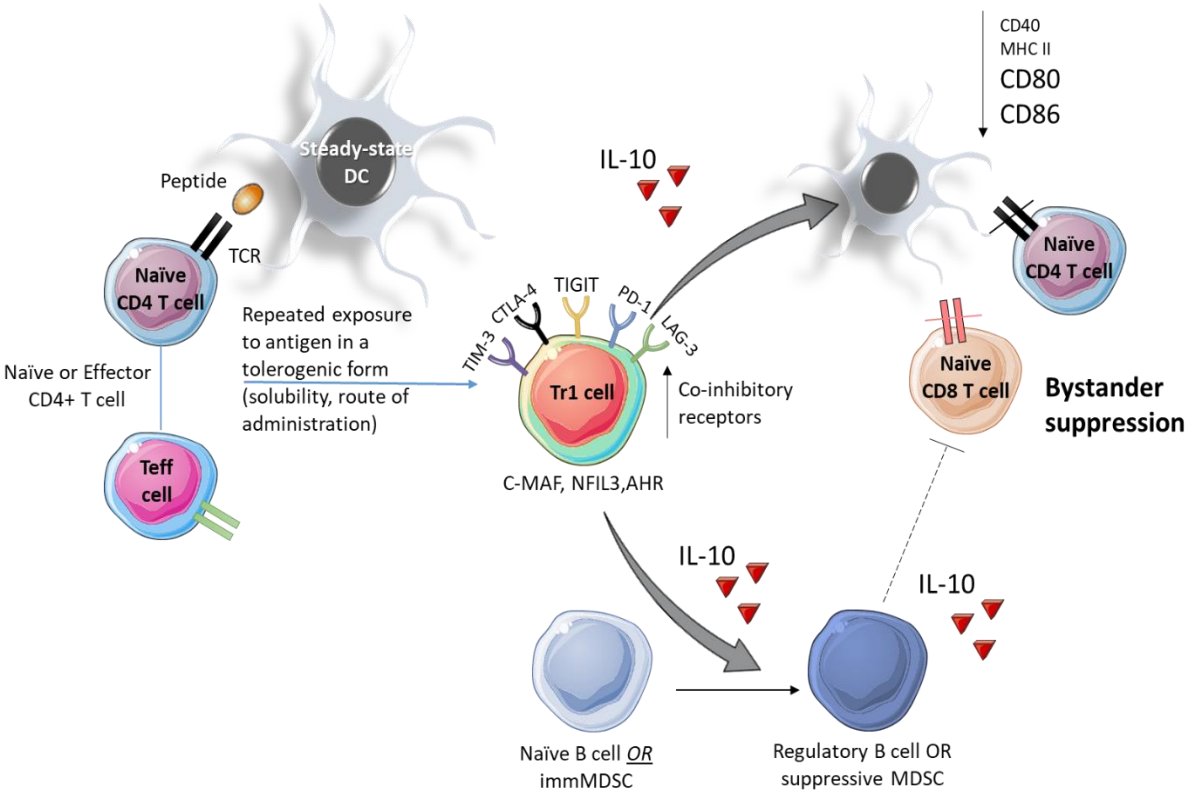



**Figure 1.8 Mechanism of action of peptide immunotherapy using soluble peptides.** Repeated doses of soluble peptides representing T cell epitopes can bind directly to MHC class II molecules on steady-state dendritic cells (ssDCs). These ssDCs are unable to properly prime and activate antigen-specific T cells, resulting in T cell anergy and conversion to IL-10$^{+}$ FoxP3$^{-}$ Tr1 cells. These tolerised Tr1 cells are no longer able to respond to the target antigen and are able to suppress the expression of co-stimulatory molecules and exert bystander or linked regulatory effects on neighbouring DCs or effector T cells to downregulate immune responses in a non-antigen specific manner. Myeloid-derived suppressor cells (MDSCs) are also generated in large numbers as a result of peptide immunotherapy, and IL-10$^{+}$ Bregs have been reported.

## 1.9 Thesis aims

To be able to successfully design tolerogenic peptides that have the ability to ameliorate autoimmune diseases, a thorough understanding of T cell responses towards autoantigens is required. Previous studies by the Wraith group have shown that T cell epitopes delivered as highly soluble peptides can induce antigen specific tolerance by giving rise to IL-10-producing Tr1 cells. The analysis after each consecutive dose of peptide treatment using a Tg4 IL-10 GFP-reporter mouse revealed a positive correlation between inhibitory molecules, including TIGIT and IL-10, as 50% of $TIGIT^+$ cells expressed IL-10 (Burton et al., 2014b). This observation indicates that TIGIT could be a useful surrogate marker for these antigen specific Tr1 cells and potentially exert a functional role on these cells and other regulatory T cells.

Chapter 3 investigates the role of TIGIT both in the regulation of central tolerance by looking at its impact on thymic Tregs and at its involvement in the maintenance of peripheral tolerance. For the latter, TIGIT was examined in the context of its ability to interfere with the generation and function of different regulatory populations (iTregs, Tr1 cells, effector Tregs) as well as their potential impact on the maturation of dendritic cells.

The identification of autoantigens involved in autoimmune diseases can be challenging, particularly in complex inflammatory diseases, where multiple antigens, potentially unknown, are involved. Multi-antigen suppression has been observed in various animal models and has also been inferred in clinical applications of antigen-specific immunotherapy, whereby tolerance induction to a single epitope/antigen, can offer broader protection. Chapter 4 introduces a system that allows the study of the mechanisms of bystander suppression both *in vitro* and *in vivo*. Antigen-specific immunotherapy gives rise to both $FoxP3^+$ Tregs and $FoxP3^-$ Tr1 cells that are involved in

different aspects of tolerance induction. However, little is known about which cell population is the most potent mediator of bystander suppression, their functional differences as well as the underlying mechanism of action; the work presented here aims to delineate that. Furthermore, this chapter aims to address the hypothesis that peptide immunotherapy not only equips *in vivo*-induced Tr1 cells and Tregs with tolerogenic properties, but also has an impact on dendritic cells, potentially rendering them tolerogenic. Finally, adoptive transfer experiments aimed to reproduce some of the *in vitro* findings in an *in vivo* model of bystander suppression to investigate their physiological relevance and the future application in a clinical setting.

Finally, chapter 5 addresses the question of how peptide immunotherapy leads to a switch from a non-suppressive to a highly suppressive phenotype among $Foxp3^+$ Treg cells. By utilising RNA sequencing techniques, differentially expressed genes were identified and molecular pathways associated with the switch in regulatory T cell function were revealed.

# CHAPTER 2: MATERIALS & METHODS

## 2.1 Experimental animals

Mice used for this thesis were housed under specific pathogen-free (SPF) conditions at the Biomedical Services Unit (BMSU) at the University of Birmingham and all the experiments were carried out in accordance with Home Office guidelines and followed the Animals (scientific Procedures) Act 1986. Mice were housed with sawdust and shredded paper as bedding, with standard laboratory mouse chow and water available *ad libitum*. All breeding, maintenance and procedures were conducted under specific regulations as stated by the Home Office Personal and in accordance with the UK Home Office Project Licence held by Professor David Wraith (P17E7ABFB). For experimental purposes, all mice were sacrificed and culled under Schedule 1 procedure, cervical dislocation. Male and female mice were used, aged between 8-12 weeks. No formal randomisation was undertaken; but wherever possible, mice were equally distributed between groups, based on age and sex.

### 2.1.1 Tg4 mice

The generation of the Tg4 mouse strain has been previously described (Liu et al., 1995). These mice, extensively backcrossed onto the B10.PL (H-2 $A^u$) background, express the αβ TCR (Vα4, Vβ8.2) of the MBP Ac1-9 specific hybridoma 1934.4, which was derived from an encephalitogenic T cell clone. TCR alpha and beta transgenic constructs were generated by inserting cDNA containing the leader and coding sequences into the human CD2 minigene. RNA splice sites and a polyA signal sequence were introduced by ligating a genomic segment of the human beta globin gene 3' to the TCR sequence. The final constructs were injected into (CBA x B10) F2 fertilized eggs and founder mice backcrossed onto the B10.PL background. The TCR transgene expression, MHC-II haplotype, T and B cell sufficiency was assessed by flow cytometric analysis of

Vβ8.2, CD4, CD19, $A^u$ levels in the peripheral blood. Approximately 95% of $CD4^+$ cells found in the Tg4 mouse are specific for the immunodominant epitope of MBP (4K peptide), therefore it serves as a model to study antigen specific $CD4^+$ T cell responses.

### 2.1.2 Tg4.TIGIT Crispr knockout mice

Using this parental Tg4 strain, a TIGIT knock out mouse was generated with the CRISPR-Cas9 technology. Mutation of the TIGIT gene was carried out using 2 guide RNAs for either end of exon 2 generated by NHEJ method (Sharma and Raghavan, 2016): guide RNA **#407**: HA10355407_MM0000134136_Tigit crRNA_Ex2_oligo#8024098841-100004 (sequence AGGCACGAUAGAUACAAAGGUUUUAGAGCUAUGCUGUUUUG) and guide RNA **#408**: HA10355408_MM0000134139_Tigit crRNA_Ex2_oligo#8024098841-100005 (CCUAUCAUACGUAUCCUGGGUUUUAGAGCUAUGCUGUUUUG) (Sigma), tracrRNA TRACRRNA05N (Sigma) and Cas9 (EnGen Cas9 NLS, NEB) by microinjection into pronucleus of single cell fertilised Tg4 mouse embryos at 0.5 days post coitum). This generated an 8bp deletion in the Crispr1 site of exon 2 of the TIGIT gene. The Crispr2 site at the 3' end of exon 2 did not show any base changes.

**Tg4/Tigit_LN7/8b**

TIGIT intron 1-2, Exon 2, intron 2-3: **F primer/ TIGIT Ex 2/ R primer G->C/** Crispr sites 1 & 2

**Tg4 wildtype sequence**

**-> F primer**

**GAGTCCATGG GAAAGGGACC** ATGGCTGGGG CTTCAGGCCT CGAGTGACAG GCAGAGGAAG AAAAACTCTG 70

GAAATCAATG ATGGTCTCTA TGGGGGGCAC CAGGAGAGAC TGCAGACTGT GGACATCTGT TCCTAGAGCC 140 AGATCTGGAC TCTGAACCCT CTGGGATTCT TCAGGAAGGT TGAAGGGCAG CTGCTGGCCA GAGACTCACG 210

**->Ex 2 Crispr1**

TGTGCTTTTC CCTCAC**CCAT AGGAGCCACA GCAGGCACGA TAGATACAAA GAGGAACATC TCTGCAGAGG** 280 **AAGGTGGCTC TGTCATCTTA CAGTGTCACT TCTCCTCTGA CACAGCTGAA GTGACCCAAG TCGACTGGAA** 350 **GCAGCAGGAC CAGCTTCTGG CCATTTATAG TGTTGACCTG GGGTGGCATG TCGCTTCAGT CTTCAGTGAT** 420 **CGGGTGGTCC CAGGCCCCAG CCTAGGCCTC ACCTTCCAGT CTCTGACAAT GAATGACACG GGAGAGTACT** 490

**Crispr2**

**TCTGTACCTA TCATACGTAT CCTGGTGGGA TTTACAAGGG GAGAATATTC CTGAAGGTCC AAGAAAGCTC** 560

**<- Ex 2**

**AG**GTAT**GTCC TTTGAGGCAA GGTGGT** 586

**<- R primer**

**Tg4/Tigit_LN7/8b**

**-> F primer**

**GAGTCCATGG GAAAGGGACC** ATGGCTGGGG CTTCAGGCCT CGAGTGACAG GCAGAGGAAG AAAAACTCTG 70

GAAATCAATG ATGGTCTCTA TGGGGGGCAC CAGGAGAGAC TGCAGACTGT GGACATCTGT TCCTAGAGCC 140 AGATCTGGAC TCTGAACCCT CTGGGATTCT TCAGGAAGGT TGAAGGGCAG CTGCTGGCCA GAGACTCACG 210

->Ex 2 Crispr1 -8bp del

TGTGCTTTTC CCTCACCCAT AGGAGCCACA GCAGGCACGA TAGA------ --GGAACATC TCTGCAGAGG 280 AAGGTGGCTC TGTCATCTTA CAGTGTCACT TCTCCTCTGA CACAGCTGAA GTGACCCAAG TCGACTGGAA 350 GCAGCAGGAC CAGCTTCTGG CCATTTATAG TGTTGACCTG GGGTGGCATG TCGCTTCAGT CTTCAGTGAT 420 CGGGTGGTCC CAGGCCCCAG CCTAGGCCTC ACCTTCCAGT CTCTGACAAT GAATGACACG GGAGAGTACT 490

Crispr2

TCTGTACCTA TCATACGTAT CCTGGTGGGA TTTACAAGGG GAGAATATTC CTGAAGGTCC AAGAAAGCTC 560

<- Ex 2

AGGTATGTCC TTTGAGGCAA GGTGGT 586

<- R primer

Changes in DNA bases following manipulation with CRISPR -Cas9 method were identified initially by DNA sequencing of an ear notch sample of tissue on an ABI 3730 sequencer (Functional Genomic Laboratory, University of Birmingham) using the primers:

**Forward: 5'** GAGTCCATGGGAAAGGGACC 3'

**Reverse: 5'** ACCACCTTGCCTCAAAGGAC 3'

Following identification of an 8bp deletion in Exon 2 of the TIGIT gene, a small sample of whole blood was stimulated with aCD3/aCD28 for 24h, then expression of TIGIT was measured by staining with anti-TIGIT-APC and evaluated by flow cytometry. Absence of TIGIT expression correlated with the presence of the 8bp deletion site. Once lines became established, some mice were culled, spleens removed and stimulated with 4K MBP peptide for 72h before staining with anti-TIGIT-APC to confirm the absence of TIGIT expression in the KO line. No TIGIT expression was observed in mice that were homozygous for the 8bp deletion in the TIGIT gene.

A bespoke PCR method developed by Transnetyx Inc to identify homozygote or heterozygote mice containing the 8bp deletion site within Exon 2 was implemented to maintain the TIGIT knock out gene breeding line. Generation, identification, and breeding of the TIGIT KO (Tg4/Tigit_LN7/8b) colonies were performed by Dr. Heather Streeter (Wraith lab), Dr. Sky Ng (Wraith lab) and Andrea Bacon (Biomedical Services Unit-BMSU).

For the purposes of genotyping, DNA was extracted from the ear notches of the different mouse strains. For the DNA extraction, the DNeasy Blood and tissue kit was used (Qiagen, Cat No 69504 and 69506) according to the manufacturer's instructions. Briefly, in each eppendorf tube containing animal tissue, 180µl Buffer ATL and 20µl proteinase K were added. The samples were vortexed thoroughly and left overnight at 56$^{o}$C for complete lysis. The following day, samples were vortexed again both before adding 200µl Buffer AL and before adding 200µl absolute (100%) ethanol. The mixture was then transferred into a DNeasy Mini spin column placed in a 2ml collection tube and spun at 6000g for 1 minute. Subsequently, the addition of 500µl of Buffer AW1 was

followed by a centrifugation step at 6000g for 1 minute, before transferring the spin column to a new 2ml micro centrifuge tube. Similarly, the columns were transferred into a new collection tube; 500µl of Buffer AW2 was added, followed by a centrifugation at 6000g for 1 minute. The final step of DNA elution was done by adding 200µl Buffer AE to the centre of the spin column membrane. The columns were left for 1 minute at room temperature to allow sufficient time for the membrane to soak and increase binding efficiency. Finally, samples were spun at 17000g for 4 minutes and kept at 4$^{o}$C until use.

The extracted DNA was amplified via Polymerase Chain Reaction (PCR) (Table 2.1). The PCR products had to be further cleaned and amplified in order to be sent for sequencing. More specifically, the micro clean protocol required the loading of 2.4µl of PCR products to a 96 well plate with 2.4µl of micro clean solution. Each PCR product occupied two wells for separate forward and reverse reactions. The plate was covered with an adhesive film lid and spun at 4000rpm for 40 minutes at room temperature. The plate was then inverted on a paper towel and spun at lowest speed (500rpm) for 30 seconds at room temperature, in order to get rid of the residual liquid. Following the micro clean, 10µl sequencing reaction mix was added to each well (for both the forward and the reverse reactions) (Table 2.2). The plate was covered with an adhesive film lid and vortexed to ensure that the reagents were properly mixed. The plate was spun down and ran on a PCR machine.

Once the fragments were amplified by PCR, the sequencing reactions were then cleaned with two ethanol washes. Firstly, 2µl 0.125M EDTA and 30µl absolute ethanol (100%) were added to each well, the plate was covered with adhesive film and spun at 2000rpm for 2 minutes at room temperature. The film was removed, and the plate was inverted on paper towel and spun at 500rpm for 30 seconds at room temperature. For the

second wash, 30µl of freshly made ethanol (70% made up with PCR grade water) was added to each well, the plate was covered and spun at 2000rpm for 10 minutes at room temperature.

The film was then removed; the plate was inverted on a paper towel and spun at 500rpm for 30 seconds at room temperature. The DNA pellet was left to air dry slightly for 1 minute, so minimal ethanol is present in wells the pellet was resuspended in 10µl formamide. The plate was covered, placed in a PCR machine, and denatured at 94$^{o}$C for 2 minutes and finally placed on ice to snap chill and prevent re-annealing.

| **Reagents** | **Volume** |
|---|---|
| PCR mix (Promega GoTaq HotStart Green Mater Mix M5122) | 12.5µl |
| Primers | 1.5µl |
| Distilled $H_2O$ | 9µl |
| Sample DNA | 2µl |
| Total volume | 25µl per sample |

**Table 2.1 Initial PCR reaction**

| **Reagents** | **Volume** |
|---|---|
| Big dye reaction mix | 0.5µl |
| Big dye sequencing buffer (5X) | 2µl |
| Primers (Forward **or** Reverse, 10pmol/ml) | 0.4µl |
| PCR grade water | 7.1µl |
| Total volume | 10µl per sample |

**Table 2.2 Sequencing reaction**

In addition to sequencing, PCR products were run on an agarose gel to confirm in a crude way that they have the expected size in terms of base pairs. In order to prepare a 2% agarose gel, 2g of agarose powder was added to 100ml of 1X TBE Buffer, mixed in a flask and placed in microwave for 2-3 minutes, until the agarose was fully dissolved. While agarose was still hot and in a liquid form, 10µl Ethidium Bromide was added and agarose was poured into mould with combs and tape on. The agarose was left to solidify for approximately 15 minutes. Once set, the agarose gel was put into the electrophoresis tank containing 1X TBE Buffer, ensuring that the tank was topped up to cover the gel properly. Finally, 10µl of each DNA sample was added to each well alongside a 1kb DNA ladder (Biolabs N32005). The gel was run at 150V for 90 minutes and visualised under UV light.

### 2.1.3 2D2 mice

2D2 TCR ($TCR^{MOG}$) transgenic mice, originally developed in the lab of Vijay Kuchroo (Bettelli et al., 2003), express a myelin oligodendrocyte glycoprotein (MOG)-specific T cell receptor (TCR) and were purchased from the Jackson Laboratory. Transgenic T cells are not deleted or tolerised and are functionally competent. The majority of thymocytes in 2D2 TCR mice express high and intermediate levels of the receptor, indicating efficient positive selection of transgenic T cells. The majority of $CD4^+$ splenocytes express the transgenic TCR (as defined by Valpha3.2 and Vbeta11 expression). For the development of these mice, a myelin oligodendrocyte glycoprotein (MOG) peptide (amino acids 35-55; MEVGWYRSPFSRVVHLYRNGK) was injected into C57BL/6 mice. T lymphocytes from lymph nodes of these immunized mice were isolated and cells expressing the T cell receptor (TCR) combination (Valpha3.2 and Vbeta11) were selected (clone 2D2). The Valpha3.2-Jalpha18 and Vbeta11-DJbeta1.1

sequences of 2D2 TCR were cloned into TCR expression cassettes, and the resulting constructs were injected into the pronuclei of fertilized C57BL/6 oocytes.

Founder mice were bred with C57BL/6J mice for many generations prior to use in experiments. Because the spontaneous disease observed in 2D2 TCR mice is similar in incidence and manifestations to those developed by multiple sclerosis (MS) patients, these mice are useful for the investigation of the role and nature of the MOG-specific, self-reactive T cell repertoire. For the typing of these mice, Vβ11 expression was measured on $CD4^+$ T cells in peripheral blood samples.

### 2.1.4 B10.PL mice

B10.PL mice, on the $A^u$ haplotype background, were originally purchased from the Jackson Laboratory. This strain was routinely phenotyped by flow cytometric analysis of CD4, CD8, Vβ8.2, CD19, $A^u$ levels in peripheral blood samples taken from tail vein bleeds after weaning. B10.PL mice display a normal complement of B and T cells and <30% $CD4^+$ T cells express the Vβ8 transgene.

### 2.1.5 C57BL/6 mice

C57BL/6 mice, on the $A^b$ haplotype background, were acquired from centralised stocks in BMSU, originally obtained from Charles Rivers.

### 2.1.6 (B10.PL x C57BL/6) F1 and (Tg4 x C57BL/6) F1 mice

Both Tg4 and B10.PL mice have the MHC haplotype $A^u$, while C57BL/6 has MHC haplotype $A^b$. Either Tg4 or B10.PL mice were crossed with C57BL/6 mice to give rise to an $A^u$ x $A^b$ heterozygote in the F1 generation, which allows the study of the binding of both MBP and MOG peptides to $A^u$ and $A^b$ MHC type,

respectively. These F1 mice were not typed; however, Tg4 mice were typed prior to crossing to monitor the frequency of Vβ8 on the $CD4^+$ T cells.

## 2.2 Reagents for cell preparations and cell cultures

### 2.2.1 RPMI-1640

Unless stated otherwise, for primary mouse cell culture, complete RPMI-1640 (Sigma-Merck; R0883) was supplemented with 5mM glutamine (Sigma-Merck; G7513), 100U/ml penicillin and 0.2µg/ml streptomycin (Sigma-Merck; P4333), 50mM 2-Mercaptoethanol (Sigma-Merck; M6250), 20nM hydroxyethyla-1-piperazineethanesulfonic acid (HEPES) buffer (1M, pH 7.0-7.6) (Sigma-Merck; H0887) and 5% heat inactivated foetal calf serum (FCS). All media were stored at 4$^o$C until use.

### 2.2.2 Cell isolation and staining buffers

FACS staining buffer: Dulbecco's PBS (Sigma-Merck; D8537) supplemented with 2mM EDTA (Sigma-Merck; 324506) and 2% sterile-filtered, heat-inactivated foetal calf serum (FBS) (ThermoFisher; 10270106), filtered through a 0.2µm filter.

MACS buffer for dendritic cell isolation: Dulbecco's PBS (Sigma-Merck; D8537) supplemented with 0.5% BSA (Sigma-Merck; A9418) and 2mM EDTA (Sigma-Merck; 324506).

EasySep buffer for Treg isolation: Dulbecco's PBS (Sigma-Merck; D8537) supplemented with 2% FBS (ThermoFisher; 10270106) and 1mM EDTA (Sigma-Merck; 324506).

Magnisort buffer for CD4+ T cell isolation: Dulbecco's PBS (Sigma-Merck; D8537) supplemented with 3% FBS (ThermoFisher; 10270106) and 10mM EDTA (Sigma-Merck; 324506).

### 2.2.3 Peptide antigens

Peptide analogues of MBP that were used for *in vitro* and *in vivo* T cell stimulation were synthesized as N-terminal acetylated peptides by fluorenylmethoxycarbonyl chemistry and were >95% pure by HPLC and mass spectrometry (GL Biochem, Shanghai, China), obtained in lyophilized form and stored at 4$^{o}$C until use. Both the native murine acetylated N-terminal peptide Ac1-9 [4K] of MBP (AcASQ***K***RPSQR) and its higher affinity MBP analogue Ac1-9 [4Y] (AcASQ***Y***RPSQR) were reconstituted at 4mg/ml in PBS and subsequently stored at -20$^{o}$C until use. The $MOG_{35-55}$ peptide (MEVGWYRSPFSRVVHLYRNGK) was not N-acetylated and was reconstituted at 4 mg/ml in PBS and stored at -20$^{o}$C with minimal freeze-thaw cycles.

For the initial optimisations, a linked/hybrid peptide$MBP_{Ac1-9}$-HFFK-$MOG_{35-55}$ (AcASQKRPSQRHFFKMEVGWYRSPFSRVVHLYRNGK) was tested, but unless otherwise stated, in the *in vitro* assays described in this thesis, separate peptides of $MBP_{Ac1-9}$ and $MOG_{35-55}$ were used for stimulation.

## 2.3 *In vitro* methods

### 2.3.1 Isolation of mouse splenocytes for analysis

Sacrificed adult mice were dissected within the BMSU facility using scissors and forceps to remove the spleen, which was then placed into 5ml serum-free RPMI-1640 medium and kept on ice. All manipulations with cells were carried out under aseptic conditions using sterile media, reagents, and plastic ware. Mechanical disaggregation was applied using a 2.5ml syringe plunger to get splenocytes suspension. When samples were not being used, tubes containing cells were kept on ice for up to 1 hour.

Splenocytes were filtered using a 40µl cell strainer (Corning cell strainer 40µm Nylon) and spun at 1500rpm for 6 minutes at 4°C. The cell pellet was lysed by adding 1ml Red Blood Cell lysing buffer Hybri-Max (Sigma Aldrich) and incubating at room temperature for 4 minutes to lyse the murine red blood cells. Brief agitation during this time was employed to facilitate the fragmentation and disaggregation of tissue. Once lysed, 9ml of medium was added to neutralise the reaction and splenocytes were spun at 1500rpm for 6 minutes at 4°C. Cell pellet was resuspended in 3.8ml medium and cells were counted using a haemocytometer under a microscope. Unless stated otherwise, cells were cultured at a density of $1.5x10^6$ cells/ml in a flat 96 well-plate for a naïve cell culture.

### 2.3.2 Cell counting using a glass haemocytometer

The glass haemocytometer and coverslip were cleaned with 70% ethanol before use. The coverslip was then moistened and affixed to the haemocytometer. The presence of Newton's refraction rings under the coverslip was indicative of proper adhesion. In order to measure the cell concentration of each culture, 10µl of cell suspension were mixed with 40µl of 0.4% Trypan blue dye (Sigma). With the coverslip already in place, one side of the haemocytometer counting chamber was filled with the cell suspension by placing the tip of the pipette at the notch. The cell number was calculated using the following formula:

$$\text{Total number of cells } (x10^6)/\text{ml} = \frac{Total\ cells\ counted x\ Dilution\ factor\ x\ 10000\ cells/ml}{Number\ of\ squares\ counted}$$

For each assay, the total number of cells required was calculated as follows:

$$\frac{Total\ number\ of\ cells}{Cells\ required\ in\ the\ final\ culture}\ \text{X Volume of resuspended cells} = \text{Volume of cell stock}$$

The volume of cell stock was then topped up with medium to reach the volume of the final cell culture, which was then plated into a well plate. This methodology of cell counting, and plating was followed throughout this study.

### 2.3.3 Live/dead separation

In some cases, live cells had to be recovered from a cell culture for further treatment, i.e., polarised T cells undergoing additional rounds of stimulation. Therefore, the separation between live and dead cells was performed using the Ficoll-Paque$^{TM}$ Premium (Ficoll-Paque Precision 1.084, GE Healthcare). Cells were resuspended in 6ml complete medium and transferred carefully on top of 3ml of Ficoll. Cells were centrifuged at 1800rpm for 35 minutes with no brake at 20$^{o}$C. Live cells that were enriched and found at the medium/Ficoll-Paque interface, were collected by carefully pipetting the cell clamps into a new falcon tube and washed twice in serum-free medium to make sure that there was no residual Ficoll in the culture.

### 2.3.4 Isolation of mouse thymocytes for analysis

To allow for T cell analysis of thymic tissue, cleaned tissue was disaggregated using cut edge frosted end glass slides (Thermo Scientific) to release the cells into a petri-dish containing RPMI-1640 medium. The slides were then washed with RPMI-1640 medium and discarded, leaving cells suspended in medium. The cell suspension was then filtered through a membrane-mesh filter into 15ml Falcon tubes (Corning Centistar RNAse/DNase free) to allow any remaining clamps to be removed prior to analysis. Centrifugation at 1400rpm for 4 minutes at 4$^{o}$C then occurred and supernatants were removed before pellets were resuspended in 2ml media and placed on ice. Cells were counted using a haemocytometer and plated in a 96 round-bottom well-plate at a density of 5x10$^{6}$ cells/well for staining.

### 2.3.5 Cell culture of naïve T cells

Splenocytes from naïve mice were cultured at a density of 1.5 x $10^6$ cells/ml in a 96 well-plate in the presence of a 10-fold titration of MBP Ac1-9 [4K], ranging from 0.1 to 100μg/ml, unless otherwise stated. Different concentrations of the administered peptide were used in order to investigate whether the responses were affected in a dose-dependent manner. Unstimulated splenocytes were used as a control.

### 2.3.6 Th1/Th2-polarised cell culture

Naïve splenocytes were plated in a 24 well-plate at a density of 2 x$10^6$ cells/ml. Cells were incubated for 7 days in humidified incubators at 37$^o$C, 5% $CO_2$ under polarising conditions. For the polarisation towards Th1 or Th2 cell lines, rmIL-12, or rmIL-4 and anti-IFN-γ (Clone XMG-1) were added in complete RPMI medium at a final concentration of 5ng/ml or 10ng/ml and 10ng/ml, respectively (Table 2.3). RhIL-2 was added at 20U/ml on day 3 to both Th1 and Th2 cultures. On day 7, live cells were recovered from the interface of a Ficoll-Paque density gradient (as described in section 2.3.3). Cells were then resuspended in 3ml complete RPMI and plated in a 96 well-plate that was pre-coated for 2 hours at 37$^o$C with aCD3 (1μg/ml diluted in PBS) for a second round of stimulation. Proliferation, cytokine secretion and expression of either surface or intracellular markers were analysed after 24, 48 or 72 hours.

| Recombinant cytokines | Supplier | Final concentration |
|---|---|---|
| Human IL-2 (rhIL-2) | R&D Systems (Abingdon, UK) | 20U/ml |
| Murine IL-12 (rmIL-12) | PeproTech EC Ltd (London, UK) | 5ng/ml |
| Murine IL-4 (rmIL-4) | PeproTech EC Ltd (London, UK) | 10ng/ml |
| Human TGF-β | PeproTech EC Ltd (London, UK) | 10ng/ml |

**Table 2.3 Recombinant cytokines**

### 2.3.7 Generation of iTregs

For the generation of Tregs *in vitro*, naïve bulk splenocytes from Tg4 mice were cultured in a 48-well plate at a density of 1 x $10^6$ cells/ml and polarised with 4K peptide, rhIL-2 (100U/ml), 10ng/ml rhTGF-β in the presence of 10nM of CAL101, a PI3K inhibitor, or DMSO control on day 0. Cultures were supplemented with rhIL-2 (20U/ml) and rhTGF-β (2ng/ml) on day 2 and day 4 and cells were used on day 7 for assessment of FoxP3 expression and downstream *in vitro* experiments.

### 2.3.8 Establishment of a CD4tol primary cell line

Tg4 mice were subjected to repeated doses of PBS or MBP Ac1-9 [4Y] as described under the *in vivo* methods, section 2.5.1. Spleens were isolated 3 days following the last peptide treatment and bulk splenocytes were cultured in complete RPMI medium in the presence of 10μg/ml 4K and 20U/ml rhIL-2 for 7 days (Round I) in 6 well-plates at a cell density of 2 x $10^6$ cells/ml. For the subsequent rounds of stimulation, cells were re-challenged once a week with 10μg/ml 4K. The $A^u$ expressing cell line PL8 was used as a source of antigen-presenting cells (APCs) and cells were cultured in a 24-well plate at a ratio of 1:2 T cells: APCs. PL8 cells were treated with Mitomycin C (Sigma; M4287)

for 40 minutes at 37ºC prior to their addition in culture, as Mitomycin C inhibits the proliferation of cells, while leaving their ability to present antigen intact. The culture was supplemented with rhIL-2 (20U/ml) 3 days after each stimulation with antigen. CD4tol cells were used for further *in vitro* assays at different rounds of stimulation as indicated.

### 2.3.9 Mouse cell isolation from splenocytes

#### *2.3.9.1 Purification of CD4⁺ T cells*

For the isolation of $CD4^+$ T cells, the MagniSort Mouse CD4 T cell enrichment Kit (Invitrogen; 8804-6821) was used according to the manufacturer's instructions. In this negative selection kit, undesired cells were labelled with a cocktail of biotinylated antibodies followed by streptavidin-coated magnetic beads. When cells were placed in the MagniSort Magnet, the undesired cells were held in place by the magnetic field, while the desired cells remained untouched and free in solution and were isolated by decanting.

Briefly, a single-cell suspension of lymphocytes at a concentration of 1 x $10^8$ cells/ml was prepared in MACS buffer and placed in a 5ml FACS tube. 20µl of MagniSort Enrichment Antibody Cocktail was added per 100µl of cells followed by a 10-minute incubation at room temperature. Cells were then washed by adding Magnisort buffer at a final volume of 4ml and spun at 300g for 5 minutes. The supernatant was discarded, the cells were thoroughly resuspended to their original volume with MACS buffer and 20µl of MagniSort Negative Selection Beads was added per 100µl of cells. After a 5-minute incubation at room temperature, MagniSort buffer was added to a final volume of 2.5ml, cells were mixed by pipetting and the tubes were inserted into the magnet and incubated at room temperature for 5 minutes. After the incubation, the supernatant was collected in a 15ml falcon tube, and the procedure was repeated one more time for a total of two

separations. The two fractions of unbound cells were pooled together and used for *in vitro* assays.

#### *2.3.9.2 Purification of CD25⁺ T regulatory cells*

For the isolation of $CD25^+$ T cells, the EasySep™ mouse CD25 Regulatory T cell positive selection kit (StemCell Technologies; 18782) was used according to the manufacturer's instructions. Briefly, a single-cell suspension of lymphocytes at a concentration of 1 x $10^8$ cells/ml was prepared in EasySep buffer and placed in a 5ml FACS tube. 50µl of FcR blocker was added per 1ml of cells and incubated at room temperature for 5 minutes. 50µl of Positive Selection cocktail was added per 1ml of cells and incubated at room temperature for 10 minutes. 20µl of PE Selection Cocktail was added per 1ml of cells and incubated at room temperature for 5 minutes. 20µl of RapidSpheres was added per 1ml of cells and incubated at room temperature for 5 minutes. The sample was then topped up with EasySep buffer to 2.5ml and placed in a magnet for 5 minutes. The supernatant was collected into a new tube ($CD25^-$ fraction) and the beads were resuspended in 2.5ml EasySep buffer for two more rounds of isolation. The isolated $CD25^+$ cells were resuspended in the appropriate medium depending on the downstream experiment.

#### *2.3.9.3 Purification of CD11c⁺ dendritic cells*

For the isolation of $CD11c^+$ dendritic cells (DCs), the CD11c MicroBeads UltraPure kit (Miltenyi Biotec; 130-125-835) was used according to the manufacturer's instructions. Briefly, a single-cell suspension of lymphocytes at a concentration of 1 x $10^8$ cells/ml was prepared in MACS buffer and placed in a 5ml FACS tube. Cells were incubated with TruStain FcX block (BioLegend; 101320) at 1:100 dilution for 10 minutes at 4°C. Cells were then centrifuged at 300g for 5 minutes at 4°C and resuspended in 400µl

MACS buffer. 100µl of CD11c Microbeads UltraPure antibody cocktail was added per $10^8$ total cells and incubated for 10 minutes at 4ºC in the dark.

Cells were washed by adding 10ml of buffer per $10^8$ cells and centrifugation for 5 minutes at 300g (4ºC). Cells were resuspended in 500µl MACS buffer and passed through a LS column that was previously rinsed with 3ml MACS buffer. The column was washed 3 more times with 3ml MACS buffer. The column was then removed from the separator and placed into a new collection tube, 5ml of MACS buffer was pipetted into the column and the magnetically labelled cells were immediately flashed out by firmly pushing the plunger into the column. The isolated $CD11c^+$ cells were resuspended in complete medium for use in downstream *in vitro* experiments.

### 2.3.10 Staining of $CD4^+$ T cells with Cell Trace Violet (CTV)

Purified $CD4^+$ T cells were spun down and washed in PBS. Cells were counted and resuspended at 5 x $10^6$ cells/ml in PBS. 1µl of CTV stain was added per 1ml of cells. The cell suspension was then incubated for 20 minutes in the dark at 37ºC and 5% $CO_2$ (exposure to light was avoided as much as possible). After 20 minutes, a minimum of 5x volume RPMI + 5% FCS was added and cells were incubated for 5 minutes in dark to quench staining. Cells were centrifuged at 300g for 5 minutes and resuspended in complete medium for downstream *in vitro* assays.

### 2.3.11 *In vitro* bystander suppression assays

Splenic $CD4^+$ T cells were isolated from 2D2 mice and stained for Cell Trace Violet (CTV) as described in 2.3.10. To assess how different populations of $MBP_{Ac1-9}$ specific Tg4 regulatory cells could interact with $MOG_{35-55}$ specific 2D2 cells *in vitro*, 1x$10^6$ $MBP_{Ac1-9}$ specific Tg4 $CD4^+$ T cells were co-cultured with 1x$10^6$ $MOG_{35-55}$ specific

2D2 $CD4^+$ CTV-labelled T cells (1:1 ratio) in the presence of $3x10^6$ (B10.PL x C57BL/6) F1 cells that acted as APCs. The number of putative suppressors were reduced by half to have different ratios of responder: suppressors (2:1, 4:1, 8:1, 16:1) and investigate whether the effect was titrating down based on the number of cells added in culture. Cells were stimulated with 100μg/ml $MBP_{Ac1-9}$ [4K] and 100μg/ml $MOG_{35-55}$ for 3 days in a humidified atmosphere at 37ºC, 5% $CO_2$ prior to flow cytometric staining and analysis.

### 2.3.12 T cell: DC co-cultures

To assess how different populations of $MBP_{Ac1-9}$-specific Tg4 regulatory cells could affect the maturation and phenotype of naïve $CD11c^+$ dendritic cells (DCs), $1x10^5$ $CD11c^+$ DCs were co-cultured with $1x10^6$ $MBP_{Ac1-9}$-specific Tg4 regulatory cells in complete RPMI + 5% FBS for 24 hours in a humidified atmosphere at 37ºC, 5% $CO_2$ prior to flow cytometric staining and analysis.

### 2.3.13 Transwell assay

To investigate whether cell contact was required in order to observe suppression, 6.5mm transwell inserts (Corning; CC405) were used to separate CD4tol putative suppressor cells from 2D2 responders. CD4tol cells were cultured either within the transwell or in the bottom of the main well in a 24-well plate while CTV-labelled 2D2 $CD4^+$ T cells were cultured in the opposite chamber, either in the bottom of the main well or within the transwell, respectively. (B10.PL x C57BL/6) F1 splenocytes were added in both chambers as antigen-presenting cells and $MBP_{Ac1-9}$ and $MOG_{35-55}$ peptides were added in both chambers at a concentration of 100μg/ml. In that setting, cells were able to exchange soluble factors, but they were separated by a semipermeable membrane. Cells were cultured for 3 days in a humidified atmosphere at 37ºC, 5% $CO_2$ prior to flow cytometric staining and analysis.

### 2.3.14 Neutralisation of IL-10R/CTLA-4 using blocking antibodies

To investigate the role of certain molecules in the suppressive capacity of CD4tol cells, two blocking antibodies were used, one against IL-10R (clone 1B1.3a; 10µg/ml) and the other one against CTLA-4 (Clone UC10-4F10-11, BD Pharmingen; 1µg/ml). Putative suppressors, CTV-stained responders and APCs were incubated in a 48-well plate for 2h at 37ºC with the blocking antibodies, prior to stimulation with cognate antigens. Cells were cultured for 3 days in a humidified atmosphere at 37ºC, 5% $CO_2$ prior to flow cytometric staining and analysis.

### 2.3.15 Assessment of cell proliferation by $^3$H-TdR incorporation

Tritiated thymidine ($^3$H-TdR) incorporation into the DNA was used as a method of measuring the proliferative capacity of $CD4^+$ T cells in response to challenge with $MBP_{Ac1-9}$ [4K]. $CD4^+$ T cells were cultured at $1.5x10^6$ cells/ml in complete RPMI medium and plated out in triplicates in round-bottomed 96 well-plates at 37ºC and 5% $CO_2$ humidified atmosphere. $MBP_{Ac1-9}$ [4K] ranging from 0.1 to 100µg/ml was added to cultures where indicated. After 24h, 48h and 72h, wells were pulsed with 25µl (0.5µCi) $^3$H-TdR (PerkinElmer, Cambridge, UK) for 16 hours prior to freezing at -20ºC. Plates were thawed and harvested onto filter paper (Cox Scientific, Kettering, UK) in ultrapure water using a Combi Cell Harvester (Skatron Molecular Devices, Lier, Norway), where DNA was trapped onto glass fibre mats. Filter papers were air-dried, sealed in sample bags with Beta Plate Scint scintillation fluid (PerkinElmer) and a Microbeta liquid scintillation counter (1450 Microbeta; Wallac) was used to measure the incorporation of tritiated thymidine.

### 2.3.16 Assessment of cytokine secretion by ELISA

The levels of certain cytokines, such as IFN-γ and IL-2 from culture supernatants were measured with the Enzyme-Linked Immunosorbent Assay (ELISA) and specifically for the measurement of IL-10, an ELISA Max$^{TM}$ Deluxe Set Mouse IL-10 kit (BioLegend; 431414) was used according to the manufacturer's instructions. For the measurement of IL-12/IL-23 (p40), an ELISA MaxTM Deluxe Set Mouse IL-12 kit (BioLegend; 431604) was used according to the manufacturer's instructions. Briefly, the capture antibody, the detection antibody and the standard were reconstituted to the recommended concentration in sterile water.

Firstly, the Nunc$^{TM}$ MaxiSorp$^{TM}$ flat-bottom 96-well plates (BioLegend) were coated with 100µl of 2µg/ml capture antibody diluted in 1x coating buffer and incubated overnight at 4$^{o}$C. Plates were then washed three times with wash buffer (0.05% Tween-20 in PBS) and then blocked with 100µl of blocking buffer (1% BSA in PBS) for 1 hour at room temperature to block unspecific binding. Plates were again washed three times with wash buffer prior to the addition of serially diluted standards in duplicates and supernatant test samples in triplicates. To create a standard curve, six 2-fold serial dilutions were performed starting from a top standard of known concentration. Plates were then incubated at room temperature for at least 2 hours before further washing three times with wash buffer. 0.25µg/ml of biotinylated detection antibody was added to each well preceding 1-hour incubation at room temperature. Plates were again washed three times before the addition of Avidin-HRP, diluted 1:1000 in diluent (1% BSA in PBS).

Plates were incubated for 30 minutes at room temperature, then washed five times, soaking for 30 seconds to 1 minute per wash. A TMB substrate solution diluted in phosphate citrate buffer (Sigma) and 30% hydrogen peroxidase (Sigma) was added to

each well and incubated in the dark for 4-30 minutes to allow colour development. In the final step, to stop the reaction, 100µl of $H_2SO_4$ was added to each well. The absorbance was read with a SpectraMax 190 microplate reader at 450nm with wavelength corrections set at 650nm. Cytokine concentrations were quantified using standard curves generated by SoftMaxPro software.

### 2.3.17 Gene expression analysis

#### *2.3.17.1 RNA extraction*

For the extraction of RNA from stimulated T cells, the RNeasy Mini kit was used (Cat No 74104; Qiagen) according to the manufacturer's instructions. Briefly, for the lysis of up to $10x10^6$ cells, 350µl buffer RLT was added to the cell pellet and vortexed thoroughly. To complete the homogenisation of the starting material, the lysate was pipetted into a QIAshredder spin column and centrifuged at full speed (16000g) for 2 min at RT. An equal volume of 70% ethanol was added to the homogenised lysate and mixed well by pipetting and transferring into a RNeasy spin column placed in a 2m collection tube. Sampled were centrifuged for 15 seconds at 8000g and any genomic DNA contamination was eliminated with on-column DNase digestion using a RNase-free DNase set (Cat No 79254; Qiagen). 500µl buffer RPE was added to the RNeasy spin column and sampled were centrifuged for 15 seconds at 8000g. Another wash with 500µl RPE was performed and sampled were spun at 8000g for 2 min to dry the membrane of the column. The RNeasy spin column was transferred into a new 1.5ml collection tube. For the final elution of RNA, 30µl of RNase-free water was added directly into the membrane of the column and sampled were centrifuged for 1 min at 8000g and the quantity of RNA was measured using a Qubit RNA HS Assay kit (Cat No Q32852; Invitrogen). Samples were stored at -80$^o$C until further use.

#### 2.3.17.2 *cDNA synthesis and real-time PCR*

For the synthesis of the first strand of cDNA, the Superscript III first-strand synthesis system for RT-PCR was used (Cat No 18080-051; Invitrogen) according to the manufacturer's instructions. Briefly, up to 5µg total RNA was mixed with 50ng/µl primers (random hexamers) and 10mM dNTP mix and incubated at 65°C for 5 min, then placed on ice for at least 1 min. A cDNA synthesis mix, consisting of 10X RT buffer, 25mM $MgCl_2$, 0.1M DTT, RNaseOUT (40U/µl) and SuperScript III RT (200U/µl) was added into the RNA/primer mixture and incubated for 10 min at 25°C, followed by 50 min at 50°C. The reaction was terminated with a 5 min incubation at 85°C, and the samples were snap chilled on ice for 1 minute. 1µl of RNase H was added to each tube and incubated for 20 min at 37°C, and cDNA was stored at -20°C until use.

The cDNA was diluted with $ddH_20$ (1:150) and added into a master mix of TaqMan Fast Advanced Master Mix (Cat No 4444557; Applied Biosystems) and primer for each target gene examined. The reaction was placed into fast 96-well plates (Cat No 4346907; Applied Biosystems) and put into a thermocycler for 40 cycles. The analysis was done based on ΔΔCT which was normalised with housekeeping gene GAPDH.

### 2.3.18 Flow cytometry

#### 2.3.18.1 *Cell surface antibody staining*

For staining, samples were loaded into a 96 round-bottom well plate (Thermo Scientific). For the staining of splenocytes, $1.5x10^6$ cells were stained, while for thymocytes, $5x10^6$ cells were stained, unless there were fewer to begin with. If this occurred, then the entire sample would be stained. Splenocytes were spun at 2000rpm for 2 minutes at 4°C, while thymocytes were spun at 1400rpm for 2 minutes at 4°C. Surface staining was completed at 4°C in the dark for 25-30 minutes using the antibodies

described in table 2.4. Once staining was completed, cells were washed with FACS buffer twice, the supernatants were flicked off and the cell pellets were resuspended in fresh FACS buffer and transferred into polystyrene 5ml FACS tubes (Falcon) to be run on the LSR Fortessa (BD).

Within staining combinations, it was imperative to include samples as controls within the combination whereby there were fluorescence minus one sample (FMO). All controls were used to set the fluorochrome level for negative staining such that positive populations could then be easily identified as levels of fluorescence above this negative gate.

**Table 2.4: Antibodies used for surface staining**

| **Antibody specificity** | **Clone** | **Fluorochrome** | **Dilution factor** | **Company** |
|---|---|---|---|---|
| CD4 | GK1.5 | AF700 | 1:100 | eBioscience |
| | RM4-5 | BV711 | 1:200 | BioLegend |
| CD8 | 53-6.7 | BV786 | 1:200 | BioLegend |
| CD25 | PC61 | BV650 | 1:800 | BioLegend |
| | | APC | 1:200 | BioLegend |
| | | PE | 1:200 | BioLegend |
| CD69 | H1.2F3 | PerCP Cy5.5 | 1:200 | BioLegend |
| | | PE-Cy7 | 1:200 | BioLegend |
| | | FITC | 1:200 | BioLegend |
| CD62L | MEL-14 | APC | 1:1500 | eBioscience |
| CD44 | IM7 | AF700 | 1:50 | eBioscience |
| Vβ8.2 | F23.1 | PE | 1:200 | BD Pharmingen |
| Vβ11 | KT11 | FITC | 1:200 | BioLegend |
| CD45.1 | A20 | APC | 1:200 | BioLegend |
| CTLA-4 | UC10-4B9 | PE-Cy7 | 1:200 | BioLegend |

| | | | | |
|---|---|---|---|---|
| LAG-3 | C9B7W | PerCP Cy5.5 | 1:200 | BioLegend |
| PD-1 | 29F.1A12 | BV421 | 1:200 | BioLegend |
| | | BV711 | 1:200 | BioLegend |
| TIGIT | 1G9 | PE | 1:200 | BioLegend |
| | | PE-Cy7 | 1:200 | BioLegend |
| TIM-3 | 8B.2C12 | APC | 1:200 | eBioscience |
| | | BV421 | 1:200 | BioLegend |
| CD80 | 16-10A1 | FITC | 1:200 | BioLegend |
| CD86 | GL-1 | BV605 | 1:400 | BioLegend |
| CD40 | 3/23 | PE-Cy7 | 1:200 | BioLegend |
| MHC II | M5.114.15.2 | PE | 1:400 | BioLegend |
| | | AF700 | 1:200 | BioLegend |
| CD11c | N418 | BV786 | 1:200 | BioLegend |
| CD19 | 6D5 | APC | 1:200 | BioLegend |

#### *2.3.18.2 Intracellular Antibody staining*

Intracellular staining was occasionally required additionally after surface staining to identify transcription factors such as FoxP3 or cytokines expressed intracellularly prior to their secretion. All staining for this was maintained in a 96 round-bottom well-plate following the initial surface staining.

For the analysis of FoxP3, a Transcription Factor Staining Buffer Set (eBioscience) was required. For this technique, cells were surface stained and then incubated with the eBioscience Fixation/Permeabilization solution; composed of 1 part fixative concentrate to 3 parts diluent with a volume of 150µl added per sample. FoxP3 staining required that cells were fixed for 40 minutes at 4$^{o}$C. Following this, cells were washed with the permeabilization buffer in the kit which required diluting from the 10x stock provided, to a 1X diluted working solution made with distilled water. This wash

was done twice. The intracellular antibodies were diluted down in 1x permeabilization buffer. Following this, cells were stained for FoxP3 for 25 minutes at 4°C. Cells were washed twice in permeabilization buffer and prior to FACS analysis (LSR Fortessa) of samples, they were ultimately resuspended in FACS buffer.

For the analysis of intracellular cytokines (ICCS), such as IFN-γ, IL-4, IL-10, and IL-2 (Table 2.5), a different treatment was used. Cells were plated in a 96 rounded-bottom well plate at a density of $1x10^6$ cells/well. Cells were spun at 2000 rpm for 2 minutes at 4°C, and stimulated for 3 hours at 37°C with phorbol 12-myristate 13-acetate (PMA), Ionomycin and Golgi stop (BD Bioscience) at 1μg/ml, 500ng/ml and 0.57μl/ml, respectively. After incubation, cells underwent viability and surface staining as described in section 2.3.18.1, after which cells were incubated for 20 minutes at 4°C with Intracellular Fixation buffer (eBioscience) to be fixed. Fixed cells were permeabilized with Permeabilization buffer (eBioscience), diluted to working solution (1X) with distilled water, for 15 minutes at 4°C and stained for intracellular cytokines for 25 minutes at 4°C. Cells were then washed twice with 1X Permeabilization buffer and resuspended in 200μl FACS buffer until analysed on the flow cytometer.

| **Antibody specificity** | **Clone** | **Fluorochrome** | **Dilution** | **Company** |
|---|---|---|---|---|
| IFN-γ | XMG1.2 | PE-Cy7 | 1:500 | eBioscience |
| IL-4 | 11B11 | PE | 1:200 | eBioscience |
| IL-10 | JES5-16E3 | APC | 1:100 | BioLegend |
| IL-2 | JES6-5H4 | BV421 | 1:200 | eBiosciences |
| FoxP3 | FJK-16s | PE-Texas Red | 1:100 | eBioscience |
| BrdU | MoBU-1 | APC | 1:50 | eBioscience |

**Table 2.5: Antibodies used for intracellular staining**

#### 2.3.18.3 *Intracellular Antibody staining for FoxP3 and IL-10*

To stain for both FoxP3 and IL-10 in the same reaction, a slightly different protocol was followed. Cells were stimulated for 4 hours with PMA/Ionomycin, and Golgi stop (containing Monensin) with Brefeldin A were added for the last 3 hours. The cell surface and live/dead staining was performed as described before in section 2.3.18.1, but then cells were fixed and permeabilized for an hour using 100µl per well in a 96 well plate of fixation and permeabilization solution from Cytofix/Cytoperm kit (BD). Cells were spun at 2000rpm for 2min at 4$^{o}$C and incubated with 1X Permeabilization Buffer (eBiosciences) for 30 minutes. Cells were washed twice with 1X Permeabilization Buffer and stained overnight for FoxP3 and IL-10. The following day, cells were washed twice in 1X Permeabilization Buffer and finally, resuspended in 200µl FACS buffer until analysed.

#### 2.3.18.4 *Flow cytometric analysis*

All samples that were stained with antibody were ready to be run on the Fortessa. The LSR Fortessa (BD) was used for all flow cytometric analysis. The machine used the BD FACSDiva$^{TM}$ software (BD Biosciences) and FlowJo 8.7.3 was used for data analysis. Because more than one colours were used, there is a need to compensate for the spectral overlap (spillover) between the different fluorophores. For the thymus work, single colour controls were used for compensation, while for analysis of splenocytes compensation beads (OneComp eBeads, Invitrogen) were used instead. In order to distinguish between viable and dead splenocytes, a viability dye eFluor$^{TM}$ 780 (eBiosciences) was used at a ratio of 1:1000. An unlabelled sample was run first to set the voltages and then either single colour controls or compensation beads were run to set the compensation against the other colours in the panel.

## 2.4 *In situ* immunofluorescent staining

Thymi from mice 6-8 weeks of age were frozen in liquid nitrogen immediately after removal. Stored sections were removed from the freezer and allowed to dry at room temperature for 30 minutes before being rehydrated in Phosphate Buffered Saline (PBS, Sigma Aldrich) for 15 minutes. During this time, antibodies were prepared and made up in 1% Bovine Serum Albumin (BSA) diluted in PBS (Sigma Aldrich). Rehydrated sections were then stained with primary antibodies (anti-CD4-biotin 1:200, anti-CD8-AF647 1:200, anti-FoxP3-FITC 1:100). All antibody steps occurred in a humidified chamber at room temperature for 30 minutes. Slides were then washed in a PBS bath for 5 minutes before staining with the secondary antibody mix (Streptavidin-AF555 1:1000, anti-FITC-AF488 1:200). For the final amplification of FoxP3 signal, slides were incubated with anti-Rabbit-AF488 (1:200) antibody for 20 min in the dark. All the above antibodies were purchased from ThermoFisher Scientific.

Following all antibody staining steps, sections were covered with 4',6-diamidino-2-phenylindole (DAPI) which is a nuclear stain and assists with cellular visualisation during immunofluorescence. After another wash in PBS, sections were covered using a coverslip (Sigma Aldrich) and sealed using 1,4 diazabicyclooctane (DABCO) in glycerol pH 7 to support the vital preservation of the 80 fluorochromes. Coverslips were then sealed using clear nail varnish around the edges and once dry, stored at -20°C. Confocal imaging was conducted using the Zeiss 780 Zen microscope. Various magnifications were used (x10, x25).

## 2.5 *In vivo* methods

All *in vivo* procedures were approved by the University of Birmingham ethical review committee and were permitted under Home Office Project License PPL, P17E7ABFB, held by Professor David C. Wraith and Personal License PIL, I8692DBAC, held by Konstantina Petkou.

### 2.5.1 Antigen administration/Dose escalation protocol

All antigen administration was performed subcutaneously (s.c.), using the high affinity $MBP_{Ac1-9}$ [4Y] peptide diluted in PBS. Mice were scruffed and 200µl of diluted peptide was administered to un-anaesthetised mice. Antigen was administered at 3–4-day intervals for a total of 6 treatments following a dose escalation protocol: 0.08µg, 0.8µg, 8µg, 80µg, 80µg, 80µg. Spleens were harvested 3 days after the final peptide dose for further *in vitro* analysis.

### 2.5.2 Bromodeoxyuridine Proliferation analysis

To support the detection of proliferating cells, the technique of Bromodeoxyuridine (BrdU) incorporation was used. For this purpose, 1.5mg BrdU was injected into mice intraperitoneally (i.p.) 1 hour prior to sacrifice. For analysis, tissues were harvested and digested as appropriate for the cell type being analysed. Once in a 96 well plate, cells were surface stained as described in section 2.3.18.1, for the identification of the desired target. Following washing of the cells after primary staining, samples were resuspended in 150µl Fix/Perm Buffer (eBioscience) for 16 hours at 4$^{o}$C. Samples were then washed with 1X Perm Buffer made with distilled water from 10X stock bottle (eBioscience) and resuspended in 100µl of diluted DNase as manufacturer's instructions and kept at 37$^{o}$C for 1 hour. Following two washes with 1X Perm Buffer, cells could then be stained for BrdU, with the antibody being made up in 1X Perm Buffer solution and

incubated at room temperature for 1 hour before being washed twice with 1X Perm Buffer. Finally, cells were resuspended in 200µl FACS Buffer and then run on the LSR Fortessa.

### 2.5.3 Preparation of CFA adjuvant

For the initial optimisations of the adoptive transfer experiments, the efficiency of the antigenic challenge with soluble peptide was compared with the antigenic challenge with peptide in adjuvant. For the preparation of peptide-containing adjuvant, a 1:1 mixture was prepared of Complete Freud's Adjuvant (CFA; Difco; 263810) supplemented with 8mg/ml *Mycobacterium Tuberculosis* H37Ra (MTb; Difco; 231141) and PBS (Sigma-Merck; D8537) containing 1mg/ml peptide. Adjuvant mixture was sonicated for 20 minutes and physically agitated by repeat pipetting using 1ml syringe until emulsified. Adjuvant consistency was checked by releasing a small droplet onto water, the droplet should retain its shape on the surface and show minimal dispersion. 100µg of peptide was delivered to each mouse under anaesthesia by two subcutaneous injections of 50µl adjuvant bilaterally at the flank of the mouse. 3 days following antigenic challenge, mice were sacrificed by cervical dislocation and spleens were collected for *in vitro* analysis.

### 2.5.4 Adoptive cell transfers in Tg4 x C57BL/6 recipients

Splenic $CD4^+$T cells from naïve 2D2 mice were purified by magnetic bead isolation to at least 90% purity. 5 x $10^6$ freshly isolated 2D2 $CD4^+$ T cells were labelled with CTV and were injected into (Tg4 x C57BL/6) F1 recipients that were treated with either PBS or $MBP_{Ac1-9}$ [4Y]. The adoptive cell transfer was done 3 days after the final dose. 24 hours post-cell transfer, recipient mice were challenged with 100µg $MBP_{Ac1-9}$

[4K] and 100µg $MOG_{35-55}$. After 3 days, spleens were harvested, $CD4^+$ T cells were purified and stained for activation markers and analysed by flow cytometry.

### 2.5.5 Adoptive cell co-transfers in B10.PL x C57BL/6 or B10.PL recipients

Splenic $CD4^+$ T cells from PBS or $MBP_{Ac1-9}$ [4Y]-treated Tg4 mice were purified by magnetic bead isolation to at least 90% purity. 5 x $10^6$ freshly isolated Tg4 $CD4^+$ cells were labelled with CTV and co-injected with equal number of either PBS or $MBP_{Ac1-9}$ [4Y]-treated Tg4 $CD4^+$ T cells via the intraperitoneal cavity into B10.PL mice (Tg4 *in vivo* system). Similarly, 5 x $10^6$ freshly isolated 2D2 $CD4^+$ cells were labelled with CTV and co-injected with equal number of either PBS or $MBP_{Ac1-9}$ [4Y]-treated Tg4 $CD4^+$ T cells via the intraperitoneal cavity into B10.PL x C57BL/6 mice (2D2 *in vivo* system). 24 hours post-cell transfer, recipient mice were challenged with 100µg peptide (either $MBP_{Ac1-9}$ [4K] alone (Tg4 system) or $MBP_{Ac1-9}$ [4K] with $MOG_{35-55}$ (2D2 system)) suspended in PBS, unless otherwise stated. After 3 days, spleens were harvested, $CD4^+$ T cells were purified and stained for activation markers and analysed by flow cytometry.

## 2.6 Bioinformatic analysis

### 2.6.1 Bulk RNA sequencing

Samples were prepared from either naive (PBS-treated) animals or treated (4Y-treated) animals. Cells were sorted based on CD4 and CD25 markers creating the following 4 biological groups: i) $CD4^+CD25^+$ 4Y-treated Tregs, ii) $CD4^+CD25^-$ 4Y-treated Tconv, iii) $CD4^+CD25^+$ PBS-treated Tregs and iv) $CD4^+CD25^-$ PBS-treated Tconv. Comparison between naive and treated samples (4Y vs PBS) as well as two different populations that were sorted from the same treatment ($CD25^+$ and $CD25^-$). The pipeline RNA-seek v1.2.1 was used for QC and to obtain RSEM counts for 12 bulk RNA-seq samples. The RSEM counts created by the RNA-seek pipeline were then used as input

for the tool iDEP (Ge et al., 2018) v0.951 for downstream analysis. Differential expression analysis was performed in iDEP with DESeq2 (Love et al., 2014) and visualised with heatmaps and volcano plots.

### 2.6.2 Single-cell RNA sequencing (scRNAseq)

The sample preparation for the scRNAseq experiment was the same as the one described in the previous paragraph 2.6.1. The sequencing of the samples was conducted according to the 10x Genomics Chromium Single Cell 3' workflow, which enables a droplet-based encapsulation of single cells using a gel bead in emulsion (GEM) approach. In this way, each gel bead is labelled with oligonucleotides that consist of a unique barcode, a 10bp unique molecular indices (UMIs), sequencing adapters/primers and an anchored 30bp oligo-dT that allows the tracking of each individual cell within the sample tested.

Despite the robustness of this method, poor-quality cells and technical artifacts can still be present in high-quality runs. Before any downstream analyses can be performed, a quality control (QC) was performed to ensure the integrity of the data. Two indicators were used to measure the integrity of the samples; nFeature_RNA that is the number of genes detected in each cell, and nCount_RNA that is the total number of molecules detected within a cell. Low nFeature_RNA is an indication of a dead/dying cell, and high nCount_RNA and/or nFeature_RNA that there is a doublet/multiplet, instead of the desired single cell per droplet. Cells with high mitochondrial percentages, low nFeature_RNA, and high nFeature_RNA counts were removed with cut-offs specific to each sample. Removing the outliers from these groups removes most of doublets, dead cells, or empty droplets. Hence, filtering is a critical pre-processing step that ensures that there are only viable, single cells in the analysed group. In a way, this step resembles the

initial gating strategy in flow cytometry, where there is a need to gate out dead cells and doublets before analysing the target population of cells.

For the bioinformatics analysis, single-cell RNA-seq samples were demultiplexed with the Cell Ranger (Zheng et al., 2017) v7.0.0 command mkfastq and feature counts generated with the count command using the Cell Ranger reference refdata-gex-mm10-2020-A. The resultant filtered matrix was used for input to Seurat (Hao et al., 2021) v4.1.1 to perform the QC mentioned above on an individual sample level. The filtered samples were integrated and annotated with SingleR (Aran et al., 2019) v1.8.1 using celldex v1.4.0 reference data for mouse to assign cell types. Annotation revealed a small cluster of ILC3 cells that were removed prior to differential expression testing. Differentially expressed genes were analysed using the model MAST (Finak et al., 2015). To be considered for differential expression the gene needed to be present in 10% of the cell for the comparison. The default average log2 fold change filter was set to 0.5.

## 2.7 Statistical analysis

Graphs were generated and analysed using GraphPad Prism software version 8.0 (GraphPad, California, USA) as described in figure legends and text. Grouped data was first assessed for normality prior to application of an appropriate parametric or non-parametric test. Asterisks denote p value significance; *p<0.05, **p<0.01, ***p<0.001, ****p<0.0001. All graphs are presented with error bars representing ±SEM. Appropriate statistical analysis was carried out as indicated for the individual assays. Paired t tests were used when comparing two groups; the corresponding one-way ANOVA was used when comparing three or more groups. Multiple comparison analysis was corrected using Tukey's or Dunnett's post-test as indicated in each figure legend.

# CHAPTER 3:

# THE ROLE OF TIGIT

# IN IMMUNE REGULATION

## 3.1 Introduction

The immune system is regulated by a variety of molecular checkpoints, a major component of which is a large set of co-stimulatory and co-inhibitory receptors that modulate the host response to foreign threats, while avoiding the destruction of host tissue (Peggs et al., 2009; Ward-Kavanagh et al., 2016). Although co-stimulation is critical for triggering the initial response following the engagement of the TCR, inhibitory pathways are equally important for regulating the overall outcome of the immune response. Co-inhibitory receptors are induced by TCR stimulation and co-stimulation and subsequently transduce negative feedback signals to provide a mechanism for ceasing T cell activation.

Either excessive co-stimulation or inadequate co-inhibition may breach peripheral self-tolerance and lead to autoimmune diseases, resulting in deleterious inflammation and destruction of self-tissues mediated by the activation of autoreactive T cells and autoantibodies (Zhang and Vignali, 2016a). It is worth mentioning that both sets of receptors are expressed by all T cell subsets, thus contributing to the net outcome of the immune response. For instance, not only are they expressed on effector T cells, but they are also expressed and have a crucial impact on regulatory T cells (Tregs) that play a critical role in the maintenance of self-tolerance (Lucca and Dominguez-Villar, 2020; Chihara et al., 2018).

In particular, the expression of co-inhibitory receptors on effector T cells ensures the appropriate contraction of effector T cell responses, whereas their expression on Tregs ensures the proper function of Tregs to control effector cells (Joller and Kuchroo, 2017). These receptors play an instrumental role in the functional outcome of T cell activation, effectively by regulating the balance between tolerance and immunity in different settings, such as autoimmunity, cancer, and viral infections (Schnell et al., 2020).

Essentially, the overexpression of these molecules in the tumour microenvironment renders T cells dysfunctional (or so-called ‘exhausted’), and therefore they cannot attack tumours, while the lack of expression as seen in cases of autoimmune diseases indicates the inability of the immune system to maintain the state of tolerance to self-antigens (Fuertes Marraco et al., 2015). Even though co-inhibitory receptors have been studied extensively in the context of cancer biology, with promising results from clinical trials of novel immune checkpoint inhibitors (Qin et al., 2019); however, their role in the control of autoimmune reactions is less understood.

It has been suggested that there is a hierarchical utilization of co-stimulatory and co-inhibitory pathways. In other words, there are ‘first-line’ and ‘second-line’ pathways affecting the overall outcome of a T cell response. CD28 co-stimulation falls under the category of a ‘first-line’ pathway essential for T cell priming, whereas co-inhibitory pathways like those involving CTLA-4 and PD-1 have a dominant ‘first-line’ inhibitory impact on T cell activation. There are also ‘second-line’ pathways, which involve co-inhibitory receptors such as Tim-3, TIGIT and LAG-3, which do not have universal impact on all autoimmune disease all the time. Therefore, their contribution is more tissue-specific and may affect the outcome in a temporary manner as these molecules are activated in a more restricted time window during the priming phase.

It has been proposed in the literature that activation of DP thymocytes induces the expression of CTLA-4, which can counteract, via ligand competition, the CD28-driven cell death of self-reactive cells following the encounter of high dose, but not low dose, specific antigen (Kwon et al., 2004). Furthermore, CD28 signalling is responsible for the induction of FoxP3 expression and differentiation of Tregs from DP cells in the thymus (Tai et al., 2005). Work from our lab using knock out mice, has demonstrated that

the absence of CTLA-4 results in an enhanced CD28-dependent expression of FoxP3 by DP cells in the thymic cortex; that led to increased frequency of self-antigen specific Tregs in the thymus as well as the periphery that provided protection against disease (Verhagen et al., 2009). A few years later, Verhagen and colleagues also demonstrated that CTLA-4 affects not only the thymic selection of FoxP3$^+$ Tregs, but also the generation of T conventional cells, by modulating the TCR repertoire (Verhagen et al., 2013). These studies showed that CTLA-4 has an impact on the generation of both thymic and peripheral Tregs and provided the basis for the hypothesis that other co-inhibitory receptors can also regulate other aspects of central, as well as peripheral tolerance.

TIGIT belongs to the next generation of co-inhibitory receptors and even though it has been studied more extensively in the context of cancer, its role in the regulation of autoimmunity remains obscure. Given that the TIGIT/CD226/CD155 pathway shares a lot of similarities with the well-characterised CTLA-4/CD28/CD80/CD86 pathway, primarily the ligand competition amongst others (described in paragraphs 1.3.1 and 1.3.2 of the Introduction, respectively), we reasoned that TIGIT may be involved in the immune regulation of regulatory T cells both in the thymus and spleen.

This chapter aims to shed light on the role of TIGIT in different regulatory cells both in the thymus and in the periphery. Two different knock-out (KO) strains were generated on the Tg4 background, using the Crispr-Cas9 technology as described in paragraph 2.1.2 from Materials & Methods, in order to test the reproducibility of the data and rule out the possibility of technical artefact or off-target effects from the Crispr-Cas9 method. For the initial experiments and unless stated otherwise, TIGIT KO refers to the Tg4/Tigit_LN7/8b strain, in which an 8bp deletion on exon 2 disrupts the expression of

TIGIT. The second KO strain was generated by a long insertion (Li) at the same site, and it is referred to as Tg4/Tigit_LN6/Li. In both strains, TIGIT is not expressed as evaluated by both sequencing and flow cytometry approaches.

Chapter aims:

- ✓ Characterise the role of TIGIT in **central tolerance** and T cell development in the thymus
- ✓ Investigate the impact of TIGIT in the maintenance of **peripheral tolerance** by examining different regulatory T cells, such as:
    - Total $CD4^+$ T cells from 4Y-treated Tg4 mice (CD4tol cells)
    - *In-vitro* generated regulatory T cells (iTregs)
    - $FoxP3^+$ Tregs from 4Y-treated Tg4 mice
- ✓ Study the capacity of $TIGIT^{-/-}$ regulatory T cells to modulate **DC maturation**

## 3.2 TIGIT expression is enhanced on thymic and peripheral Tregs

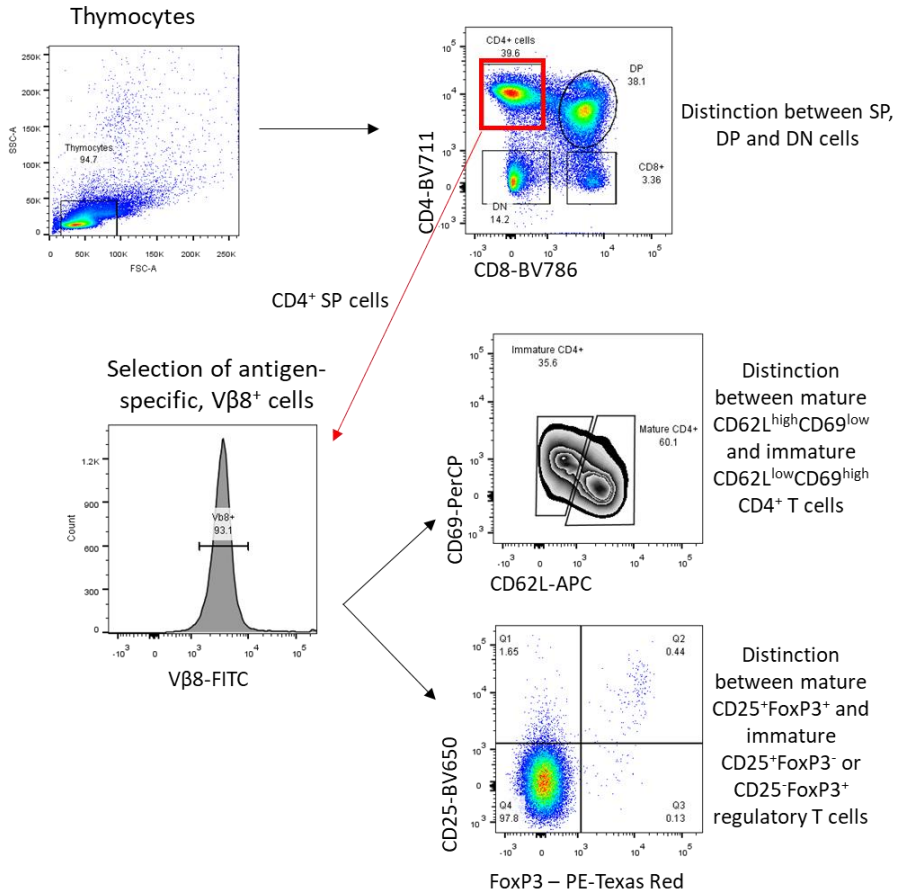
To start dissecting the impact of TIGIT on central tolerance, firstly, we investigated its expression on the different subsets of T cells in the thymus, by gating on the different populations of thymocytes as shown in Fig. 3.1A. During the functional maturation process of developing T cells that takes place in the thymus, different cell types arise at different stages of development, with the first ones being the $CD4^{-}CD8^{-}$ double negative (DN) cells that appear at the early stages of development from early thymus progenitors and go through 4 different stages of maturation and express different markers prior to TCR rearrangement: $CD44^{+}CD25^{-}$ (DN1), $CD44^{+}CD25^{+}$ (DN2), $CD44^{-}CD25^{+}$ (DN3) and $CD44^{-}CD25^{-}$ (DN4) (Ceredig and Rolink, 2002).

After TCR rearrangement, thymocytes mature to double-positive (DP) $CD4^{+}CD8^{+}$ T cells that appear during positive selection in the cortex and subsequently mature into single-positive (SP), either $CD4^{+}$ or $CD8^{+}$ during negative selection in the medulla. $CD4^{+}$ T cells can be further progress from an immature ($CD62L^{low}CD69^{high}$) to a mature ($CD62L^{high}CD69^{low}$) phenotype (Germain, 2002). In addition to conventional $CD4^{+}$ and $CD8^{+}$ T cells, $CD25^{+}FoxP3^{+}$ Tregs, a subset of $CD4^{+}$ T cells, also mature in the thymus from immature $CD25^{-}FoxP3^{+}$ or $CD25^{+}FoxP^{-}$ precursors (Owen et al., 2019).

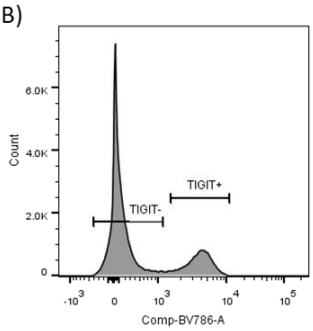
Using the Tg4 mouse model, the expression of TIGIT was analysed on different populations of T cells. Fig. 3.1B shows a representative histogram with the gating for $TIGIT^{+}$ and $TIGIT^{-}$ cells as gated on $CD4^{+}CD25^{+}FoxP3^{+}$ Tregs. Furthermore, total $CD4^{+}$ T cells, total $CD8^{+}$ T cells, different populations of Tregs (mature and immature), different populations of DN cells and DP cells in the thymus (Fig. 3.1C). TIGIT was predominantly expressed on fully mature, $CD25^{+}FoxP3^{+}$ Tregs (approximately 10% of total $CD4^{+}$ T cells), as well as immature $CD25^{+}FoxP3^{-}$ and $CD25^{-}FoxP3^{+}$ Tregs (5%),

but not on Tconv cells, either $CD4^+$ or $CD8^+$, double-positive cells or double-negative (Fig. 3.1C). Interestingly, TIGIT was also expressed by $FoxP3^+$ Tregs in the spleen, but not Tconv, indicating that there are either some $TIGIT^+$ thymic Tregs that entered the periphery or that TIGIT was also upregulated on peripherally induced Tregs (Fig. 3.1D). In either way, the expression of TIGIT of both thymic and peripheral Tregs indicates that it can potentially play a role in the function of these cells.

(A) **Gating strategy for thymic T cell populations**

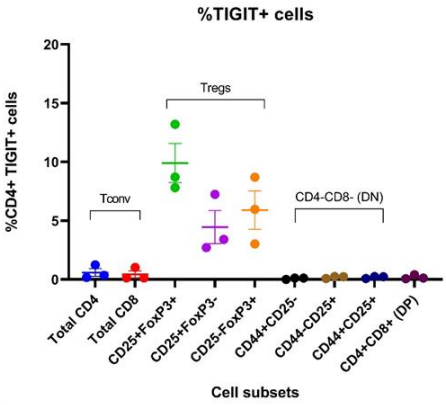



(B)




Gated on viable CD4+ CD25+FoxP3+

(C) **Thymus**




(D) **Spleen**

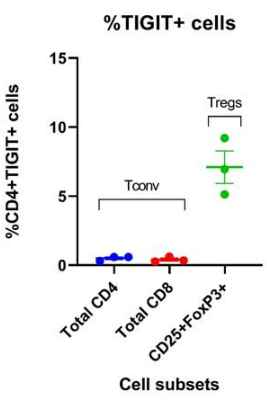


Figure 3.1: **TIGIT expression is enhanced on Tregs in the thymus and spleen.** Thymi and spleens from age-matched (8—10 weeks old) mice were harvested, stained for lineage markers and TIGIT and analysed by flow cytometry. **(A)** Gating strategy followed for the analysis of different cell lineages in the thymus. **(B)** Representative histogram from $TIGIT^{+}$ and $TIGIT^{-}$ cells, gated on $CD4^{+}CD25^{+}FoxP3^{+}$ Tregs. **(C)** Summarising bar graph with % of $CD4^{+}TIGIT^{+}$ T cells in the thymus. **(D)** Summarising bar graph with % of $CD4^{+}TIGIT^{+}$ T cells in the spleen. The error bars show the standard error mean (SEM) and are representative of two independent experiments.

## 3.3 Phenotypic characterisation of the TIGIT KO mice

To be able to characterise the TIGIT KO mice, we assessed the size and cellularity of thymi from TIGIT KO and Tg4 mice. Even though the number of thymocytes was slightly lower in the TIGIT KO mice compared to the Tg4 control, this difference was not significant (Fig. 3.2A). Furthermore, the number of total $CD8^+$ T cells (Fig. 3.2B) and total $CD4^+$ T cells (Fig. 3.2C) remained unaffected in the absence of TIGIT, as well as the number of both mature $CD69^-CD62L^+$ (Fig. 3.2D, i) and immature $CD69^+CD62L^-$ $CD4^+$ T cells (Fig. 3.2D, ii). Double positive $CD4^+CD8^+$ cells (Fig. 3.2E) and double negative $CD4^-CD8^-$ cells during the different stages of maturation (Fig. 3.2D from i – early stage, to iv – latest stage) were not impacted by TIGIT.

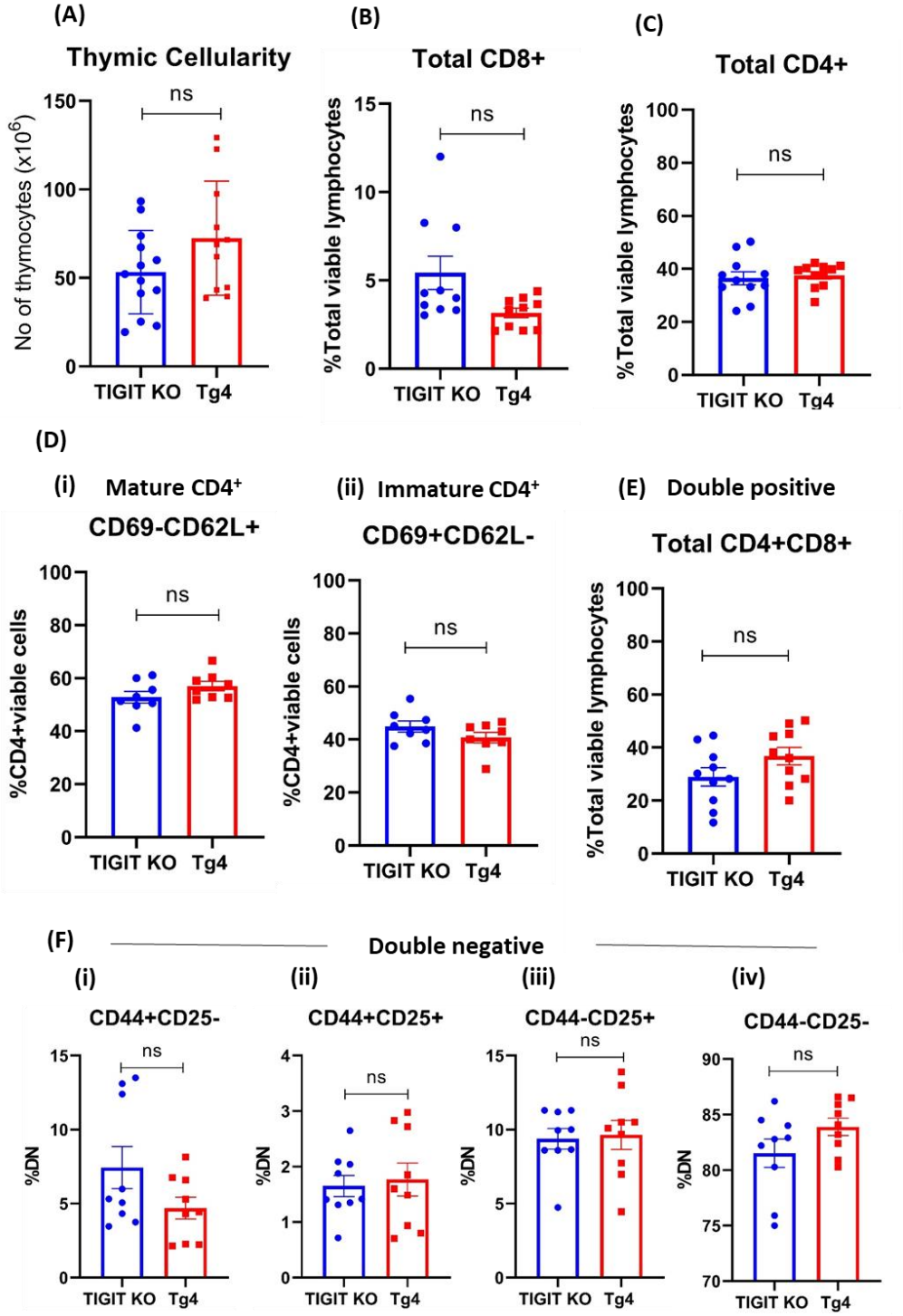


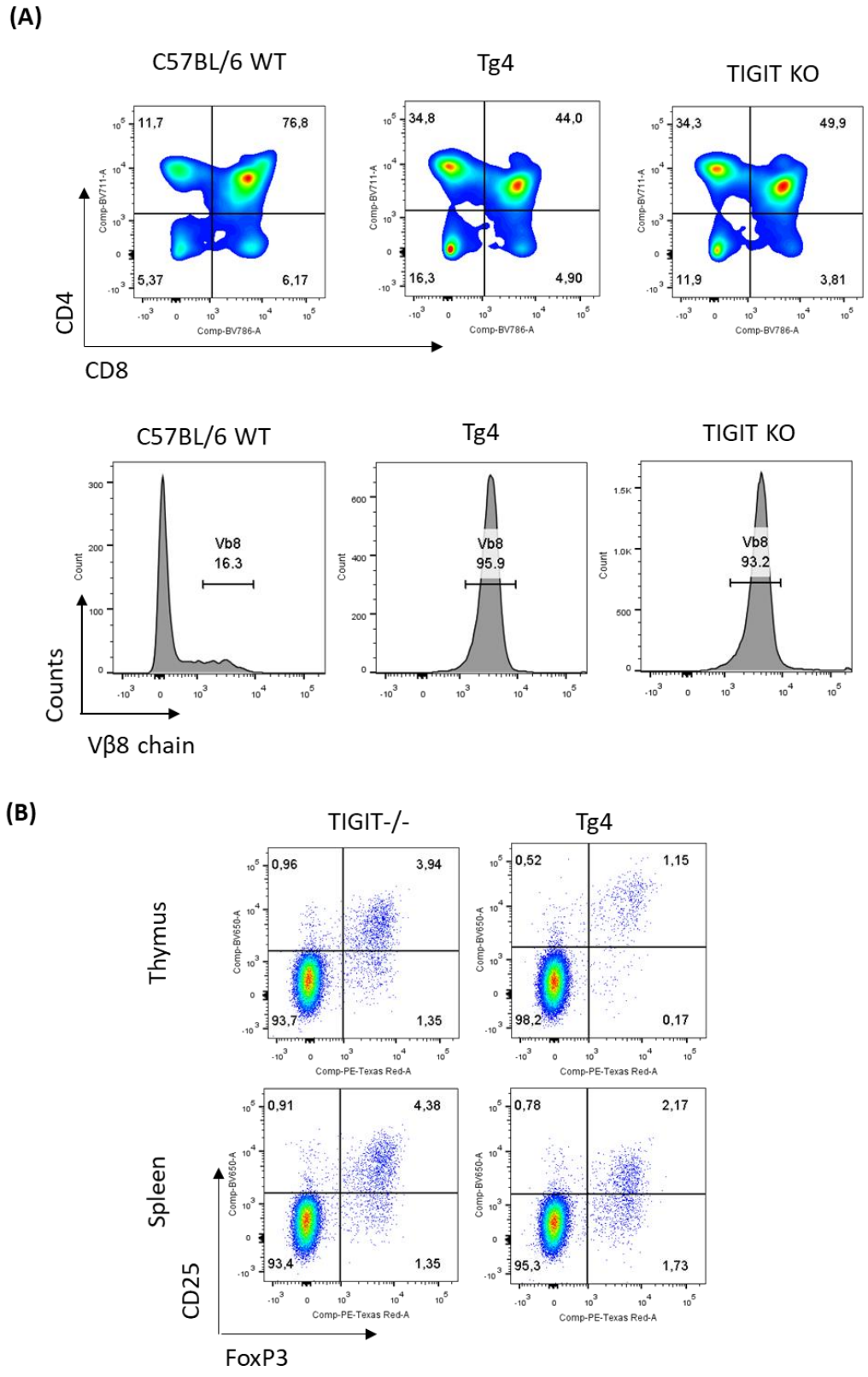

**Fig. 3.2 Phenotypic characterisation of T cell subsets in the thymus of TIGIT KO mice and Tg4 controls. (A)** Thymi harvested from either TIGIT KO mice (Tg4/Tigit_LN7/8b) or Tg4 controls were dissociated and the total cell numbers were measured with trypan blue staining. Cells were stained for T cell markers to distinguish between the different subpopulations and the percentage of each cell type was assessed by flow cytometry. Percentage of total $CD8^+$ **(B)**, total $CD4^+$ **(C)**, mature $CD4^+$ **(D, i)** and immature $CD4^+$ **(D, ii)**, $CD4^+CD8^+$ (double positive) **(E)**, and $CD4^-CD8^-$ (double negative) **(F)** from early stages (i) to middle (ii and iii) and late (iv) that were gated on single, live cells is shown. Statistical significance was calculated by unpaired t test. Results are pooled together from 3 independent experiments and presented as standard error of the mean (SEM).

### 3.3.1 Tg4 mice lacking TIGIT display increased frequencies of FoxP3$^+$ Tregs

As mentioned previously, the TIGIT KO was generated on the Tg4 background, therefore in this model, approximately 95% of CD4$^+$ T cells express the Vβ8 transgene from a T cell specific for the immunodominant peptide of MBP, MBP$_{Ac1-9}$ [4K peptide] (Liu et al., 1995). Given that this is an MHC class II-restricted model, most developing thymocytes are forced to become CD4$^+$ T cells, compared to a wild-type mouse. As part of the characterisation of the new KO strains, thymi from both TIGIT KO and Tg4 mice were harvested and stained for lineage markers and Vβ8. As expected, both TIGIT KO and Tg4 mice had similar percentages of CD4$^+$, CD8$^+$ and CD4$^+$CD8$^+$ T cells, but the percentage of CD4$^+$ SP T cells was much higher (35% of viable, single cells) compared to the C57BL/6 wild type control (12%) (Fig. 3.3A, upper panel). Furthermore, in both TIGIT KO and Tg4 mice, almost all the CD4$^+$ T cells express the Vβ8 chain of the TCR, while in the C57BL/6 wild type control <20% of cells express Vβ8 (Fig. 3.3A, lower panel).

Interestingly, when CD4$^+$Vβ8$^+$ T cells from both TIGIT KO and Tg4 mice were analysed for the frequencies of regulatory cells, there was an upregulation in the number of Tregs, both in the thymus (Fig. 3.3B, upper panel) and in the periphery (Fig. 3.3B, lower panel) of TIGIT KO mice. This difference in cell numbers of thymic Tregs was more significant in fully mature CD25$^+$FoxP3$^+$ Tregs and CD25$^+$FoxP3$^-$ Tregs, but not in the precursor population of CD25$^-$FoxP3$^+$ Tregs, potentially because the percentage of these cells was so low that made the detection of any difference challenging (Fig. 3.3C, i). Intriguingly, this enhanced percentage of CD25$^+$FoxP3$^+$ Tregs was also observed in the spleen (Fig. 3.3C, ii), in line with previous data from the CTLA-4$^{-/-}$ mice (Verhagen et al., 2009).

**Fig. 3.3** (Continued on the next page)



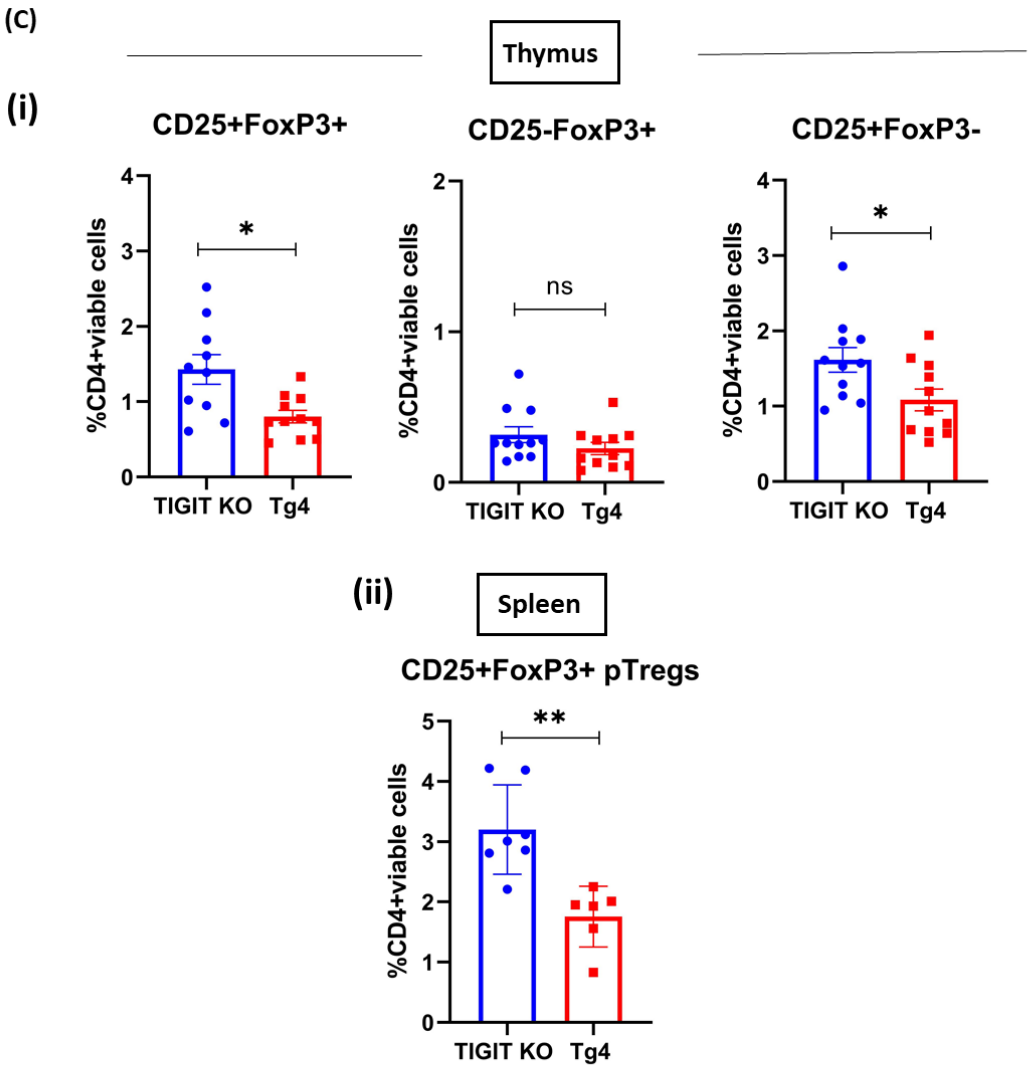



**Figure 3.3: TIGIT$^{-/-}$ mice display higher frequencies of FoxP3$^{+}$ Tregs both in the thymus and spleen.** **(A)** Isolated thymocytes from C57BL/6 WT, Tg4 or TIGIT$^{-/-}$, ages 6-8 weeks, stained with anti-CD4, anti-CD8 and anti-Vβ8 antibodies to determine percentage of CD4SP and CD4CD8DP thymocytes and expression of the transgene. Gated on live single cells. Images are representative of nine (Tg4, TIGIT$^{-/-}$) or three (C57BL/6) thymi analysed. **(B)** Representative FACS plots of CD25 and FoxP3 expression on live CD4SP thymocytes (upper panel) or splenocytes (lower panel) from Tg4 or TIGIT-/- mice (6-8 weeks) directly *ex vivo*. Minimum of 2 x $10^6$ live thymocytes analysed for each thymus or spleen. **(C)** Thymi harvested from either TIGIT KO (8b) mice or Tg4 controls were dissociated and cells were stained for CD4, CD25 and FoxP3 to identify Tregs. In the thymi of TIGIT KO mice, both number of mature CD25$^{+}$FoxP3$^{+}$ Tregs and immature, either CD25$^{-}$FoxP3$^{+}$ or CD25$^{+}$FoxP3$^{-}$ Tregs were increased (i). Numbers of FoxP3$^{+}$ Tregs were also elevated in the spleen (ii). Statistical significance was calculated by unpaired t test. Results are pooled together from 3 independent experiments and presented as standard error of the mean (SEM).

### 3.3.2 Investigation of the proliferative capacity of Tregs from TIGIT KO and Tg4 mice

Following the observation that there is a higher percentage of both thymic and splenic FoxP3$^+$ Tregs in the TIGIT KO mice, the question that we aimed to address next was what the driving force behind the difference seen in numbers might be. One explanation would be that FoxP3$^+$ Tregs that lack TIGIT display enhanced proliferative capacity. To test this hypothesis, mice were injected intraperitoneally (i.p.) with BrdU, an analogue of thymidine that identifies proliferation rates *in vivo* by incorporating into newly synthesised DNA of actively proliferating cells. One hour post injection, tissues were harvested, processed, and stained for lineage markers and BrdU (Fig. 3.4A).

Surprisingly, the levels of BrdU$^+$ cells in thymic Tregs, both mature and immature, was quite low and there were no significant differences between the TIGIT KO and Tg4 control mice (Fig. 3.4B). Similarly, the levels of BrdU$^+$ FoxP3$^+$ Tregs in the spleen were at the same levels and any differences were negligible (Fig. 3.4C). Therefore, the increased percentage of FoxP3$^+$ Tregs in the TIGIT KO mice in unlikely to be due to elevated levels of proliferation.

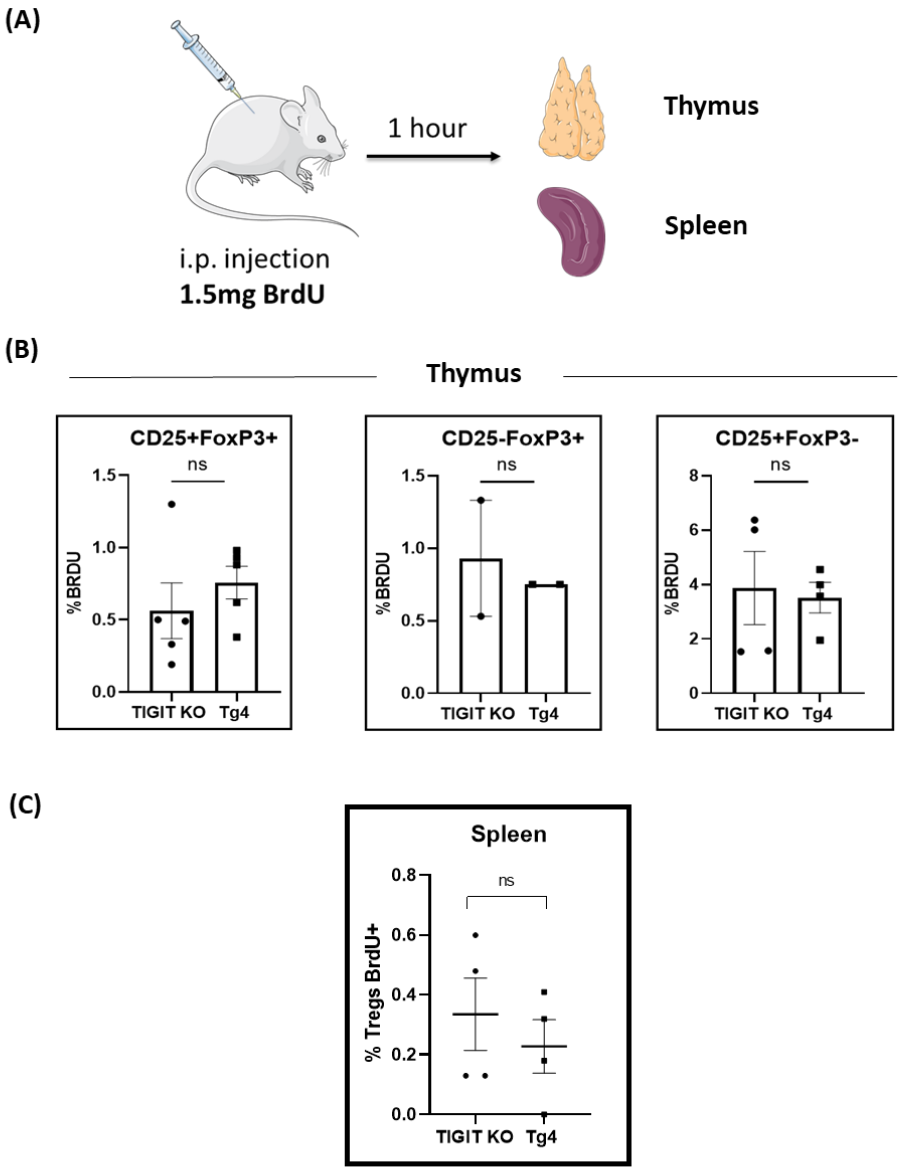


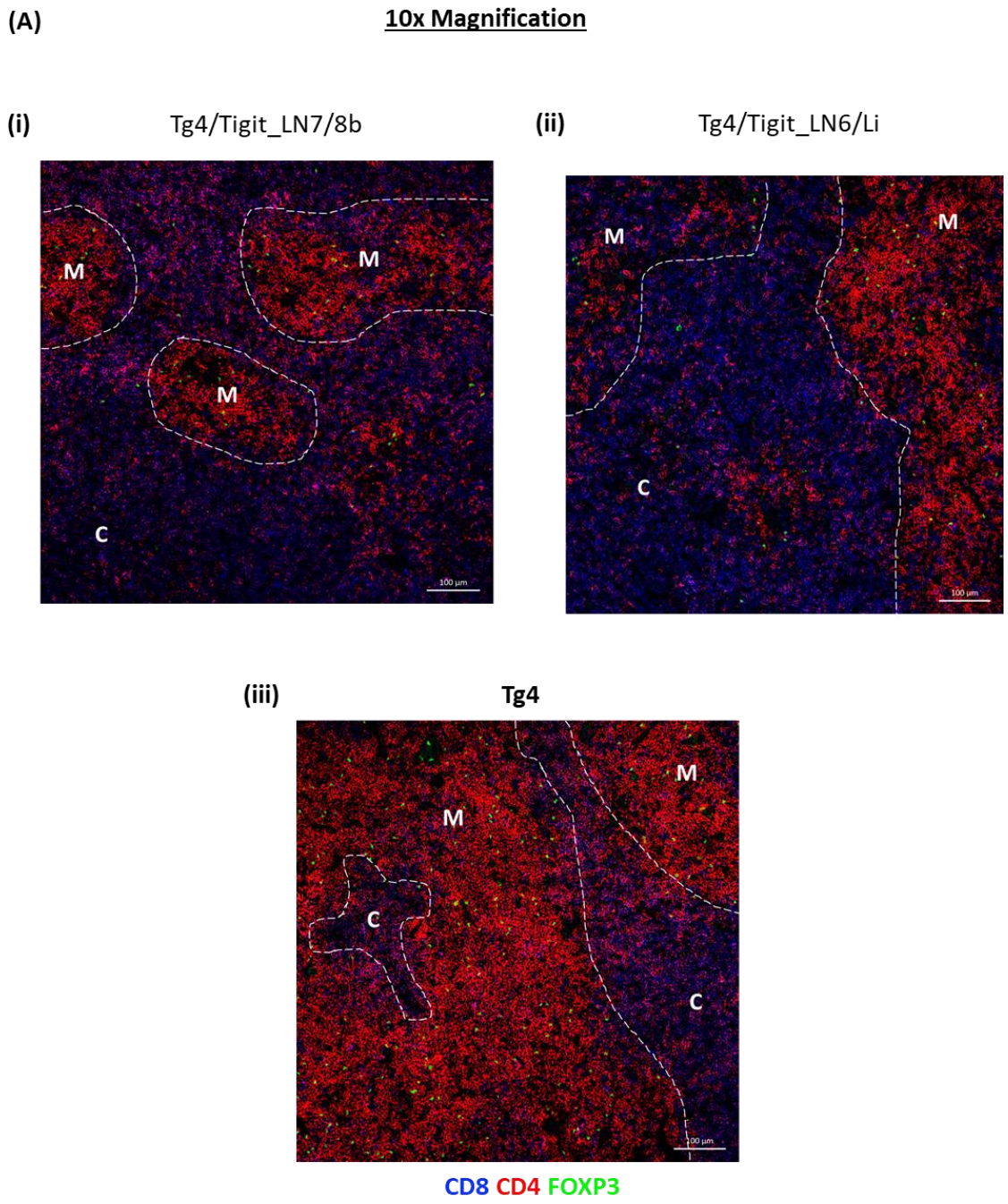

**Figure 3.4: Assessment of Treg proliferation with BrdU. (A)** To support the detection of proliferating cells, 1.5mg of BrdU, an intercalating dye that binds to DNA, was injected into mice intraperitoneally (i.p). After one hour, mice were sacrificed and tissues (thymus, spleen) were harvested and digested as appropriate for the cell type being analysed. Cells were surface stained to define the desired population, fixed overnight and then stained intracellularly for BrdU. **(B)** Percentage of proliferating, fully mature ($CD25^{+}FoxP3^{+}$) and immature ($CD25^{-}FoxP3^{+}$ and $CD25^{+}FoxP3^{-}$) thymic Tregs based on BRDU incorporation as analysed by flow cytometry. **(C)** Percentage of proliferating, splenic $CD25^{+}FoxP3^{+}$ Tregs. Statistical significance was calculated by unpaired t test. Results are pooled together from 2 independent experiments and presented as standard error of the mean (SEM).

### 3.3.3 Localisation of TIGIT$^{-/-}$ Tregs in the thymus

Given that proliferation of FoxP3$^{+}$ Tregs was not compromised due to TIGIT, we reasoned that the discrepancy seen in Treg numbers could be due to altered negative selection in the thymic medulla. The localisation of developing thymocytes reflects their developmental stage. In wild type mice, during positive selection that takes place in the thymic cortex, CD4$^{+}$ or CD8$^{+}$ SP developing thymocytes upregulate CCR7, which is required for the migration of SP cells to the medulla, where negative selection takes place (Kurd and Robey, 2016). We hypothesised that the absence of TIGIT might interfere with the ability of T cells to undergo negative selection. To address this, we followed an imaging approach, in which frozen sections from thymi of TIGIT KO and Tg4 mice were stained for CD4 and CD8 to be able to visualise the areas of cortex (C) and medulla (M) that is mostly populated by CD4$^{+}$ T cells and FoxP3 to detect Tregs and visualised at different magnifications under a Zeiss LSM 710 confocal microscope.

In this way, we wanted to investigate both the localisation of Tregs as well as their absolute numbers. Interestingly, at the lower magnification of 10x, in both TIGIT KO strains, Tg4/Tigit_LN7/8b (Fig. 3.5A, i) and Tg4/Tigit_LN6/Li (Fig. 3.5A, ii), FoxP3$^{+}$ Tregs were found within the medullary regions, similar to the Tg4 control (Fig. 3.5A, iii). Furthermore, using the higher magnification of 25x, we were able to see that the numbers of FoxP3$^{+}$ Tregs were very similar between the Tg4/Tigit_LN7/8b (Fig. 3.5B, i), Tg4/Tigit_LN6/Li (Fig. 3.5b, ii) and Tg4 control (Fig. 3.5B, iii). Therefore, with the approaches we followed we were not able to give a conclusive answer regarding the differences seen in Tregs number between the TIGIT KO and Tg4 mice. Further analysis of the involvement of TIGIT on central tolerance was beyond the scope of this thesis, and the next paragraphs focus on the role of TIGIT in peripheral tolerance.

**Fig 3.5: The absence of TIGIT does not interfere with the localisation of Tregs in the thymus** (Continued on the next page)



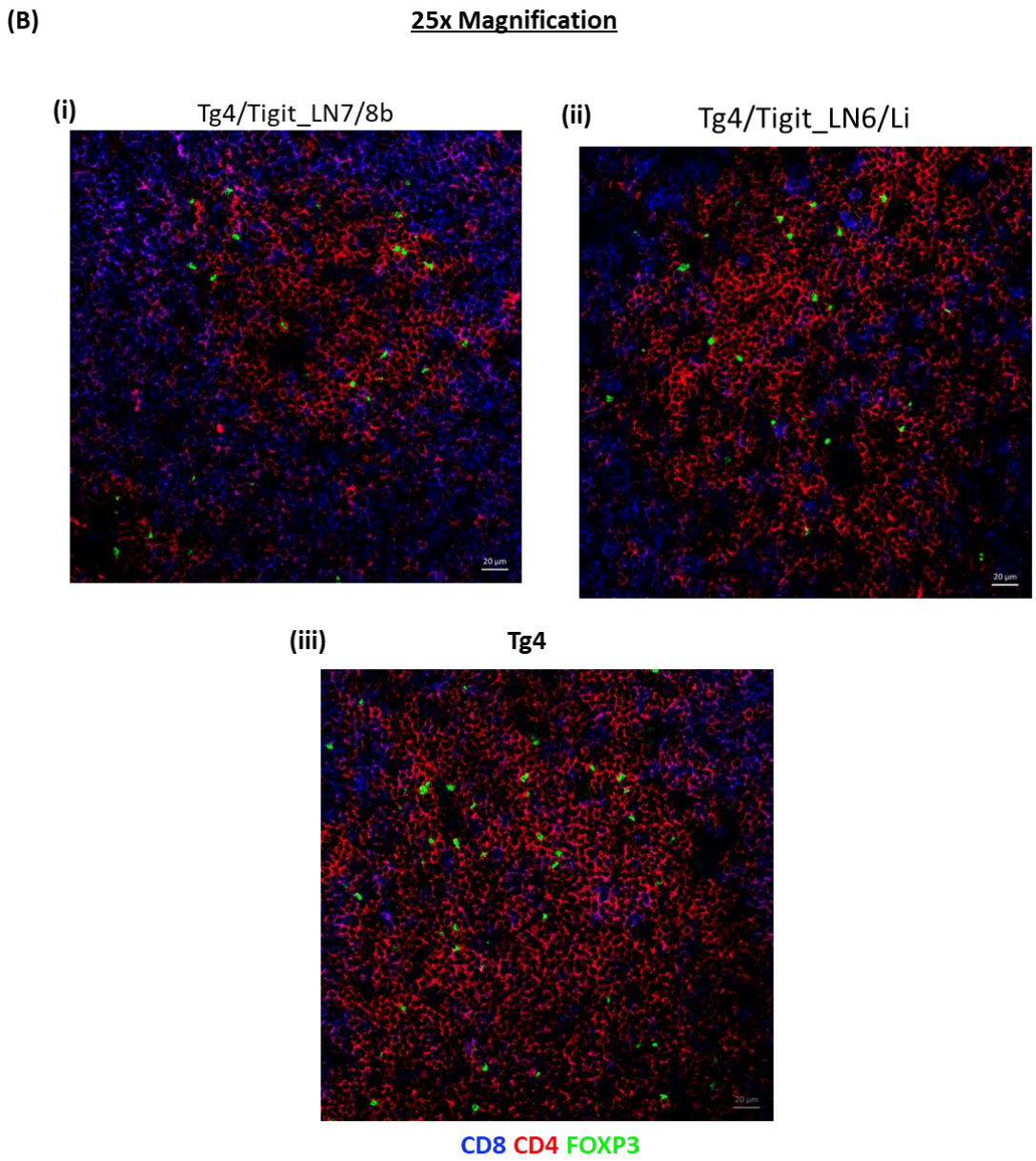



**Figure 3.5: The absence of TIGIT does not interfere with the localisation of Tregs in the thymus.** Thymi from either Tg4/Tigit_LN7/8b (i), Tg4/Tigit_LN6/Li (ii) or Tg4 mice (iii) that were 6-8 weeks of age were frozen in liquid nitrogen immediately after removal. Seven-micrometre sections were fixed in acetone, washed in PBS and stained with anti-CD4, anti-CD8, anti-FoxP3 and DAPI and images were taken with a confocal microscope at either 10x magnification **(A)** or 25x magnification **(B)**. The dotted lines mark the areas of medulla (M) and cortex (C). Images are representative of 3 independent experiment (N=3) showing similar results. $CD8^+$ cells are shown in blue, $CD4^+$ cells in red and $FoxP3^+$ cells in green.

## 3.4 Development of protocol for *in vitro* expansion of CD4$^+$ T cells from 4Y-treated mice (CD4$^+$tol)

To investigate the role of TIGIT in the maintenance of peripheral tolerance mediated by different regulatory T cells, different approaches were followed. The dose escalation protocol, in which Tg4 mice are given increasing doses of the high affinity MBP analogue, MBP$_{Ac1-9}$[4Y] *in vivo* to give rise to IL-10$^+$ peripherally-induced tolerant cells has been studied extensively (Sundstedt et al., 2003; Gabrysova et al., 2009; Nicolson et al., 2009; Burton et al., 2014). However, this protocol has not been applied to TIGIT KO mice before, therefore a couple of pilot experiments were conducted first to ensure the safety of this method as a tool to give rise to tolerant CD4$^+$ T cells, hereafter referred to as **CD4tol cells**.

TIGIT KO mice did not exhibit any signs of clinical pathology or development of EAE or any other adverse side effect during the course of tolerance induction. Therefore, TIGIT KO and Tg4 mice were subjected to subcutaneous administration of increasing doses of the 4Y peptide and spleens were harvested 3 days after the final treatment and expanded *in vitro* for subsequent rounds of stimulation (Fig. 3.6A). For the first round, bulk splenocytes of tolerant Tg4 mice were expanded in the presence of 4K and IL-2 because there were some APCs in that bulk population of cells to allow antigen presentation to T cells. After 7 days, isolated CD4$^+$ T cells were re-stimulated with 4K and PL8 cells, an A$^u$-expressing, antigen presenting B cell lymphoma cell line that was used instead of APCs (Wraith et al., 1992). Cell cultures were supplemented with IL-2 three days after stimulation with 4K and viable CD4$^+$ T cells were used after each subsequent round for *in vitro* assays or further expansion.

This protocol was developed in compliance with the 3Rs policy (Replacement, Reduction, Refinement), so that we could use CD4tol cells expanded in culture for further experiments, instead of repeating the tolerance induction using more mice each time. Before using the cells in assays, a quick assessment of their phenotype was conducted to ensure the stability of the cell line, primarily to ensure that they maintained the production of IL-10, which is the main characteristic of these cells and also the fact that they don't express FoxP3, the main difference between peptide-induced tolerant cells and other naturally occurring FoxP3$^+$ Tregs.

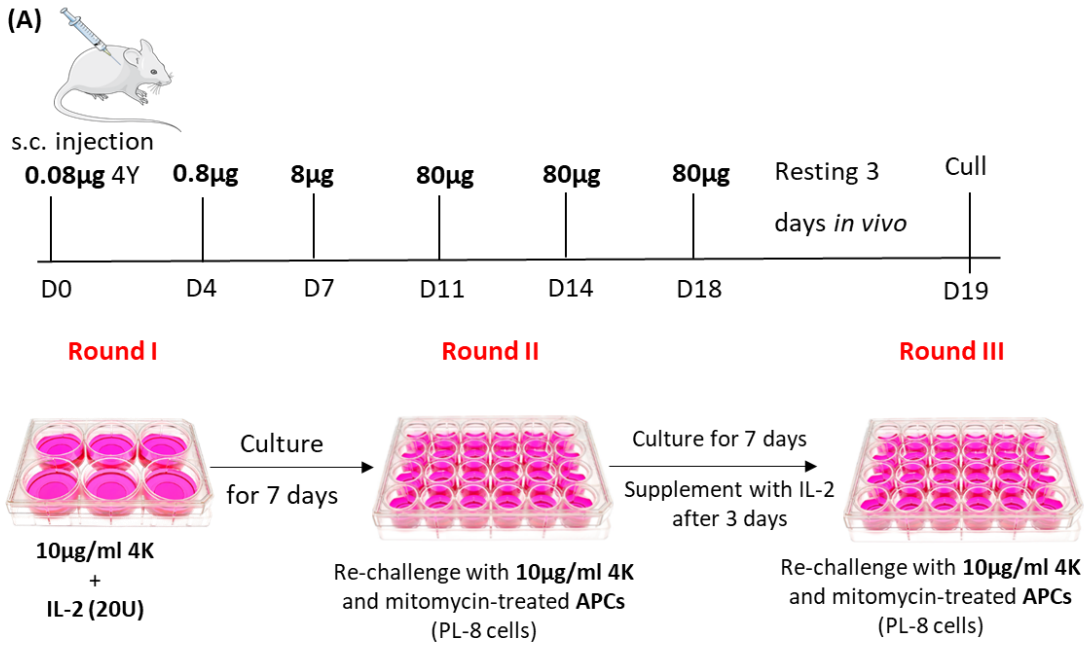
Previous data has shown that CD4tol cells are anergic, fail to produce IL-2, but can produce high levels of IL-10 following antigen encounter; however, this state of anergy is reversible upon addition of exogenous IL-2 (Anderson et al., 2005). Importantly, external IL-2 did not induce the transcription of *Il2* gene in these cells, therefore these cells remained unable to sustain their survival and proliferation through production of their own IL-2, but relied on IL-2 produced by T effector cells, a characteristic also seen in FoxP3$^+$ Tregs (Chinen et al., 2016). To confirm these observations in CD4tol cells from Tg4 mice and compare the phenotype to their counterparts in the TIGIT KO mice, cells were stimulated with either the low [4K] or high [4Y] affinity peptides for three days, with or without IL-2, and cells were pulsed with [3H]-thymidine for the last 16h of culture to measure the levels of proliferation.

Interestingly, without external IL-2, CD4tol cells from both TIGIT KO mice and Tg4 controls remained undivided (ccpm below 2000) upon stimulation with either 4K (Fig. 3.6B, ii) or 4Y (Fig. 3.6B, iv), confirming their state of anergy, which was not reversed even with the strong TCR stimulation with 4Y. Naïve CD4$^+$ T cells were used as a positive control for proliferation, since they were able to proliferate readily across

peptide concentrations. The low levels of proliferation seen upon stimulation with the high dose (100μg/ml) peptide, either 4K or 4Y, can be due to the fact that a high proportion of cells undergo induced cell death when exposed to strong TCR stimulation (Lissy et al., 1998). However, when IL-2 was added into the cultures, cells were able to overcome this state of unresponsiveness and proliferate upon stimulation with 4K (Fig. 3.6B, i) or 4Y (Fig. 3.6B, iii). Strikingly, the re-stimulation with 4K only partially reversed the anergic phenotype (ccpm around 20000), while re-stimulation with 4Y provided a strong signal that enhanced the proliferation drastically (ccpm above 60000), reaching levels similar to the ones seen with naïve $CD4^+$ T cells. This indicates that this state of anergy imprinted to CD4tol cells following peptide immunotherapy is reversible and it depends on both TCR signals as well as environmental cues from cytokines, such as IL-2.

Surprisingly, TIGIT did not appear to play a role in the establishment of the anergic phenotype of CD4tol cells in the IL-2-free cultures and did not interfere with the reversion of this phenotype upon addition of IL-2, since the levels of proliferation between the two TIGIT KO strains (8b deletion and long insertion) and the Tg4 control were similar across the different conditions tested. There is a trend of slightly higher proliferation in the CD4tol cells from TIGIT KO, especially the ones that were re-stimulated with 4K and IL-2 (Fig. 3.6B, i); however, the difference seen was not statistically significant. This indicates that TIGIT plays a subtle, if any, role in the proliferative capacity of CD4tol cells.

**Fig. 3.6: Protocol for tolerance induction and establishment of anergy** (Continued on the next page)



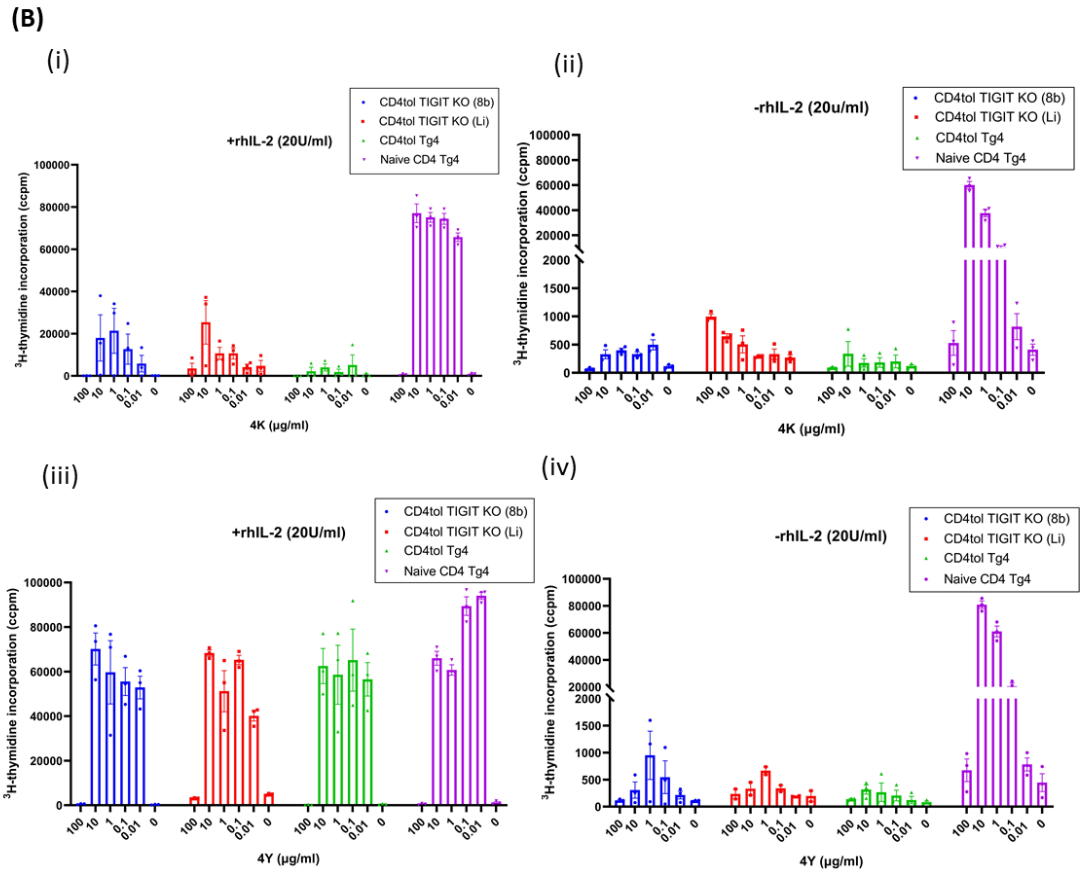



**Figure 3.6: Protocol for tolerance induction and establishment of anergy. (A)** Mice were treated with 6 increasing doses of $MBP_{Ac1-9}$ [4Y]. Spleens were harvested 3 days after the last dose and CD4tol cells were expanded *in vitro* for 7 days in the presence of 10µg/ml 4K with rhIL-2 (20U/ml) (Round I). Cells were then re-stimulated with 10µg/ml 4K in the presence of PL8 cells that acted as APCs (Round II) and the culture was supplemented with IL-2 (20U/ml) on day 3 after antigen stimulation. **(B)** 7 days after the first round of stimulation with 4K (Round I), a fraction of $CD4^+$ T cells from the initial culture was further stimulated with the low-affinity peptide analogue $MBP_{Ac1-9}$ [4K] for 3 days either in the presence (i) or absence (ii) of rhIL-2 (20U/ml) or with the high-affinity peptide analogue $MBP_{Ac1-9}$ [4Y] for 3 days either in the presence (iii) or absence (iv) of rhIL-2 (20U/ml) and cells were then pulsed with 0.18MBq/ml [3H]-thymidine for 16-20 hours. [3H]-thymidine incorporation was measured on a scintillation reader as corrected counts per minute (ccpm). Bar graphs display individual and mean average values of 3 mice per group (SEM), collated from 3 independent experiments. Statistical significance calculated by two-way ANOVA with Dunnett's multiple comparisons between CD4tol cells from the two TIGIT KO strains and theTg4 control. Non-statistically significant changes were accepted where $p>0.05$ (no *). Naïve $CD4^+$ T cells from Tg4 mice were used to demonstrate the levels of proliferation without any treatment and were excluded from the analysis.

### 3.4.1 Assessment of the cytokine profile of $CD4^+$tol from $TIGIT^{-/-}$ and Tg4 mice after *in vitro* re-challenge with $MBP_{Ac1-9}$ analogues

Even though TIGIT did not seem to play a major role in the proliferative capacity of CD4tol cells, we hypothesised that it could play a role in the capacity of these cells to produce pro- or anti-inflammatory cytokines, since it was previously shown that there is a positive correlation between TIGIT and IL-10 (Burton et al., 2014). Therefore, we reasoned that TIGIT may play a role in the ability of CD4tol cells to produce IL-10. Furthermore, even though CD4tol cells have differentiated towards an anergic, IL-10-producing phenotype, they are still able to produce IFN-γ in response to antigen, revealing their Th1 origin (Gabryšová et al., 2009); therefore we were keen to investigate the implications of the lack of TIGIT on the ability of CD4tol cells to produce both IL-10 and IFN-γ.

Interestingly, upon *in vitro* re-challenge of CD4tol cells with 4K, there were high levels of IL-10 in culture supernatants both with (Fig. 3.7A, i) and without (Fig. 3.7A, ii) exogenous IL-2. This effect was dose-dependent and with the addition of IL-2, cells were able to produce high levels of IL-10 at lower doses compared to the cultures that did not have IL-2. Naïve $CD4^+$ T cells were used as an untreated control for the background levels of IL-10 production. Upon re-stimulation with 4Y, there was again a clear, dose-dependent effect for IL-10 production; however, the strong TCR stimulation potentiated CD4tol cells to produce high levels of IL-10 even at low doses (0.1 or even 0.01) in the presence of IL-2 (Fig. 3.7B, i) and less so without IL-2 (Fig. 3.7B, ii). In all the conditions mentioned above, differences in the levels of IL-10 production between the TIGIT KO strains and Tg4 controls were not significant.

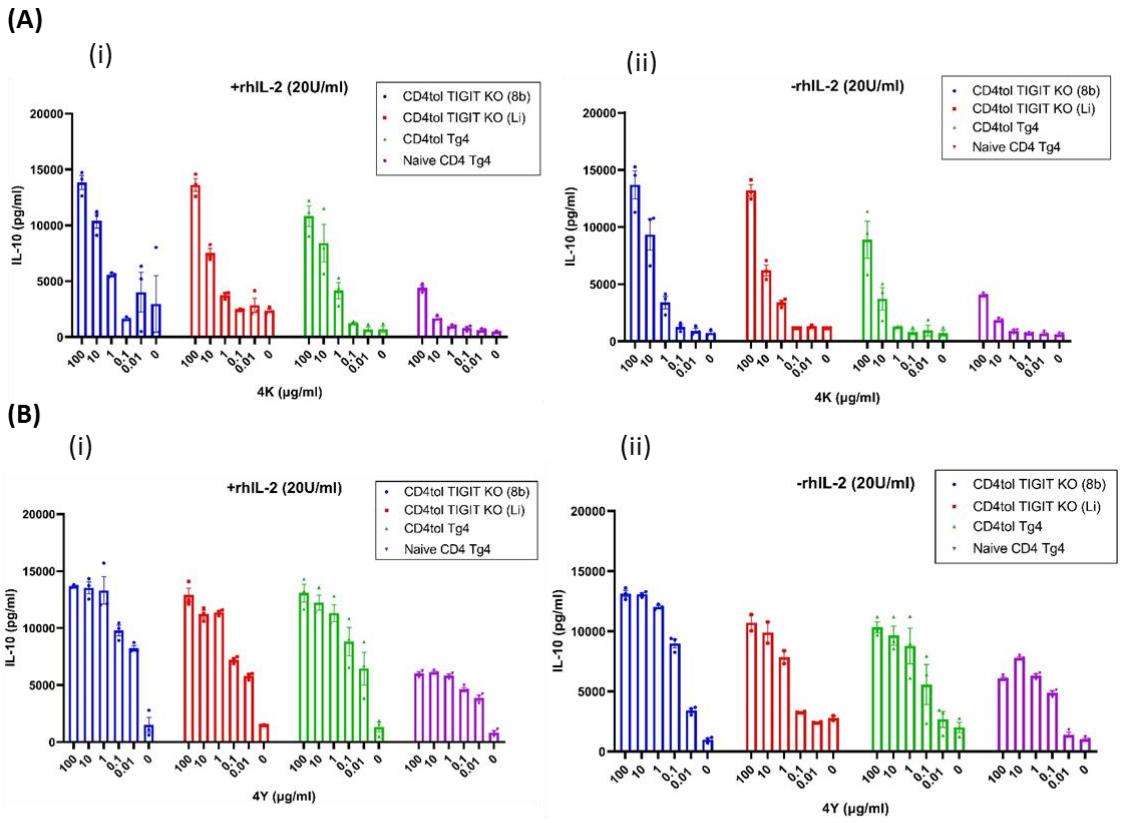



**Figure 3.7: IL-10 levels of CD4tol cells deriving from either TIGIT$^{-/-}$ or Tg4 mice after *in vitro* re-challenge with MBP analogues of different affinity.** Mice were treated with 6 increasing doses of $MBP_{Ac1-9}$ [4Y] *in vivo*. Spleens were harvested 3 days after the last dose and CD4tol cells were expanded *in vitro* for 7 days as described previously. **(A)** 7 days after the first round of stimulation with 4K (Round I), a fraction of CD4$^+$ T cells from the initial culture was further stimulated with the low-affinity peptide analogue $MBP_{Ac1-9}$ [4K] for 3 days either in the presence (i) or absence (ii) of rhIL-2 (20U/ml) or **(B)** with the high-affinity peptide analogue $MBP_{Ac1-9}$ [4Y] for 3 days either in the presence (i) or absence (ii) of rhIL-2 (20U/ml) and levels of IL-10 were measured in the supernatants of the culture by sandwich ELISA according to the manufacturer's instructions. Bar graphs display individual and mean average values of 3 mice per group (SEM), collated from 3 independent experiments. Statistical significance calculated by two-way ANOVA with Dunnett's multiple comparisons between CD4tol cells from the two TIGIT KO strains and theTg4 control. Non-statistically significant changes were accepted where $p>0.05$ (no *). Naïve CD4$^+$ T cells from Tg4 mice were used to demonstrate the levels of proliferation without any treatment and were excluded from the analysis.

In addition to IL-10, levels of IFN-γ produced by CD4tol cells in response to antigen were measured in cell culture supernatants. Similar conditions were investigated, where CD4tol cells were re-stimulated *in vitro* with either the high affinity, 4Y, or low affinity, 4K peptide, in the presence or absence of external IL-2. Again, in the presence of 4K peptide and without IL-2, there was a dose-dependent effect for IFN-γ production that was very similar between the two different TIGIT KO strains and the Tg4 control (Fig. 3.8A, ii) and the levels of IFN-γ increased in the presence of IL-2, but still the absence of TIGIT did not alter the production of IFN-γ (Fig. 3.8A, i). Re-stimulation with 4Y peptide had a similar impact on CD4tol cells; however, the production of IFN-γ was quite high even at the low doses of 0.1 and 0.01μg/ml peptide without exogenous IL-2 (Fig. 3.8B, ii) and these levels were slightly higher at the same peptide doses but with exogenous IL-2. In all the cases, it appeared that TIGIT was dispensable and did not interfere with the ability of CD4tol cells to produce IFN-γ following peptide stimulation.

In a last attempt to test the role of TIGIT on CD4tol cells, a different approach was used. After one round of *in vitro* expansion, CD4tol cells were re-stimulated with PMA and Ionomycin for 4h and stained for surface markers and intracellular cytokines. Levels of intracellular IL-10, IFN-γ, IL-2, and IL-4 were measured on $CD4^+$ viable cells from either 4Y-treated or untreated Tg4 mice (Fig. 3.9A). Data from 4 independent experiments showed that there were no significant differences in the % or MFI of $IL\text{-}10^+$ cells (Fig. 3.9B, i and ii), in the % or MFI of $IFN\text{-}\gamma^+$ cells (Fig. 3.9C, i and ii), in the % or MFI of $IL\text{-}2^+$ cells (Fig. 3.9D, i and ii) and in the % or MFI of $IL\text{-}4^+$ cells (Fig. 3.9E, i and ii). From all the experiments presented in this paragraph, it was clear that TIGIT did not play a role in the development and phenotype of CD4tol cells.

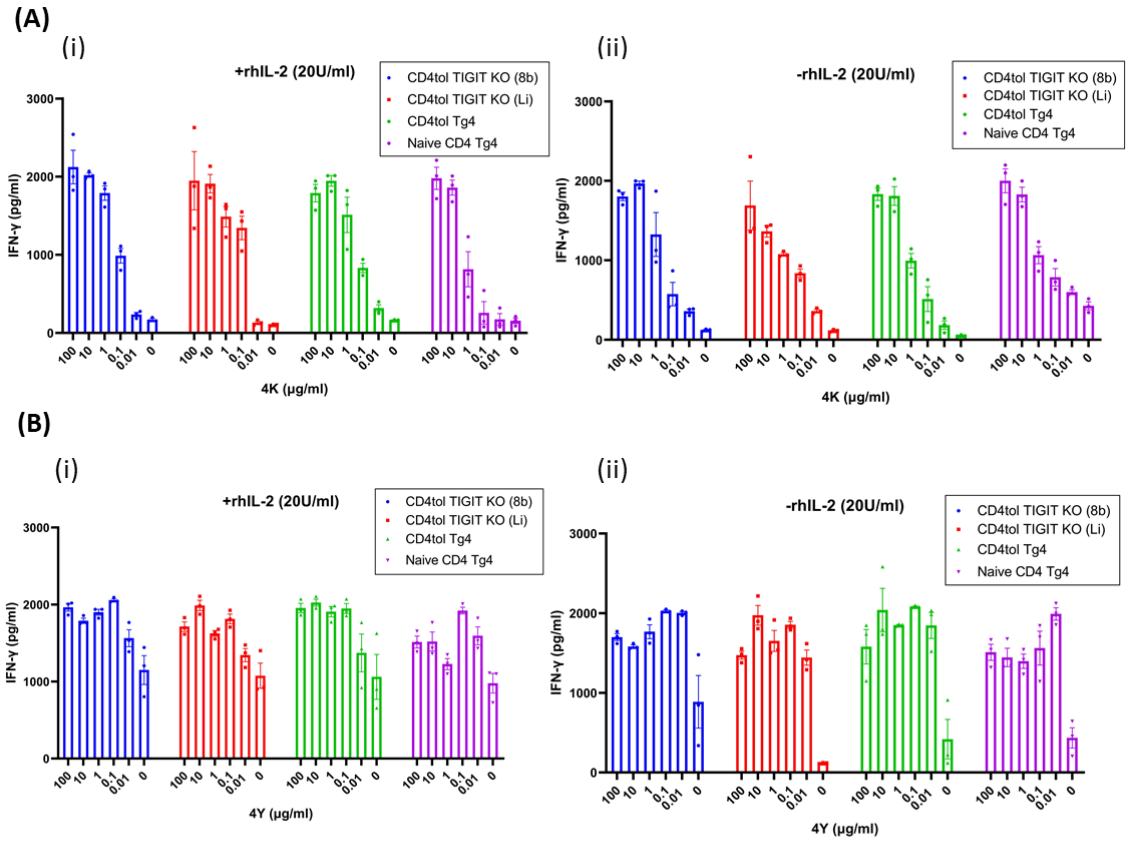



**Figure 3.8: IFN-γ levels of CD4tol cells deriving from either TIGIT$^{-/-}$ or Tg4 mice after *in vitro* re-challenge with MBP analogues of different affinity.** Mice were treated with 6 increasing doses of $MBP_{Ac1-9}$ [4Y] *in vivo*. Spleens were harvested 3 days after the last dose and CD4tol cells were expanded *in vitro* for 7 days as described previously. **(A)** 7 days after the second round of stimulation with 4K, a fraction of the culture was further stimulated with the low-affinity peptide analogue $MBP_{Ac1-9}$ [4K] for 3 days either in the presence (i) or absence (ii) of rhIL-2 (20U/ml) or **(B)** with the high-affinity peptide analogue $MBP_{Ac1-9}$ [4Y] for 3 days either in the presence (i) or absence (ii) of rhIL-2 (20U/ml) and levels of IFN-γ were measured in the supernatants of the culture by sandwich ELISA according to the manufacturer's instructions. Bar graphs display individual and mean average values of 3 mice per group (SEM), collated from 3 independent experiments. Statistical significance calculated by two-way ANOVA with Dunnett's multiple comparisons between CD4tol cells from the two TIGIT KO strains and the Tg4 control. Non-statistically significant changes were accepted where $p>0.05$ (no *). Naïve $CD4^+$ T cells from Tg4 mice were used to demonstrate the levels of proliferation without any treatment and were excluded from the analysis.

**Fig. 3.9**: **Cytokine profile of tolerant cells deriving from either TIGIT$^{-/-}$ or Tg4 mice after stimulation with PMA/Ionomycin.** (Continued on the next page)

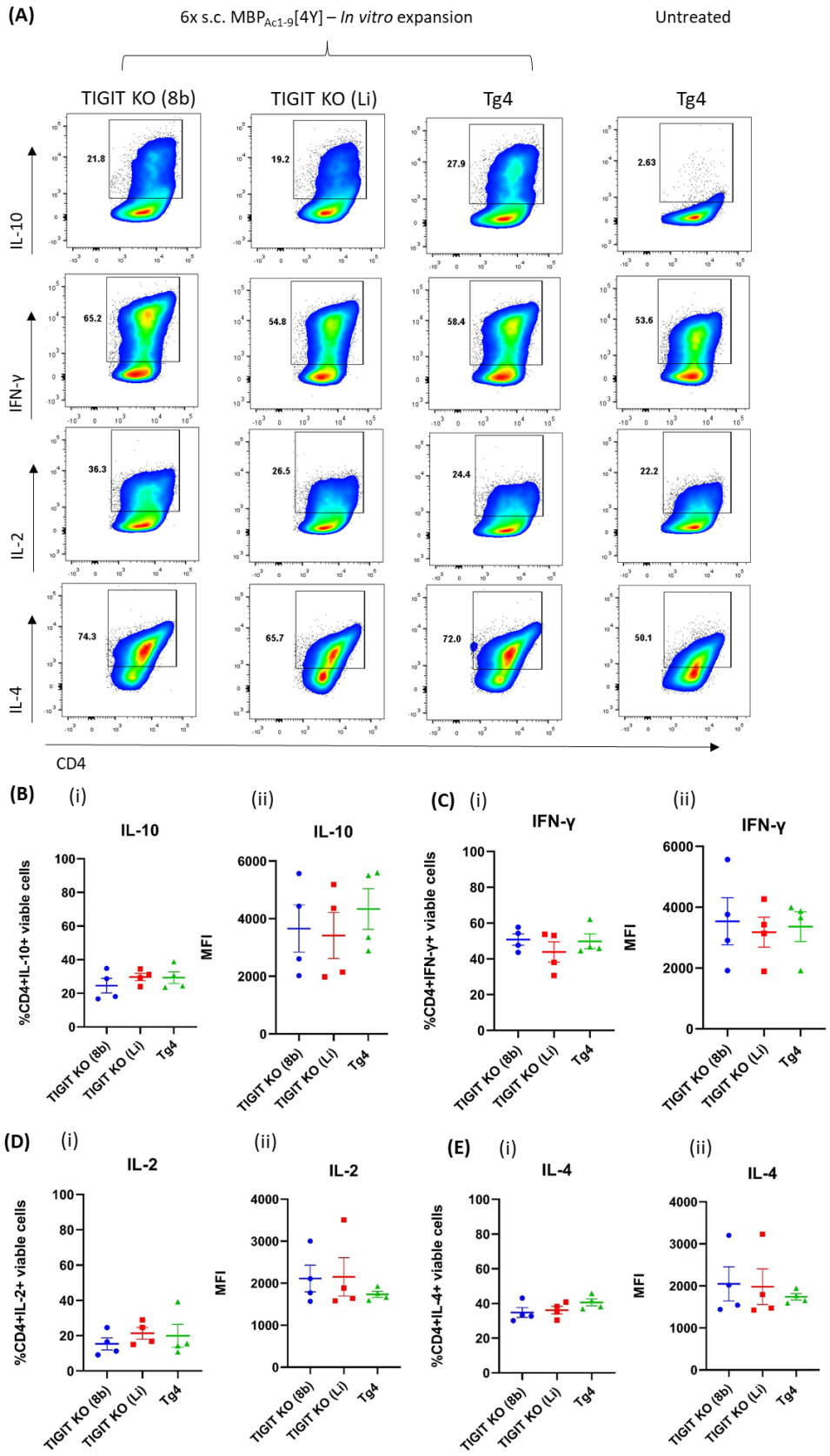


**Figure 3.9: Cytokine profile of tolerant cells deriving from either TIGIT$^{-/-}$ or Tg4 mice after stimulation with PMA/Ionomycin.** Mice were treated with 6 increasing doses of $MBP_{Ac1-9}$ [4Y]. Spleens were harvested 3 days after the last dose and CD4tol cells were expanded *in vitro* for 7 days in the presence of 10μg/ml 4K with rhIL-2 (20U/ml) (Round I). 7 days after the first round of stimulation with 4K, a fraction of the culture was stimulated with PMA and Ionomycin for 4 h in the presence of Golgi Stop. Cells were surface stained with anti-CD4 AF700 and eF780 (viability dye) and intracellularly with anti-IL-10 APC, anti-IFN-γ PE-Cy7, anti-IL-2 BV421 and anti-IL-4 PE. **(A)** Representative FACS plots of Il-10, IFN-γ, Il-2 and IL-4 expression on live CD4$^+$ T cells from either 4Y-treated TIGIT$^{-/-}$ or Tg4 mice or naïve Tg4 controls. **(B-E)** Levels of IL-10 production are presented either as percentage of CD4$^+$ IL-10$^+$ viable cells (B, i) or as mean fluorescence intensity (MFI) (B, ii) and similarly for IFN-γ$^+$ cells (C), IL-2$^+$ cells (D) and IL-4$^+$ cells (E). Fluorescence intensity was measured on a BD LSR II flow cytometer (BD) and analysed using Flowjo (Tree Star, Inc.) FACS analysis software. Bar graphs display individual and mean average values of 3 mice per group (SEM), collated from 4 independent experiments. Statistical significance calculated by two-way ANOVA with Dunnett's multiple comparisons between the CD4tol cells from the two TIGIT knock out strains and the CD4tol cells from the Tg4 control. Non-statistically significant changes were accepted where $p>0.05$ (no *).

## 3.5 The role of TIGIT in the generation of iTregs

Moving on from CD4tol cells, we were interested to study the role of TIGIT in the generation and phenotype of *in vitro*-generated Tregs (iTregs). For the generation of iTregs, bulk splenocytes from TIGIT KO or Tg4 mice were cultured with TFG-β and IL-2 and CAL101, a PI3K inhibitor that was previously shown from our lab to enhance FoxP3 expression (unpublished data) or DMSO control. The role of PI3K pathway in the stability of Tregs has been controversial; however, several different publications have confirmed that inhibition of this pathway results in increased expression of FoxP3 (Soond et al., 2012; Harada et al., 2010; Patterson et al., 2011). Furthermore, a titration of 4K peptide was used to define the optimal concentration for the generation of a population with a high percentage of $FoxP3^+$ cells in the Tg4 model.

Firstly, it was clear that CAL101 increased the selective survival of $FoxP3^+$ cells at the higher doses of antigen, as evidence by the percentage of $FoxP3^+$ cells across the different peptide concentrations compared with the DMSO control (Fig. 3.10A). The low peptide concentration of 0.1μg/ml 4K gave rise to the highest percentage of $CD25^+FoxP3^+$ Tregs in the cultures treated with CAL101 (Fig. 3.10B, i) or DMSO (Fig. 3.10B, ii); however, the lack of TIGIT did not affect the ability of naïve $CD4^+$ T cells to acquire FoxP3 expression under polarising conditions. The same observation was true when the MFI of FoxP3 was assessed in cultures with (Fig. 3.10C, i) or without (Fig. 3.10C, ii) CAL101. Therefore, from the data presented in the paragraphs above, it becomes clear that TIGIT does not play a role in the phenotype of either *in vivo*-generated CD4tol cells or *in vitro*-generated iTregs.

**Fig 3.10: TIGIT is dispensable for the generation of iTregs** (Continued on the next page)

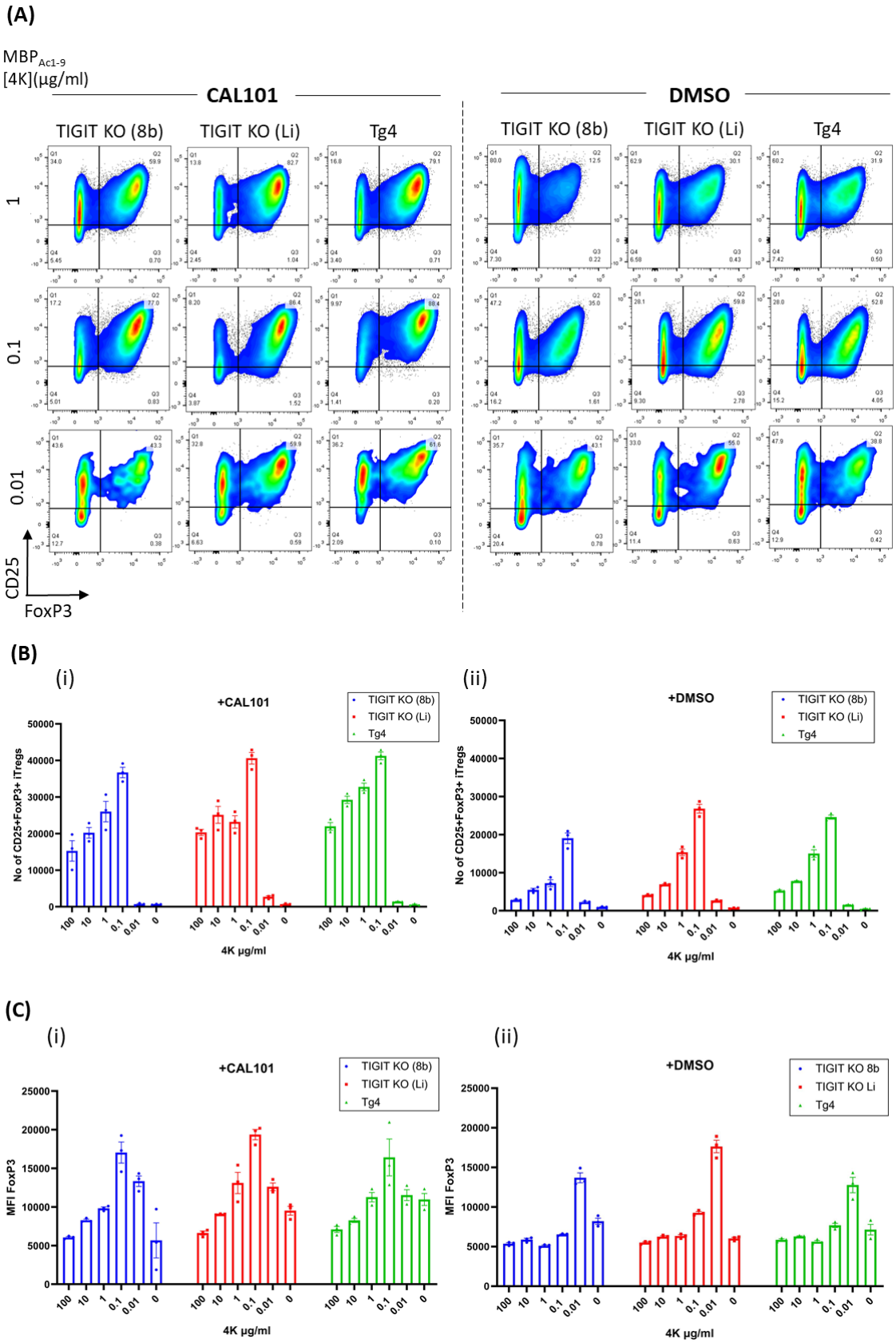


**Fig. 3.10: TIGIT is dispensable for the generation of iTregs.** Splenocytes were cultured in the presence of CAL101 (10nM) or DMSO, TGF-β (10ng/ml) IL-2 (100U/ml) and $MBP_{Ac1-9}$ [4K] (titration) for 7 days and the culture was further supplemented with TGF-β (2ng/ml) and IL-2 (20U/ml) on day 2 and day 4. On day 7, cells were surface stained for anti-CD4 AF700, anti-CD25 BV650 and ef780 (viability dye), fixed, permeabilised and stained intracellularly with anti-FoxP3 PE-Texas Red. **(A)** Representative FACS plots of FoxP3 and CD25 expression of live $CD4^+$ T cells from either $TIGIT^{-/-}$ or Tg4 mice that have been treated with either CAL101 (left panel) or DMSO (right panel). Results are representative of three independent experiments showing similar results. **(B)** Absolute numbers of $CD25^+FoxP3^+$ iTregs after treatment with CAL101 (i) or DMSO (ii). **(C)** Mean fluorescence intensity (MFI) of FoxP3 as measured on $CD4^+$ live cells that have been treated with CAL101 (i) or DMSO (ii). Fluorescence intensity was measured on a BD LSR II flow cytometer (BD) and analysed using Flowjo (Tree Star, Inc.) FACS analysis software. Bar graphs display individual and mean average values of 3 mice per group (SEM), collated from 3 independent experiments. Statistical significance calculated by two-way ANOVA with Dunnett's multiple comparisons between the CD4tol cells from the two TIGIT knock out strains and the CD4tol cells from the Tg4 control. Non-statistically significant changes were accepted where $p>0.05$ (no *).

## 3.6 TIGIT is dispensable for the suppressive capacity of different regulatory T cells

With the previous experiments, the generation and phenotype of CD4tol and iTregs was assessed in relation to TIGIT expression, in a first, exploratory attempt to identify the involvement of TIGIT in different pathways implicated in the maintenance of immune tolerance. To expand this analysis further, we were keen to assess the function of regulatory cells that did not express TIGIT and study their suppressive capacity in an *in vitro* setting.

Different regulatory T cell populations (CD4tol, iTregs, 4Y-treated FoxP3$^+$ Tregs) were co-cultured with Cell Trace Violet (CTV)-stained CD4$^+$ T cells from the 2D2 mouse, another transgenic mouse, in which CD4$^+$ T cells recognise the MOG$_{35-55}$ peptide. (C57BL/6 x B10.PL) F1 splenocytes that are able to present both MBP$_{Ac1-9}$ and MOG$_{35-55}$ were used as APCs and both peptides were added in culture to stimulate both 2D2 responders and Tg4 putative suppressors. This *in vitro* system allows the study of bystander suppression mechanisms and is described more extensively in Chapter 4. However, it is introduced here for the first time since this system allowed us to assess the contribution of TIGIT towards bystander suppression mediated by regulatory T cells *in vitro*.

### 3.6.1 Evaluation of the suppressive capacity of TIGIT$^{-/-}$ iTregs, CD4tol and 4Y-treated FoxP3$^{+}$ Tregs

The different putative suppressors were co-cultured with 2D2 responder cells at different cell ratios for 3 days, and proliferation and activation of CD4$^{+}$Vβ11$^{+}$CTV$^{+}$ 2D2 cells were assessed by flow cytometry. In the presence of iTregs from TIGIT KO mice (either 8b or Li), around 20% of 2D2 cells remained undivided and this percentage dropped proportionally to the number of iTregs added in culture (Fig. 3.11A, i). Similar percentages of undivided 2D2 cells were observed in the presence of iTregs from the Tg4 control and the differences between TIGIT KO and Tg4 iTregs were not statistically significant. This effect was also reflected on the activation status as measured by the activation markers CD25 (Fig. 3.11B, i) and CD69 (Fig. 3.11B, ii) expressed on 2D2 cells in the presence of iTregs. Again, the suppression of the activation markers was proportional to the iTreg cell number, since there was a lower percentage of either CD25$^{+}$ or CD69$^{+}$ 2D2 cells at the highest ratio (1:1) and it titrated out when iTreg:2D2 ratios dropped to 1:4; however, the level of suppression observed was not altered in TIGIT$^{-/-}$ iTregs.

Furthermore, the ability of TIGIT$^{-/-}$ CD4tol cells to mediate bystander suppression was investigated in the same setting. Unsurprisingly, in the presence of both TIGIT KO CD4tol cells and Tg4 CD4tol cells, around 80% of 2D2 cells remained undivided at the highest ratio (1:1) and this percentage dropped down in a proportional manner to the number of CD4tol cells added in the culture (Fig. 3.11A, ii). Finally, the percentage of CD25$^{+}$ (Fig. 3.11C, i) and CD69$^{+}$ (Fig. 3.11C, ii) 2D2 cells was almost identical in the presence of either TIGIT KO or Tg4 CD4tol cells.

**Fig. 3.11: TIGIT is dispensable for the suppressive capacity of CD4tol and iTregs**
(Continued on the next page)

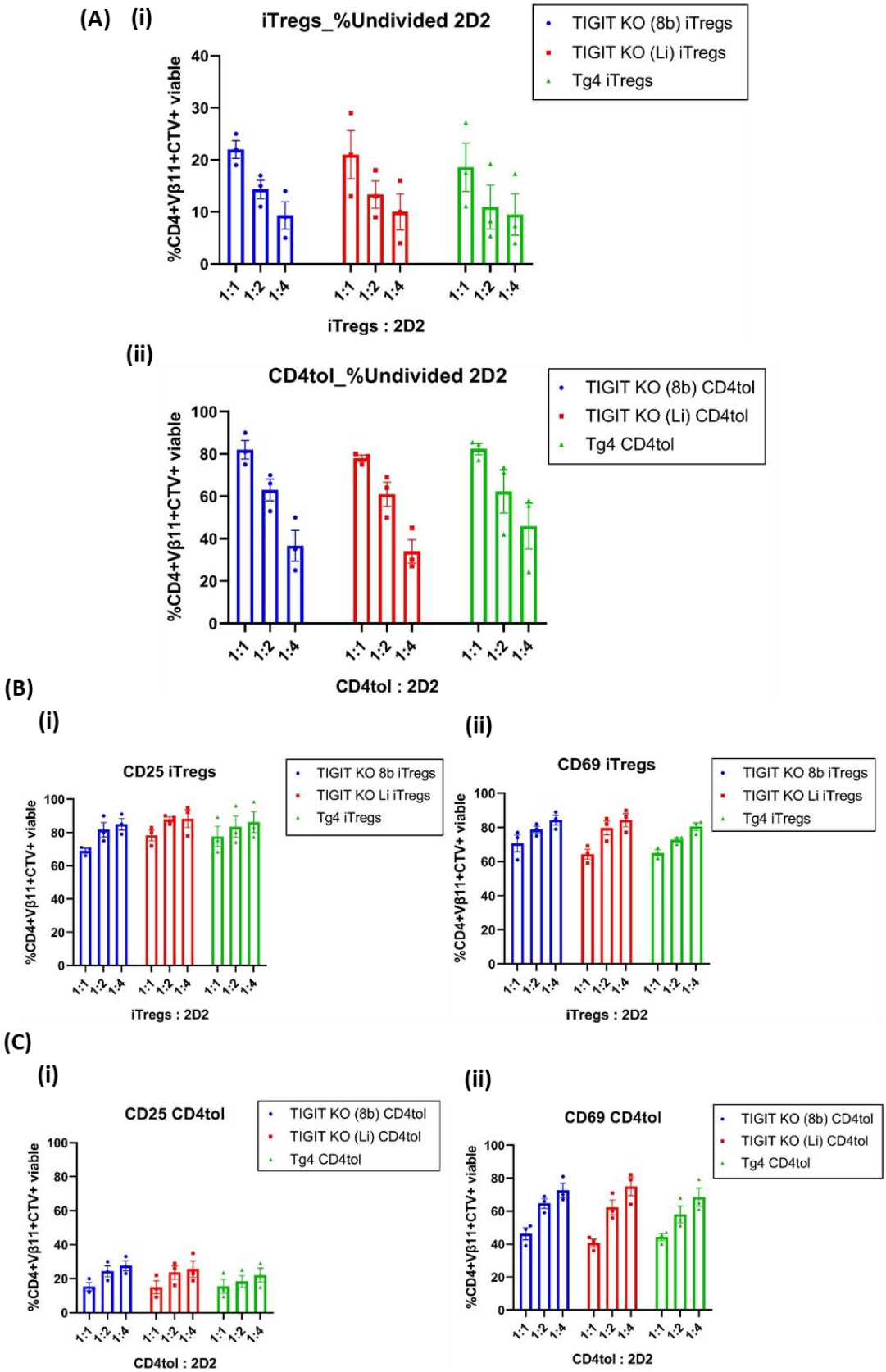


**Fig. 3.11 : TIGIT is dispensable for the suppressive capacity of CD4tol and iTregs. (A)** iTregs (i) or CD4tol cells (ii) derived from either the two different TIGIT KO strains (8b, Li) or the Tg4 control were co-cultured with different ratios of CTV-stained 2D2 $CD4^+$ responder T cells in the presence of (C57BL/6 x B10.PL) F1 splenocytes and 100µg/ml $MOG_{35-55}$ and 100µg/ml $MBP_{Ac1-9}$ separate peptides. After 3 days of culture, proliferation of 2D2 cells was assessed through measurement of CTV levels by flow cytometry. **(B)** The activation profile of 2D2 $CD4^+$ T cells was evaluated after 3 days of co-culture with different rations of iTregs and the levels of CD25 (i) and CD69 (ii) were measured on the surface of $CD4^+V\beta11^+CTV^+$ 2D2 cells. Bar graphs display individual and mean average values of 3 mice per group (SEM), collated from 3 independent experiments. Statistical significance calculated by two-way ANOVA with Dunnett's multiple comparisons between the CD4tol cells from the two TIGIT knock out strains and the CD4tol cells from the Tg4 control. Non-statistically significant changes were accepted where $p>0.05$ (no *).

In addition to total CD4tol cells, which consist of both $FoxP3^+$ and $FoxP3^-$ populations of 4Y-treated $CD4^+$ T cells, we wanted to specifically look at the role of TIGIT on 4Y-treated $FoxP3^+$ Tregs, which is a subpopulation of CD4tol cells. These cells are proven to be highly suppressive, as demonstrated in further detail in the next chapter; therefore, we wanted to study a potential role of TIGIT on these potent suppressors.

To study these cells, a fraction of the culture was stimulated with PMA and Ionomycin and stained for surface markers as well as intracellular FoxP3 and IL-10 (Fig. 3.12A, i). The difference between the levels of FoxP3 (Fig. 3.12A, ii) and IL-10 (Fig. 3.12A, iii) between TIGIT KO and Tg4 mice was not significant. When these cells were added in co-culture with 2D2 responders, a strikingly high percentage of responder cells (approximately 95%) remained undivided both with TIGIT KO and Tg4 Tregs from 4Y-treated Tg4 mice at a 1:1 ratio (Fig. 3.12B).

In line with this phenotype, in the presence of 4Y-treated Tregs, only 20% of 2D2 cells expressed CD25 (Fig. 3.12C, i) and 40% of 2D2 cells expressed CD69 (Fig. 3.12C, ii) at different ratios of responder to suppressor cells. Taken together, it appears that TIGIT deficiency does not have an impact on the suppressive capacity of CD4tol, iTregs or 4Y-treated Tregs in the context of bystander suppression.

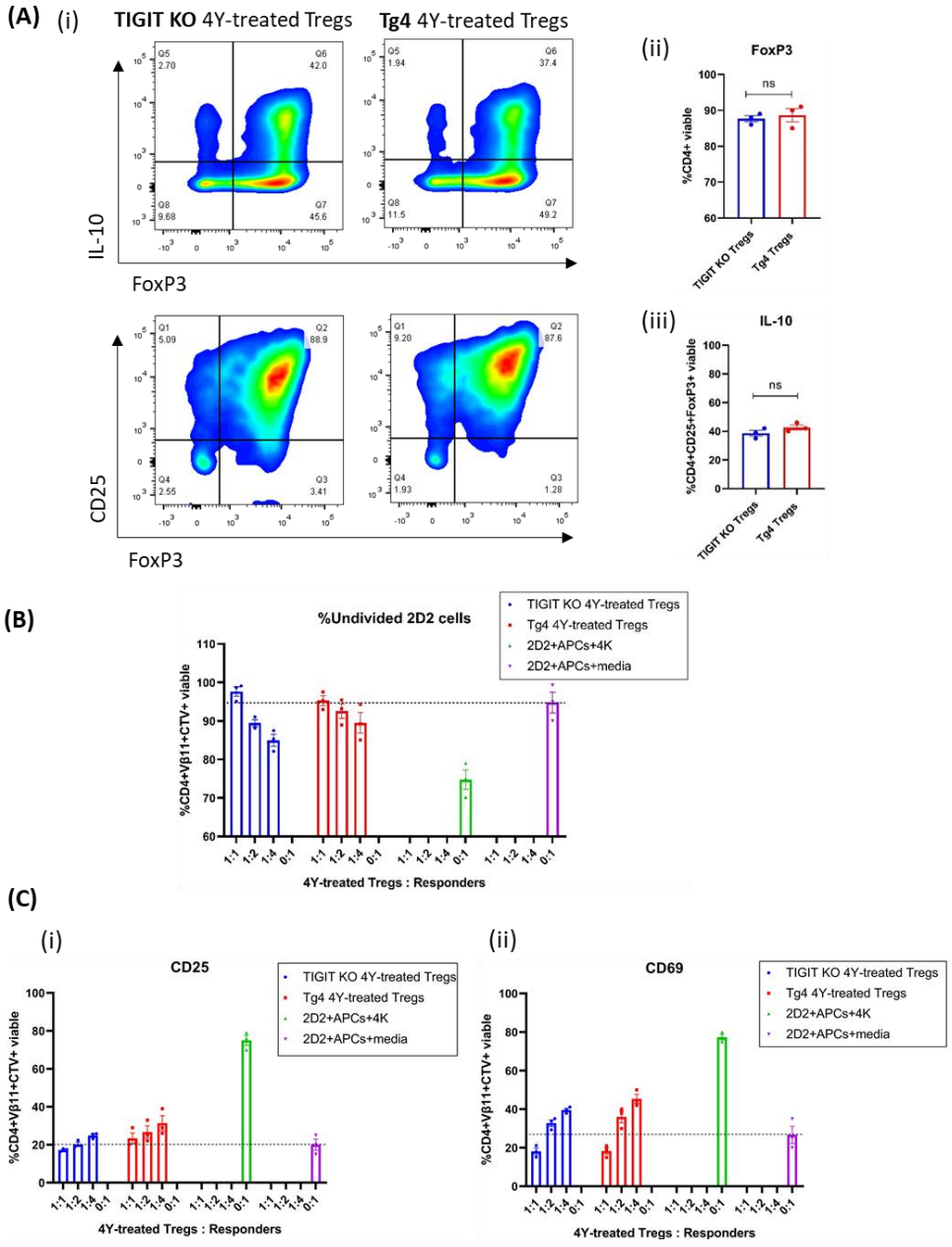



**Fig. 3.12: TIGIT does not play a role in the suppressive capacity of tolerised FoxP3⁺ Tregs. (A)** TIGIT KO or Tg4 mice were injected with increasing doses of 4Y peptide and spleens were harvested three days after the final dose and $CD4^+CD25^+$ Tregs were isolated. A fraction of the cells was stimulated with P/I for 4h and stained for surface and intracellular markers. Representative FACS plots slowing expression of CD25, FoxP3 and IL-10 (i) and corresponding graphs summarising the % of $CD4^+$ viable cells expressing FoxP3 (ii) and % of $CD4^+CD25^+FoxP3^+$ Tregs expressing IL-10 (iii). **(B)** Tregs from either TIGIT KO or Tg4 mice were co-cultured at different cell ratios with CTV-stained $CD4^+$ 2D2 responder cells in the presence of (C57BL/6 x B10.PL) F1 APCs for 3 days. Responder cells were analysed for proliferation by CTV dilution by flow cytometry. (C) Graphs summarising the percentage of CD4+Vβ11+CTV+ 2D2 cells expressing CD25 (i) and CD69 (ii). Bar graphs display individual and mean average values of 3 mice per group (SEM), collated from 2 independent experiments. Statistical significance calculated by two-way ANOVA with Dunnett's multiple comparisons between the CD4tol cells from the T|IGIT KO and the CD4tol cells from the Tg4 control. Non-statistically significant changes were accepted where $p>0.05$ (no * or ns).

### 3.6.2 Impact of TIGIT on the ability of responder cells to produce pro- or anti-inflammatory cytokines *in vitro*

To be able to give a complete functional characterisation of TIGIT$^{-/-}$ regulatory T cells, we were keen to assess the ability of Tg4-derived TIGIT$^{-/-}$ Tregs to influence cytokine production by T effector cells of different antigen specificity (2D2 cells). We chose the 4Y-treated Tregs as a representative population of regulatory T cells since this population was highly suppressive *in vitro*. The level of each cytokine was measured by both sandwich ELISA in the culture supernatants following peptide stimulation with $MBP_{Ac1-9}$ and $MOG_{35-55}$ (Fig. 3.13, right column), and intracellular cytokine staining following stimulation of cells with PMA and Ionomycin (Fig. 3.13, left column).

In the presence of either TIGIT KO or Tg4 FoxP3$^+$ Tregs, the levels of pro-inflammatory cytokines, IFN-γ (Fig. 3.13A, i and ii) and IL-2 (Fig. 3.13B, i and ii), as well as the levels of anti-inflammatory cytokine, IL-10 (Fig. 3.13C, i and ii) were very similar. The condition where 2D2 responders were cultured with F1 APCs and medium alone (dotted line in the graphs) was used as a control to set the threshold for cytokine production following TCR stimulation. Even though there was a clear titration in the production of IFN-γ and IL-2, which was inversely proportional to the number of FoxP3$^+$ Tregs added in culture, while for IL-10 the correlation was directly proportional, the difference between TIGIT-deficient and TIGIT-sufficient 4Y-treated FoxP3$^+$ Tregs was not significant.

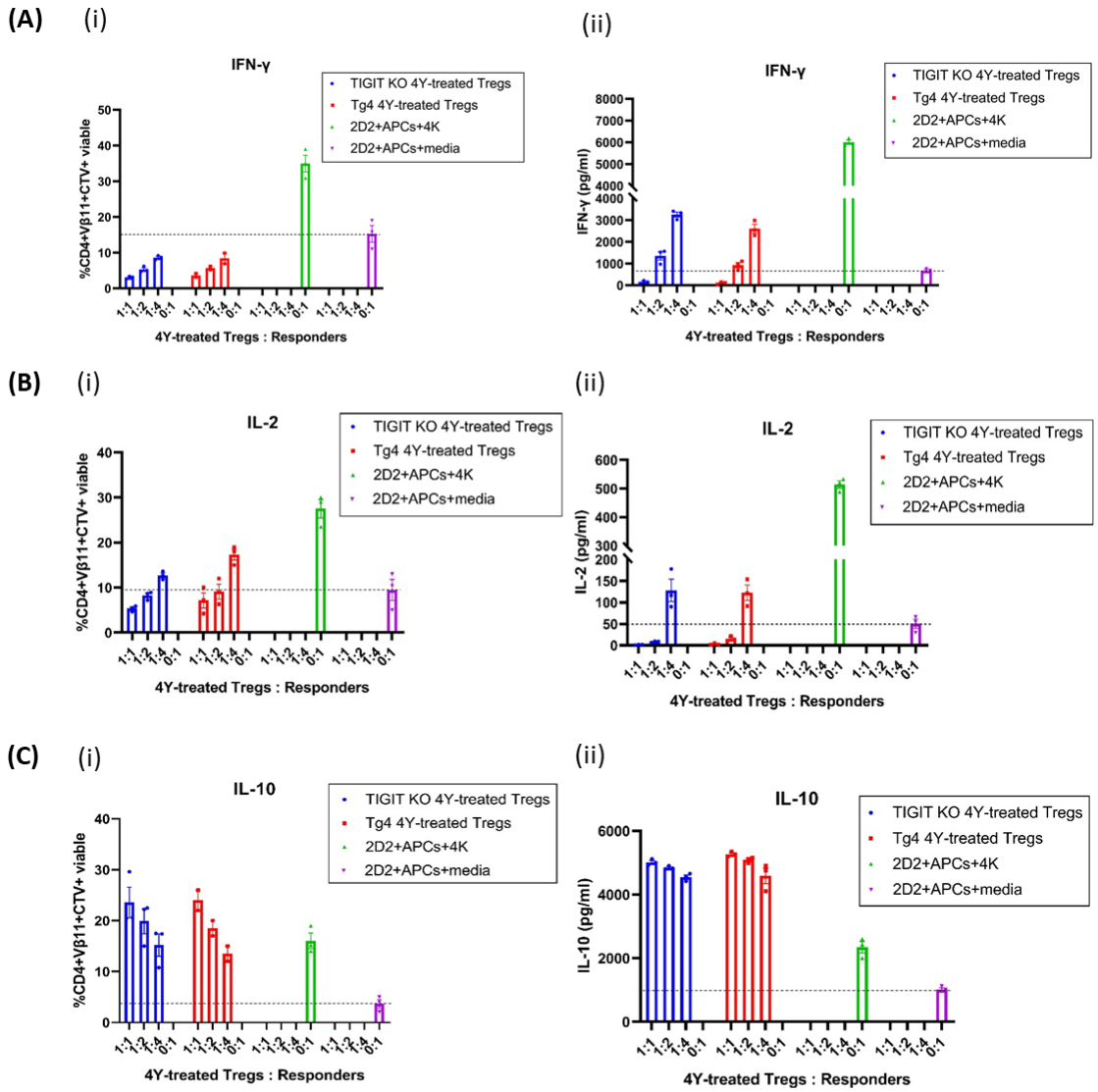



**Fig. 3.13: The absence of TIGIT does not interfere with the ability of responder cells to produce pro- or anti-inflammatory cytokines.** Tregs from either TIGIT KO or Tg4 mice were co-cultured at different cell ratios with CTV-stained $CD4^+$ 2D2 responder cells in the presence of (C57BL/6 x B10.PL) F1 APCs for 3 days. Supernatants were collected and cytokine levels were measured by ELISA. Cells were stimulated with P/I, stained intracellularly for each cytokine and analysed by flow cytometry. **(A)** Graphs showing IFN-γ production by $CD4^+V\beta11^+CTV^+$ responder cells following P/I stimulation (i) or in culture supernatants following peptide stimulation (ii) at different cell ratios. **(B)** Graphs summarising IL-2 production by responder cells (i) or in culture supernatants (ii). **(C)** IL-10 levels produced by responder cells (i) or in cell culture supernatants (ii). Bar graphs display individual and mean average values of 3 mice per group (SEM), collated from 2 independent experiments. Statistical significance calculated by two-way ANOVA with Dunnett's multiple comparisons between the CD4tol cells from the T|IGIT KO and the CD4tol cells from the Tg4 control. Non-statistically significant changes were accepted where $p>0.05$ (no * or ns).

## 3.7 The role of TIGIT in the T-cell mediated inhibition of dendritic cell maturation

Regulatory T cells can exert their suppressive phenotype either directly on other T cells or indirectly by modulating the maturation of dendritic cells and compromising their ability for antigen presentation that would subsequently initiate an immune response. To investigate the impact of TIGIT-deficient regulatory T cells on DC maturation, an overnight co-culture of the putative suppressors with splenic $CD11c^+$ DCs was set up. The following day, levels of co-stimulatory molecules, such as CD80, CD86, CD40 and MHC II were assessed on the surface of $CD3^-CD19^-CD11c^+$MHC $II^+$ viable DCs (Fig. 3.14A), and pro- or anti-inflammatory cytokines were measured in culture supernatants (Fig. 3.15).

Interestingly, in the presence of CD4tol cells, both CD80 (Fig. 3.14B, i) and CD86 (Fig. 3.14B, ii) were significantly downregulated compared to naïve $CD4^+$ T cells that acted as a positive control; however, there was no difference in the levels of suppression between TIGIT KO and Tg4 CD4tol cells or iTregs. Furthermore, MHC II (Fig. 3.14B, iii) and CD40 (Fig. 3.14B, iv) were not influenced by the presence of CD4tol cells or iTregs coming from either TIGIT KO mice or Tg4 controls. Finally, the levels of IL-10 or IL-12 were measured in the cell culture supernatants in the presence of different regulatory T cell populations. Consistent with all the previous data shown in this chapter, no difference was observed between TIGIT KO and Tg4 CD4tol or iTregs in terms of IL-10 production, both after stimulation with 100μg/ml 4K (Fig. 3.15A, i) or without antigen (Fig. 3.15A, ii). Moreover, levels of the pro-inflammatory cytokine, IL-12 were very similar between the TIGIT-deficient iTregs and CD4tol cells and Tg4 controls after stimulation with 100μg/ml 4K (Fig. 3.15B, i) or without antigen (Fig. 3.15B, ii).

**Fig. 3.14** (Continued on the next page)

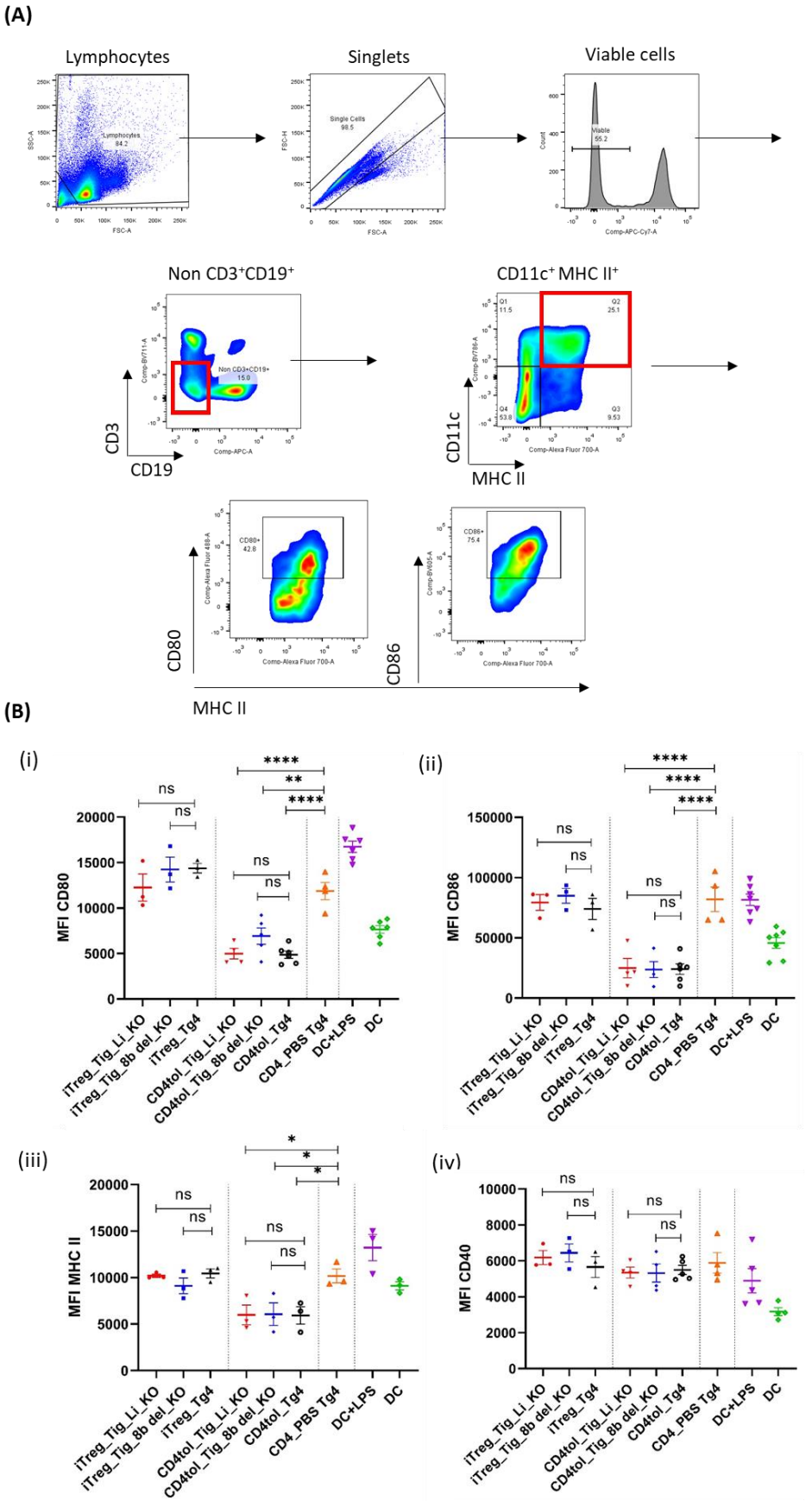


**Fig. 3.14: The absence of TIGIT does not interfere with the ability of CD4tol cells or iTregs to modulate DC maturation. (A)** Gating strategy applied for analysis of expression of molecules on DCs after overnight co-culture with the different regulatory T cells. **(B)** Graphs showing the mean fluorescence intensity (MFI) of CD80 (i), CD86 (ii), MHC II (iii) and CD40 (iv) on $CD11c^+$ DCs. Bar graphs display individual and mean average values of 3 mice per group (SEM), collated from 3 independent experiments. Statistical significance calculated by two-way ANOVA with Dunnett's multiple comparisons between the iTregs or CD4tol cells deriving from either the two TIGIT knock out strains (referred to as Tig_Li_KO or Tig_8b del_KO) or the Tg4 control and naïve Tg4 cells (CD4_PBS) that were used as a positive control. DCs alone were used as a control to set the baseline expression of co-stimulatory molecules without stimulation, and DCs with LPS were used as a positive control for expression of these markers under strong stimulatory conditions and they were excluded from the statistical analysis. Non-statistically significant changes were accepted where $p>0.05$ (no * or ns).

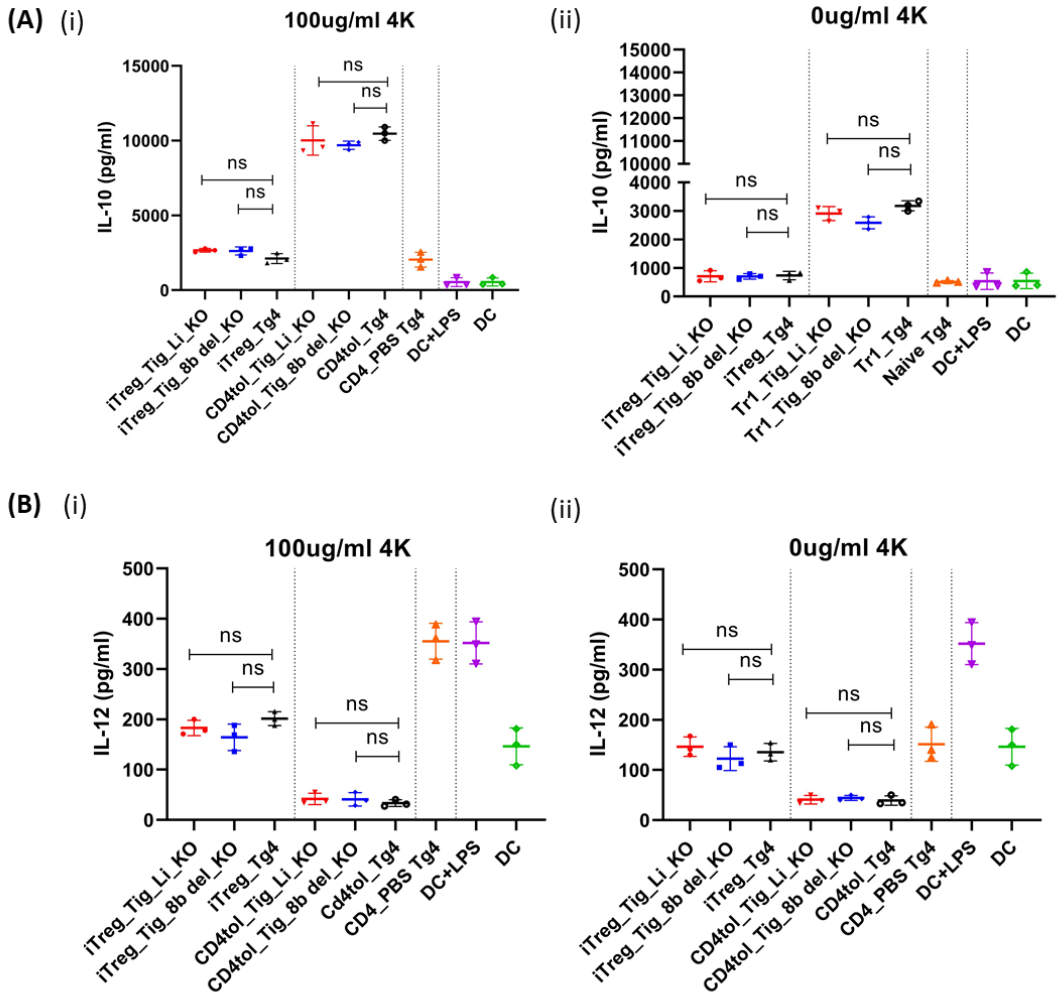



**Fig. 3.15: The absence of TIGIT does not interfere with cytokine production from CD4tol cells or iTregs in co-cultures with dendritic cells.** Cell culture supernatants were collected 24h after co-culture of different regulatory T cell populations with DCs and pro- and anti-inflammatory cytokines were measured by sandwich ELISA according to the manufacturer's instructions. **(A)** Summarising graphs demonstrating the levels of IL-10 production (pg/ml) after stimulation with 100µg/ml 4K (i) or without antigen (ii). **(B)** Summarising graphs demonstrating the levels of IL-12 production (pg/ml) after stimulation with 100µg/ml 4K (i) or without antigen (ii). Bar graphs display individual and mean average values of 3 mice per group (SEM), collated from 3 independent experiments. Statistical significance calculated by two-way ANOVA with Dunnett's multiple comparisons between the iTregs or CD4tol cells deriving from either the two TIGIT knock out strains (referred to as Tig_Li_KO or Tig_8b del_KO) or the Tg4 control and naïve Tg4 cells (CD4_PBS) that were used as a positive control. DCs alone were used as a control to set the baseline expression of co-stimulatory molecules without stimulation, and DCs with LPS were used as a positive control for expression of these markers under strong stimulatory conditions and they were excluded from the statistical analysis. Non-statistically significant changes were accepted where $p>0.05$ (no * or ns).

## 3.8 Discussion

Co-inhibitory receptors play a pivotal role in the negative feedback regulation of immune responses and the perturbation in their expression can give rise to immune-mediated pathologies (Zhang and Vignali, 2016; Nagai, 2020). While it is well established that prolonged expression of co-inhibitory receptors can result in the progression of chronic inflammatory diseases, the downregulation of T cell activation mediated by these co-inhibitory pathways can also function as a safety switch to provide protection against excessive immune responses (Thaventhiran, 2013). TIGIT belongs to the family of co-inhibitory receptors and acts as a critical immune checkpoint for limiting both $CD4^+$ T cell-driven inflammation and $CD8^+$ T cell-dependent anti-tumour immunity (Johnston et al., 2014).

TIGIT has been studied extensively as a promising target in cancer immunotherapy, since it is an instrumental inhibitor of anti-tumour responses that can hinder multiple steps of the cancer immunity cycle (Ge et al., 2021). In particular, TIGIT overexpression was found in the tumour microenvironment and was strongly associated with immune escape and poor prognosis in several types of tumours, such as lung (Sun et al., 2020), kidney (Dai et al., 2021), liver (Liu et al., 2019), glioma (Hung et al., 2018), melanoma (Chauvin et al., 2015), colorectal carcinomas (Masson et al., 2001), neuroblastomas (Tahara-Hanaoka et al., 2006), and gastric cancer (Castriconi et al., 2004).

Intriguingly, utilising a transgenic mouse that has cells that specifically recognise the hepatitis B surface antigen (HBsAg), Zong and colleagues showed that the absence of TIGIT can result in a breach in peripheral tolerance that can eventually lead to chronic hepatitis and liver fibrosis mediated by $CD8^+$ cytotoxic T lymphocytes (CTLs)

(Zong et al., 2019). Conversely, overexpression of TIGIT on PBMCs marked a state of **T cell dysfunction or exhaustion**, characterised by significantly high numbers of $TIGIT^{+}PD\text{-}1^{+}CD8^{+}$ T cells in patients suffering with chronic lymphocytic leukaemia (CLL) compared to healthy controls (Hajiasghar-Sharbaf et al., 2021). Interestingly, in the field of cancer immunotherapy, several clinical trials have studied blocking monoclonal antibodies (mAbs) against TIGIT either as a monotherapy (Sanchez-Correa et al., 2019), or in combination with anti-PD1/PD-L1 mAbs for the treatment of solid malignancies (Raphael et al., 2021; Xiao et al., 2021; Banta et al., 2022), with a promising recent first-in-human phase 1 study in non-small-cell lung cancer patients (Niu et al., 2022). In addition to its well-documented role in cancer immunity, TIGIT has been also implicated in the control of immune pathology during influenza and chronic viral infection with LCMV (Schorer et al., 2020), HIV-1 (Holder and Grant, 2020) or human retrovirus (Yasuma-Mitobe and Matsuoka, 2018).

Even though there is a solid body of evidence in the literature to support the implications of TIGIT in cancer and viral immunity, there is still a gap of knowledge on its role in $CD4^{+}$ T cells and its implications in the regulation of autoimmunity. It has been previously shown that TIGIT is constitutively expressed on Tregs even at steady-state (Kurtulus et al., 2015), enabling them to acquire a highly suppressive phenotype and suppress effector T cell responses either in a direct **(T cell intrinsic)** or indirect **(T cell extrinsic, via APCs)** manner. Joller and colleagues, by using agonistic anti-TIGIT mAbs in the absence of any APCs, demonstrated that T cell intrinsic TIGIT signalling can directly inhibit T cell activation and proliferation, by attenuating TCR signalling, (Joller et al., 2011). Interestingly, in these experiments, TIGIT engagement affected the

expression of molecules upstream in the T cell activation process, thus preventing T cell expansion without inducing cells to undergo anergy or deletion from the repertoire.

To further expand on the characterisation of TIGIT on $CD4^+$ T cells, we aimed to study the impact of TIGIT deletion on the development, phenotype, stability, and function of different regulatory T cell populations, such as IL-$10^{high}$FoxP$3^{low}$ CD4tol cells generated *in vivo* by peptide immunotherapy, iTregs generated *in vitro*, and in naturally occurring peripheral $FoxP3^+$ Tregs generated *in vivo* by the same protocol as CD4tol cells. Previous studies with CTLA-4 KO mice in the Tg4 background have shown that CTLA-4 reduces the signalling via TCR and CD28 on developing thymocytes leading to a change in the repertoire of cells selected and in particular, altering the percentage of $FoxP3^+$ cells (Verhagen et al., 2009, 2013). This work has provided the rationale to study the implications of TIGIT deficiency in central tolerance.

Our initial findings confirmed the expression of TIGIT on both thymic and peripheral Tregs. Interestingly, in the TIGIT KO mice, there was a slight upregulation of $FoxP3^+$ Tregs; however, the percentage of these cells was quite low in both TIGIT KO and Tg4 controls (<5% within the $CD4^+$ viable gate), indicating that this difference seen in numbers, even though consistent between different experiments, could be due to limitations of the sensitivity of the staining method. To investigate the properties of thymic Tregs in the TIGIT KO and Tg4 controls, we looked at their proliferative capacity and localisation in the thymus and found no differences that could be attributed to the absence of TIGIT. At that point, the focus of the project was shifting towards a different direction, focusing mainly on studying TIGIT on peripheral tolerance; therefore, additional work on the involvement of TIGIT on thymic selection was not possible.

Notably, ablation of TIGIT can lead to hyperproliferation, inflammation and a significant reduction in IL-10 levels produced by T cells (Lozano et al., 2012). To further understand the impact of TIGIT on T cell intrinsic inhibition of peripherally induced regulatory T cells, we investigated the proliferative capacity and cytokine profile of IL-10-producing CD4tol cells in the Tg4 transgenic model. Previous work from our lab using an $Tg4^{Il10/GFP}$ reporter mouse, established a strong link between the different co-inhibitory receptors, including TIGIT, and IL-10 (Burton et al., 2014). To build upon these observations, we generated CD4tol cells from either TIGIT KO or Tg4 mice and investigated their proliferative capacity upon *in vitro* re-challenge with either the high- or low-affinity MBP analogues, 4Y or 4K, respectively. Addition of external IL-2 also was used as a tool to examine whether TIGIT interferes with TCR signalling in this system and the ability of these cells to restore their state of anergy. Even though it has been reported that TIGIT interferes with TCR signalling (Josefsson et al., 2018), in our system, it appears that TIGIT did not play a role in the proliferative capacity or cytokine profile of expanded CD4tol cells and it did not affect their ability to suppress other T effector cells.

Additionally, TIGIT was studied in the context of iTreg generation, a process dependent both on TCR stimulation and environmental cues, such as provision of TGF-β and IL-2. Again, bulk splenocytes were able to give rise to iTregs, regardless of TIGIT expression and these iTregs had very similar properties in terms of suppressive capacity against other T cells or even DCs. Finally, it has been proposed in the literature that TIGIT is involved in both the establishment and restoration of the suppressive capacity of $FoxP3^+$ Tregs (Lucca et al., 2019); therefore, we were keen to study its role in the highly suppressive population of peptide-treated $FoxP3^+$ Tregs. Data presented in this

chapter demonstrated that both TIGIT-deficient and TIGIT-sufficient 4Y-treated Tregs were able to exert a highly suppressive phenotype *in vitro*. Taking these results together, we can conclude that TIGIT does not play a role in T cell intrinsic suppression mediated by a wide array of regulatory T cell populations derived from the Tg4 mouse.

Moreover, *in vivo* engagement of TIGIT to one of its ligands, CD155, on APCs can result in indirect suppression of T cells mediated by a marked increase in IL-10 production by **tolerogenic DCs** (Zhang et al., 2018; Wang et al., 2018; Yu et al., 2008) , with a concomitant reduction in IL-12, a pro-inflammatory cytokine secreted by APCs upon activation (Chen et al., 2016; Noguchi et al., 2019). TIGIT-deficient regulatory cells were co-cultured with DCs to confirm the hypothesis that TIGIT might interfere with the ability of regulatory T cells to inhibit the maturation of DCs, since it was previously shown that $TIGIT^+$ Tregs are functionally distinct from their $TIGIT^-$ counterparts in terms of *in vitro* suppressive capacity (Joller et al., 2014). To our surprise, TIGIT-deficient CD4tol or iTregs had the same suppressive capacity as their Tg4 counterparts both in terms of ability to suppress CD80 and CD86 on DCs and influence the production of pro-inflammatory cytokine, IL-10, and anti-inflammatory cytokine, IL-12, by DCs.

Although TIGIT deficiency does not lead to spontaneous autoimmunity or tissue inflammation, loss of TIGIT in a genetically susceptible background can result in autoimmune disease as observed in 2D2 X $TIGIT^{-/-}$ mice that developed EAE (Lozano et al., 2012). However, we have not observed any significant difference in the incidence of EAE in the TIGIT knockout Tg4. The difference between our results and those in the 2D2 mouse suggest that TIGIT has a subtle impact on the threshold for T cell activation, which impacts disease susceptibility in the 2D2 mouse but not the Tg4. The extensive work

described in this chapter further shows that TIGIT does not have an essential role in either the differentiation or function of different Treg subsets.

# CHAPTER 4:

# CHARACTERISATION OF THE ROLE OF DIFFERENT REGULATORY T CELLS IN BYSTANDER SUPPRESSION

## 4.1 Introduction

Bystander suppression refers to the phenomenon where T cells specific for antigen A can suppress responses of T cells specific for antigen B either in either a cell-contact mediated (direct) or cytokine mediated (indirect) manner. Suppression against multiple antigens has been observed in various murine models (Miller et al., 1991; Anderton and Wraith, 1998) and has also been reported in clinical setting, where induction of tolerance towards a single antigen can be 'spread' and provide protection against other antigens. However, even though this has been reported as a phenomenon, little is known about the cellular and molecular mechanisms underlying the bystander effect.

Understanding bystander suppression as a means of reducing immune responses to multiple antigens by inducing tolerance to a small number of immunodominant ones would be an extremely powerful tool, which will provide the basis for the application of peptide immunotherapy to a wider range of autoimmune and autoinflammatory conditions. Although several autoantigenic epitopes are well-defined in some autoimmune diseases, including multiple sclerosis (MS), there are other conditions, where we do not know which (if any) of these epitopes are the key targets recognised by T cells initiating and subsequently driving the disease. Therefore, a suppressive T cell population recognising a defined myelin epitope could suppress a proinflammatory population recognising other (perhaps unknown) myelin epitopes if their localisation was sufficiently close. In this way, the need to induce antigen-specific tolerance to each and every antigen involved in the initiation and progression of complex autoimmune diseases can be bypassed.

Transgenic Tg4 mice serve as a good model for studying antigen-specific responses in $CD4^+$ T cells *in vivo*, since the precursor frequency of antigen-specific cells is

sufficiently high to measure the effect of antigen administration directly. Particularly in this murine model, virtually all $CD4^+$ T cells (approximately 95%) can recognise the immunodominant peptide $MBP_{Ac1-9}$. Repeated exposure to increasing doses of the high affinity soluble analogue of this epitope $MBP_{Ac1-9}$ [4Y] can render them tolerant to both $MBP_{Ac1-9}$ and MBP as a whole protein. In addition to the Tg4 model, the transgenic 2D2 model was also used in the experiments described in this chapter, which allowed the assessment of T cell responses towards the immunodominant $MOG_{35-55}$ peptide.

To investigate bystander suppression both *in vitro* and *in vivo*, the F1 generation of wildtype B10.PL and C57BL/6 mice was used. These (B10.PL x C57BL/6) F1 mice, hereafter referred to as F1 strain, carry both MHC Class II molecules $A^u$ and $A^b$. Due to MHC restriction, expression of $A^u$ allows the presentation of the immunodominant epitope of myelin basic protein $MBP_{Ac1-9}$, while $A^b$ expression allows the recognition of the immunodominant epitope of myelin oligodendrocyte glycoprotein epitope $MOG_{35-55}$. Moreover, $MBP_{Ac1-9}$-specific T cells are restricted exclusively to $V\beta8^+$ T cells; however, not all $V\beta8^+$ T cells are specific for $MBP_{Ac1-9}$. Similarly, $MOG_{35-55}$-specific T cells in 2D2 mice all express Vβ11, but not all $V\beta11^+$ T cells are specific for $MOG_{35-55}$. In addition to the wild type (B10.PL x C57BL/6) F1 mice, Tg4 mice were also crossed with C57BL/6 mice to be able to generate a transgenic mouse (Tg4 x C57BL/6) that can be tolerised against $MBP_{Ac1-9}$ and at the same time can recognise $MOG_{35-55}$.

To confirm that in the (B10.PL x C57BL/6) F1 mice there are T cells that recognise both $MBP_{Ac1-9}$ and $MOG_{35-55}$ peptides, tail vain bleeds were stained for TCR Vβ8 and Vβ11 chains, an indication on the existence of cells that carry compatible TCRβ chains for $MBP_{Ac1-9}$ and $MOG_{35-55}$ reactive T cells, respectively. A linked hybrid peptide that contained both $MOG_{35-55}$ and $MBP_{Ac1-9}$ epitopes covalently linked together using a HFFK

linker region, hereafter called $MBP_{Ac1-9}$-$MOG_{35-55}$, was synthesised in order to deliver both antigens on the same APC. This is a great tool to compare T cell responses to $MBP_{Ac1-9}$-$MOG_{35-55}$ where both epitopes are presented to the same APC (linked suppression), vs $MBP_{Ac1-9}$ and $MOG_{35-55}$ delivered separately (*bona fide* bystander suppression). However, it should be noted that even when peptides are given separately, there is a chance that some APCs can capture and present both on their surface.

Chapter aims:

- ✓ Establishment of an *in vitro* system to study bystander suppression
- ✓ Characterisation of the molecular mechanisms underpinning bystander suppression
    - Does bystander suppression rely on antigens being presented in proximity (contact-dependant)
    - Identification of molecules that could contribute to the suppressive capacity
- ✓ Assessment of the impact of regulatory T cells on the maturation of DCs *in vitro*
- ✓ Establishment of an *in vivo* system of bystander and antigen-specific suppression
- ✓ Phenotypic assessment of $CD11c^+$ DCs after tolerance induction *in vivo*

## 4.2 Introduction to the *in vitro* model of bystander suppression: co-cultures of putative suppressive Tg4 T cell populations and 2D2 $CD4^+$ T responder cells

To assess whether we could observe bystander suppressive effects between T cells of different antigen specificities *in vitro*, a series of co-culture experiments was conducted, in which transgenic Tg4 $CD4^+$ T cells ($MBP_{Ac1-9}$-specific) and transgenic 2D2 $CD4^+$ T cells ($MOG_{35-55}$-specific) can be monitored. Figure 4.1A summarises the protocol schematic. Putative suppressor cells were derived from Tg4 mice that were naïve or had been tolerised with repeated s.c. injection of $MBP_{Ac1-9}$ [4Y] peptide prior to splenic $CD4^+$ T cell isolation (hereafter called CD4tol cells) or $CD4^+CD25^+$ T cells isolation ($FoxP3^+$ Tregs).

Alternatively, splenocytes from naïve Tg4 mice were cultured in the presence of TGF-β and IL-2 for one week to give rise to *in vitro*-generated Tregs (iTregs). Furthermore, naïve splenic $CD4^+$ T cells were isolated from 2D2 mice, stained using proliferation dye Cell Trace Violet (CTV) and acted as responder T cells with bulk splenocytes from (B10.PL x C57BL/6) F1 mice used as antigen-presenting cells (APCs). Proliferation of 2D2 $CD4^+$ T cells can be assessed alongside additional activation markers, such as CD25 and CD69, in response to stimulation with antigen (Figure 4.1B).

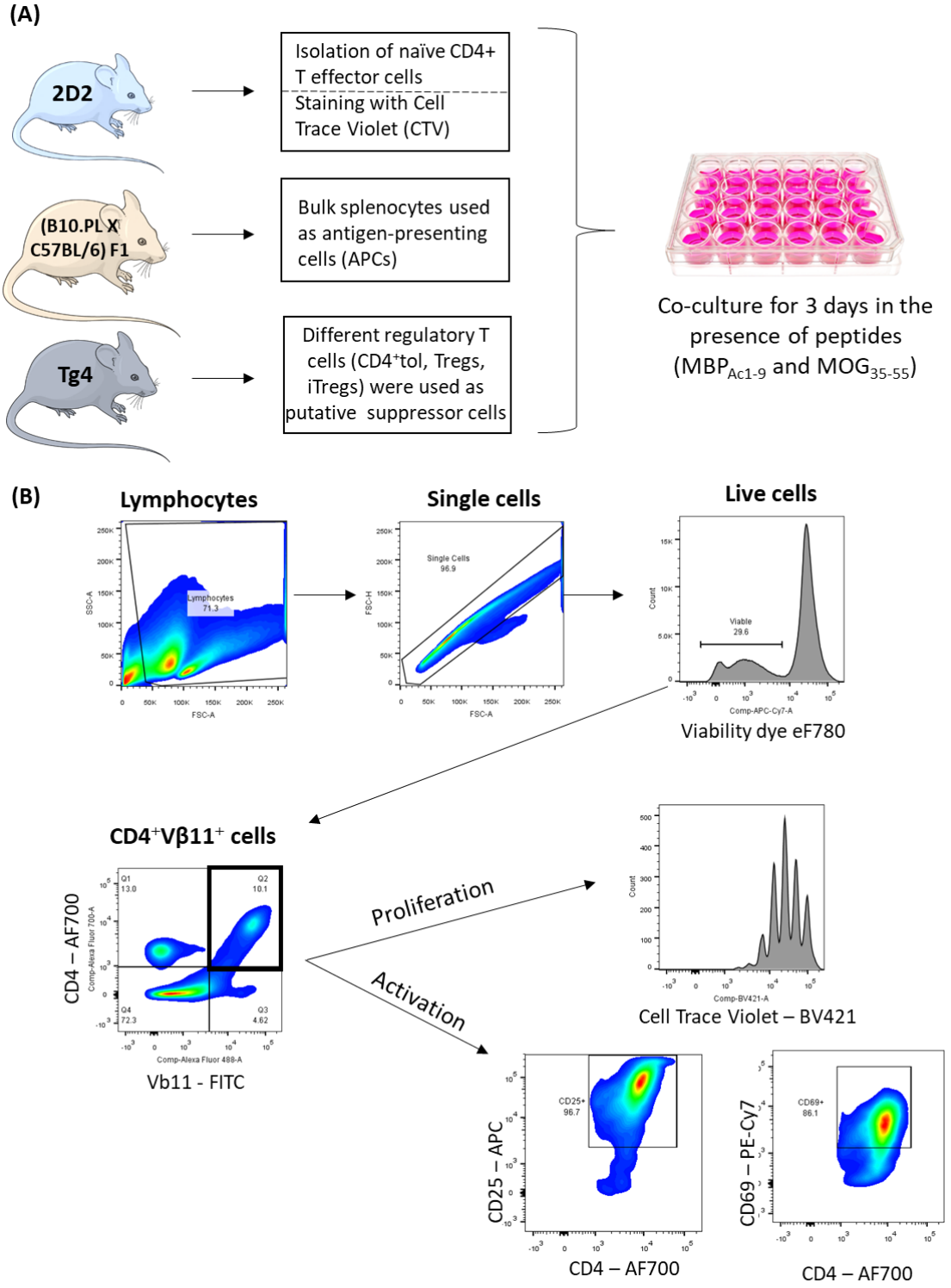



**Fig. 4.1 : Proliferation of $MOG_{35-55}$ specific $CD4^+$ T cells from 2D2 mice can be monitored by Cell Trace Violet *in vitro*. (A)** Regulatory T cells from Tg4 mice, bearing a Vβ8 TCR chain were co-cultured with naïve Cell Trace Violet (CTV)-stained $CD4^+$ T cells from 2D2 mice (Vβ11 TCR chain) and (B10.PL X C57BL/6) F1 splenocytes that served as antigen-presenting cells (APCs). Cells were stimulated with either $MBP_{Ac1-9}$-$MOG_{35-55}$ linked peptide or $MBP_{Ac1-9}$ + $MOG_{35-55}$ separate peptides for 3 days prior to antibody staining and flow cytometry analysis. **(B)** Gating strategy for $V\beta11^+CD4^+$ cells from 2D2 mice, which had been stained for CTV on day 0, cultured for 3 days and subsequently stained with a viability dye (eF780), CD4, Vβ11 and activation markers (CD69, CD25).

Tg4 and 2D2 cells can be distinguished by the presence of TCR genes Vβ8 and Vβ11, respectively. To confirm the antigen-specificity of the cells deriving from these transgenic mice, $CD4^+$ T cells from Tg4 mice were cultured with either $MBP_{Ac1-9}$ or $MOG_{35-55}$ for 3 days in the presence of F1 APCs. As expected, Tg4 cells did not respond to $MOG_{35-55}$ (Fig. 4.2A, i), but did respond by proliferation and upregulation of CD69 when they were stimulated with $MBP_{Ac1-9}$ (Fig. 4.2A, ii). On the other hand, 2D2 cells were able to respond to $MOG_{35-55}$ and proliferate (Fig. 4.2B, i), while they remained undivided upon encounter with $MBP_{Ac1-9}$ (Fig. 4.2B, ii). This indicates that the responses mounted by these cells are antigen specific.

Furthermore, $CD4^+$ T cells from 2D2 mice were cultured with a titration of both the linked $MBP_{Ac1-9}$-$MOG_{35-55}$ peptide (Fig. 4.2C, i) or separate peptides (Fig. 4.2C, ii) to define the optimal dose to use for subsequent *in vitro* assays. It appears that the highest dose (100μg/ml) was optimal for both peptides, since this stimulation allowed the highest percentage of $CD4^+V\beta11^+$ 2D2 T cells to respond and proliferate. Once the peptide dose was defined, both the linked and separate peptides were used in co-cultures with CD4tol putative suppressors and CTV-stained 2D2 responders and F1 APCs to examine whether this *in vitro* system can be used as a reliable readout for suppression.

It was clear that with either linked (Fig. 4.3B, i) or separate (Fig. 4.3B, ii) peptides alone, 2D2 cells were able to proliferate, while upon encounter with CD4tol cells, a great proportion of 2D2 cells remained undivided, especially when stimulated with the linked peptide at the highest CD4tol:2D2 ratio (Fig. 4.3A). For the purposes of this thesis, the focus was to study the mechanisms of bystander rather than linked suppression; therefore, for all the experiments that are described in this chapter, the two separate $MBP_{Ac1-9}$ and $MOG_{35-55}$ peptides were used instead of the linked peptide.

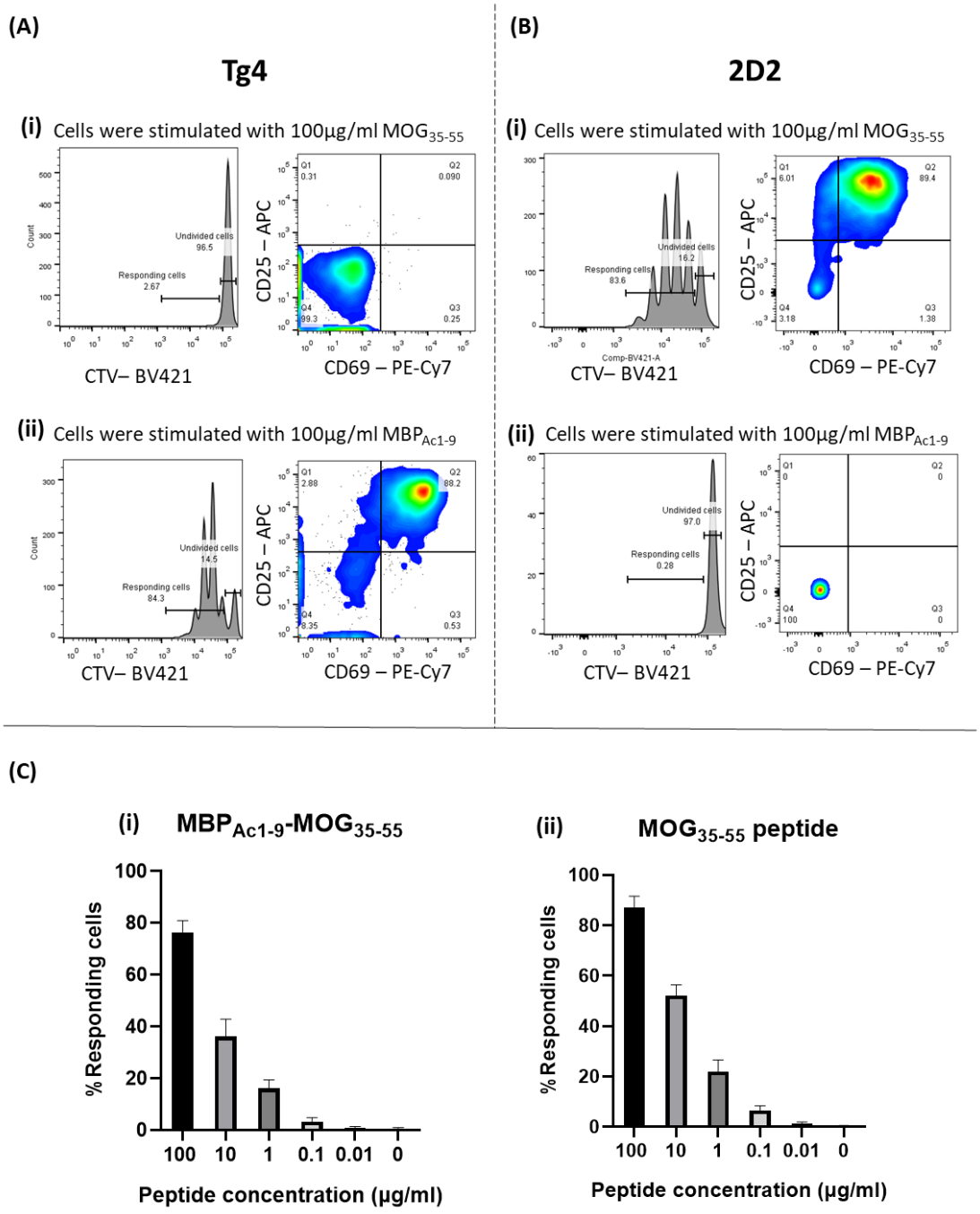



**Fig. 4.2: Tg4 cells are $MBP_{Ac1-9}$-specific, while 2D2 cells are $MOG_{35-55}$-specific and can respond to both linked $MBP_{Ac1-9}$-$MOG_{35-55}$ and $MOG_{35-55}$ at 100µg/ml. (A)** $CD4^+$ T cells from a Tg4 mouse were isolated, stained with CTV and cultured in the presence of either 100µg/ml $MOG_{35-55}$ (i) or 100µg/ml $MBP_{Ac1-9}$ (ii) for 3 days. **(B)** $CD4^+$ T cells from a 2D2 mouse were isolated, stained with CTV and cultured in the presence of either 100µg/ml $MOG_{35-55}$ (i) or 100µg/ml $MBP_{Ac1-9}$ (ii) for 3 days. **(C)** $CD4^+$ T cells from a 2D2 mouse were isolated, stained with CTV and cultured in the presence of different concentrations of either linked $MBP_{Ac1-9}$-$MOG_{35-55}$ (i) or $MOG_{35-55}$ (ii) peptide for 3 days. Results shown are representative of 2 independent experiments.

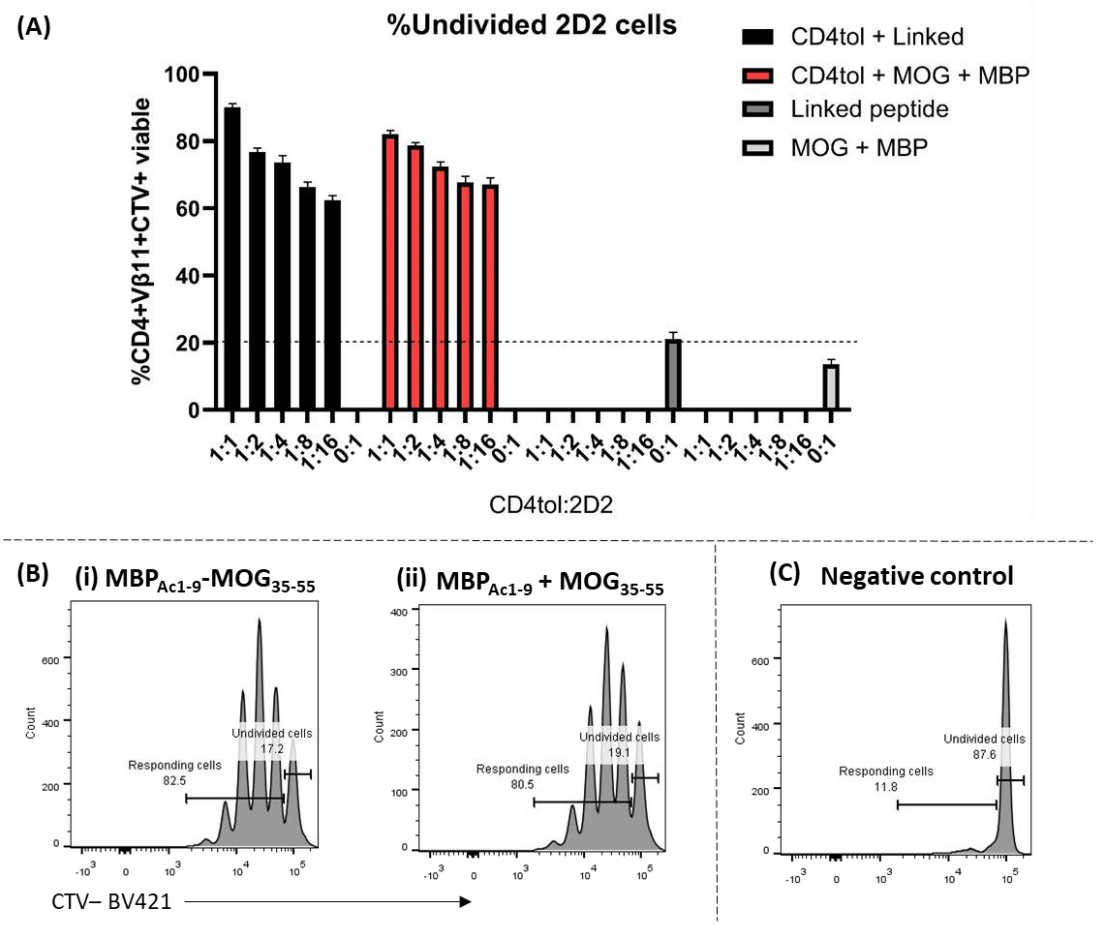



**Fig. 4.3 : Both separate $MOG_{35-55}$ + $MBP_{Ac1-9}$ and linked peptides can stimulate CD4tol and 2D2 cells.** **(A)** CTV-stained $CD4^+$ T cells deriving from a 2D2 mouse were co-cultured with (B10.PL x C57BL/6) F1 cells as APCs and decreasing numbers of Tg4 Cd4tol cells (2-fold dilutions), in the presence of either the linked or the separate peptides at a concentration of 100µg/ml for 3 days. As a positive control, 2D2 cells were stimulated with either 100µg/ml linked or separate peptides in the presence of F1 APCs without CD4tol cells. **(B)** Representative FACS plots of the CTV dilution peaks that demonstrate the proliferation of 2D2 cells following stimulation with the linked (i) or separate (ii) peptides in the absence of CD4tol cells. **(C)** CTV-stained 2D2 $CD4^+$ T cells cultured with F1 APCs in the absence of any peptide were used as negative control.

## 4.3 CD4tol cells are potent mediators of bystander suppression *in vitro*

Our working hypothesis was that regulatory T cells that derive from the Tg4 mouse model and are specific for $MBP_{Ac1-9}$ can exert their suppressive phenotype once activated by their cognate antigen and can subsequently suppress either T cells of different specificity, such as 2D2 cells that are specific for a different myelin epitope, $MOG_{35-55}$ and may modulate the function of dendritic cells (DCs). To test this hypothesis, MBP-specific regulatory T cells (either CD4tol cells or iTregs) were co-cultured with MOG-specific CTV-stained 2D2 cells in the presence of $MBP_{Ac1-9}$ and $MOG_{35-55}$ peptides and F1 APCs that can present both peptides. The impact of each regulatory cell type on 2D2 cells was assessed on day 3 by measuring the levels of proliferation by CTV dilution and activation by measuring the expression of CD25 and CD69.

Interestingly, in the presence of Tg4 CD4tol cells, most of the 2D2 cells ($CD4^+V\beta11^+CTV^+$) remained undivided and this was proportional to the number of CD4tol cells added in culture (Fig. 4.4A – blue line), with the highest ratio of CD4tol cells (i) giving the strongest effect of suppression that titrated down when the number of CD4tol cells was reduced by 2-fold (ii) or 4-fold (iii). In the presence of $FoxP3^+$ iTregs (Fig. 4.4A – red line), 2D2 cells were able to undergo up to 4 cell divisions and only a small percentage remained undivided, and this phenotype was very similar to Tg4 Th1 cells (Fig. 4.4 – green line), which possess effector rather than suppressive properties and were used as a control for the measured effect (suppression). This indicates that CD4tol cells were more successful at mediating bystander suppression compared to iTregs even at lower cell number (Fig. 4.4B). This observation was also reflected by the expression

of CD25 (Fig. 4.4C, i and ii) and CD69 (Fig. 4.4D) whose expression was suppressed on the surface of 2D2 cells that were co-cultured with CD4tol cells, but not iTregs.

**Fig. 4.4 CD4tol cells are potent mediators of bystander suppression** (Continued on the next page)

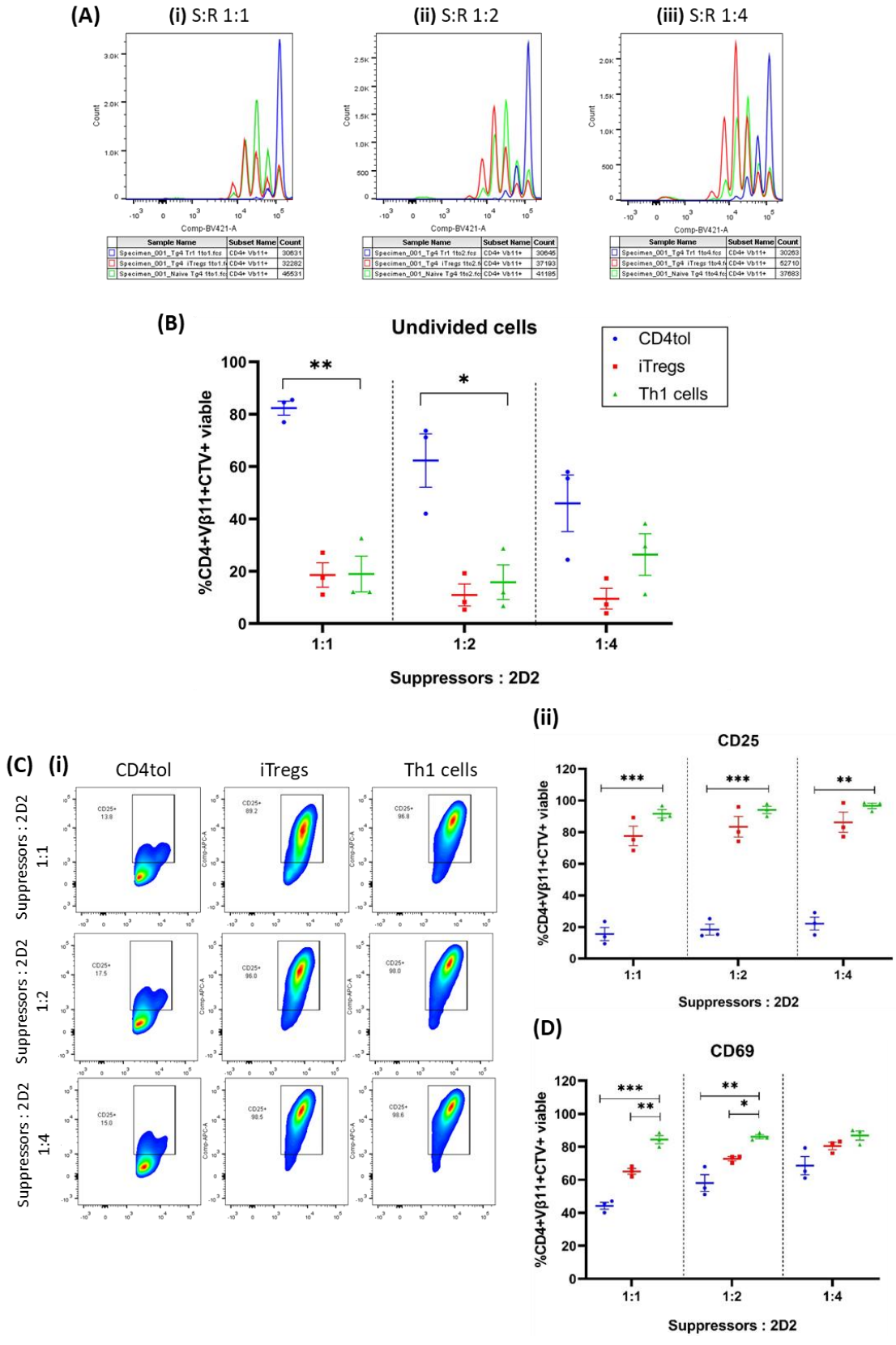


**Fig. 4.4 CD4tol cells are potent mediators of bystander suppression.** Different Tg4-derived regulatory T cells were co-cultured at different ratios with CTV-stained 2D2 $CD4^+$ T cells for 3 days in the presence of separate $MBP_{Ac1-9}$ and $MOG_{35-55}$ peptides and F1 APCs. **(A)** Overlays of CTV peaks of 2D2 cells at a ratio of 1:1 Suppressors: Responders (i), 1:2 (ii) or 1:4 (iii). **(B)** Graph depicting the percentage of 2D2 cells that remained undivided in the presence of each putative suppressor cells. **(C)** Representative FACS plots of CD25 expression by 2D2 cells (i) and graph displaying surface expression of CD25 on 2D2 cells in the presence of decreasing numbers of CD4tol cells (ii). **(D)** Graph displaying CD69 expression on 2D2 cells. Statistical significance calculated by one-way ANOVA with Dunnett's multiple comparisons test of each putative suppressor cells against Th1 cells that were used as negative control for suppression. Results are representative of 3 independent experiments showing similar results and presented as standard error of the mean (SEM).

## 4.4 Requirement for cell-contact for bystander suppression mediated by CD4tol cells *in vitro*

From the initial *in vitro* suppression assays, it was clear that Tg4 CD4tol cells are potent mediators of bystander suppression as they can successfully inhibit the proliferation and activation of effector 2D2 cells. To further elucidate the mechanisms underpinning this phenomenon, a series of experiments was performed to address whether this type of suppression is cell contact-dependent, and which molecules are involved.

### 4.4.1 Antigen presentation by a central APC versus separate APCs

Initially, the bystander assays were set up in the presence of either APCs that can present both antigens on the same, central APC, or separate APCs to examine whether there is a more profound suppressive effect when suppressors and responders come in proximity during antigen-presentation. As a negative control for this experiment, B10.PL ($A^u$) splenocytes were used as APCs, since they can present $MBP_{Ac1-9}$ and activate CD4tol cells; however, they are not able to present $MOG_{35-55}$, therefore 2D2 cells cannot recognise their cognate antigen and remain undivided. (Fig. 4.5A, i).

On the other hand, C57BL/6 ($A^b$) splenocytes can present $MOG_{35-55}$ and activate 2D2 responder cells, but they are unable to present $MBP_{Ac1-9}$ and give a stimulatory signal for CD4tol cells (Fig. 4.5A, ii). This condition was used as a positive control since 2D2 cells were activated and able to proliferate without being influenced by the impact of CD4tol cells. Furthermore, F1 APCs ($A^u$ x $A^b$) can present both peptides on their surface (central APC), bringing 2D2 responders and CD4tol suppressors in proximity during antigen presentation and subsequent activation (Fig. 4.5A, iii). Finally, a combination of B10.PL and C57BL/6 APCs was used to stimulate both suppressors and responders, with

antigen presentation taking place on separate APCs (Fig. 4.5A, iv). In that way, both CD4tol and 2D2 effector cells receive a stimulus, without having to come into contact during TCR activation.

In the presence of B10.PL APCs, most of the 2D2 responder cells remained undivided, regardless of the number of CD4tol cells added in culture (Fig. 4.5B, i) as expected, since CD4tol cells were not able to recognise their cognate antigen. The fact that in the presence of CD4tol cells, there was a slightly higher percentage of undivided cells compared to the control (0:1 - no CD4tol cells added), can be explained by the fact that CD4tol cells can have a residual activity and exert some minor suppressive effect even without TCR stimulation. This observation was also reflected by the activation status, where expression of CD69 on 2D2 cells was only slightly downregulated at a highest ratio of 1:1 (Fig. 4.6A, i), while CD25 expression on 2D2 cells was not affected (Fig. 4.6B, i).

In the presence of C57BL/6 APCs, 2D2 cells were able to respond to $MOG_{35-55}$ and readily start to proliferate since their function was not altered by CD4tol cells, who remained inactivated. Therefore, only a small percentage of 2D2 cells remained undivided in that condition and again, that could be due to some suppressive effect coming from CD4tol cells even when they are not stimulated via their TCR (Fig. 4.5B, ii). Similarly, expression of CD69 was not affected by the presence of CD4tol cells (Fig. 4.6A, ii), while CD25 expression was only inhibited at the highest ratio of CD4tol cells added in culture (Fig. 4.6B, ii).

Interestingly, when both $MBP_{Ac1-9}$ and $MOG_{35-55}$ were presented on the same APC, a great percentage of 2D2 cells remained undivided especially at the highest ratio

of CD4tol cells (>80%) and this effect was directly proportional to the number of CD4tol cells added in culture (Fig. 4.5B, iii). This suppressive effect was also mirrored on the expression of CD69 (Fig. 4.6A, iii) and CD25 (Fig. 4.6B, iii), which were significantly downregulated, highlighting that in the presence of F1 APCs, 2D2 cells can proliferate, as shown by the small percentage of undivided cells in the absence of CD4tol cells (ratio CD4tol: 2D2 0:1), but when 2D2 cells are close to CD4tol cells which have also been activated, a strong suppressive effect occurs (linked suppression).

Intriguingly, when $MPB_{Ac1-9}$ and $MOG_{35-55}$ peptides were presented on different APCs (*bona fide* bystander suppression), there was a significant percentage of 2D2 cells that remained undivided at the highest ratio (approximately 60%) (Fig. 4.5B, iv), and these cells also downregulated both CD69 (Fig. 4.6A, iv) and CD25 (Fig. 4.6B, iv). However, the suppressive effect seen with F1 APCs was much stronger, highlighting that in addition to soluble factors that may be involved in this phenomenon, there is also an element of cell-contact that is required for successful suppression to occur.

**Fig 4.5** (Continued in the next page)

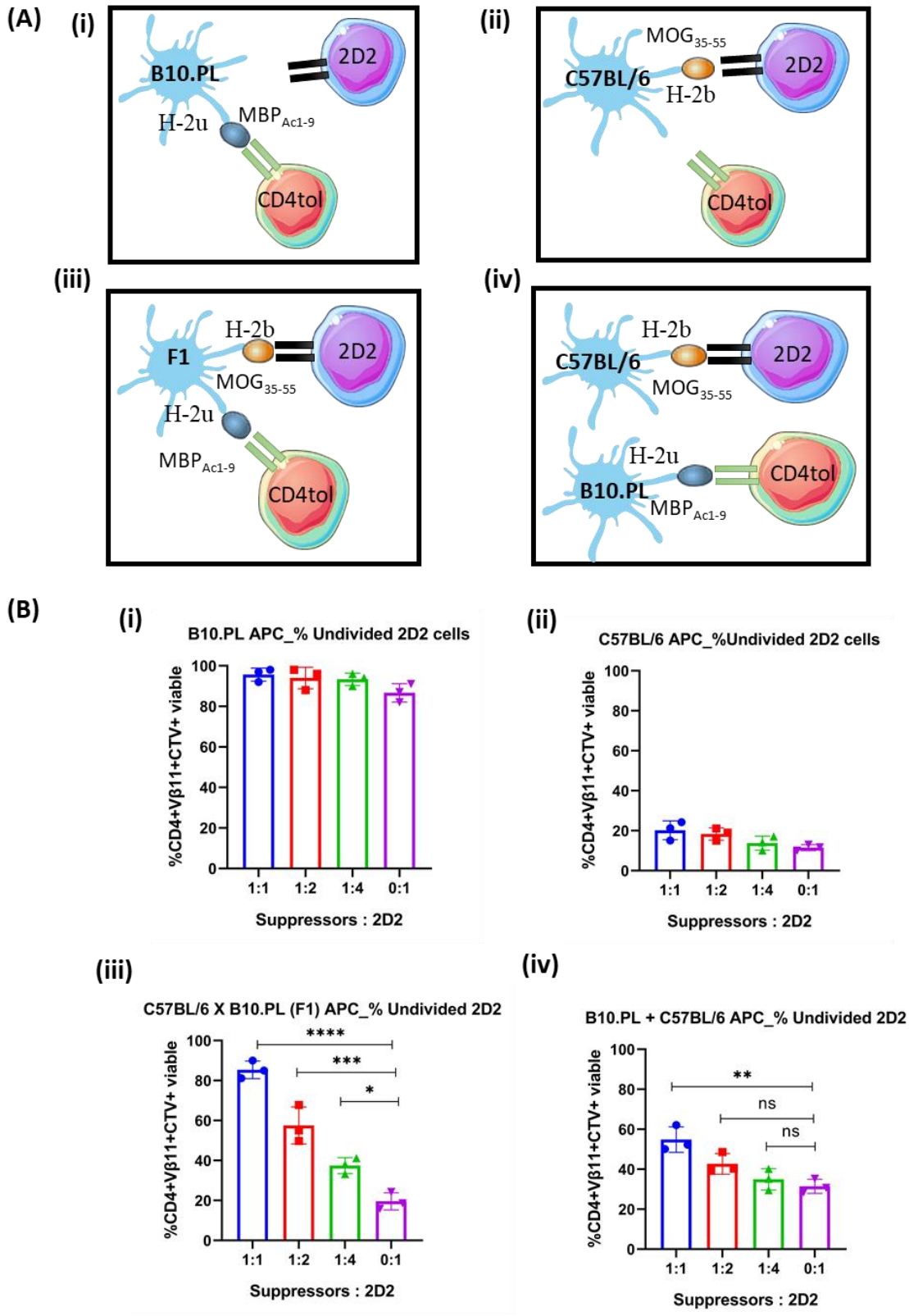


**Fig. 4.5 : (B10.PL x C57BL/6) F1 splenocytes can present both $MBP_{Ac1-9}$ and $MOG_{35-55}$ on the same APC and facilitate the establishment of suppression in a more effective way compared to the combination of B10.PL + C57BL/6. (A)** Schematic representation of the bystander suppression model *in vitro*. (i) B10.PL cells can present $MBP_{Ac1-9}$ and activate CD4tol cells, but they can not present $MOG_{35-55}$. (ii) C57BL/6 cells can present $MOG_{35-55}$ and activate 2D2 cells, but they can not present $MBP_{Ac1-9}$. (iii) F1 APCs can present both antigens on the same APC. (iv) The combination of C57BL/6 and B10.PL cells allows both antigens to be presented, however on different APCs. **(B)** The graphs represent the % of 2D2 cells that remained undivided after 3 days of co-culture with different ratios of Suppressors : 2D2 cells in the presence of 100µg/ml $MOG_{35-55}$ and $MBP_{Ac1-9}$ peptides, presented by B10.PL (i), C57BL/6 (ii), F1 (iii) or C57BL/6 + B10.PL APCs (iv). Statistical significance calculated by one-way ANOVA with Dunnett's multiple comparisons test against the culture condition where no CD4tol cells were added. Results are pooled together from 3 independent experiments and presented as standard error of the mean (SEM).

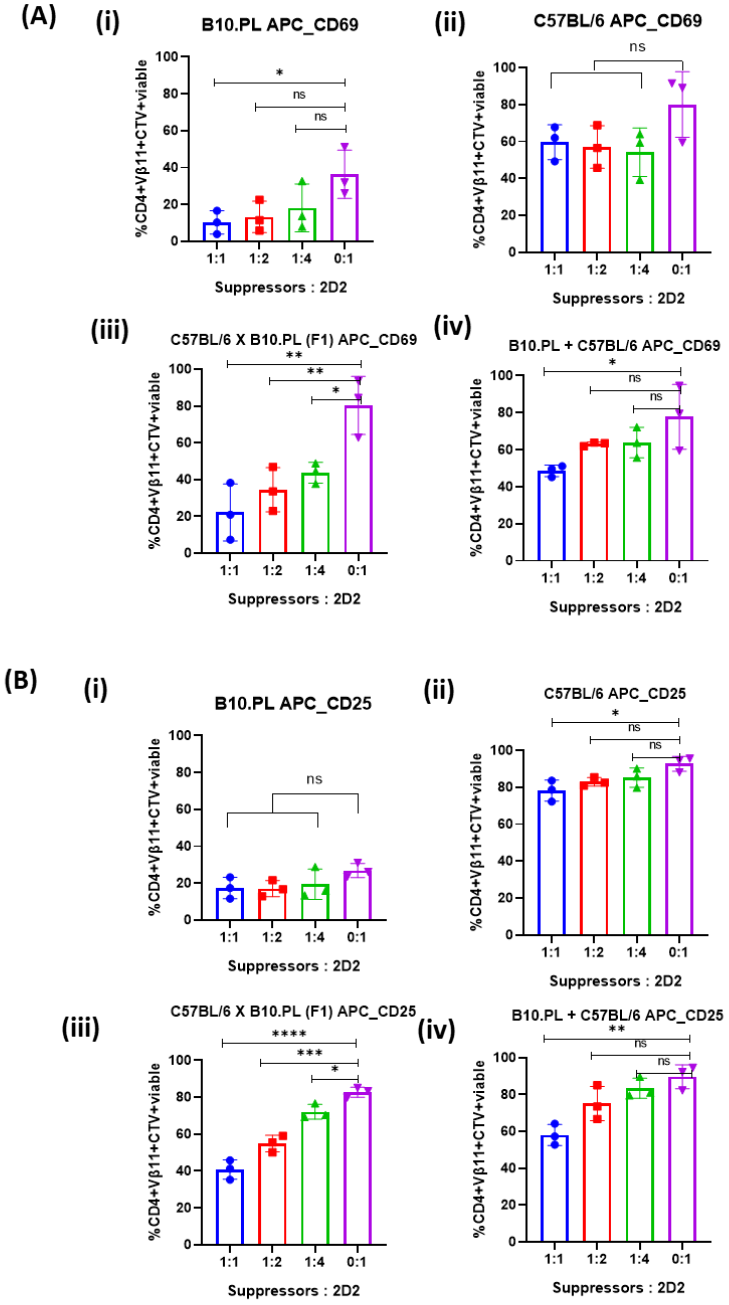



**Fig. 4.6: Antigen-presentation in the context of (B10.PL x C57BL/6) F1 splenocytes can lead to downregulation of activation markers on 2D2 cells in the presence of CD4tol cells. (A)** The graphs represent the % of $CD4^{+}V\beta11^{+}$ viable cells that express CD69 after 3 days of co-culture with different numbers of CD4tol cells in the presence of 100µg/ml MOG and MBP peptides presented by B10.PL (i), C57BL/6 (ii), F1 (iii) or C57BL/6 + B10.PL (iv) APCs. **(B)** The graphs represent the % of $CD4^{+}V\beta11^{+}$ viable cells that express CD25 after 3 days of co-culture with different numbers of CD4tol cells in the presence of 100µg/ml MOG and MBP peptides presented by B10.PL (i), C57BL/6 (ii), F1 (iii) or C57BL/6 + B10.PL (iv) APCs. Statistical significance calculated by one-way ANOVA with Dunnett's multiple comparisons test against the culture condition where no CD4tol cells were added. Results are from 3 independent experiments and presented as standard error of the mean (SEM).

### 4.4.2 Co-cultures of CD4tol suppressor cells and 2D2 responders in a transwell setting

To be able to conclusively determine whether contact between suppressor and responder cells was required for the bystander effect to occur, a transwell assay was developed. This assay allows the separation of the regulatory T cells from the responder cells via a semi-permeable membrane and one lineage is placed in the cultured well and the other one in the inserted transwell, referred to hereafter as the transwell system (Fig. 4.7A). In this setting, cells were able to exchange soluble factors, such as cytokines, but contact was prevented.

In the transwell system, MBP-specific CD4tol cells were co-cultured with MOG-specific CTV-stained 2D2 cells in the presence of both $MBP_{Ac1-9}$ and $MOG_{35-55}$ peptides and F1 APCs that can present both peptides. CD4tol cells were cultured either within the transwell or within the main well, with the 2D2 cells being on the opposite side of the membrane. On both sides of the membrane, F1 APCs were added together with the two peptides. The impact of CD4tol cells on 2D2 responder cells was assessed on day 3 by measuring the levels of proliferation. When suppressor CD4tol cells were separated from responder 2D2 cells, there was a clear reversion in suppression as 2D2 cells were able to proliferate both when they were placed within the transwell or within the main well with CD4tol cells on the opposite side of the membrane (Fig. 4.7B, i).

However, 2D2 proliferation was inhibited when the two cell populations were in contact either within the transwell (Fig. 4.7B, ii) or within the main well (Fig. 4.7B, iii). In addition to the impact on the proliferation of 2D2 cells (Fig. 4.7C, i), cell contact was also required for CD4tol cells to downregulate activation markers on 2D2 cells, such as CD25 (Fig. 4.7C, ii) and CD69 (Fig. 4.7C, iii).

**Fig 4.7 Cell contact is required for the suppressive function of CD4tol cells**
(Continued on the next page)

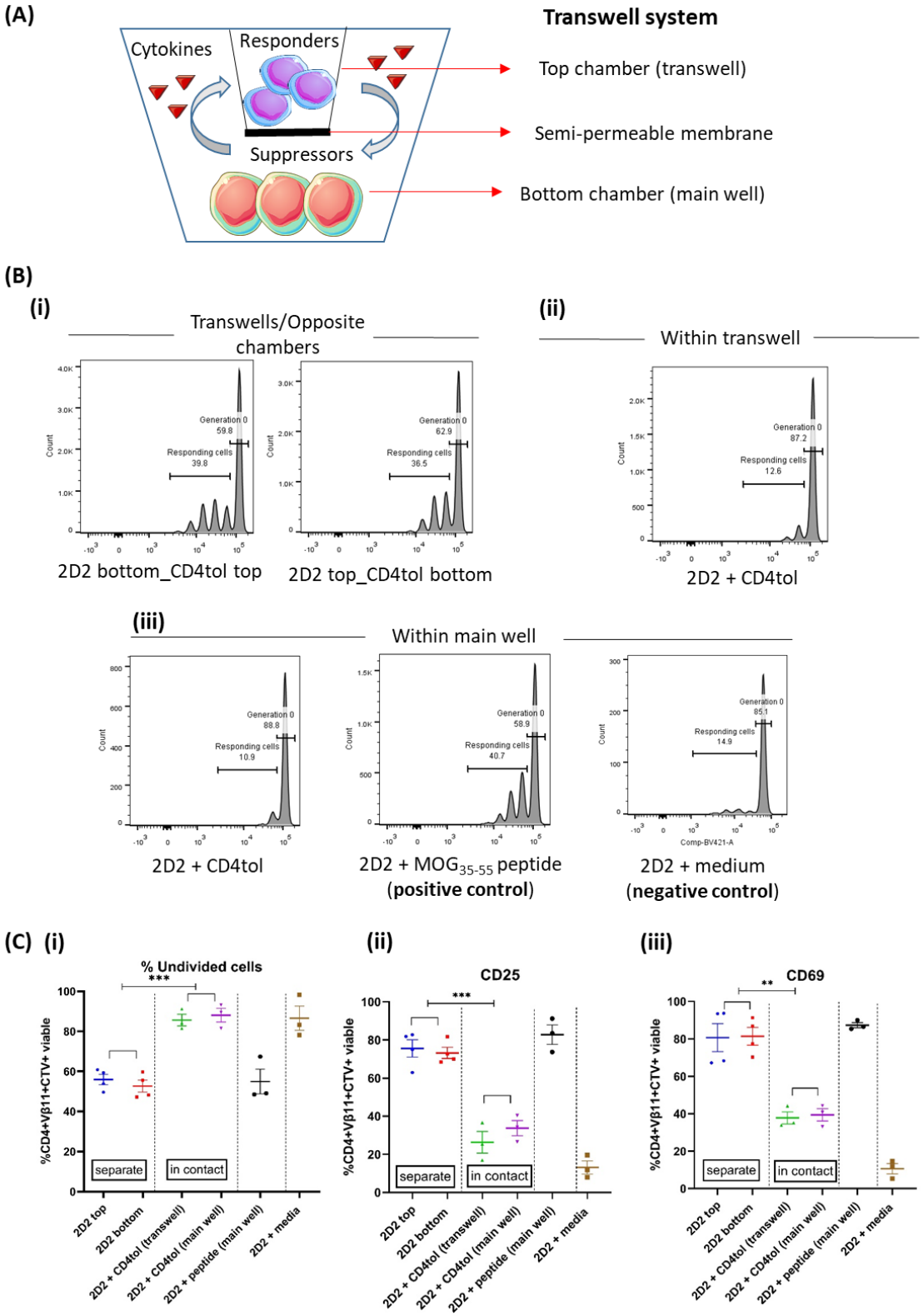


**Fig. 4.7: Cell contact is required for the suppressive function of CD4tol cells. (A)** Schematic of experimental set up of co-culture of CD4tol suppressor cells and 2D2 responders in a transwell assay. **(B)** Representative FACS plots of CTV dilution peaks of 2D2 cells when they were cultured with CD4tol cells in separate chambers that prevented cell contact (i), when cultured in contact with CD4tol cells within the transwell (ii) and when cultured within the main 24 well (iii) with (left) or without (middle and right) CD4tol cells. **(B)** Graphs summarising the % of undivided 2D2 cells (i) and levels of expression of CD25 (ii) and CD69 (iii) at the different conditions indicated. Statistical significance calculated by one-way ANOVA with Tukey's multiple comparisons test. Results are pooled together from 3 independent experiments and presented as standard error of the mean (SEM).

Even though with the transwell system, in theory, it is presumed that cytokines can travel readily through the semi-permeable membrane and impact the population on the opposite side of the membrane, it must be noted that this is an artificial system and can be limited in terms of how physiologically relevant this setting can be. Therefore, to validate the results from the transwell experiments showing that cell-contact was essential for the suppressive phenotype of CD4tol cells, a different experiment was developed to address the same hypothesis from a different angle.

In this experiment, CTV-stained responder 2D2 cells were co-cultured with different ratios of CD4tol cells as before (Fig. 4.8A – left), or with cell culture supernatants of optimally stimulated CD4tol cells (Fig. 4.8A – right). CD4tol cells or supernatants were co-cultured for further 3 days with 2D2 cells before analysis by flow cytometry. It was clear that with CD4tol cells, 2D2 cells remained undivided, while with CD4tol supernatants there was no effect (Fig. 4.8B, i).

Similarly, CD4tol supernatants alone were not able to suppress CD25 (Fig. 4.8B, ii) or CD69 (Fig. 4.8B, iii). This result shows that the soluble factors found in CD4tol supernatants such as IL-10 and TGF-β, are not sufficient to drive the suppressive effect. Potentially there is a requirement for the cells to be the source of constant and localised secretion of certain cytokines that will establish a successful suppression together with other potentially contact-dependent mechanisms, such as ligation of inhibitory receptors found of the cell surface of CD4tol cells.

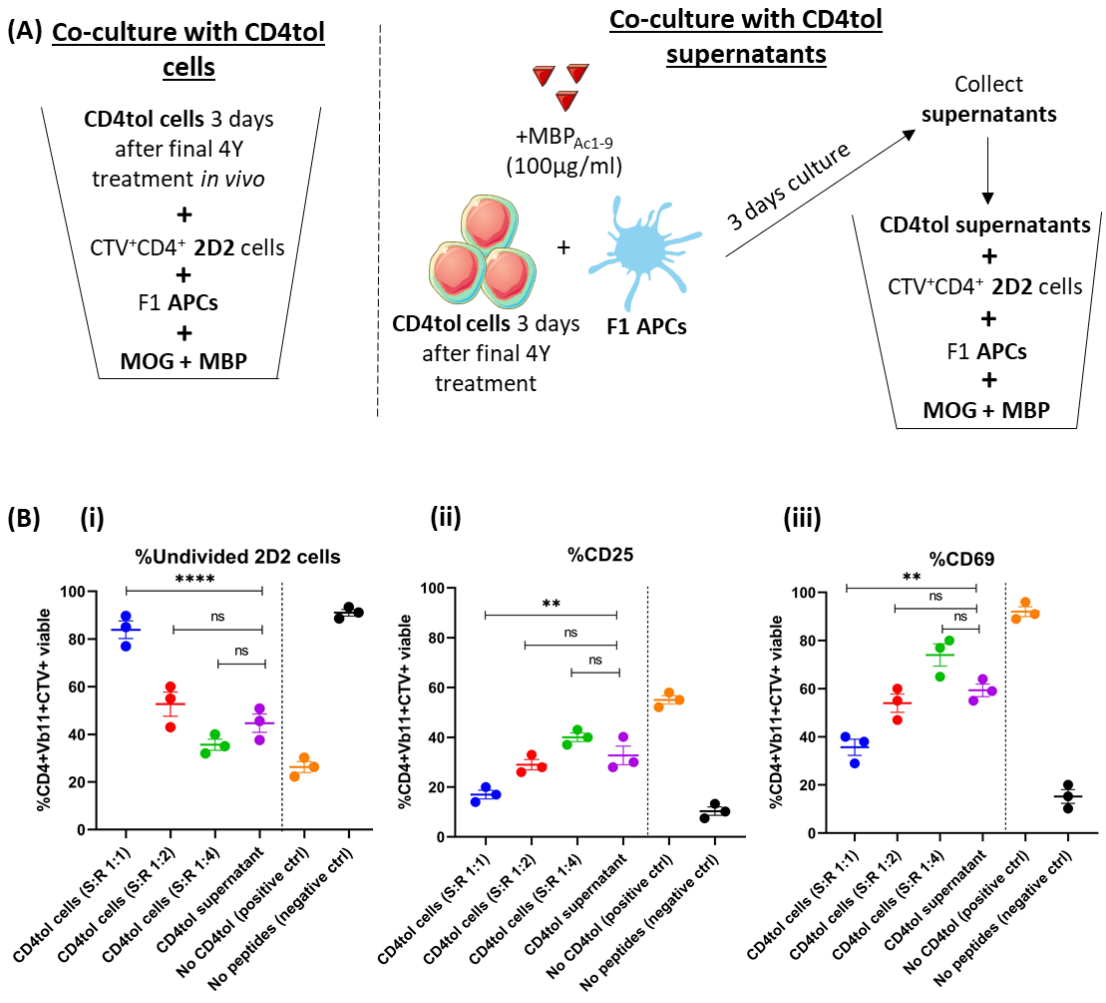



**Fig. 4.8: Soluble factors secreted in culture supernatants of CD4tol cells are not able to mediate bystander suppression. (A)** Schematic representation of the co-culture system with CD4tol cells (left) or CD4tol supernatant (right). **(B)** Graphs showing the proliferation of 2D2 cells after 3 days in culture with CD4tol cells at different ratios or CD4tol supernatants (i), and the expression of activation markers such as CD25 (ii) and CD69 (iii). Statistical significance calculated by one-way ANOVA with Dunnett's multiple comparisons test. Results are pooled together from 2 independent experiments and presented as standard error of the mean (SEM).

### 4.4.3 A role for CTLA-4 and IL-10 in bystander suppression mediated by CD4tol cells *in vitro*

To further dissect the factors that make CD4tol cells potent suppressors, blocking antibodies were used against IL-10R, CTLA-4 or both and incubated with suppressor and responder T cells and APCs for 2h at 37ºC before stimulating with $MBP_{Ac1-9}$ and $MOG_{35-55}$. Intriguingly, the suppression of 2D2 proliferation was only reversed when both molecules were neutralised at the same time (Fig. 4.9A), and in particular, at the highest CD4tol ratios of 1:1 (i) or 1:2 (ii) suppressors: responders.

However, there was still an effect on the expression of CD25 (Fig. 4.9B, i) and CD69 (Fig. 4.9C, i) when either IL-10R or CTLA-4 was blocked individually. This effect was again more profound after simultaneous blockade even at lower CD4tol numbers (1:2 and 1:4 suppressors: responders) as measured by CD25 (Fig, 4.9B, ii and iii) and CD69 (Fig. 4.9B, ii and iii), respectively. Therefore, it appears that there is an additive effect between IL-10 and CTLA-4, as they both play a role in the suppressive phenotype of CD4tol cells individually, but this effect was amplified when both molecules were neutralised at the same time.

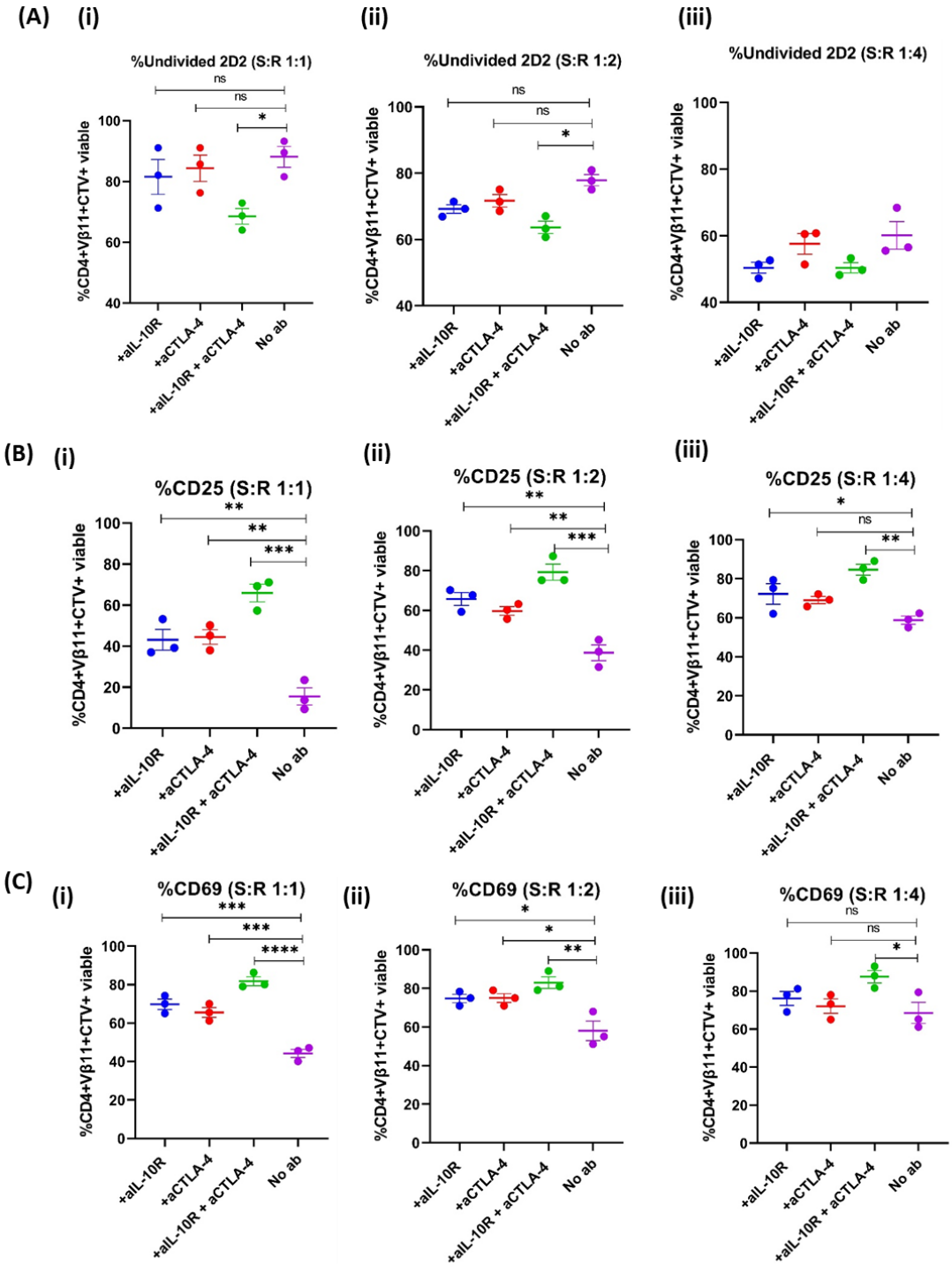



**Fig. 4.9: Simultaneous neutralisation of CTLA-4 and IL-10 reverses the suppression mediated by CD4tol cells. (A)** Graphs showing the percentage of 2D2 cells that remained undivided after 3 days in culture with CD4tol cells at a ratio of Suppressors : Responders (S:R) 1:1 (i), 1:2 (ii) or 1:4 (iii) following initial blockade of IL-10R, CTLA-4 or both. **(B)** Percentage of 2D2 cells that express CD25 after co-cultured with CD4tol cells at 1:1 S:R (i), 1:2 (ii) or 1:4 (iii). **(C)** Percentage of 2D2 cells that express CD25 after co-cultured with CD4tol cells at 1:1 S:R (i), 1:2 (ii) or 1:4 (iii). Statistical significance calculated by one-way ANOVA with Dunnett's multiple comparisons test against the condition where no blocking antibody was added in culture. Results are pooled together from 2 independent experiments and presented as standard error of the mean (SEM).

## 4.5 Evidence of bystander suppression *in vivo*

To recapitulate the *in vitro* findings of bystander suppression in an *in vivo* setting, two different approaches were followed. Firstly, we wanted to address the impact of tolerance induction on the ability of the recipient mice to suppress the adoptively transferred cells using the (Tg4 x C57BL/6) F1 model. Secondly, we aimed to investigate the ability of tolerant $CD4^+$ T cells to mediate bystander (antigen nonspecific) or antigen-specific suppression *in vivo*. To do that, tolerant Tg4 $CD4^+$ T cells were co-transferred with either CTV-stained responder $CD4^+$ 2D2 T cells into (B10.PL x C57BL/6) F1 mice (bystander model) or CTV-stained responder $CD4^+$ Tg4 T cells into B10.PL mice (antigen-specific model).

### 4.5.1 (Tg4 x C57BL/6) F1 model

The advantage of the (Tg4 x C57BL/6) F1 model lies in the fact that it can be tolerised against $MBP_{Ac1-9}$ and at the same time, be able to recognise both $MBP_{Ac1-9}$ and $MOG_{35-55}$. To investigate the effect of peptide-immunotherapy on recipient mice, (Tg4 x C57BL/6) F1 mice were treated with increasing doses of 4Y peptide (tolerance induction), or PBS as described previously. Three days after the final dose, CTV-stained $CD4^+$ T cells from the 2D2 mice were administered s.c. and 24h later mice were challenged with 100μg/ml of the low-affinity peptide analogue of $MBP_{Ac1-9}$ [4K peptide] and 100μg/ml $MOG_{35-55}$. Three days after the peptide challenge, spleens were harvested and analysed *in vitro* to assess the proliferation and activation status of transferred 2D2 cells (Fig. 4.10A).

Cells were gated on $CD4^+V\beta11^+CTV^+$ to be able to track only the labelled 2D2 cells that were transferred and distinguish them from the endogenous cells of the recipient mice that express the Vβ11 chain. Interestingly, when 2D2 cells were transferred into 4Y-

treated recipients, a significantly higher percentage remained undivided (approximately 85%) compared to PBS treated recipients (around 70%) (Fig. 4.10B, ii). This was shown qualitatively with the overlays of CTV peaks of 2D2 cells transferred into either 4Y-treated (blue line), where they remained mostly undivided, or PBS-treated (red line) recipient mice, where they were able to undergo up to three divisions (Fig. 4.10B, i).

This phenotype was also reflected by the activation status of the 2D2 cells. When these responder cells were transferred into 4Y-treated recipients, the expression of CD69 was significantly suppressed on the surface of 2D2 cells as measured by both percentages of $CD4^+V\beta11^+CTV^+CD69^+$ cells (Fig, 4.11A, i) as well as MFI (Fig. 4.11A, ii). The expression of CD25 was also suppressed even though to a lesser extend (Fig. 4.11B). CD69 seems to be a more reliable marker in this system since there is a good proportion of cells expressing this marker (>10% within the $CD4^+V\beta11^+CTV^+$ gate), while there is a much lower proportion of 2D2 cells expressing CD25 (<5%) and this may be due to the kinetics of CD25 that potentially goes down much quicker than CD69, therefore it reaches a very low level by day 3 post antigenic challenge *in vivo*. Even so, it is clear that there is a downregulation of both activation markers on 2D2 cells when these were administered to recipient mice that were previously subjected to treatment with increasing doses of 4Y peptide.

Taken together, these data indicate that peptide immunotherapy established a highly tolerogenic environment in recipient mice, by either giving rise to regulatory populations such as CD4tol cells and $FoxP3^+$ Tregs, which actively suppress the transferred 2D2 cells, or also by giving rise to tolerogenic DCs that are unable to activate the adoptively transferred 2D2 cells that subsequently, remained undivided.

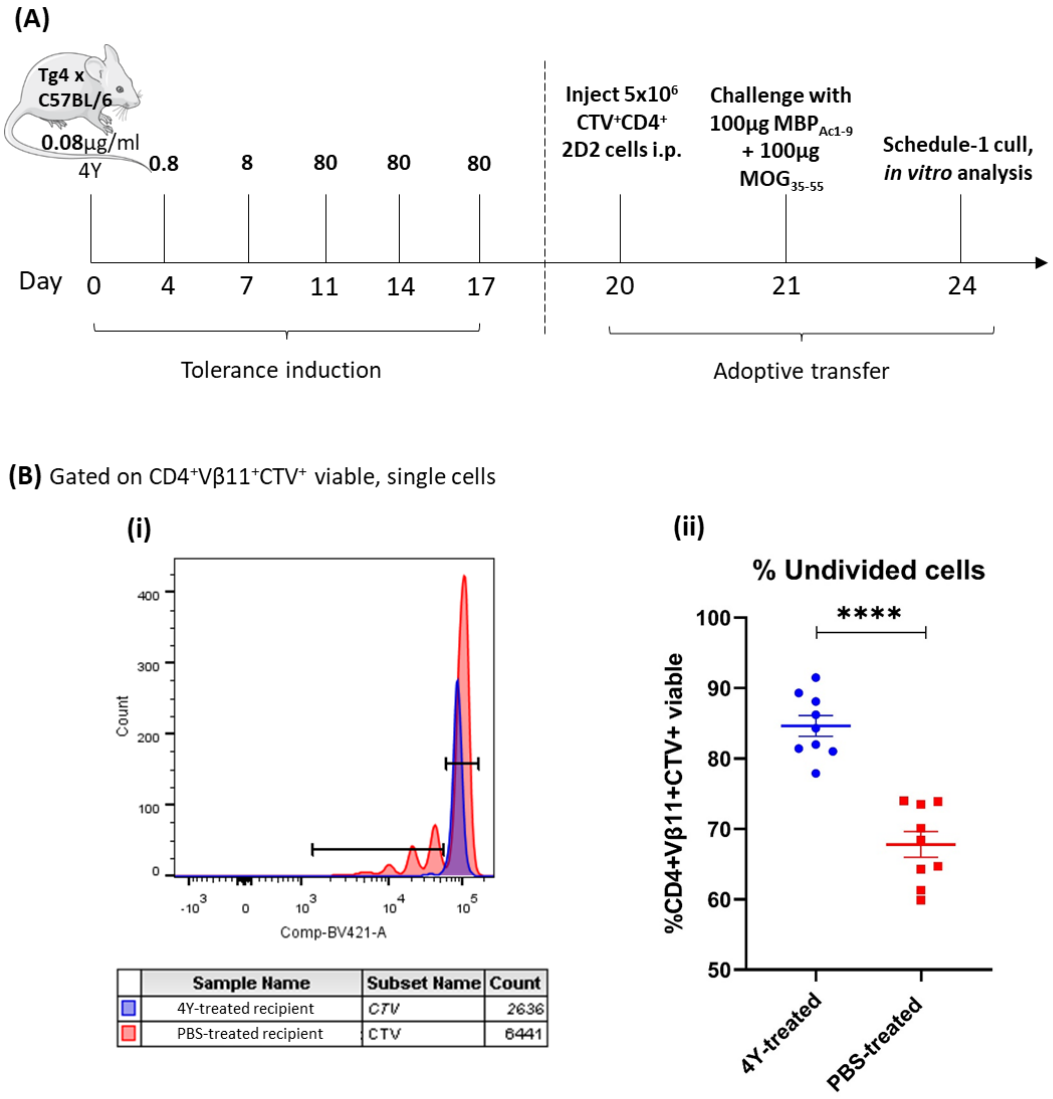



**Fig. 4.10: Peptide treatment establishes a tolerogenic environment that prevents the proliferation of adoptively transferred naïve T cells. (A)** Schematic of the tolerance induction protocol followed by the adoptive transfers. **(B)** Spleens were removed from (Tg4 x C57BL/6) F1 recipient mice three days after antigenic challenge and proliferation of $CD4^+V\beta11^+CTV^+$ transferred 2D2 cells was analysed by looking at the CTV dilution peaks of 2D2 cells. **(i)** Overlays of CTV peaks of 4Y-treated recipient (blue) and PBS-treated recipient mice (red). **(ii)** Corresponding bar graph where results from three independent experiments were pooled together (N=9). Statistical significance was calculated by unpaired student t test. Results are presented as standard error of the mean (SEM).

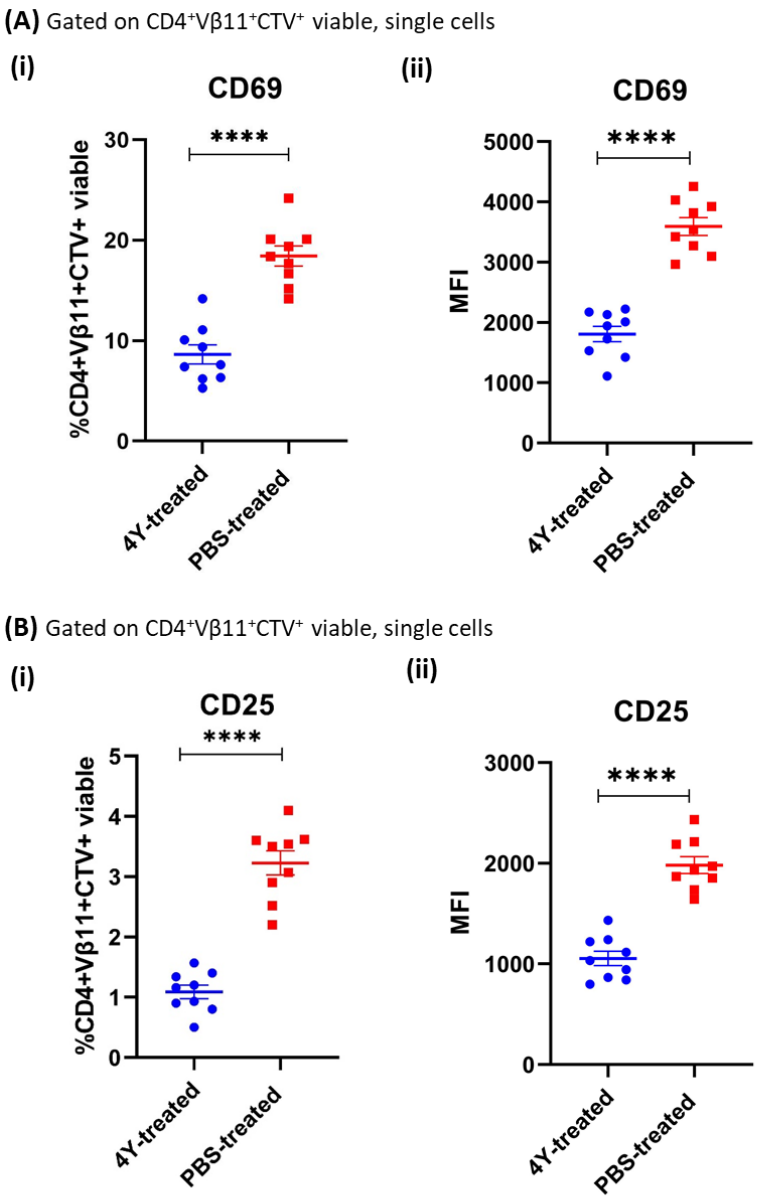



**Fig. 4.11: Peptide treatment establishes a tolerogenic environment that prevents the activation of adoptively transferred naïve T cells. (A)** Summarising bar graphs with the percentage (i) or MFI (ii) of $CD4^+V\beta11^+CTV^+$ 2D2 cells that express CD69 on cells when transferred into tolerised recipients (4Y-treated) or naïve recipients (PBS-treated). **(B)** Summarising bar graphs with the percentage (i) or MFI (ii) of $CD4^+V\beta11^+CTV^+$ 2D2 cells that express CD25 on cells when transferred into tolerised recipients (4Y-treated) or naïve recipients (PBS-treated). Statistical significance was calculated by unpaired t test. In the corresponding bar graph results from three independent experiments were pooled together (N=9). Results are presented as standard error of the mean (SEM).

### 4.5.2 Adoptive co-transfers of 2D2 responder cells with Tg4 CD4tol cells into (B10.PL x C57BL/6) F1 recipient mice

To investigate whether CD4tol cells were able to mediate bystander suppression *in vivo*, CTV-stained $CD4^+$ 2D2 responder T cells were co-transferred with an equal number of CD4tol cells from Tg4 mice into (B10.PL x C57BL/6) F1 recipient mice. 24h post adoptive transfer, mice were challenged with the low affinity $MBP_{Ac1-9}$ peptide [4K] and $MOG_{35-55}$ and three days later, spleens were harvested and analysed *in vitro* (Fig. 4.12A). Cells were gated on $CD4^+V\beta11^+CTV^+$ to track the transferred 2D2 responder cells in the recipient mice.

In line with the *in vitro* data, it was clear that in the presence of CD4tol cells from Tg4 mice, a higher percentage of 2D2 responder cells remained undivided (blue line), while in the presence of PBS-treated $CD4^+$ cells, 2D2 responders were able to undergo up to 3 cell divisions (Fig. 4.12B, i – red line). Collective date from two independent experiments, showed that around 65% of 2D2 cells were not able to proliferate in the presence of CD4tol cells, while this percentage dropped to just below 60% in the presence of PBS-treated $CD4^+$ cells. Furthermore, the expression of CD69 was suppressed on the surface of 2D2 cells as measured by both % of $CD69^+$ 2D2 cells as well as at the population level with the measurement of MFI (Fig. 4.12C, i). Expression of CD25 was also suppressed on 2D2 cells that were co-transferred with CD4tol cells (Fig. 4.12C, ii). Taken together, this data indicates that CD4tol cells from the Tg4 mice can suppress the proliferation and activation of 2D2 responder cells and mediate bystander suppression *in vivo*.

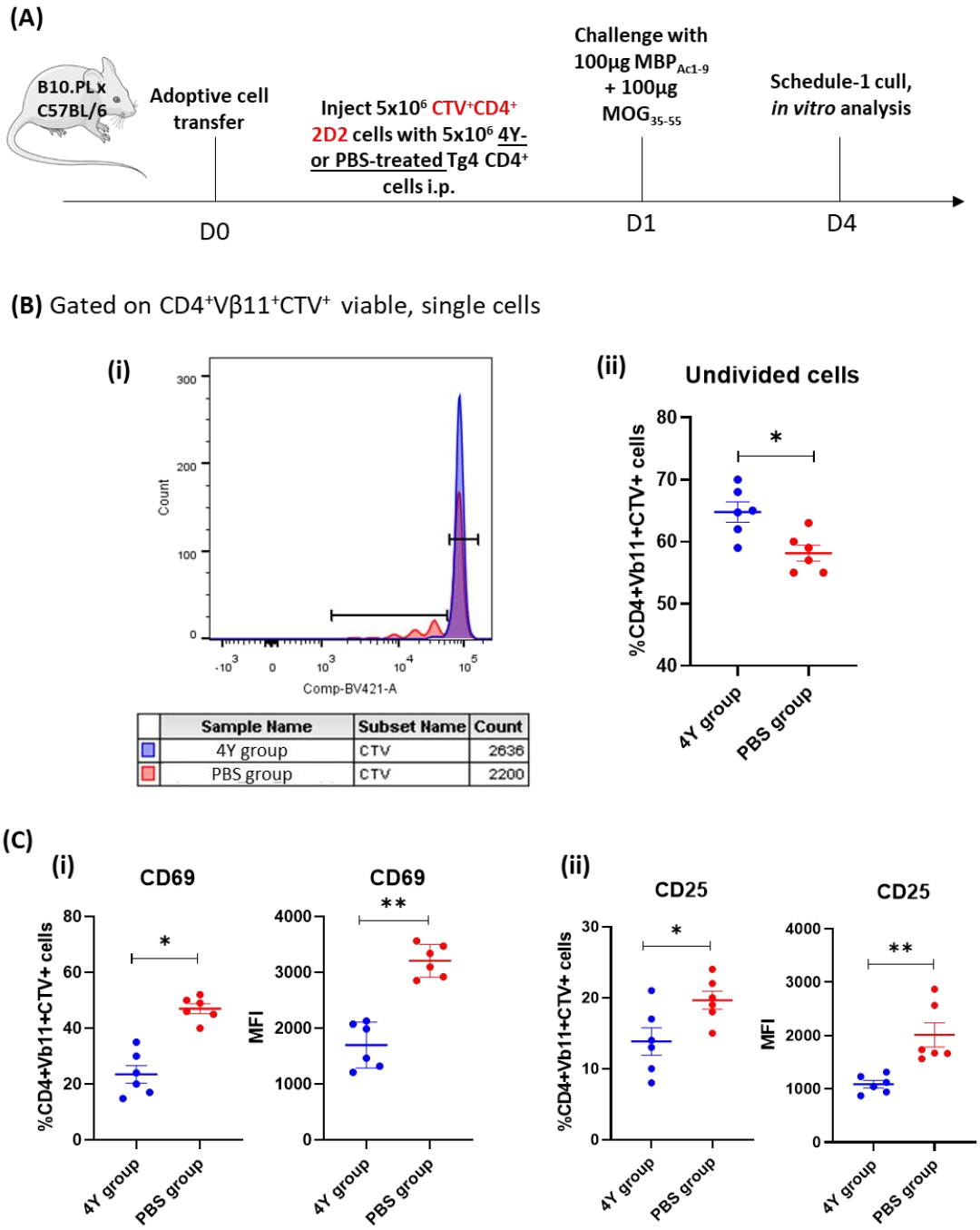



**Fig. 4.12: CD4tol cells are able to mediate bystander suppression *in vivo*. (A)** Schematic of tolerance induction protocol followed by the adoptive co-transfers. **(B)** Spleens were removed from (B10.PL x C57BL/6) F1 recipient mice and proliferation of $CD4^+V\beta11^+CTV^+$ transferred 2D2 cells was analysed. Overlays of CTV dilution peaks of 2D2 cells when transferred with equal numbers of 4Y-treated $CD4^+$ Tg4 cells (blue line) or PBS-treated $CD4^+$ Tg4 cells (red line), with the corresponding bar graph (ii) which summarises the percentage of responder cells that remained undivided in each condition. **(C)** Expression of activation markers, CD69 (i) and CD25 (ii) on $CD4^+V\beta11^+CTV^+$ transferred 2D2 cells with the corresponding MFIs. Statistical significance was calculated by unpaired t test. Results are pooled together from 2 independent experiments and presented as standard error of the mean (SEM).

### 4.5.3 Adoptive co-transfers of Tg4 responder cells with Tg4 CD4tol cells into B10.PL recipient mice

In a similar setting, CTV-stained $CD4^+$ Tg4 responder T cells were co-transferred with an equal number of tolerant $CD4^+$ Tg4 T cells into B10.PL recipient mice. 24h post adoptive transfer, mice were challenged with the low affinity $MBP_{Ac1-9}$ peptide [4K] and three days later, spleens were harvested and analysed *in vitro* (Fig. 4.13A). Cells were gated on $CD4^+V\beta8^+CTV^+$ to track the transferred 2D2 responder cells in the recipient mice.

In this experiment, both responders and putative suppressors come from the same Tg4 mouse strain; however, they can easily be distinguished because the naïve Tg4 responder cells were labelled with CTV to track proliferation. A way to improve this system, would be to use CD45.1 Tg4 responders and CD45.2 tolerant $CD4^+$ Tg4 T cells as putative suppressors to have an additional marker to track the responders. For the purposes of this experiment, CTV staining would suffice for the distinction between the different populations.

As expected, tolerant $CD4^+$ Tg4 T cells were able to supress the proliferation of other T cells with the same antigen-specificity (both coming from the Tg4 mouse strain), as shown by the fact that there was a higher percentage of undivided $CD4^+V\beta8^+CTV^+$ Tg4 responder cells (Fig. 4.13B, ii). Overlays from CTV peaks show that in the presence of CD4tol cells from Tg4 mice, a higher percentage of Tg4 responder cells remained undivided, with only a few cells undergoing one division (blue line), while in the presence of PBS-treated $CD4^+$ cells, Tg4 responders were able to undergo up to 4 cell divisions (Fig. 4.13B, i – red line).

Furthermore, on those cells the expression of both CD69 (Fig. 4.13C, i) and CD25 (Fig. 4.13C, ii) was suppressed as shown by both % expression of each marker and MFI. Therefore, CD4tol cells can successfully mediate both bystander and antigen-specific suppression *in vivo*.

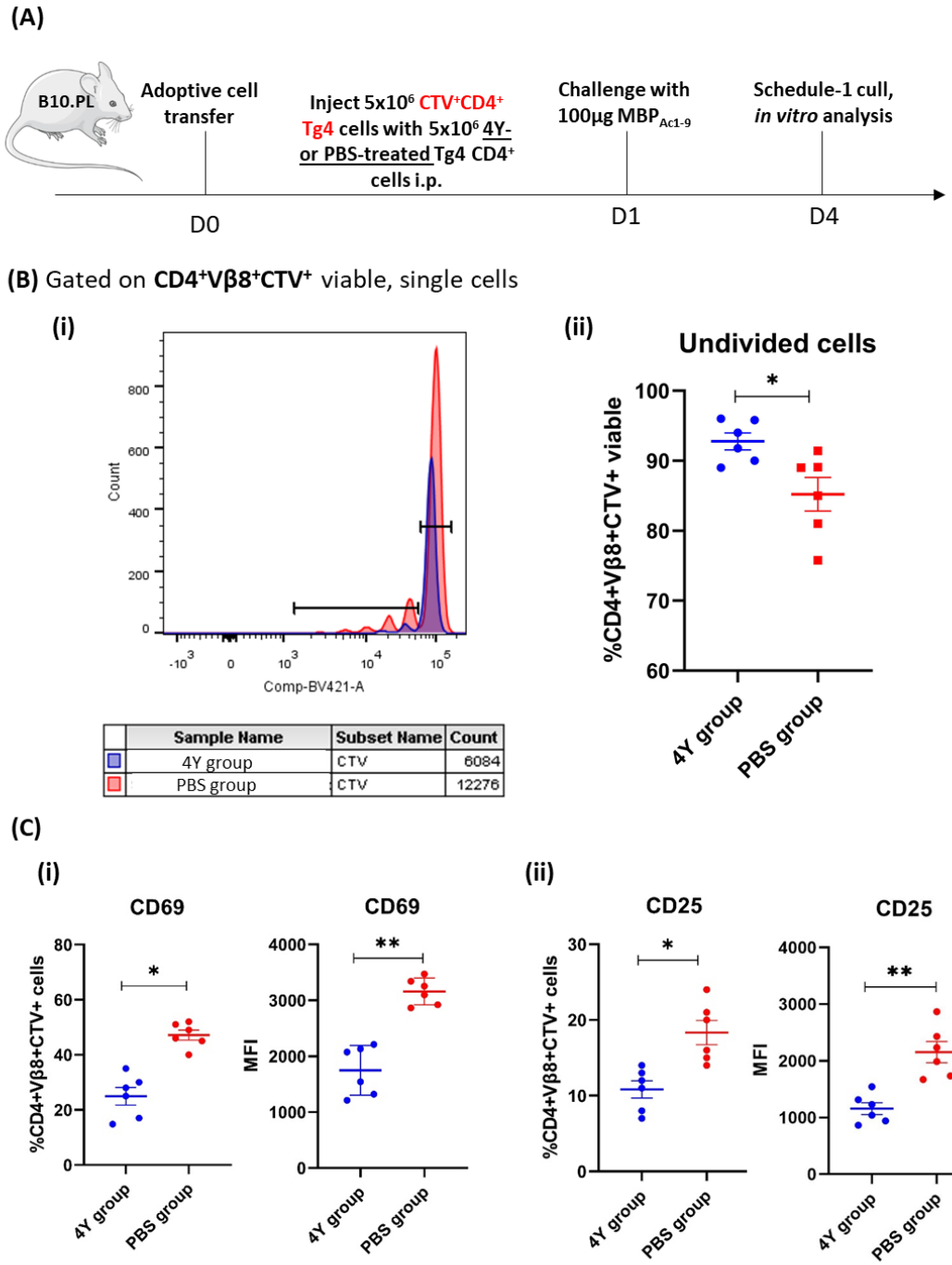



**Fig. 4.13: CD4tol cells are able to mediate antigen-specific suppression *in vivo*. (A)** Schematic of tolerance induction protocol followed by the adoptive co-transfers. **(B)** Spleens were removed B10.PL recipient mice and proliferation of $CD4^+V\beta8^+CTV^+$ transferred Tg4 cells was analysed by looking at the CTV dilution peaks of Tg4 cells when transferred with equal numbers of 4Y-treated $CD4^+$ T cells (blue line) or PBS-treated $CD4^+$ T cells (red line), with the corresponding bar graph (ii) which summarises the percentage of responder cells that remained undivided. **(C)** Expression of activation markers, CD69 (i) and CD25 (ii) on $CD4^+V\beta8^+CTV^+$ transferred Tg4 cells with the corresponding MFIs. Statistical significance was calculated by unpaired t test. Results are pooled together from 2 independent experiments and presented as standard error of the mean (SEM).

### 4.5.4 Dendritic cells are modulated by tolerance induction *in vivo*

To assess whether antigen-presenting cells from (Tg4 x C57BL/6) F1 mice were affected by tolerance induction, 4Y- or PBS-treated Tg4 mice were culled 3 days after their last *in vivo* dose of peptide treatment and spleens were collected. Splenocytes were stained for dendritic cell markers (CD11c, MHC II), in addition to co-stimulatory molecules CD80, CD86 and CD40. Expression of MHC II and CD40 by MFI was not significantly different between naïve and peptide-treated mice (data not shown); however, CD80 (Fig. 4.14A) and CD86 (Fig. 4.14B) were significantly suppressed in tolerised mice. That is in line with the *in vitro* co-culture data (paragraph 4.7.1), and it indicates that DCs in tolerised mice may provide co-stimulatory molecules at a level that is below the threshold required to fully activate subsequent T cells

Taken together, it can be concluded that repeated antigen stimulation sufficient to induce antigen-specific T cell tolerance is able to affect the T cell priming capacities of DCs. This in turn may be an effective means of mediating bystander suppression.

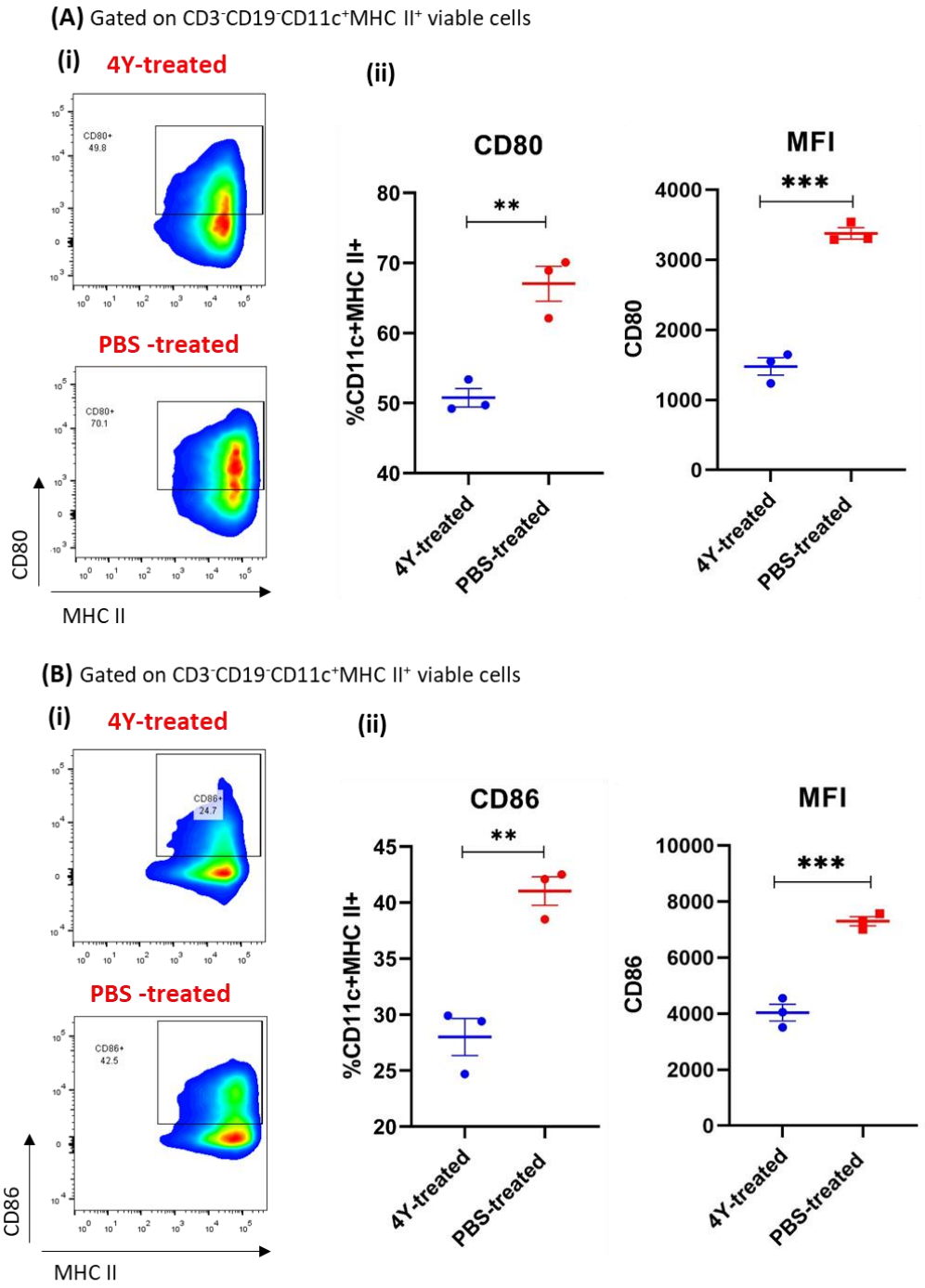



**Fig. 4.14: Tolerance induction has an impact on DCs *in vivo*, making them downregulate CD80 and CD86.** Three days after the final peptide treatment, spleens were harvested, and bulk splenocytes were stained for surface markers and analysed by flow cytometry. **(A)** Representative FACS plots showing CD80 expression on $CD3^-CD19^-CD11c^+MHC\ II^+$ viable dendritic cells coming from either 4Y-treated mice (i, upper panel) or PBS-treated mice (i, lower panel) and corresponding bar graph with % of $CD80^+$ DCs together with MFI (ii). **(B)** Representative FACS plots showing CD86 expression on $CD3^-CD19^-CD11c^+MHC\ II^+$ viable dendritic cells coming from either 4Y-treated mice (i, upper panel) or PBS-treated mice (i, lower panel) and corresponding bar graph with % of $CD86^+$ DCs together with MFI (ii). Statistical significance was calculated by unpaired t test. Results are coming from 1 experiment and presented as standard error of the mean (SEM).

## 4.6 Peptide immunotherapy licenses FoxP3$^+$ Tregs to acquire a highly suppressive phenotype *in vitro*

All the experiments described previously, both *in vitro* and *in vivo*, tested the capacity of **total CD4$^+$ T cells from 4Y-treated Tg4 mice**, referred to as **CD4tol** cells in previous paragraphs, to mediate suppression. There are some discrepancies with the nomenclature of these cells, as they have been also named **peptide-induced tolerant cells (PItol)** (Sundstedt et al., 2003) or even **Tr1-like T cells** (White and Wraith, 2016) in the past. In this thesis, they were called CD4tol cells, rather than Tr1 cells, which are defined as IL-10$^+$ cells. In the Tg4 mouse, only 30-40% of the CD4tol cells express IL-10 (data not shown).

Furthermore, CD4tol cells consist of both FoxP3$^-$IL-10$^+$ Tr1 cells and FoxP3$^+$ Tregs. Historically, our lab has investigated extensively the properties of Tr1 cells, but the impact of peptide immunotherapy on FoxP3$^+$ Tregs was far less understood. Previous work has shown that during the course of tolerance induction the expression of FoxP3 is upregulated (Burton et al., 2014); however, it was not clear whether this means there was an expansion of the initial population of Tregs, or whether there was *de novo* generation of Tregs. Intriguingly, the properties, phenotype, and function of these Tregs coming from 4Y-treated mice have not been studied before, and we were keen to start teasing apart the impact of peptide immunotherapy on this specific population of regulatory T cells.

To address the function of these cells, naïve FoxP3$^+$ Tregs were isolated from Tg4 mice using a CD4$^+$CD25$^+$ positive selection kit (see Materials and Methods, section 2.3.9.2) and added in co-culture with 2D2 cells in the presence of F1 APCs and $MBP_{Ac1-9}$ and $MOG_{35-55}$ peptides to investigate their capacity to mediate bystander suppression.

Interestingly, the proliferation of 2D2 cells was not affected in the presence of naïve FoxP3$^+$ Tregs, since there was a low proportion of CD4$^+$Vβ11$^+$CTV$^+$ 2D2 cells that remained undivided, and the levels were similar to the ones seen in the presence of Th1 cells that were used as a negative control for suppression (Fig. 4.15A, i). Similarly, the expression of CD69 (Fig. 4.15A, ii) and CD25 (Fig. 4.15A, iii) on 2D2 cells remained unaltered when in culture with naïve FoxP3$^+$ Tregs.

We then moved on to test the suppressive capacity of FoxP3$^+$ Tregs that derived from Tg4 mice that were treated with increasing doses of 4Y peptide. Interestingly, when 2D2 cells were co-cultured with tolerised FoxP3$^+$ Tregs, virtually all the responder 2D2 cells remained undivided, not only at the highest ratio but even when the number of putative suppressors was reduced by 4-fold (Fig. 4.15B, i). This striking effect was even more profound than the one seen with CD4tol cells (4Y-treated total CD4$^+$ T cells) before, indicating that potentially the main driver for bystander suppression is the population of FoxP3$^+$ Tregs rather than CD4tol cells, despite the fact that they only comprise a small proportion of total CD4$^+$ T cells (<10%). This strong suppressive effect of tolerant FoxP3$^+$ Tregs was also confirmed by the significant downregulation of CD69 (Fig. 4.15B, ii) and CD25 (Fig. 4.15B, iii) on 2D2 cells following a 3-day co-culture with tolerised FoxP3$^+$ Tregs.

Furthermore, the impact of the different regulatory T cells on cytokine production was investigated. To do that, two different methods were used; either total levels of the pro-inflammatory cytokine, IFN-γ, and anti-inflammatory cytokine, IL-10, were measured on the cell culture supernatants by ELISA (section 2.3.16 from Materials & Methods), or cells were stimulated with PMA and Ionomycin and stained intracellularly for IFN-γ and IL-10 and analysed by flow cytometry (section 2.3.18.2). The advantage of

the latter method is that enables us to look specifically at the production of each cytokine by $CD4^+V\beta11^+CTV^+$ 2D2 cells only and exclude any other cell type that was in the initial co-culture.

Strikingly, in the presence of tolerised $FoxP3^+$ Tregs, the production of IFN-γ was completely switched off following antigenic stimulation in the co-culture with 2D2 cells, even at very low number of Tregs (1:16, Suppressors: 2D2 Responders) (Fig. 4.16A, i). This downregulation of IFN-γ production was significantly more profound with 4Y-treated $FoxP3^+$ Tregs, followed by total 4Y-treated $CD4^+$ T cells, and lastly PBS-treated $FoxP3^+$ Tregs. As expected, IFN-γ levels were high in the control culture of effector Th1 cells. This phenotype was also mirrored in the intracellular staining results, since a significantly lower proportion of 2D2 cells secreted IFN-γ when co-cultured with 4Y-treated Tregs (<%5 across the different ratios), as opposed to PBS-treated Tregs (approximately 15%) (Fig. 4.16A, ii).

On the other hand, the expression of IL-10 follows the opposite trend. In the co-cultures of 2D2 cells with 4Y-treated $FoxP3^+$ Tregs, there was a significant upregulation of IL-10 production, compared to PBS-treated $FoxP3^+$ Tregs, following peptide stimulation (Fig. 4.16B, i). IL-10 levels were also high in the presence of 4Y-treated total $CD4^+$ T cells, and relatively low with Th1 cells, as expected. Moreover, when 2D2 cells were stimulated with PMA and Ionomycin, there was a higher percentage of $IL\text{-}10^+$ 2D2 cells across the decreasing ratios of 4Y-treated $FoxP3^+$ Tregs (>10% of the $CD4^+V\beta11^+CTV^+$ 2D2), while this percentage was significantly lower with PBS-treated $FoxP3^+$ Tregs (<10% for the higher ratios, approximately 10% for the lower Treg ratio) (Fig. 4.16B, ii). In the presence of total 4Y-treated $CD4^+$ T cells, there was a high

percentage of 2D2 cells expressing IL-10, slightly higher than the one seen with 4Y-treated FoxP3$^+$ Tregs across the different rations.

This indicates that the different regulatory T cell populations can have an imprinting effect on naïve 2D2 cells and potentiate them to produce more IL-10 and acquire a tolerogenic phenotype (infectious tolerance). It appears that the total CD4$^+$ T cells from 4Y-treated mice are the major drivers for IL-10 production, even though it was shown previously that 4Y-treated FoxP3$^+$ Tregs are the most potent mediators of bystander suppression, and this highlights the fact that in addition to IL-10, there are other molecules that make FoxP3$^+$ Tregs superior suppressors.

Taken together, there is a certain degree of hierarchy in terms of suppressive capacity amongst regulatory T cells following peptide immunotherapy. FoxP3$^+$ Tregs from 4Y-treated mice are the most potent mediators of bystander suppression *in vitro*, followed by total CD4$^+$ from 4Y-treated mice (CD4tol), with PBS-treated FoxP3$^+$ Tregs and iTregs being the least suppressive populations.

**Fig 4.15** (Continued on the next page)

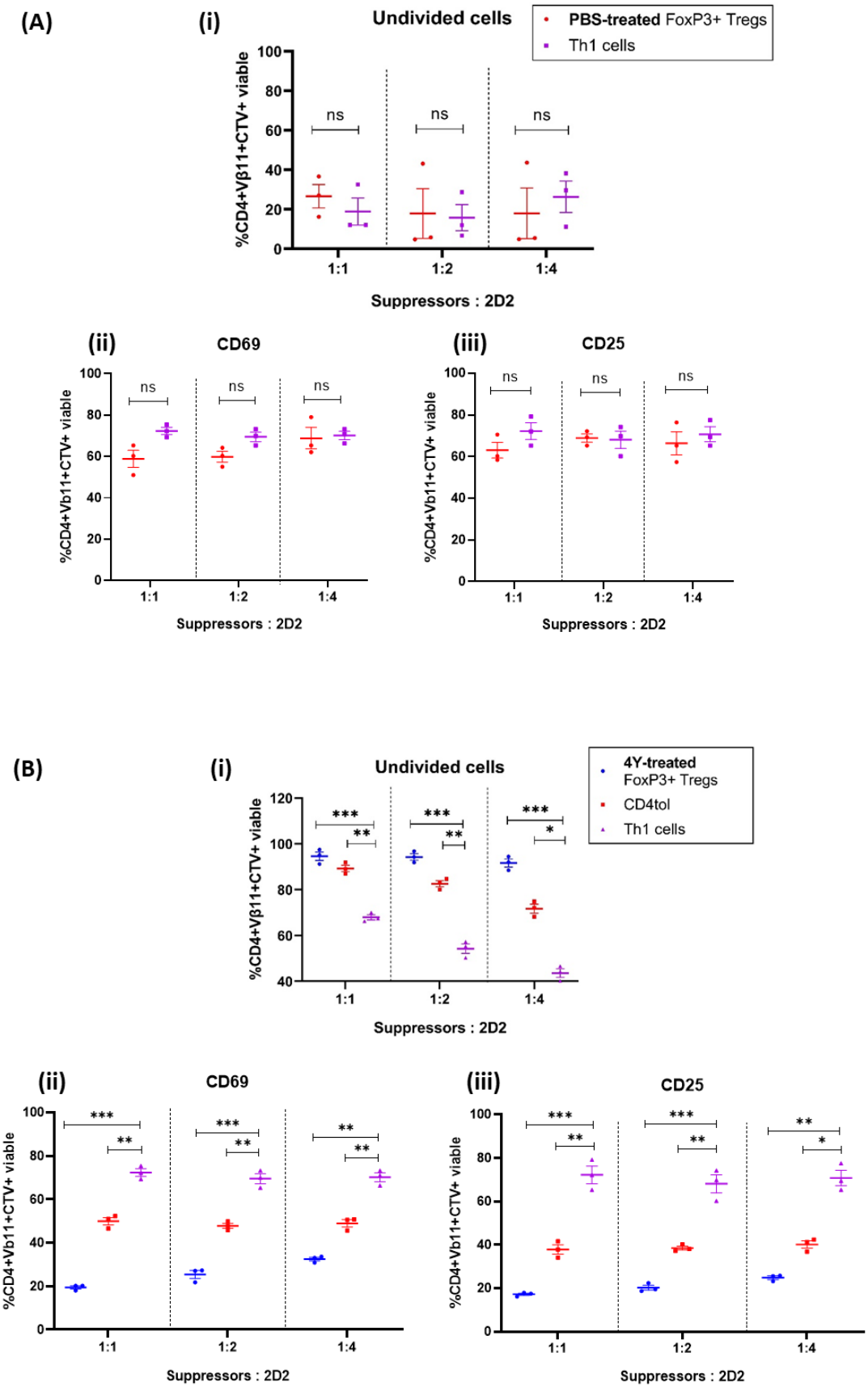


**Fig. 4.15: FoxP3$^+$ Tregs from peptide-treated Tg4 mice are able to suppress responder 2D2 cells even at low ratios, while naïve FoxP3$^+$ Tregs are not suppressive. (A)** The graph demonstrates the percentage of undivided 2D2 cells in the presence of either naïve FoxP3$^+$ Tregs or Th1 cells at decreasing ratios of putative suppressors (i). Expression of CD69 (ii) and CD25 (iii) on 2D2 cells after 3 days of culture. **(B)** Percentage of undivided 2D2 cells when cultured with FoxP3$^+$ Tregs from peptide-treated mice (i) and expression of activation markers, CD69 (ii) and CD25 (iii). Statistical significance calculated by one-way ANOVA with Dunnett's multiple comparisons test. Results are representative of 3 independent experiments showing similar results and presented as standard error of the mean (SEM).

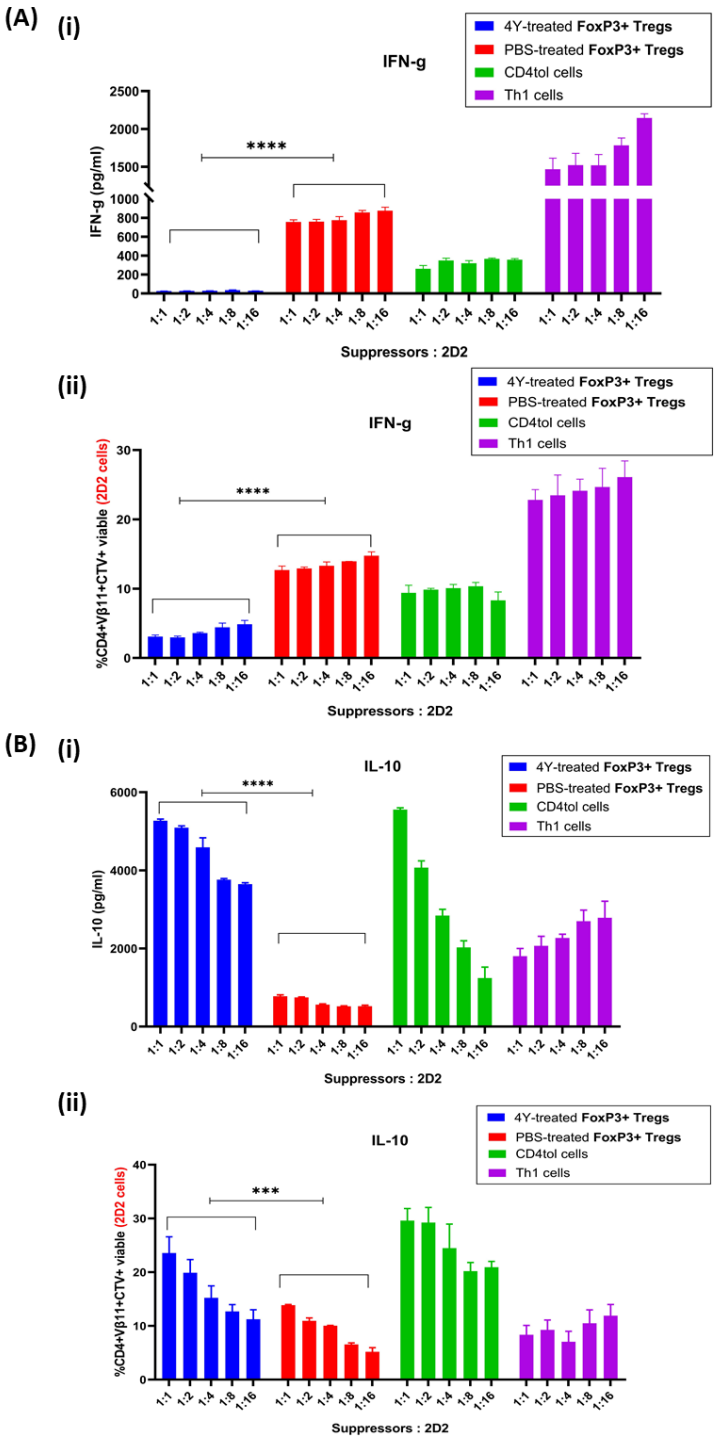



**Fig. 4.16: FoxP3$^+$ Tregs from peptide-treated Tg4 mice are able to completely switch off IFN-γ production and promote IL-10 production.** CTV-stained CD4$^+$ 2D2 cells were co-cultured with each population of putative suppressors in the presence of (C57BL/6 x B10.PL) F1 APCs and $MOG_{35-55}$ and $MBP_{Ac1-9}$ peptides. After 3 days, supernatants were collected from the cultures and levels of IFN-g (A, i) or IL-10 (B, i) were measured by sandwich ELISA. The remaining cells were stimulated with PMA/Ionomycin for 4h, fixed, permeabilised and stained intracellularly for IFN-g (A, ii) and IL-10 (B, ii). The levels of each cytokine was measured on CD4$^+$Vβ11$^+$CTV$^+$ 2D2 cells. Statistical significance calculated by one-way ANOVA with Tukey's multiple comparisons test. Results are coming from 3 independent experiments showing similar results and presented as standard error of the mean (SEM).

The previous data clearly demonstrated that 4Y-treated Tregs were more suppressive compared to their PBS-treated counterparts. The question that arises from that observation is whether the full course of tolerance induction is required for the **licensing** of Tregs, or whether a single dose of 4Y peptide *in vivo* would suffice for Tregs to acquire their tolerogenic properties. In other words, is it the repeated exposure to antigen **(tolerisation)** that makes FoxP3$^+$ Tregs highly suppressive or would a single encounter with the antigen **(priming)** be enough to achieve the same phenotype?

To answer this question, Tg4 mice were given either 80μg 4Y s.c. or PBS and 3 days later spleens were harvested, FoxP3$^+$ Tregs were isolated and placed in culture with 2D2 cells, F1 APCs and $MBP_{Ac1-9}$ and $MOG_{35-55}$ peptides for 3 days. A fraction of isolated Tregs were kept aside, stimulated with PMA and Ionomycin and stained intracellularly for FoxP3 and IL-10 to assess the effect of the *in vivo* priming on these markers. Interestingly, even with one single dose of 4Y peptide, expression of IL-10 was upregulated (approximately 15% of total live CD4$^+$ cells) compared to the levels seen in PBS-treated mice (2%) (Fig. 4.17A). In the presence of primed Tregs, there was a slightly higher percentage of 2D2 cells that remained undivided, especially at the higher ratio of suppressors to responders (Fig. 4.17B and 4.17C, i). Furthermore, primed FoxP3$^+$ Tregs were more potent at suppressing CD25 (Fig. 4.17C, ii) and CD69 (Fig. 4.17C, ii) on the surface of 2D2 cells compared to naïve FoxP3$^+$ Tregs, but only at the highest ratio. This shows that the initial encounter with antigen *in vivo*, initiates the re-programming of Tg4 CD4$^+$ T cells to upregulate IL-10 and become suppressive. However, the phenotype of primed Tregs is far less profound compared to fully tolerised Tregs, in which around 40% express IL-10 and are suppressive even at lower ratios. Therefore, the full course of peptide immunotherapy is required for the more effective licensing of FoxP3$^+$ Tregs.

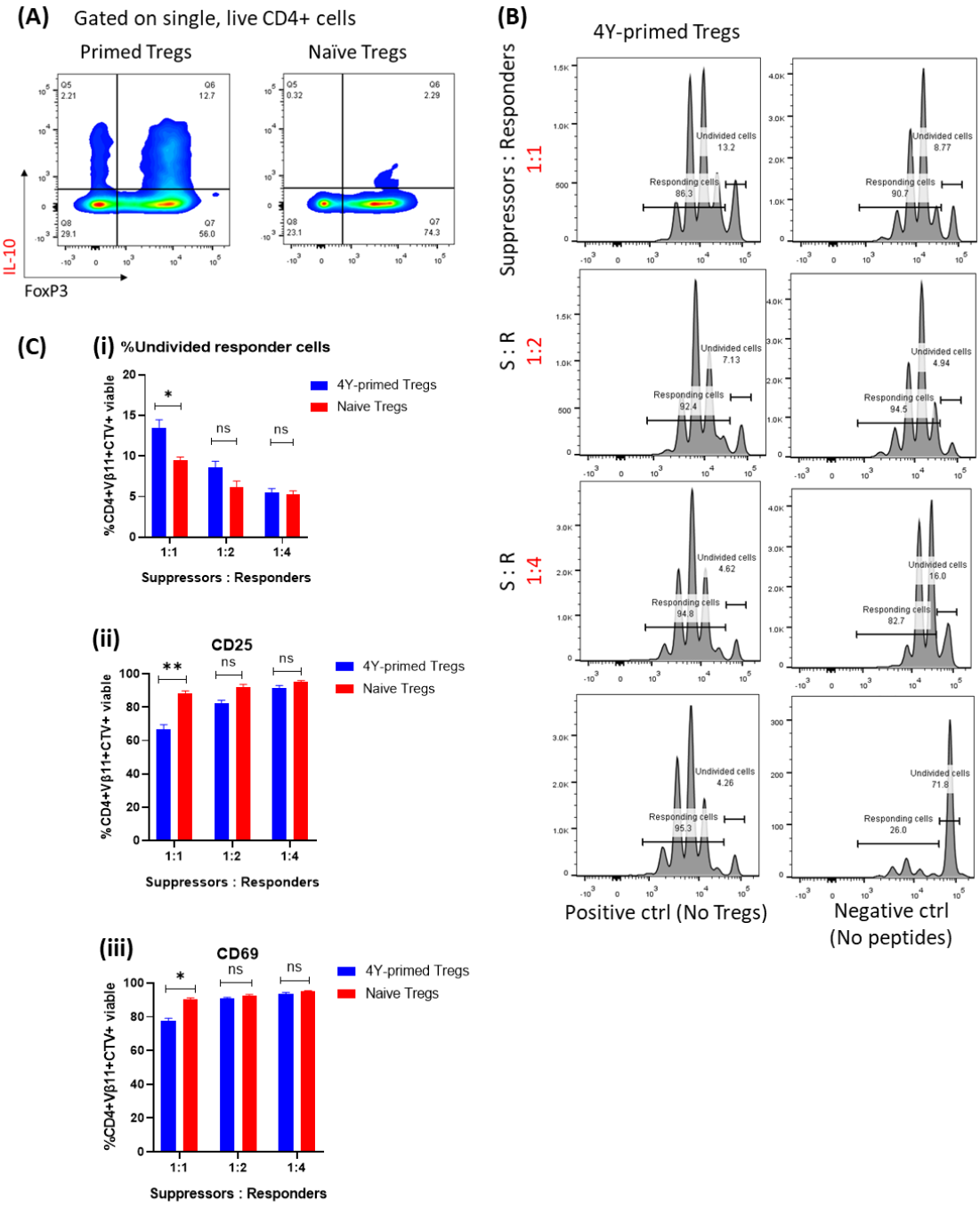



**Fig. 4.17: The full course of tolerance induction is required for the complete licensing of Tregs. (A)** $CD4^+CD25^+$ regulatory T cells were isolated from mice that received either 80ug 4Y or PBS 3 days prior to schedule-1 cull. A fraction of Tregs was stimulated with PMA and Ionomycin for 4h and then stained for surface markers and intracellularly for IL-10 and FoxP3. **(B)** Representative FACS plots of the CTV dilution peaks of responder cells when co-cultured with either 4Y-primed Tregs (left panel) or naïve Tregs (right panel) at different ratios. **(C)** Corresponding bar graphs of the percentage of undivided responder cells (i) and expression of CD25(ii) and CD69 (iii) on these cells ($CD4^+V\beta11^+CTV^+$). Statistical significance calculated by one-way ANOVA with Sidak's multiple comparisons test. Results are coming from 2 independent experiments and presented as standard error of the mean (SEM).

## 4.7 Naïve antigen-presenting cells are modulated by co-culture with different regulatory T cells *in vitro*

The data presented in previous paragraphs investigated the capacity of different regulatory T cells to suppress other T cells of different antigen specificity. To better characterise the function of these cells, we aimed to study their ability to exert their suppressive effects on DCs. To do that, a series of co-culture experiments was devised in which specific pathways could be manipulated. In that system, naïve $CD11c^+$ DCs from B10.PL mice were cultured together with different regulatory T cells (CD4tol, iTregs, 4Y-treated Tregs, PBS-treated Tregs) and naïve $CD4^+$ T cells (CD4_PBS) were used as a positive control for suppression. Purity of isolated $CD11c^+$ DCs was > 90% (data not shown).

Cells were stimulated overnight with different concentrations of 4K peptide (either 100μg/ml or 10μg/ml) to assess any dose-dependent effect or medium alone (0μg/ml 4K) as a control and expression of co-stimulatory molecules, such as CD80 and CD86, was assessed by flow cytometry the following day and cells were gated on $CD3^-CD19^-$ $CD11c^+MHC\ II^+$ DCs, based on the gating strategy shown in Figure 4.18A.

### 4.7.1 Dendritic cell modulation by co-culture with different regulatory T cells *in vitro*

For the generation of the different regulatory T cells, different approaches were used. For the generation of CD4tol cells (4Y-treated total $CD4^+$ T cells), Tg4 mice were administered s.c. increasing doses of the high affinity [4Y] peptide *in vivo* as described previously, and three days after the final dose, $CD4^+$ T cells from peptide-treated mice were isolated and used as CD4tol cells. It is worth noting that tolerant $CD4^+$ T cells consist

of both FoxP3$^+$ Tregs (<5%) and FoxP3$^-$IL-10$^+$ CD4tol cells (approximately 25-30% of total CD4$^+$), even though proportionally CD4tol cells outnumber Tregs in the total CD4$^+$ T cell pool.

Furthermore, iTregs were generated from naïve Tg4 splenocytes after *in vitro* differentiation with TGF-β and IL-2 and approximately 90% of total cells that were used for the co-cultures with DCs were FoxP3$^+$ (data not shown). For the purification of naturally occurring, peripheral FoxP3$^+$ Tregs from either PBS- or 4Y-treated mice were enriched based on CD4 and CD25 expression and approximately 85% of the cells used in the co-cultures were FoxP3$^+$. Naïve CD4$^+$CD25$^-$ T cells do not express FoxP3.

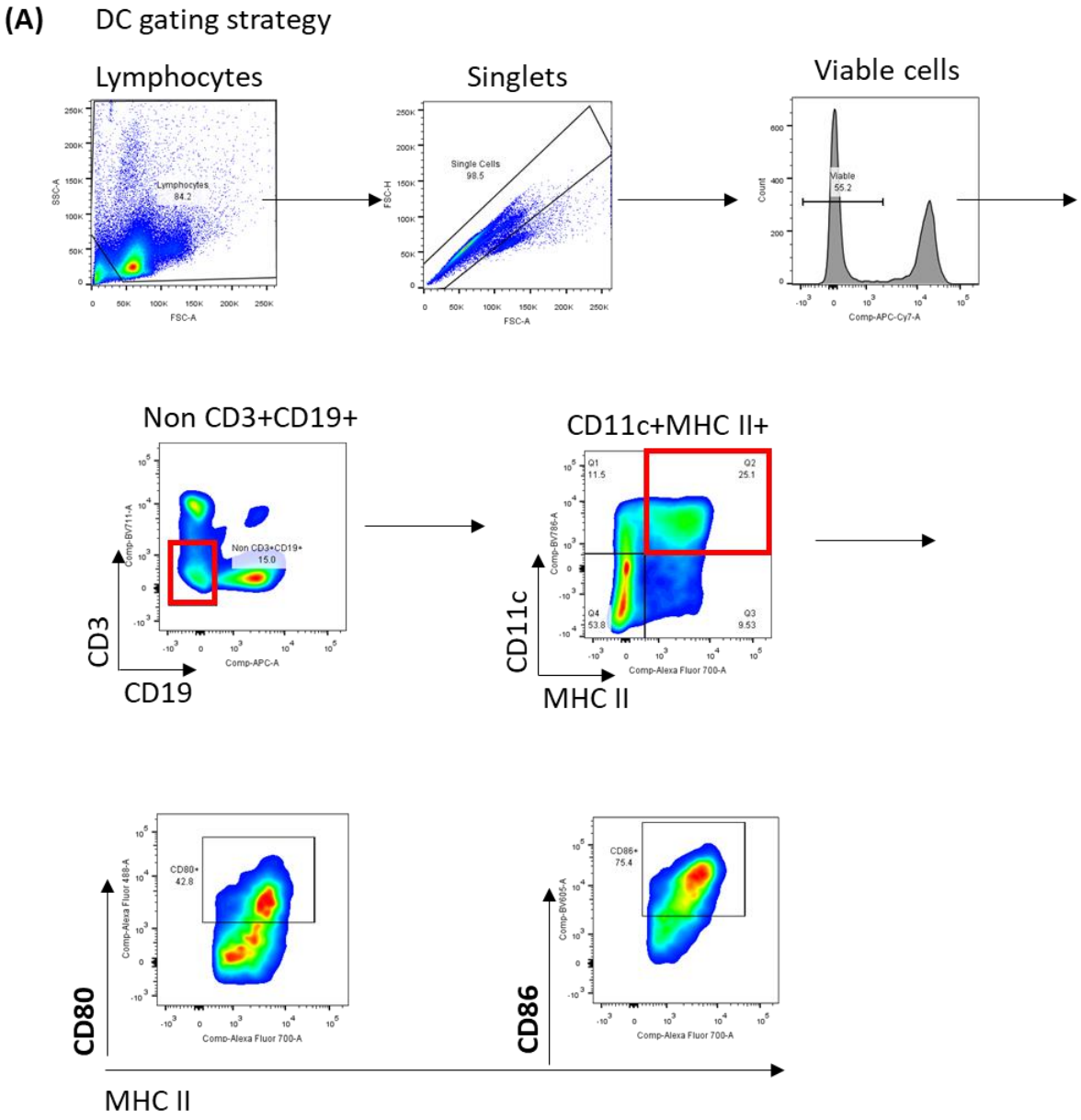
Each regulatory population was co-cultured with DCs at a ratio of 2:1 in a 96 well plate for 24h. Figure 4.18B summarises the MFI of CD80 on DCs following stimulation with 100μg/ml 4K (i), 10μg/ml (ii) or without antigen (iii), and Figure 4.18C summarises the expression of CD86 following stimulation with 100μg/ml 4K (i), 10μg/ml (ii) or without antigen (iii). DC expression of both CD80 and CD86 were very potently inhibited when exposed to 4Y-treated FoxP3$^+$ Tregs, followed by CD4tol cells and PBS-treated FoxP3$^+$ Tregs. Expression of CD40 and MHC II were not impacted significantly (data not shown).

In the presence of naïve CD4$^+$ T cells, there is an upregulation of both CD80 and CD86 upon activation with antigen as compared to the background level (untouched DC) that indicates DC maturation, which was abrogated when DCs were exposed to 4Y-treated Tregs, with the levels of expression being lower than the background showing the strong suppressive effect. Expression of CD86 follows a very similar pattern; DCs co-cultured with naïve CD4$^+$ T cells upregulate CD86 expression, yet when those DCs were

exposed to either 4Y-treated Tregs or CD4tolcells this upregulation was completely prevented.

These data repeat key experiments published previously on the *in vitro* effect of tolerised $CD4^+$ T cells on DC phenotype and very closely resembles the suppression observed (Gabrysova et al., 2009). However, the novelty of this new finding relies on the fact that it demonstrates that the main driver of the suppression is tolerised $FoxP3^+$ Tregs rather than $IL\text{-}10^+$ Tr1 cells.

**Fig 4.18** (Continued on the next page)



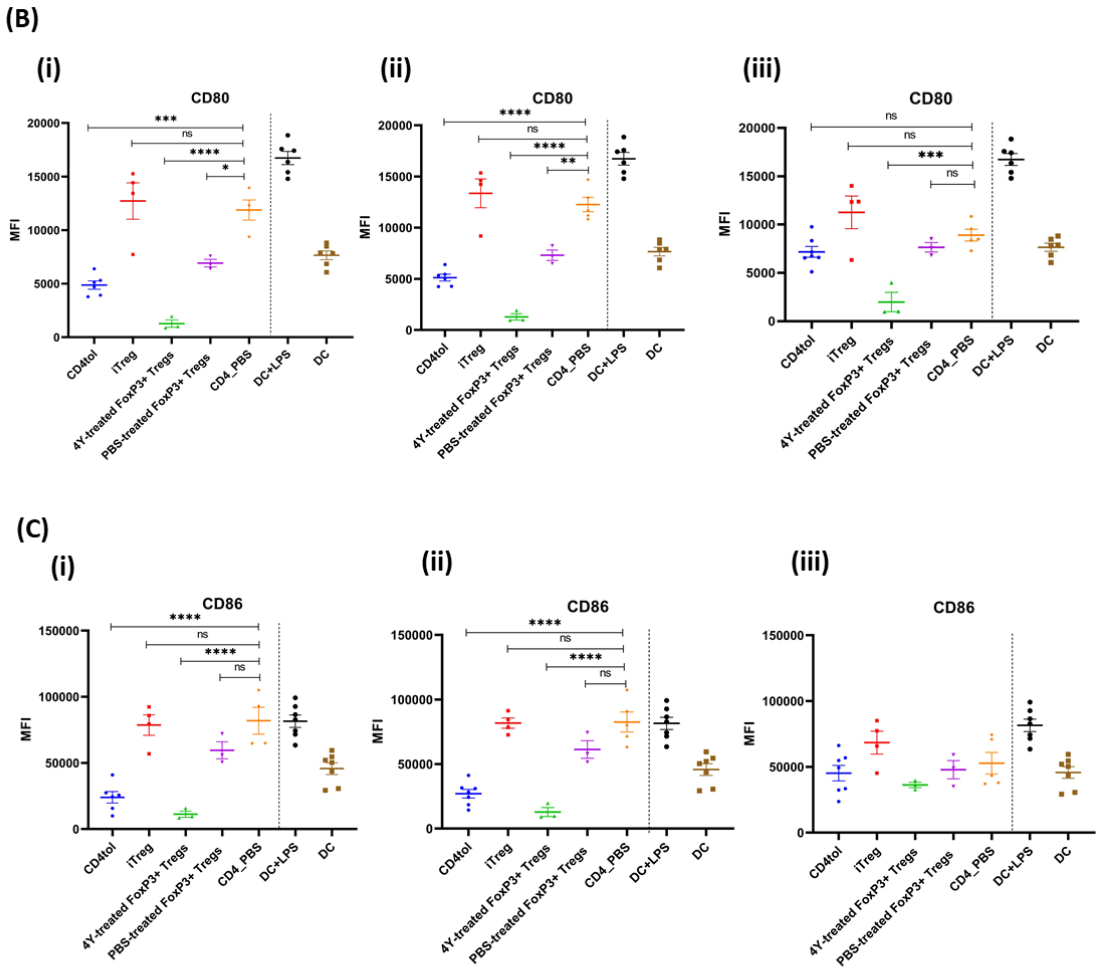



**Fig. 4.18: FoxP3$^+$ Tregs from peptide-treated Tg4 mice are the most potent suppressors of CD80 and CD86 expression on dendritic cells, followed by CD4tol cells. (A)** Gating strategy followed to study the impact of each regulatory T cell population of DCs. Results are coming from CD3$^-$CD19$^-$CD11c$^+$MHC II$^+$ DCs. **(B)** Mean fluorescence intensity (MFI) of CD80 after co-culturing DCs with each regulatory T cell population overnight in the presence of 100μg/ml 4K (i), 10μg/ml 4K (ii) or 0μg/ml 4K (iii). **(C)** MFI of CD86 after co-culturing DCs with each regulatory T cell population overnight in the presence of 100μg/ml 4K (i), 10μg/ml 4K (ii) or 0μg/ml 4K (iii). DC stimulated with LPS served as a positive control, while DCs alone show the background expression of each marker and they were excluded from the statistical analysis. Statistical significance calculated by one-way ANOVA with Dunnett's multiple comparisons test against naïve CD4$^+$FoxP3$^-$ Tg4 cells, which served as a positive control. Results are coming from 3 independent experiments and presented as standard error of the mean (SEM).

### 4.7.2 Production of IL-10 and IL-12 by DC co-culture with regulatory T cells *in vitro*

To investigate the impact of each regulatory T cell population on cytokine production, cell culture supernatants from T cell: DC co-cultures were collected, and levels of secreted anti-inflammatory cytokine, IL-10, and pro-inflammatory cytokine, IL-12p70 were measured by sandwich ELISA. It should be noted that with ELISA, it is not possible to identify the cellular source of measured cytokine; therefore, it cannot be determined whether the expression of these cytokines derived from the DC or T cell component of the co-culture.

Ideally, intracellular staining for IL-10 and IL-12 within DCs, both with and without stimulation with exogenous peptide antigen and/or LPS would be the best way to define whether these cytokines are deriving from DCs. However, by including DCs in medium alone as a control for background cytokine production and DC stimulated with LPS as a measurement for secretion of these cytokines upon activation, we can infer some information about the impact of each regulatory population on the overall cytokine profile of the co-culture.

In the presence of CD4tol cells, there was a significantly high production of IL-10 upon stimulation with 100µg/ml 4K (Fig. 4.19A, i), 10µg/ml 4K (Fig. 4.19A, ii) and even without antigen (Fig. 4.19A, iii). 4Y-treated Tregs also produced high levels of IL-10 both with and without antigen. IL-10 can come from the regulatory cells themselves, or it can come from their increased capacity to potentiate DCs to produce IL-10, rendering them tolerogenic and establishing a negative feedback mechanism that prevents further activation of naïve and effector T cells by DCs.

IL-12 production is restricted to DCs, and it relies on CD40-CD40L interaction (Heufler et al., 1996). Co-culture of DCs with naïve $CD4^+$ T cells secreted very high concentrations of IL-12, similar to that seen upon stimulation with LPS, promoting in turn the expansion of Th1 cells in response to $MBP_{Ac1-9}$ (Fig. 4.19B). However, in the presence of CD4tol cells and 4Y-treated Tregs, there was a significant downregulation of IL-12 production both after stimulation with 100μg/ml 4K (Fig. 4.19B, i) and 10μg/ml 4K (Fig. 4.19B, ii) and even to some degree without antigen (Fig. 4.19B, iii). This is not surprising, since both CD4tol and 4Y-treated Tregs produce IL-10 in the absence of antigen, potentially due to previous TCR signals they received *in vivo* during 4Y-treatment, and hence are able to subsequently suppress DC maturation and IL-12 production *in vitro*. iTregs and naïve peripheral Tregs are also able to downregulate IL-12, but not as efficiently as CD4tol and 4Y-treated Tregs.

Taken together, the data presented in the previous paragraphs demonstrate that peptide immunotherapy gives rise to superior suppressive cells, both $FoxP3^+$ Tregs and $FoxP3^-$ CD4tol cells that can exert their inhibitory effect either by modulating other T cells of different antigen specificity, or by modulating the ability of dendritic cells to prime other T cells by downregulating CD80 and CD86, secrete high levels of IL-10, which can then in turn lead to downregulation of IL-12. It will be useful to also have an APC-free system, where T cells can be stimulated with monoclonal antibodies against CD3 and CD28 to be able to demonstrate direct suppression between T cells, which is not mediated via APCs.

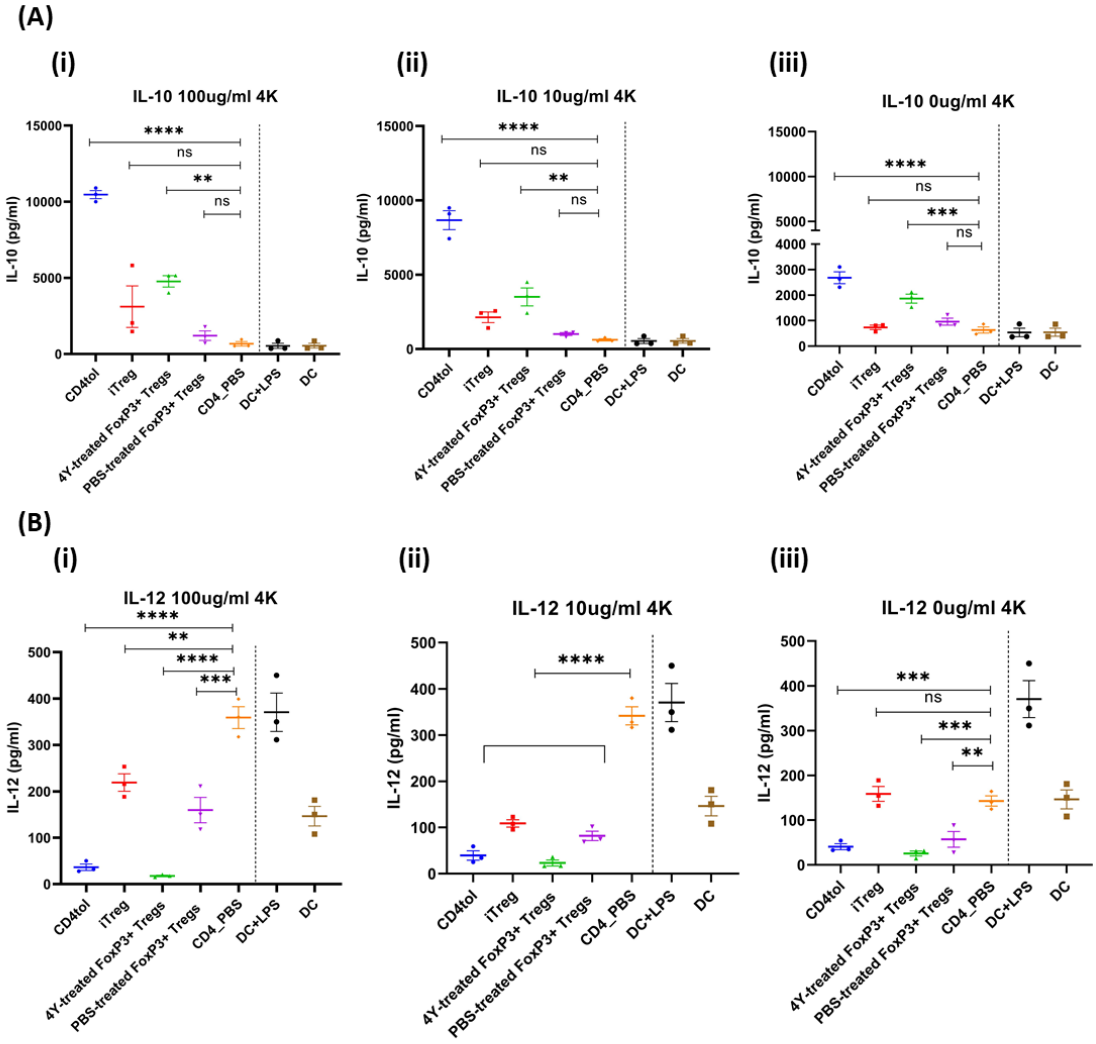



**Fig. 4.19: In the presence of 4Y-treated FoxP3$^{+}$ Tregs and FoxP3$^{-}$ CD4tol cells, the secretion of IL-10 was enhanced, while IL-12 was downregulated.** **(A)** After 24h of T cell: DC co-culture, supernatants were collected and levels of IL-10 were measure by ELISA after stimulation with 100µg/ml 4K (i), 10µg/ml 4K (ii) or 0µg/ml 4K (iii). **(B)** Levels of IL-12 were measure by ELISA after stimulation with 100µg/ml 4K (i), 10µg/ml 4K (ii) or 0µg/ml 4K (iii). DC stimulated with LPS served as a positive control, while untouched DCs show the background production of each cytokine and were excluded from the statistical analysis. Statistical significance calculated by one-way ANOVA with Dunnett's multiple comparisons test against naïve CD4+ Tg4 cells (CD4_PBS), which served as a positive control. Non-statistically significant changes were accepted where p>0.05 (no * or ns). Results are coming from 3 independent experiments and presented as standard error of the mean (SEM).

### 4.7.3 Requirement for cell-contact for inhibition of DC maturation by regulatory T cells

Having shown that both 4Y-treated FoxP3$^+$ Tregs and total CD4$^+$ from 4Y-treated mice (CD4tol cells) were able to downregulate CD80 and CD86, the question we aimed to address next was whether this suppression was mainly driven by cell contact or by soluble factors secreted by the regulatory cells. To do that, CD4tol cells were chosen as a representative regulatory population and were put in co-culture with CD11c$^+$ DCs as previously described, with or without antigen for 24h. Furthermore, CD4tol supernatants from optimally stimulated cultures (see section 4.4.2 of this chapter) were also added in culture with DCs to investigate whether soluble factors found in the supernatants were sufficient to drive the downregulation of co-stimulatory molecules on DCs. Naïve Tg4 CD4$^+$ T cells were used as a positive control for suppression.

It was clear that CD4tol supernatants alone were not able to downregulate CD80 either after stimulation with 100μg/ml 4K (Fig. 4.20A, i) or 10μg/ml 4K (Fig. 4.20A, ii) or without antigen (Fig. 4.20A, iii) as measured by MFI. CD86 MFI was similar when CD4tol supernatants or naïve CD4$^+$ T cells were added in culture and stimulated with 100μg/ml 4K (Fig. 4.20B, i) or 10μg/ml 4K (Fig. 4.20B, ii) or without antigen (Fig. 4.20B, iii). Therefore, soluble factors found in the supernatants of regulatory T cells are not sufficient to mediate the downregulation of CD80 and CD86 and there is a requirement for cell contact for this type of suppression to occur.

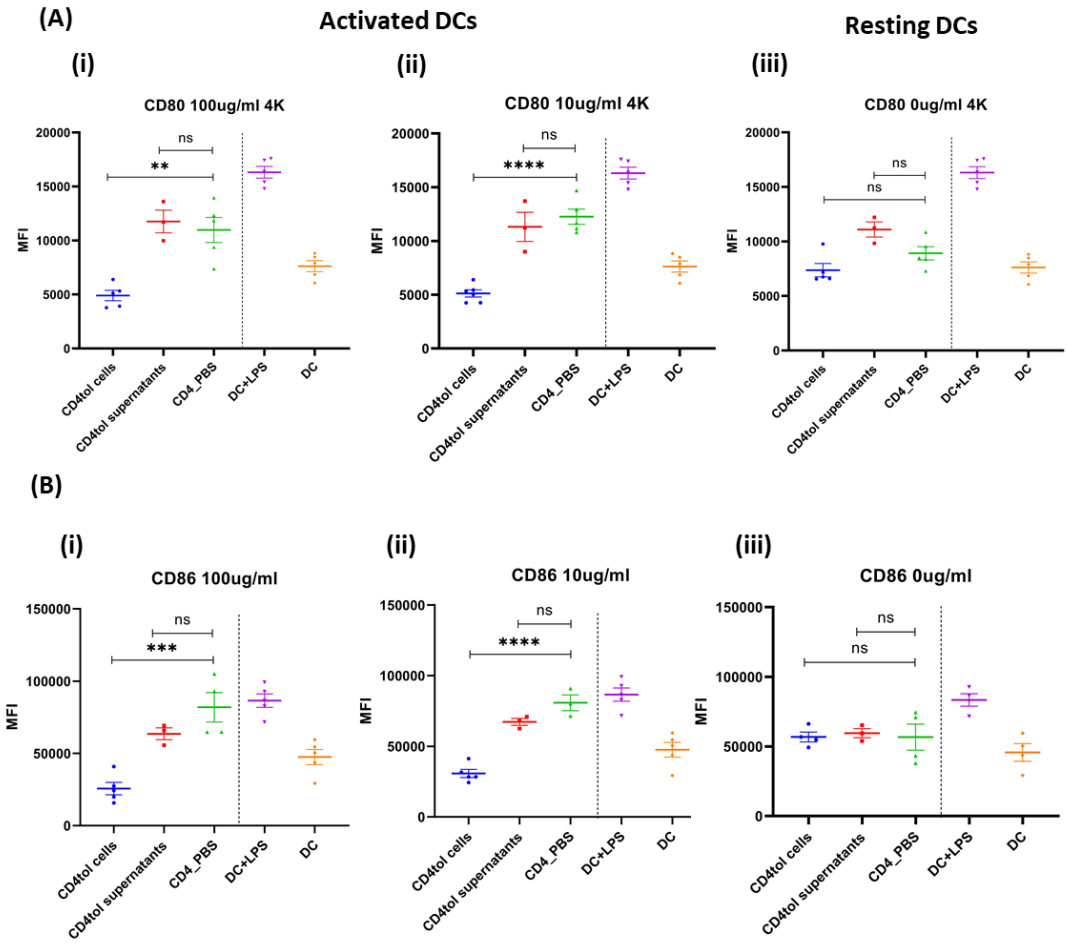



**Fig. 4.20: Soluble factors secreted in CD4tol culture supernatants were not sufficient to downregulate CD80 and CD86 on dendritic cells. (A)** Either CD4tol cells or CD4tol supernatants were added in culture with DCs overnight and expression of CD80 on DCs was measured 24h later after stimulation with either 100ug/ml 4K (i), 10ug/ml (ii) or 0ug/ml 4K (iii). **(B)** The mean fluorescence intensity of CD86 on DCs was measured after stimulation with either 100ug/ml 4K (i), 10ug/ml (ii) or 0ug/ml 4K (iii) in the presence of either CD4tol cells or CD4tol supernatants. DC stimulated with LPS served as a positive control, while DCs alone show the background production of each cytokine and they were excluded from the statistical analysis. Statistical significance calculated by one-way ANOVA with Dunnett's multiple comparisons test against naïve CD4+ Tg4 cells (CD4_PBS), which served as a positive control. Non-statistically significant changes were accepted where $p>0.05$ (no * or ns). Results are coming from 2 independent experiments and presented as standard error of the mean (SEM).

### 4.7.4 Role of CTLA and IL-10 in the suppressive effect of regulatory T cells on DCs

Prior data using the Tg4 IL-$10^{-/-}$ revealed that suppression of CD80 and CD86 *in vivo* was reliant on the presence of IL-10, and that without IL-10 mice are not able to control EAE development when treated with tolerogenic peptide (Gabrysova et al., 2009; Burkhart et al., 1999; O'Neill et al., 2006). To assess the role of IL-10 together with CTLA-4, we used blocking antibodies against IL-10R and CTLA-4, respectively. CD4tol cells were co-cultured with DCs, with or without antigen as before (control) and CD4tol cells were also co-cultured with either anti-IL-10R or anti-CTLA-4 antibodies or both for 2h at 37$^{o}$C prior to antigenic stimulation.

Interestingly, the *in vitro* results from the DC co-cultures confirmed the previous *in vivo* results, since suppression of CD86 was reversed when IL-10R was blocked, while antibodies against CTLA-4 alone did not have a significant effect on the capacity of regulatory T cells to downregulate CD86 on DCs, both with (Fig. 4.21A, i) or without antigen (Fig. 4.21A, ii). Similar phenotype was seen with CD80, since its expression was restored only when IL-10R was blocked but not when CTLA-4 was blocked, in the presence (Fig. 4.21B, i) or absence of antigen (Fig. 4.21B, ii).

Taken together, all the results from the blockade of IL-10R and CTLA-4, demonstrate the ability of regulatory T cells to mediate bystander suppression against other cells is driven by both IL-10 and CTLA-4, while the ability of the same cells to inhibit the maturation of DCs, relies mostly on IL-10 expression.

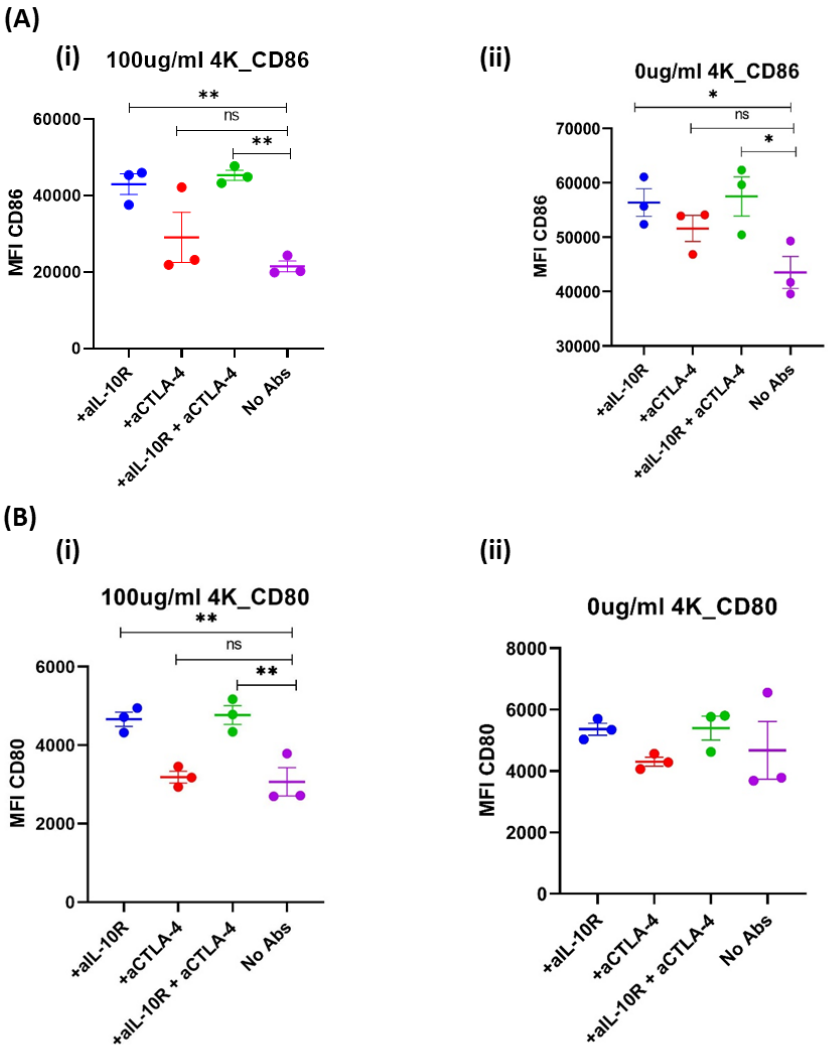



**Fig. 4.21: Neutralisation of IL-10R but not CTLA-4 reversed the downregulation of CD80 and CD86 on DCs mediated by CD4tol cells. (A)** DCs and CD4tol cells were incubated with either aIL-10R blocking antibody, aCTLA-4 or both for 2h at 37°C prior to stimulation with 4K. Cells were stained 24h later and the MFI of CD86 was measured following stimulation with 100µg/ml 4K (i) or at steady state (ii). **(B)** Similarly, CD80 MFI was measured after stimulation with 100µg/ml 4K (i) or at steady state (ii). Statistical significance calculated by one-way ANOVA with Dunnett's multiple comparisons test against the condition where no blocking antibody was added in culture, which served as a positive control. Non-statistically significant changes were accepted where $p>0.05$ (no * or ns). Results are coming from 2 independent experiments and presented as standard error of the mean (SEM).

## 4.8 Discussion

The work that was done previously in the Wraith lab has mainly focused on understanding the mechanisms of action of antigen specific immunotherapy by studying the impact on IL-10$^{+}$ Tr1 cells, which is the predominant population in tolerant CD4$^{+}$ T cells. Analysis of the transcriptome has shown that during the dose escalation, there are certain transcription factors, such as c-Maf, NFIL3, and co-inhibitory receptors, including TIGIT, TIM-3 and LAG-3, whose expression was strongly linked to the immunoregulatory cytokine, IL-10 (Burton et al., 2014). However, there was an unmet need to study the functional properties of these cells, by examining both their capacity to mediate bystander suppression on T cells with different antigen specificity and by also dissecting the mechanism of action.

The data presented in this chapter provides an in-depth analysis of the ability of different regulatory T cells to mediate bystander suppression *in vitro*. CD4tol cells were highly suppressive as they strongly inhibited the proliferation and activation of other T cells in co-culture experiments. It was demonstrated that their mechanism of action relies predominantly on cell contact, with CTLA-4 being involved in their suppressive mechanism of action on other T cells, but not on DCs. It appeared that their ability to modulate DC maturation was IL-10-dependent, in line with previous *in vivo* data (Gabryšová et al., 2009). IL-10 was critical for the ability of these cells to exert both bystander suppression as well as inhibition of CD80 and CD86 on DCs, highlighting the already established importance of this cytokine for the function of these cells (Brockmann et al., 2017).

Interestingly, it was also shown that these cells can mediate both linked and bystander suppression, because in the initial experiments, the suppression mediated by

CD4tol cells was more profound with the peptides that are covalently linked, rather than the separate peptides, consistent with the work from Bullock and colleagues who were amongst the first ones to describe this phenomenon almost 4 decades ago (Bullock et al., 1975). Intriguingly, when antigen presentation was taking place on the same F1 APC, that allows responders and suppressors to come in proximity, a stronger suppressive effect was observed, further reinforcing the hypothesis that cell contact is a prerequisite for suppression. This hypothesis was confirmed with transwell experiments and it was in line with previous work, which demonstrated that this state of induced tolerance can be self-perpetuating and long-lasting, as long as the putative suppressors and responders are in the vicinity of one another (Turley and Miller, 2007; Navarro et al., 2014). This state of infectious tolerance, holds great therapeutic potential for the fields of autoimmunity, allergy and transplantation (Kendal and Waldmann, 2010; Qin et al., 1993).

Furthermore, we wanted to recapitulate some of these findings in a more physiologically relevant environment. This was done by two different approaches; firstly, by assessing whether the APC populations are affected by the tolerance induction protocol themselves to exert bystander suppression *in vivo,* or by investigating whether introduction of tolerant $CD4^+$ T cells using adoptive transfers was sufficient to mediate bystander suppression when given together with naïve 2D2 cells into naive F1 mice. With the first set of experiments in the (Tg4 x C57BL/6) F1 mouse, it was clearly shown that induction of tolerance established a highly suppressive environment, which does not allow the adoptively transferred, CTV-labelled naïve responders to proliferate. In that model, it was also shown that the expression of CD80 and CD86 was suppressed on DCs *in vivo,* and that can partially explain the suppression seen. In addition to the impact of peptide treatment on DCs, another reason for the suppression would be the involvement

of the different populations of regulatory T cells that expand after tolerance induction and can exert their suppressive phenotype via different mechanisms, such as killing of neighbouring APCs or T cells via granzyme B (Cao et al., 2007), consumption of IL-2 that prevents the survival and expansion of T effector cells (Höfer et al., 2012), IL-10-mediated inhibition of either T cells directly (Taylor et al., 2009) or indirectly via induction of tolerogenic APCs (Bhattacharyya et al., 2004), amongst others. Their phenotype is explained more extensively in the Tg4 model in the following chapter.

Therefore, by inducing tolerance to the recipient mice, both T cells and APCs acquire a more tolerogenic phenotype that prevents the expansion of naïve T cells. It would be interesting to investigate whether bystander suppression is driven by IL-10 *in vivo*, and follow up previous observations which showed that suppression of proliferation of naïve Tg4 T cells transferred into tolerised Tg4 recipients was reversed by neutralisation of IL-10 (Sundstedt et al., 2003).

It is easier to observe suppression in the (Tg4 x C57BL/6) F1 model, since there is a great number of regulatory T cells and tolerogenic DCs that can orchestrate the suppression. Therefore, we were keen to devise a series of co-transfer experiments, where naïve recipient mice were given $5x10^6$ tolerant Tg4 $CD4^+$ (CD4tol cells), with an equal number of responder cells, either 2D2 responders (bystander model) or Tg4 responders (antigen-specific model). It was shown in both models that this cell number is sufficient to drive the suppressive phenotype in an otherwise naïve recipient mouse that does not have any other IL-$10^+$ CD4tol cells. This experiment clearly shows that the strong suppressive capacity of these cells is sufficient to establish bystander suppression *in vivo*.

The shortcoming of the previous experiments is the purity of CD4tol cells used. In our system, tolerant $CD4^+$ T cells were referred to as CD4tol cells since there was a high percentage of cells (around 40%) expressing IL-10. Previous studies on CD4tol cells (also referred to PItol since they derive from peptide-induced, 'tolerised' mice) have shown that $CD4^+$ T cells from the tolerant Tg4 mouse were predominantly $CD25^-FoxP3^-$, highlighting that CD4tol cells are distinct both in origin and function to the natural $CD4^+CD25^+FoxP3^+$ Tregs (Nicolson et al., 2006). Furthermore, $FoxP3^+$ Tregs were not required for the generation of the CD4tol populations. However, in that population of CD4tol cells, there will still be a small population of cells that express FoxP3 following tolerance induction (Burton et al., 2014).

To be able to isolate different regulatory T cell populations at higher purity, an IL-10 reporter Tg4 mouse would be the best model to use to be able to isolate a pure population of $IL\text{-}10^+$ Tr1 cells. Ideally, to be able to successfully define CD4tol cells and differentiate them from Tregs, we would need to generate an IL-10 and FoxP3 double-reporter as described by other groups (Brockmann et al., 2018; Rubtsov et al., 2008) and cross it with the Tg4 background to generate $FoxP3^+IL\text{-}10^-$ or $FoxP3^+IL\text{-}10^+$ Tregs and $FoxP3^-IL\text{-}10^+$ Tr1 cells at high purities and compare their phenotypic and functional differences.

Despite the limitations arising from the models used and the inherent heterogeneity that characterises the regulatory T cell populations, it was clearly demonstrated that peptide immunotherapy is responsible not only for giving rise to the suppressive population of CD4tol cells, but also for the licensing of $FoxP3^+$ Tregs. Tregs from 4Y-treated mice were the most potent mediators of bystander suppression, followed by total $CD4^+$ T cells from tolerant mice, which comprised both $FoxP3^+$ Tregs and $FoxP3^-$ CD4tol

cells, and lastly naïve FoxP3$^{+}$ Tregs and iTregs, which were not suppressive in our *in vitro* system. Both tolerised CD4tol and Tregs express high levels of IL-10; however, CD4tol cells are the more dominant source numerically.

Despite the high levels of IL-10 found in CD4tol cultures, it was interesting to show that the supernatants from CD4tol cultures failed to block the upregulation of CD80 and CD86 on naïve DCs and had no effect on T cell proliferation. Hence, even though IL-10 is a critical cytokine that can partially account for the highly suppressive phenotype of regulatory T cells, it is not the only molecule involved in bystander suppression, since there are other pathways that are involved in this type of suppression. For example, Homann and colleagues showed that T cells specific for one antigen in insulin B chain, can suppress autoreactive T cells specific for a different self-antigen (LCMV-NP) in a mechanism that was highly dependent on the IL-4/Stat6 pathway (Homann et al., 1999).

Notably, the hierarchy in terms of suppressive capacity amongst the different populations of regulatory T cells highlights the heterogeneity and plasticity seen in Tregs that reflects their diverse functions under inflammatory conditions or in specific tissues (Cretney et al., 2013). Upon first encounter with the antigen, Tregs retain a naïve-like phenotype, but they start to produce low levels of IL-10 and gradually differentiate into effector, fully mature Tregs; however, they only acquire their highly suppressive phenotype after repeatedly encountering their cognate antigen. This indicates that during chronic exposure to antigen, when there is a persistent triggering of the TCR, Tregs undergo a re-programming process that makes them acquire a more tolerogenic phenotype to be able to suppress excessive immune pathology and restore immune homeostasis.

Furthermore, prior data using the Tg4 IL-$10^{-/-}$ model revealed that the expression of CD80 and CD86 *in vivo* was reliant on the presence of IL-10 and that without IL-10, mice were not able to control EAE development when treated with tolerogenic peptide (Burkhart et al., 1999a; O'Neill et al., 2006b; Gabrysova et al., 2009). Our *in vitro* data using a blocking antibody against IL-10R, confirmed that observation. It will be interesting to investigate the role of inhibitory receptors on this phenomenon by either using blocking antibodies against the different receptors or by generating knock out mice on the Tg4 background and testing the suppressive capacity of the relevant regulatory T cells to further dissect the mechanisms and pathways involved in bystander suppression.

In conclusion, the analysis of T cell populations (CD4tol and Treg cells) and DCs from the Tg4 mouse represents a novel view of how diverse subsets of lymphocytes are modified as a result of peptide immunotherapy using $MBP_{Ac1\text{-}9}$[4Y] and suggests multiple avenues for the bidirectional interaction between T cells and DCs, which is central for bystander suppression.

Concluding statement

The data presented on this chapter demonstrate that repeated exposure to tolerogenic antigen stimulation mimics the course of chronic infection and it gives rise to different regulatory T cell populations, each one of them having a distinct capacity to mediate bystander suppression. This type of suppression is cell-contact dependent, with CTLA-4 being one of the cell surface molecules that is involved in the inhibition of responder cells. IL-10 also played a role in driving the bystander effect, by enabling regulatory T cells to inhibit the expression of CD80 and CD86 on DCs. The influence of IL-10 on DC

function reveals a classical, negative feedback loop that has evolved to control the immune response to antigen and limit immune pathology. Finally, some of these findings were also reproduced *in vivo*, showing that during the course of tolerance induction, peptides delivered in a highly soluble form that are known to bind steady-state DCs (Shepard et al., 2021) and present antigen in a tolerance-inducing manner can give rise to both CD4tol cells and tolerant Tregs as well as tolerogenic DCs. In this way, T cell responses can be self-limiting in the context of peripheral tolerance to a self-antigen.

# CHAPTER 5:

# IMPACT OF PEPTIDE IMMUNOTHERAPY ON THE TRANCRIPTIONAL RE-PROGRAMMING OF REGULATORY T CELLS

## 5.1 Introduction

In chapter 4, it was shown that Tregs derived from peptide-treated mice were able to inhibit the proliferation of responder cells even at low ratios of suppressors: responders (1:16), while naïve Tregs were not functionally suppressive *in vitro*. The critical question that we aim to address in this chapter is how peptide immunotherapy leads to a switch from a non-suppressive to a highly suppressive phenotype among FoxP3$^{+}$ Tregs. We hypothesise that the change in phenotype was a result of repeated cell activation, which subsequently results in differential expression of genes associated with the differentiation and function of Tregs following repeated exposure to antigen.

Previous work from the Wraith lab has not focused heavily on the phenotype of FoxP3$^{+}$ Tregs following tolerance induction, since the generation of FoxP3$^{-}$ Tr1 cells was a more striking effect of peptide immunotherapy. Furthermore, using a RAG$^{-/-}$ Tg4 mouse model that lacks endogenous FoxP3$^{+}$ Tregs, it was shown that peptide immunotherapy can induce Tr1 cells *in vivo* independently of Tregs, (Nicolson et al., 2006). Burton and colleagues (Burton et al., 2014) have performed detailed immunophenotyping during dose escalation immunotherapy using $MBP_{Ac1\text{-}9}$ [4Y] and shown that antigen-specific CD4$^{+}$ T cells undergo a progressive transcriptional re-programming, rendering them resistant to production of inflammatory cytokines.

Furthermore, Bevington and colleagues (Bevington et al., 2020) have shown that dose escalation has an effect not only on the transcriptome, but also in the epigenome of tolerant CD4$^{+}$ T cells, where epigenetic priming creates an accessible chromatin environment for immunosuppressive genes, while for immune response genes the threshold of TCR/CD28 signalling for activation remains high, rendering these loci less responsive to stimulus.

The studies described above focused on tolerance induction in the total $CD4^+$ population of tolerant cells, which mainly consists of $FoxP3^-$ Tr1 cells; however, in RAG-sufficient Tg4 mice there is also a small percentage of $FoxP3^+$ Tregs (5-10% of total $CD4^+$ T cells) that undergo phenotypic changes following repeated exposure to antigen. Therefore, this chapter attempts to shed light on both $FoxP3^-$ Tr1 and $FoxP3^+$ Treg cells to delineate how these regulatory T cell subsets compare in their ability to mediate immune suppression and to define whether they share phenotypic and functional markers of tolerance induction.

It should be acknowledged that the bulk RNA sequencing described in this chapter was done in collaboration with Azenta Life Sciences and the initial bioinformatics analysis of the raw data was kindly done by Dr Sky Ng from the Wraith lab. For the single-cell RNA sequencing, I spent three months of my PhD at the National Institutes of Health (NIH) in Bethesda, USA under the supervision of Dr Ethan Shevach. During that time, I was able to observe part of the sequencing and subsequent bioinformatics analysis, which was done at a core facility of the National Institute of Allergy and Infectious Diseases (NIAID). Finally, the DNA demethylation analysis was done in collaboration with Dr Shimon Sakaguchi's lab in Osaka University, Japan.

<u>Chapter aims:</u>

- Phenotypic characterisation of Tregs and Tr1 cells
- Analysis of the differentially expressed genes amongst the different regulatory populations using bulk and single-cell RNA sequencing techniques
- Epigenetic analysis of the CNS2 region

## 5.2 Characterisation of the phenotype of tolerised CD4$^+$ T cells

In the previous chapter, we were able to dissect the suppressive capacity of both total tolerised CD4$^+$ T cells (CD4tol) and to delve into the enriched population of FoxP3$^+$ Tregs from either naïve or peptide treated Tg4 mice and study them in the context of bystander suppression. In addition to the functional studies, to be able to fully understand the heterogeneous nature of both FoxP3$^+$ Tregs and FoxP3$^-$ Tr1, a thorough characterisation of the phenotype and genotype of these cells was done to further elucidate the pathways that are affected by peptide immunotherapy.

### 5.2.1 Expansion of IL-10$^+$FoxP3$^-$ Tr1 cells and FoxP3$^+$ Tregs following peptide treatment

To be able to characterise the immunophenotype of Tregs and Tr1 cells, Tg4 mice were subjected to the tolerance induction protocol, as described previously in section 2.5.1 of Materials & Methods, and spleens were harvested three days after the final 4Y treatment. CD25$^+$ cells were purified from either the 4Y- or PBS-treated group and used as the Treg fraction of the bulk CD4$^+$ T cell population. The CD25$^-$ fraction, essentially the Treg-depleted population, from the 4Y-treated mice was called 4Y-treated T conventional cells, while the CD25$^-$ fraction from PBS-treated mice was referred to as PBS-treated T conventional cells. These 4 groups were stimulated with PMA and Ionomycin (P/I) prior to staining for surface and intracellular markers.

There was a good correlation between CD25 and FoxP3 expression, since both in the peptide-treated and naïve mice, most of the CD25$^+$ cells also expressed FoxP3 (Fig. 5.1A). This confirms that the purification process was successful because the CD25$^+$ fraction consists almost entirely of FoxP3$^+$ Tregs. On the other hand, in the CD25$^-$ fraction of 4Y-treated cells, there was still a small percentage of FoxP3$^+$ cells (around 10%), while

this was not the case in PBS-treated cells, indicating that during 4Y-treatment, there are some cells that downregulate CD25 even though they still express FoxP3 (Fig. 5.1A). This should be accounted for when analysing these cells, which even though they are primarily $FoxP3^-$ and they would otherwise be referred to as Tr1 cells, we prefer to call them 4Y-treated T conventional cells, due to the impurities deriving from our methodology.

Furthermore, in the 4Y-treated cells, there was enhanced expression of IL-10, both in Tregs and T conventional cells (approximately 37% $IL\text{-}10^+$ cells within the $CD4^+$ gate), while there was only a small percentage of $IL\text{-}10^+$ cells in the PBS-treated Tregs (12%) and virtually no expression of IL-10 in the PBS-treated T conventional cells (Fig. 5.1B). To better define the subpopulations of regulatory T cells within each one of the 4 groups that were analysed, the percentage of $FoxP3^+IL\text{-}10^+$, $FoxP3^+IL\text{-}10^-$ or $FoxP3^-IL\text{-}10^+$ cells was measured by flow cytometry.

As expected, in the PBS-treated T conventional group, there were very low percentages (<5% of $CD4^+$ T cells) of any regulatory population, while in the 4Y-treated T conventional group, the dominant population of cells was $IL\text{-}10^+FoxP3^-$ (around 35% of $CD4^+$ T cells) (Fig. 5.1C). In the PBS-treated Tregs, the main population of cells was $FoxP3^+IL\text{-}10^-$, with low percentages of IL-10-producing cells, while in the 4Y-treated Tregs, the predominant population was again $FoxP3^+IL\text{-}10^-$ (45-50% of $CD4^+$ T cells); however, there was a substantial increase in the proportion of cells that were expressing both FoxP3 and IL-10 (35%) (Fig. 5.1C).

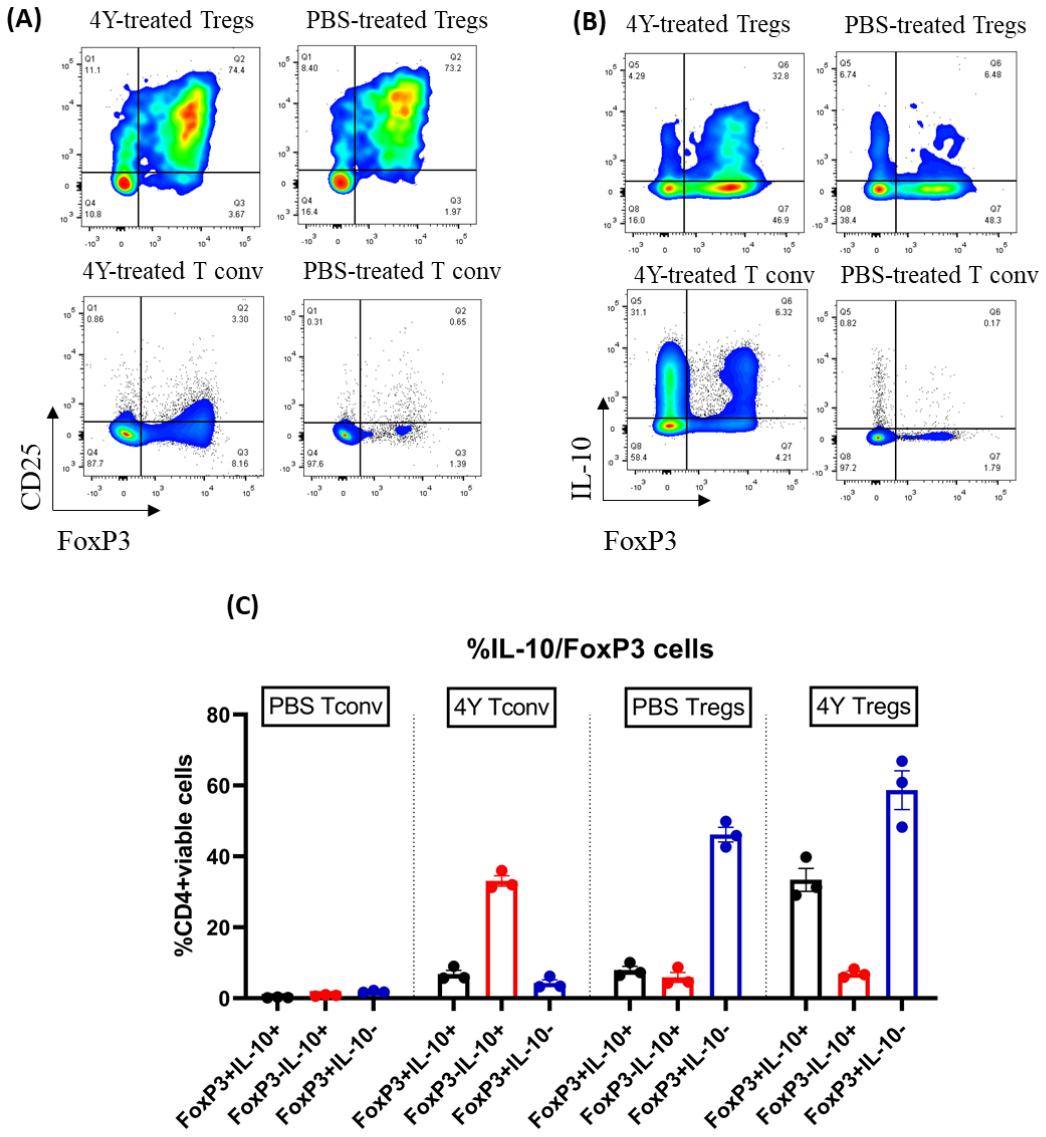


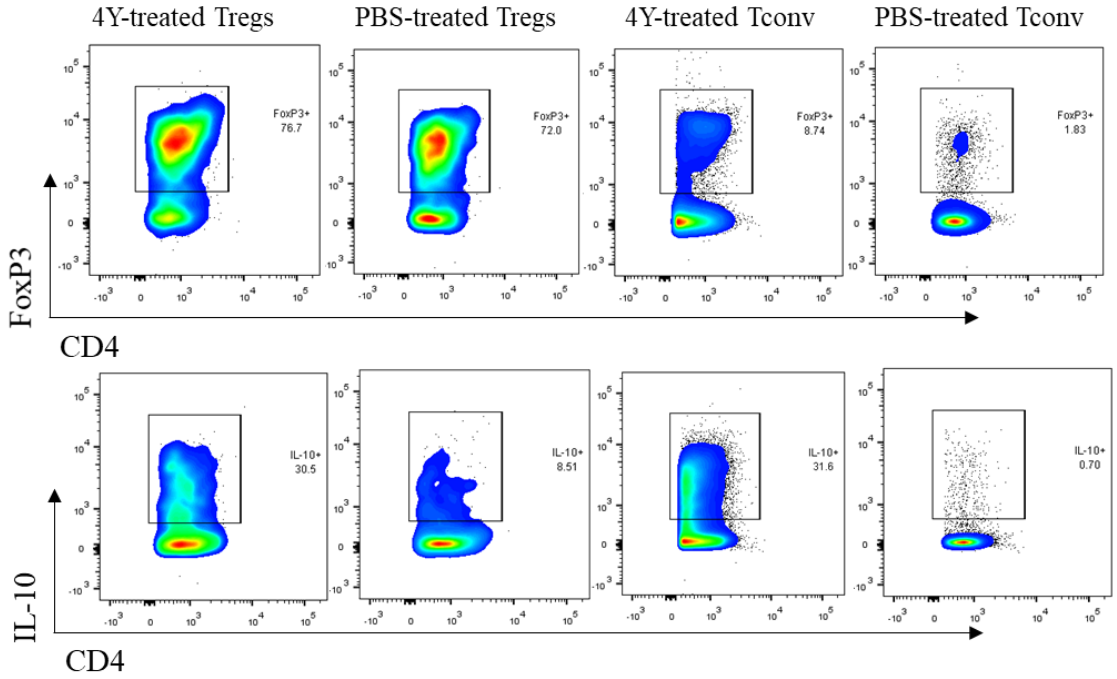

**Figure 5.1 Evaluation of the purity of the isolated fractions and correlation between FoxP3 and IL-10.** **(A)** 3 days after the final treatment with 4Y or PBS, spleens were isolated and Tregs were positively selected based on CD25 expression. The CD25- fraction (Treg-depleted) was used as the T conventional group. All groups were stimulated with PMA/Ionomycin for 4h, stained for surface markers, fixed and permeabilised and stained intracellularly for FoxP3 and IL-10 overnight. Representative FACS plots showing the expression of FoxP3 in relation to CD25. **(B)** Representative FACS plots from all 4 biological groups showing the expression of IL-10 in relation to FoxP3. **(C)** Bar graphs display individual and mean average values of 3 mice per group (± SEM), collated from 3 repeat experiments showing the percentage of $FoxP3^{+}IL\text{-}10^{+}$, $FoxP3^{-}IL\text{-}10^{+}$ and $FoxP3^{+}IL\text{-}10^{-}$ cell subsets within each one of the groups (PBS T conv, 4Y T conv, PBS Tregs, 4Y Tregs).

It is clear from previous experiments (sections 4.6, 4.7.1 and 4.7.2 of Chapter 4) that Tregs from 4Y-treated mice have superior suppressive capacity and we reasoned that one of the molecules responsible for this function would be the immunoregulatory cytokine IL-10, which also plays a fundamental role in the function of Tr1 cells (Sundstedt et al., 2003). Following tolerance induction, there was a clear expansion of IL-$10^+$ T cells within the bulk population of $CD4^+$ T cells (Fig. 5.2A) in line with previous data in the literature (Gabrysova et al., 2009); however, it is not clear whether this IL-10 is coming primarily from $FoxP3^+$ Tregs or $FoxP3^-$ Tr1 cells.

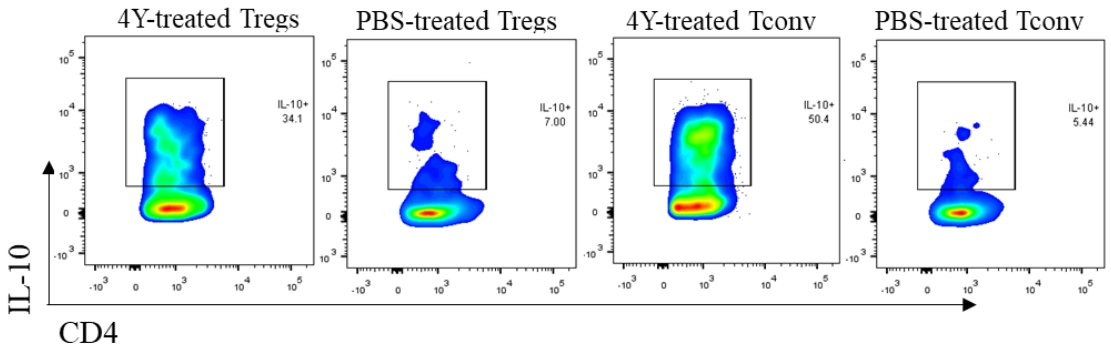
To start teasing this apart, IL-10 levels were measured both in the $CD4^+FoxP3^+$ and $CD4^+FoxP3^-$ gated populations found within the 4 groups analysed (4Y-treated Tregs, PBS-treated Tregs, 4Y-treated Tconv, PBS-treated Tconv) (Fig. 5.2B). Interestingly, there was an expansion of IL-$10^+$ cells both in the $FoxP3^+$ and $FoxP3^-$ population of cells following peptide treatment; however, this expansion was more profound in the $FoxP3^+$ population both in terms of percentage of IL-$10^+$ cells (Fig. 5.2C, i), as well as mean fluorescence intensity (MFI) (Fig. 5.2C, ii), indicating that there is a positive correlation between FoxP3 and IL-10.

In summary, tolerance induction expands the IL-$10^+$ populations within both 4Y-treated Tconv and 4Y-treated Tregs. The fact that antigen-specific immunotherapy can potentiate $FoxP3^+$ Tregs to produce IL-10 in the Tg4 mouse has not been revealed previously. This novel finding highlights the significant impact of peptide treatment on a diverse subset of immune cells.

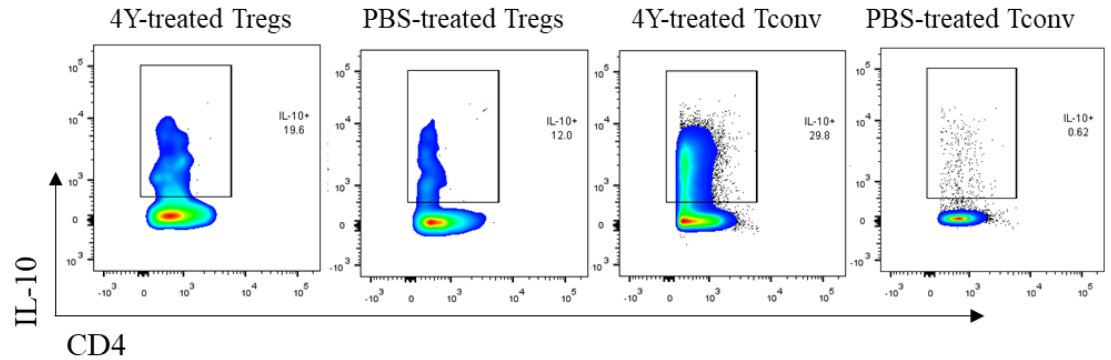
**(A)** **Gated on total CD4+single viable cells**




**(B)** **Gated on total CD4+FoxP3+single viable cells**




**Gated on total CD4+FoxP3-single viable cells**



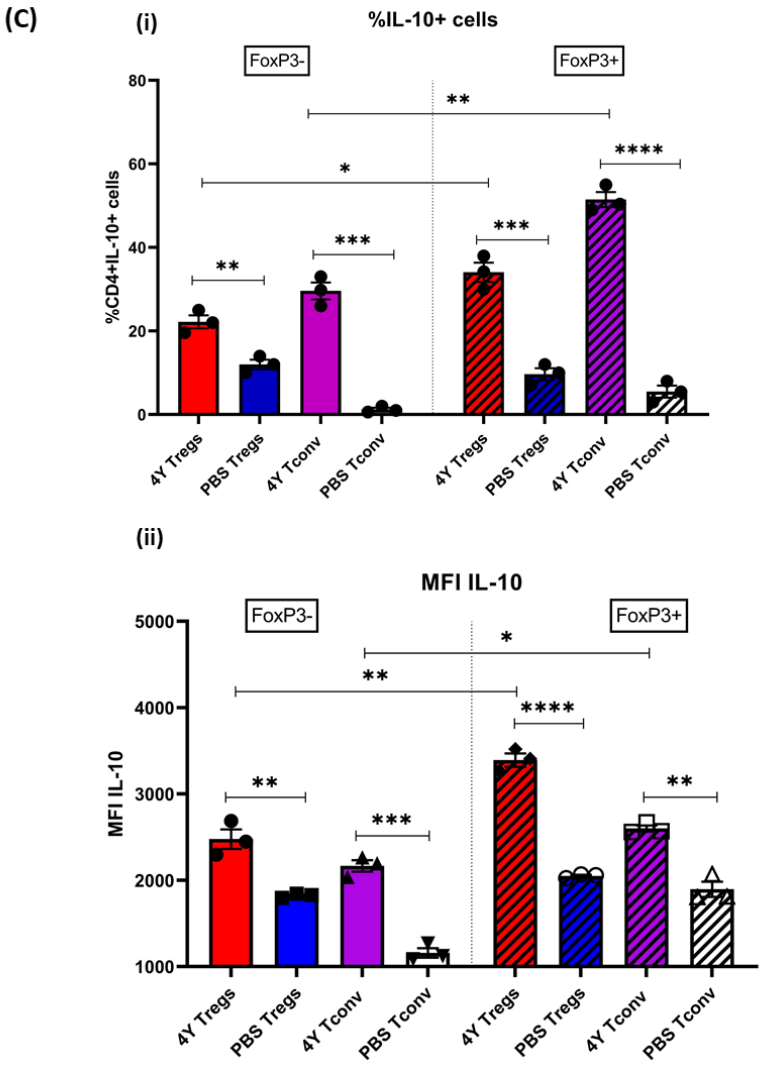



**Figure 5.2 Tg4 mice undergo IL-10$^+$ cell expansion of both CD4$^+$FoxP3$^+$ Tregs and CD4$^+$FoxP3$^-$ Tr1 cells following tolerance induction with MBP$_{Ac1-9}$ [4Y] peptide.** Tg4 mice were treated as previously with increasing doses of 4Y or PBS and three days after the final treatment CD25$^+$ Tregs were isolated and the CD25$^-$ fraction was used as T conv. Cells were stimulated with PMA and Ionomycin and stained intracellularly for FoxP3 and IL-10. **(A)** Representative FACS plots showing levels of FoxP3 and IL-10 within the CD4+ gate. **(B)** Representative FACS plots showing levels IL-10 within the CD4$^+$FoxP3$^+$ gate (upper panel) and CD4$^+$FoxP3$^-$ gate (lower panel). **(C)** Corresponding graph with the percentage of CD4$^+$IL-10$^+$ cells (i) or mean fluorescence intensity (MFI) within the FoxP3$^-$ and FoxP3$^+$ subpopulations found in the 4 different groups. Bar graphs display individual and mean average values of 3 mice per group (± SEM) from two independent experiments. Statistical significance calculated by one way ANOVA with Tukey's multiple comparisons test.

### 5.2.2 The expression of co-inhibitory receptors is upregulated both in Tr1 and Tregs following tolerance induction

It was previously shown that $CD4^+$ T cells from tolerised Tg4 mice express higher levels of co-inhibitory receptors (IRs) as measured by both mRNA levels and protein expression and that the expression of these IRs strongly correlates with IL-10 (Burton et al., 2014). To confirm this observation at the protein level and to assess IR cell surface expression of Tregs alongside Tr1 cells, spleens from Tg4 mice were harvested 3 days after the final treatment with 4Y peptide and Tregs from the different treatment groups were enriched based on CD25 expression as before, giving rise to the 4 biological groups mentioned in the previous paragraph. Cells were then treated with P/I and stained for FoxP3 and IL-10 together with the IRs, TIGIT, CTLA-4, TIM-3, LAG-3, and PD-1.

It was shown in the previous paragraph (section 5.2.1) that there is an expansion of $IL\text{-}10^+$ cells both in 4Y-treated Tregs and Tconv. There were two distinct questions that we wanted to address; firstly, whether tolerance induction enhances the expression of IRs on Tregs, since it was previously shown that it does on Tr1 cells (Burton et al., 2014); secondly, whether there is a strong correlation with the expression of IRs and IL-10 in each of the regulatory T cell populations, in an effort to investigate the molecular pathways that are involved in the function of these cells. To do that, $CD4^+$ T cells from 4Y-treated Tregs or Tconv were divided into $IL\text{-}10^+$ and $IL\text{-}10^-$ populations and expression of IRs was evaluated on each fraction (Fig. 5.3A).

Interestingly, the expression of CTLA-4 was increased in the $IL\text{-}10^+$ fraction of 4Y-treated Tregs (30% of total $CD4^+$ T cells) compared to the $IL\text{-}10^-$ fraction (20%), but it was not significantly affected in 4Y-treated Tconv (Fig. 5.3B, i). Surprisingly, the levels of TIGIT were not upregulated in the $IL\text{-}10^+$ fraction of either Tregs or Tconv compared

to their IL-10$^{-}$ counterparts, following tolerance induction (Fig, 5.3B, ii). TIM-3 expression was strongly upregulated in the population of IL-10$^{+}$ cells found in 4Y-treated Tregs (45%) compared to IL-10$^{-}$ Tregs (20%); however, a similar difference was not seen in 4Y-treated Tconv, where levels of TIM-3 were below 20% both in IL-10$^{+}$ and IL-10$^{-}$ cells (Fig. 5.3B, iii). Furthermore, the expression of LAG-3 was significantly upregulated on the IL-10$^{+}$ cells of 4Y-treated Tconv, and this observation is in line with the literature where LAG-3 has been proposed to be a good marker for FoxP3$^{-}$Il-10$^{+}$ Tr1 cells (Gagliani et al., 2013). An even higher proportion of CD4$^{+}$LAG-3$^{+}$ cells was found within the IL-10$^{+}$ population of 4Y-treated Tregs (Fig. 5.3B, iv). Finally, expression of PD-1 was upregulated in the IL-10$^{+}$ subpopulation of cells found within the 4Y-treated Treg biological group (90%) compared to IL-10- cells within the same group (65%) (Fig. 5.3B, v). Similar differences, but even more profound (80% versus 40%), were found between IL-10$^{+}$ and IL-10$^{-}$ cells in the 4Y-treated Tconv, respectively.

Taken together, there was a clear correlation between IL-10 and all the IRs, except TIGIT, and this was quite profound on 4Y-treated Tregs and less so on Tconv.

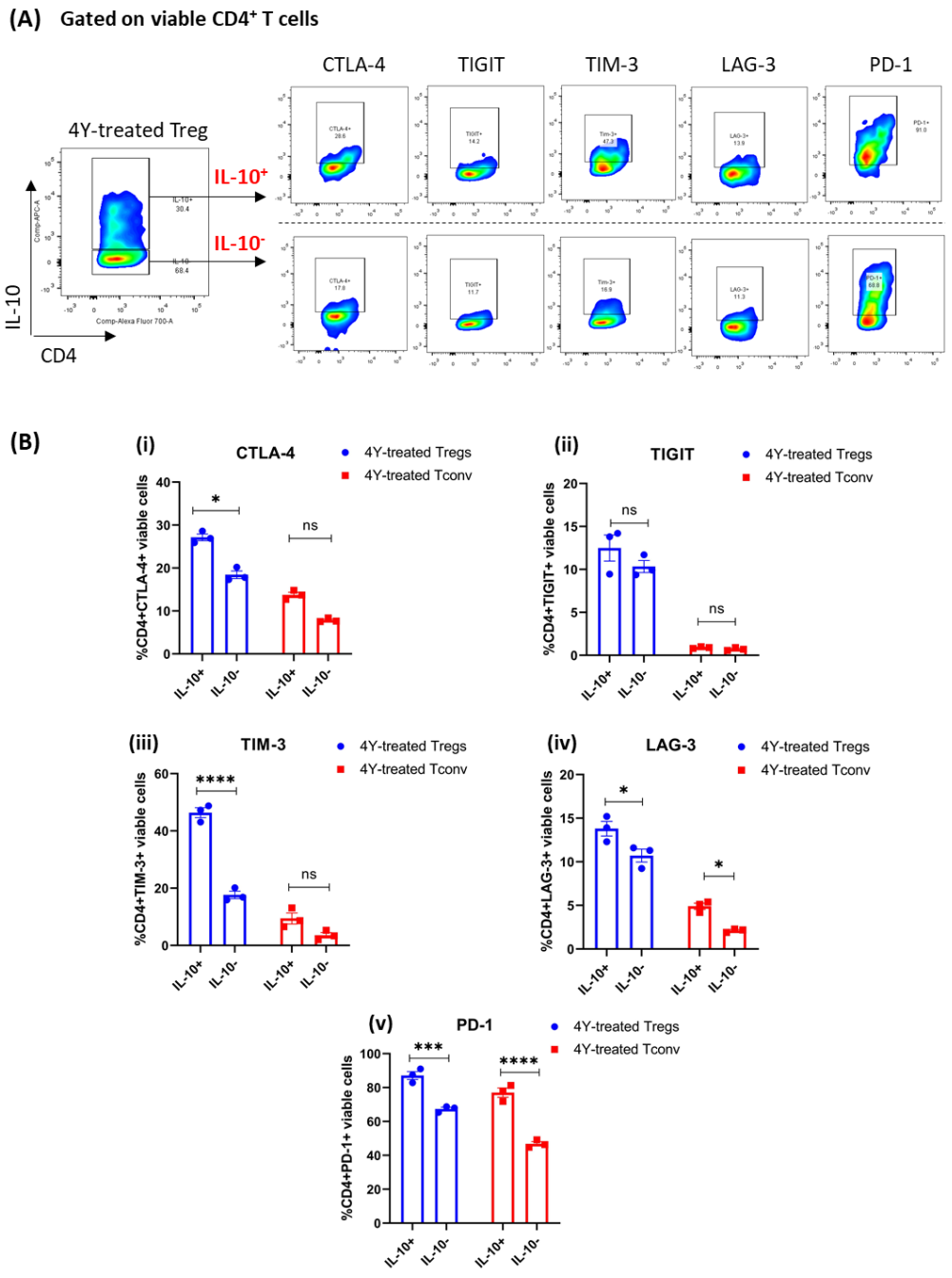



**Figure 5.3 Tg4 mice after tolerance induction with MBPAc1-9 [4Y] peptide undergo expansion of inhibitory receptors, which correlates with IL-10 expression.** Tg4 mice were treated with as previously and 3 days after the final treatment, CD25+ Tregs were purified from either the 4Y or PBS group. Cells were stimulated with P/I and stained for cell surface expression of inhibitory receptors and intracellularly for IL-10. **(A)** Gating strategy and representative FACS plots for 4Y-treated Tregs. Identical gating was applied to 4Y-treated Tconv samples. A fluorescence minus one (FMO) control was used to set the gates. (B) Summary graphs with the different cell subsets (4Y-treated Tregs or Tconv) expressing **i)** CTLA-4, **ii)** TIGIT, **iii)** TIM-3, **iv)** LAG-3 and **v)** PD-1. Bar graphs display the mean average values of 3 mice per group (± SEM) and results are representative of 2 independent experiments with similar results. Statistical significance between the biological groups was calculated by 2way ANOVA with Sidak's multiple comparison test.

## 5.3 Optimisation of the *in vitro* conditions for stimulation of regulatory T cells

The previous paragraphs of this chapter aimed to investigate the impact of peptide immunotherapy on the phenotype of Tregs and Tconv cells by analysing the expression pattern of FoxP3 and IL-10 within each group and correlating these two intracellular markers with the surface expression of different IRs. To further build upon the characterisation of the different regulatory T cells, we aimed to analyse the transcriptional signatures that distinguish naïve from peptide-treated Tregs as well as naïve Tconv from peptide-treated Tconv to explain the functional differences seen previously in terms of suppressive capacity. To be able to do this, the optimal conditions for stimulation of these regulatory T cells had to be established before proceeding into the analysis of the RNA profile of the cells. The conditions had to closely resemble the ones used for the *in vitro* bystander assays to be able to associate the functional profile of these cells with certain changes in the RNA transcripts.

In the suppression assays, each putative suppressor was able to recognise their cognate antigen and stay in culture with the responder cells for three days to exert their suppressive function. However, in this case we want to study the regulatory T cells alone; therefore, an antigenic stimulation *in vitro* would not be possible, since it requires the presence of APCs for the antigen presentation and subsequent activation. Hence, the resulting mixed population of regulatory T cells and APCs would need further purification prior to RNA extraction, which creates technical problems because the numbers of Tregs isolated using magnetic beads for positive selection had low yield of Tregs. This limitation created the need for minimum manipulations to avoid further losses in cell numbers.

To circumvent this, we reasoned that the regulatory T cells could be activated *in vivo*; instead of harvesting the spleens 3 days after the final 4Y treatment, it could be done 2h following the final dose. This time point was previously shown to fall within the optimal time window for *in vivo* activation of T cells in the Tg4 model, since the APC loading following peptide administration reached a peak between 1h and 4h using either the intranasal (Metzler et al., 2000) or subcutaneous route (Burton et al., 2014; Shepard et al., 2021).

To examine whether the same regime would work for optimal stimulation of Tregs *in vivo*, Tg4 mice were given either a single dose of 80μg of 4Y or PBS and 2h later, spleens were harvested and stained for CD25 and FoxP3. Previous data from our lab showed that 2h after *in vivo* administration of 4Y, the expression of all three chains of the IL-2 receptor was upregulated at the RNA level (Fig. 5.4A). The high affinity IL-2 receptor consists of all three subunits, IL-2Rα (CD25), IL-2Rβ (CD122) and γc (CD132) that are readily found on Tregs and recently antigen-activated T conventional cells (Malek and Castro, 2010). Given that CD25 is constitutively expressed on Tregs and on T conv upon activation, we were keen to examine whether 2h post antigen administration would be sufficient time to upregulate CD25 on $CD4^+FoxP3^-$ T conv.

To confirm the RNA data at the protein level, we measured CD25 expression by flow cytometry 2h post 4Y administration. Bulk $CD4^+$ T cells in 4Y-treated Tg4 mice upregulated both CD25 (8% of $CD4^+$ T cells) and CD69 (94.5%) compared to PBS-treated Tg4 mice (4% and 8% for CD25 and CD69, respectively) (Fig. 5.4B). Intriguingly, only 47% of $CD4^+CD25^+$ cells in the 4Y-treated mouse expressed FoxP3 compared to 83% in the PBS-treated mouse (Fig. 5.4C). This result clearly shows that almost half of the $CD4^+CD25^+$ cells in the 4Y-treated mouse are $FoxP3^-$, indicating that this is a mixed

population of both $CD25^{+}FoxP3^{+}$ Tregs and $CD25^{+}FoxP3^{-}$ activated, effector T cells. For consistency purposes, we need to utilise the expression of CD25 for the isolation of Tregs in line with the method used previously, therefore in this case, CD25 is not a good marker, since it is expressed not only on Tregs but also on activated T cells. Due to the aforementioned limitations, the *in vivo* stimulation of Tregs was not the best approach to follow.

An alternative option for *in vitro* stimulation that does not require antigen, would be the use of functional, monoclonal antibodies against CD3 and CD28 for TCR triggering (Bashoura et al., 2014). To be able to determine the optimal conditions for stimulation in our system, different time points were examined (4h or 6h) as well as different combinations of antibody delivery (soluble or plate-bound). Treatment of cells with P/I for 4h was used as a positive control since it gives a potent stimulus for T cell activation. For optimisation purposes, $CD4^{+}$ T cells were used due to cell number restrains and mice availability at the time. Cells were stimulated with the different conditions tested and expression of CD25 and CD69 were used as a readout for their activation status (Fig. 5.5A).

In addition to the activation profile, the amount of RNA extracted after each condition as measured by Qubit assay was also taken into account, since we aimed to achieve not only optimal activation, but also high yields of extracted RNA (Fig. 5.5D). In addition to the quantity of RNA, the quality of RNA was assessed by measuring the RNA integrity number (RIN), which ranges between 1(totally degraded) and 10 (intact) (Fig. 5.5E). Any number above 6 corresponds to a decent quality of RNA (Schroeder et al., 2006).

Based on the expression of CD25 (Fig. 5.5B) and CD69 (Fig. 5.5C), as well as the quantity and quality of RNA, the optimal conditions for T cell stimulation involved stimulation with soluble anti-CD3 and anti-CD28 antibodies for 4h. These were the conditions used for the *in vitro* stimulation of Tregs and T conv cells prior to RNA sequencing (bulk and single cell) as well as epigenetic analysis (DNA demethylation) described in later paragraphs of this chapter.

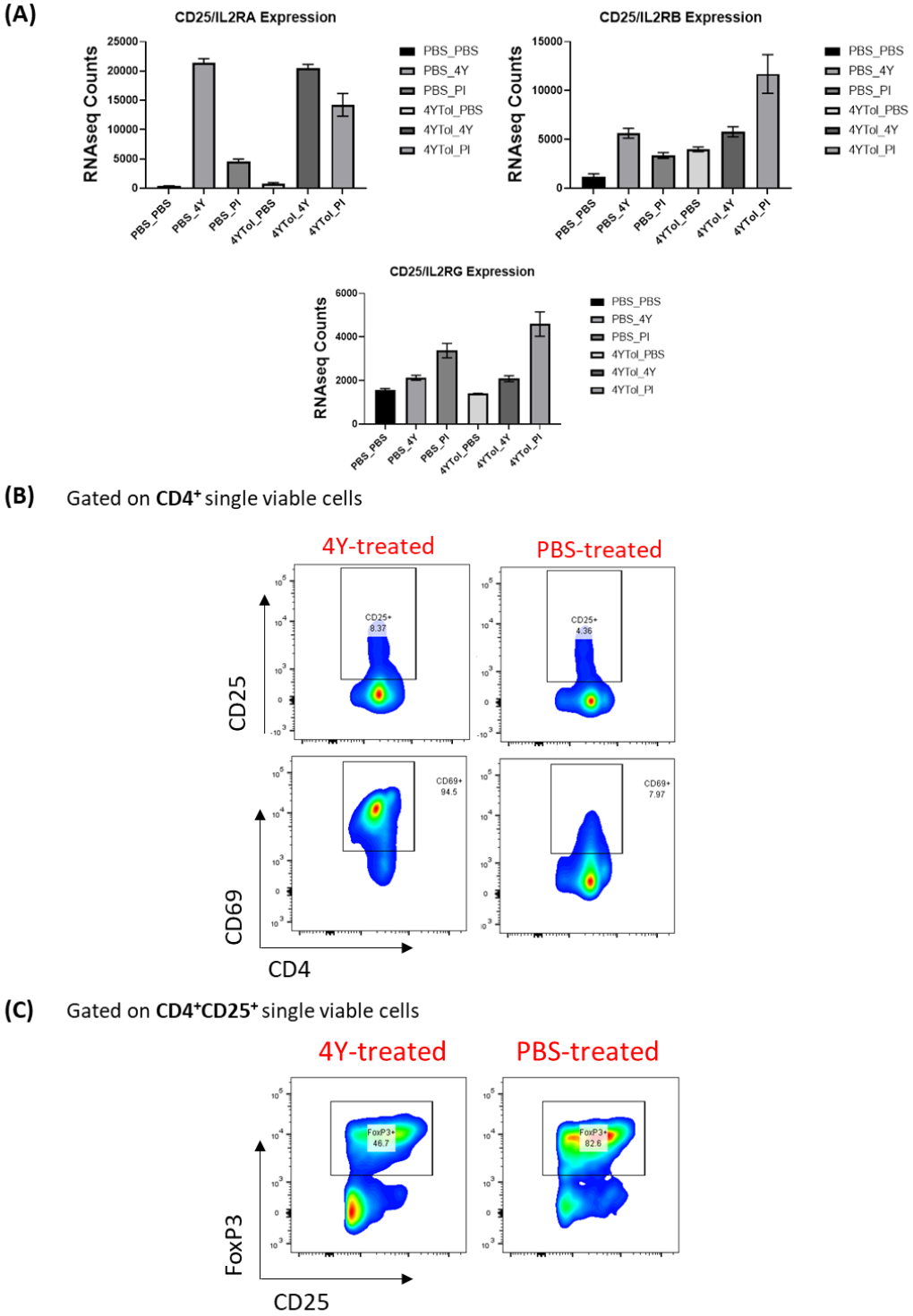



**Figure 5.4 CD25 expression 2h after *in vivo* treatment with a single dose of 80µg 4Y. (A)** RNA transcripts (raw counts) of all three chains, alpha, beta and gamma that together constitute the high-affinity IL-2 receptor (CD25). The RNA levels were measured in naïve mice (PBS-treated *in vivo*) at the steady state (PBS_PBS) or after *in vivo* priming with a single dose of 80µg of 4Y (PBS_4Y), or after *in vitro* re-challenge with PMA/Ionomycin (PBS_PI). Similar restimulation approaches were followed in mice that were subject to tolerance induction with 4Y *in vivo* (4YTol). **(B)** Representative FACS plots showing the expression of CD25 and CD69 2h post-treatment with either 80µg 4Y or PBS. **(C)** Representative FACS plots showing the expression of FoxP3 on $CD4^+CD25^+$ cells from mice that were either primed with a single dose of 4Y or with PBS.

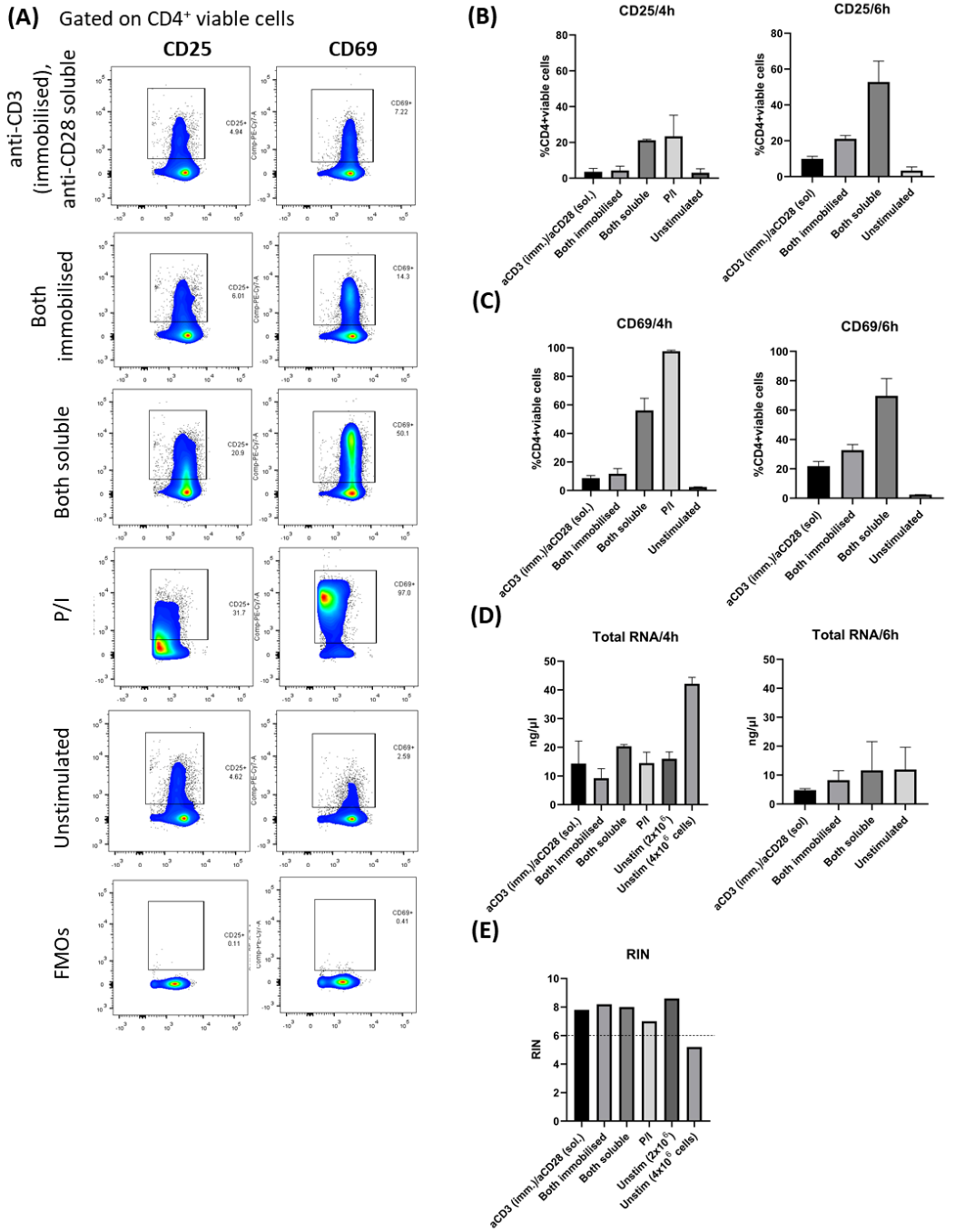



**Figure 5.5 The optimal *in vitro* re-stimulation regime for Tregs is with soluble anti-CD3/anti-CD28 monoclonal antibodies for 4 hours.** Spleens from naïve Tg4 mice were harvested and $CD4^+$ T cells were negatively isolated according to the manufacturer's instructions. Cells were plated at a density of $2x10^6$ cells/well in a 48 well plate and stimulated with the respective conditions of either monoclonal antibodies (anti-CD3, anti-CD28) or PMA and Ionomycin (P/I) for either 4h or 6h at 37°C. **(A)** Representative FACS plots of CD25 and CD69 levels for each condition tested at 4h. **(B)** Summarising graphs with the levels of CD25 expression at 4h and 6h. **(C)** Summarising graphs with the levels of CD69 expression at 4h and 6h. **(D)** Summarising graphs with the amount of total RNA extracted at 4h and 6h. **(E)** Evaluation of the quality of RNA extracted from each condition by assessing the RNA integrity number (RIN). Any value above 6 is considered acceptable quality of RNA. Bar graphs display individual and mean average values of 3 mice per group (± SEM), collated from 3 repeat experiments. The data on RIN value comes from a single experiment.

## 5.4 Bulk RNA sequencing

Three days after the final peptide treatment, spleens were harvested, $CD25^+$ and $CD25^-$ fractions were isolated from either the 4Y- or PBS-treated groups and cells were stimulated *in vitro*, prior to RNA extraction (see section 2.3.17.1 from Materials and Methods). The RNA was kept at -80$^o$C before sending to GeneWiz Azenta Life Sciences for sequencing. The initial bioinformatics analysis was performed with the help of Dr Sky Ng from our lab, and the pipeline is described in section 2.6.1 of Chapter 2.

### 5.4.1 Hierarchical clustering and pathway analysis

Initially, we wanted to investigate how peptide treatment affects the global transcriptional signatures of the 4 different samples tested. In this initial exploratory analysis, a Principal Component Analysis plot (PCA) and a hierarchical clustering tree were generated using the iDEP software. The PCA plot is used to reduce the dimension of the data, simplify and achieve a better visualisation in two dimensions, assuming that there is a linear relationship between the samples (Jollife and Cadima, 2016). It reflects the variance of the whole dataset, with Principal Component 1 (PC1) capturing most of the variability in the data, while the residual variability is captured by Principal Component 2 (PC2), which is independent of PC1. Each dot in the PCA plot essentially represents the entirety of the data from each individual mouse (3 mice per biological group).

Surprisingly, it appears that 4Y- and PBS-treated Tregs are clustered together, while 4Y Tconv and PBS Tconv occupied separate areas of the plot and were not clustered together (Fig. 5.6A). This indicates that peptide immunotherapy primarily has an impact on Tconv cells, since there are more transcriptional signatures that differentiate 4Y from PBS Tconv cells; however, this is not a case for Tregs in this particular analysis. It is also

interesting to note that Tregs and Tconv fall into two distinct populations, indicating a high degree of variability that confirms that these populations are independent and have different determining pathways for their growth, differentiation and function as demonstrated previously in humans (Kunicki et al., 2018), mice (Maynard et al., 2007) and more specifically in the Tg4 mouse (Nicolson et al., 2006).

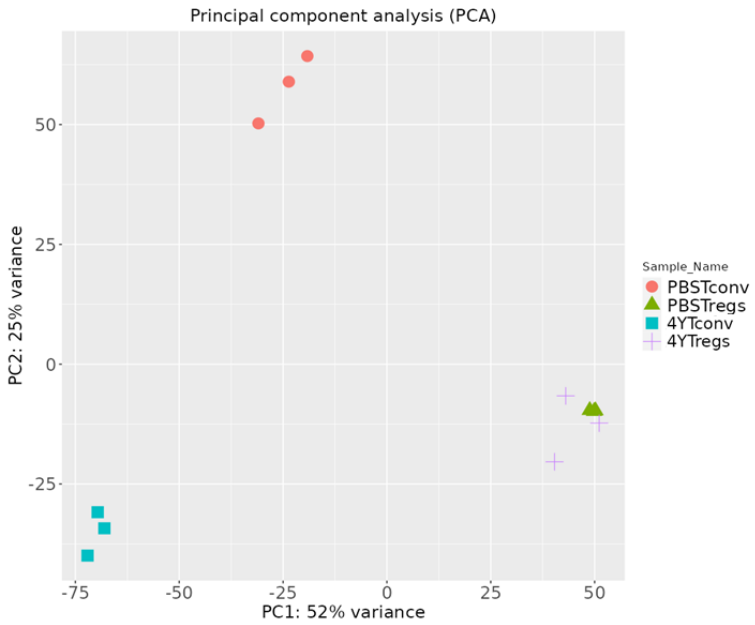
A similar observation was seen in the hierarchical clustering tree, where there was a higher degree of similarity between 4Y and PBS Tregs and between 4Y and PBS Tconv and a divergence between Tregs and Tconv from both treatment groups (Fig. 5.6B). The triplicates within each group were clustered together in both types of analysis, ensuring the robustness and reproducibility of the results.

Furthermore, additional clustering analysis using a heatmap as a readout revealed the existence of 4 clusters amongst the biological groups. Red colour denotes upregulated genes, while green colour is indicative of downregulated genes. In cluster A and B, it appears that the upregulated genes are those relevant to the identity of the cell subset rather than the impact of peptide immunotherapy as there are 746 upregulated genes in Tregs (both 4Y and PBS) in cluster A, and 343 upregulated genes in Tconv (both 4Y and PBS) within cluster B (Fig. 5.6C). In cluster C and cluster D, there are 344 and 567 upregulated genes, respectively, found in the 4Y Tconv group. In cluster D but not cluster C, there appears to be a minor upregulation of the relevant genes in 4Y Tregs (Fig. 5.6C).

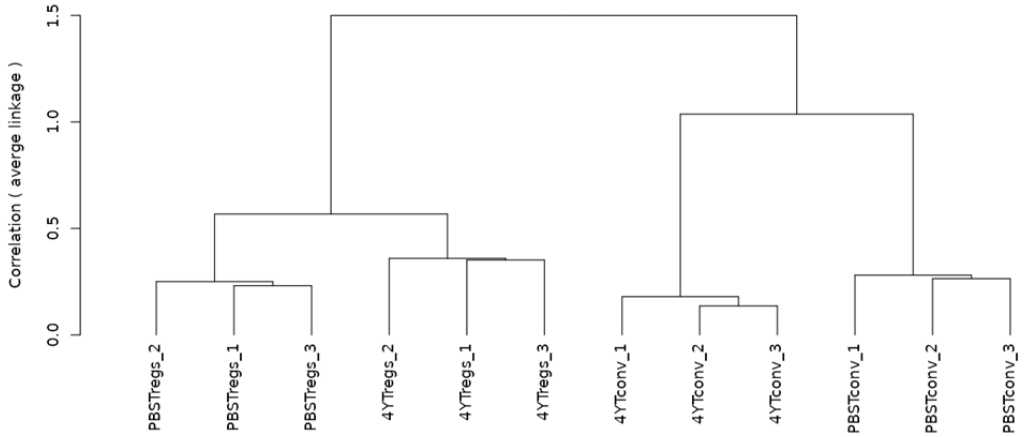
Fig. 5.6D shows a summary of the biological processes that are involved in each cluster, with cluster A and B mainly include pathways that determine the identity of Tregs versus Tconv cells (i.e., development, cell adhesion, chemotaxis, locomotion) as well as response to stimulus (i.e., activation or regulation of immune response). Cluster C

includes responses against external inflammatory stimuli (bacterial origin), stress and innate immune responses, while cluster D again includes similar pathways to cluster C, with the additional responses to cytokine stimulus (interferon-beta) as well as mitotic cell cycle processes (division) (Fig. 5.6D).

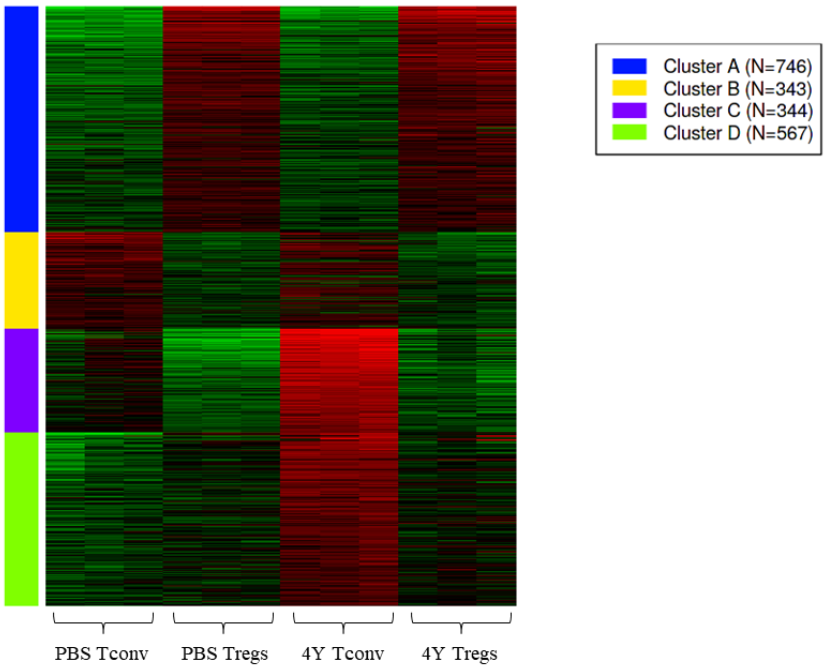
(A)


Principal component analysis (PCA)
PC2: 25% variance
PC1: 52% variance
50
25
0
-25
-75
-50
-25
0
25
50
Sample_Name
PBSTconv
PBSTregs
4YTconv
4YTregs

(B)


Correlation ( averge linkage )
1.5
1.0
0.5
0.0
PBSTregs_2
PBSTregs_1
PBSTregs_3
4YTregs_2
4YTregs_1
4YTregs_3
4YTconv_1
4YTconv_2
4YTconv_3
PBSTconv_1
PBSTconv_2
PBSTconv_3

(C)


Cluster A (N=746)
Cluster B (N=343)
Cluster C (N=344)
Cluster D (N=567)
PBS Tconv
PBS Tregs
4Y Tconv
4Y Tregs

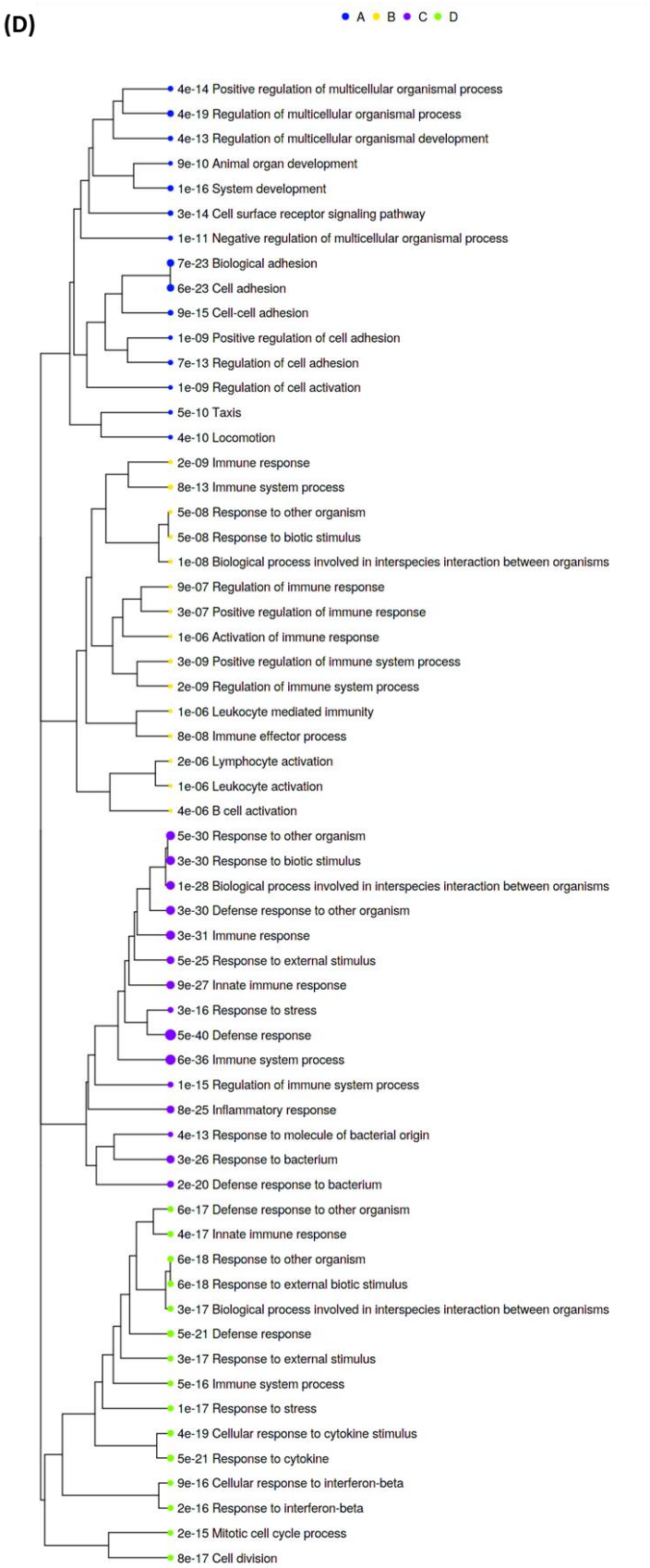



**Figure 5.6 PCA plot and hierarchical clustering tree showing the clustering of the 12 samples based on similarity.** The pipeline RNA-seek v1.2.1 was used for QC and to obtain RSEM counts for 12 bulk RNA-seq samples. The RSEM counts created by the RNA-seek pipeline were then used as input for the tool iDEP v0.951 for downstream pathway analysis.

## 5.5 Single-cell RNA sequencing

In addition to bulk RNA sequencing (RNAseq), a single-cell RNAseq (scRNAseq) approach was used to validate the results and to provide further insight into the transcriptional signatures of each biological group not only at the populational level, but also at the single cell level. Bulk RNAseq essentially studies the average global gene expression, while scRNAseq allows a high resolution study of the heterogeneity within each sample, taking into account the cell-to-cell variability, thus enabling the exploration of more complex biological systems and inferring regulatory networks across the samples (Hwang et al., 2018).

### 5.5.1 Expression of selected genes

Initially, the first genes to be analysed were *Il10* and *FoxP3*, to confirm the flow cytometry data shown in section 5.2.1 at the single-cell RNA level and ensure the purity of the populations. As expected, *Il10* is mainly expressed in cells that have been subjected to peptide treatment, primarily the FoxP3$^+$ Treg population and less so in the 4Y-treated Tconv as shown in the UMAPs for each sample (Fig. 5.10A). Also, PBS-treated Tregs express *Il10* at lower levels and this is clearer in the violin plots shown in Fig. 5.11A. Therefore, we can conclude that Tregs express *Il10*, even when they are not stimulated, but the levels are much higher once they encounter their cognate antigen repeatedly.

However, intracellular expression of IL-10 as measured by flow cytometry showed similar levels of expression in 4Y-treated Tregs and Tconv (around 35-40% of total CD4$^+$ T cells), while the first group has higher RNA expression. This would indicate that the chromatin encompassing the IL-10 locus may be uniquely modified in each of the different cell types and the post-transcriptional modifications may also be cell specific,

resulting in different degrees of RNA degradation amongst regulatory T cells (Mosser and Zhang, 2008).

Furthermore, *FoxP3* was predominantly expressed in Tregs (PBS- and 4Y-treated) as shown by the frequency of the blue-coloured dots on the UMAP plot (Fig. 5.7B); the darker the colour of each dot, the higher the expression of FoxP3 in that cell. However, there were some cells that expressed *FoxP3* even in the Tconv group (both PBS and slightly more in 4Y group) (Fig. 5.8B), confirming the minor impurities found within the samples that were first picked up with the flow cytometry staining (section 5.2.1). Similarly, *Il2ra*, the gene for CD25, which was used as a marker for positive selection of Tregs was also found to be expressed also on PBS-treated Tconv and less so in 4Y-treated Tconv (Fig. 5.8E). Even though the gene is transcribed in Tconv cells (4Y and PBS), it is barely expressed on the surface of the cells as shown by flow cytometry data; therefore, it could be argued that this minor discrepancy does not interfere with the eligibility of CD25 to be used as a selective marker for Tregs, both naïve and 4Y-treated.

Interestingly, *Maf* was also expressed in Tregs, particularly the 4Y-treated Tregs as shown by the UMAPs (Fig. 5.7C). The expression pattern of *Maf* is clearer in the violin plots where there is a high expression in 4Y-treated populations, predominantly Tregs, but also Tconv and it is less expressed in PBS-treated Tregs and at very low levels in PBS-treated Tconv (Fig. 5.8C). This transcriptional profile is reminiscent of *Il10* expression, since *Maf* has been shown to positively regulate *Il10* gene expression in $CD4^+$ T cells both *in vitro* (Rutz et al., 2011; Xu et al., 2009; Apetoh et al., 2010) and *in vivo* (Gabryšová et al., 2018).

Finally, *Prdm1* was predominantly expressed in 4Y-treated FoxP3$^{+}$ Tregs, followed by PBS-treated Tregs and finally 4Y-treated Tconv as shown in the UMAP plots (Fig. 5.7D), as well as the violin plots (Fig. 5.8D). It was previously shown that in Tregs, Blimp-1, the zinc finger protein that is the product of the transcription of *Prdm1*, cooperates with interferon regulatory factor 4 (IRF4) to establish a Treg cell effector program, including the expression of IL-10 and Granzyme B, particularly in non-lymphoid tissues (Cretney et al., 2011; Vasanthakumar et al., 2015).

Taken together, from the analysis of the first regulatory genes in our data set, it appears that peptide immunotherapy drives the transcriptional re-programming of Tregs, converting them from a population of naïve, non-suppressive cells to a population of highly suppressive, effector Tregs **(eTregs)**.

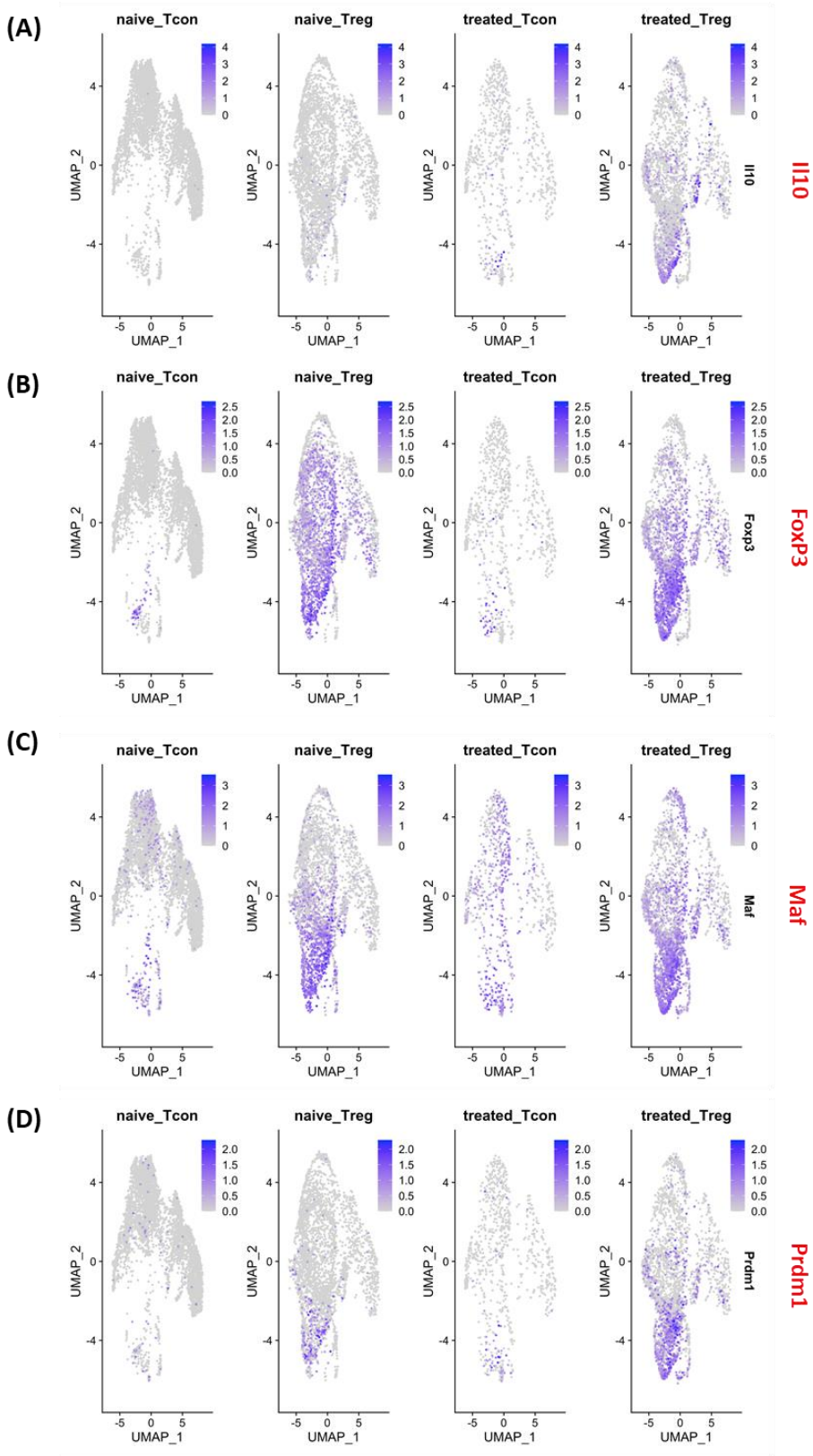



**Figure 5.7 Selected gene expression across the UMAP with feature plots.** Il10 **(A)**, FoxP3 **(B)**, Maf **(C)** and Prdm1 (Blimp1) **(D)** gene expression is shown across the UMAPs that are split by biological sample (Naïve_Tcon, naïve_Treg, treated_Tcon and treated_Treg).

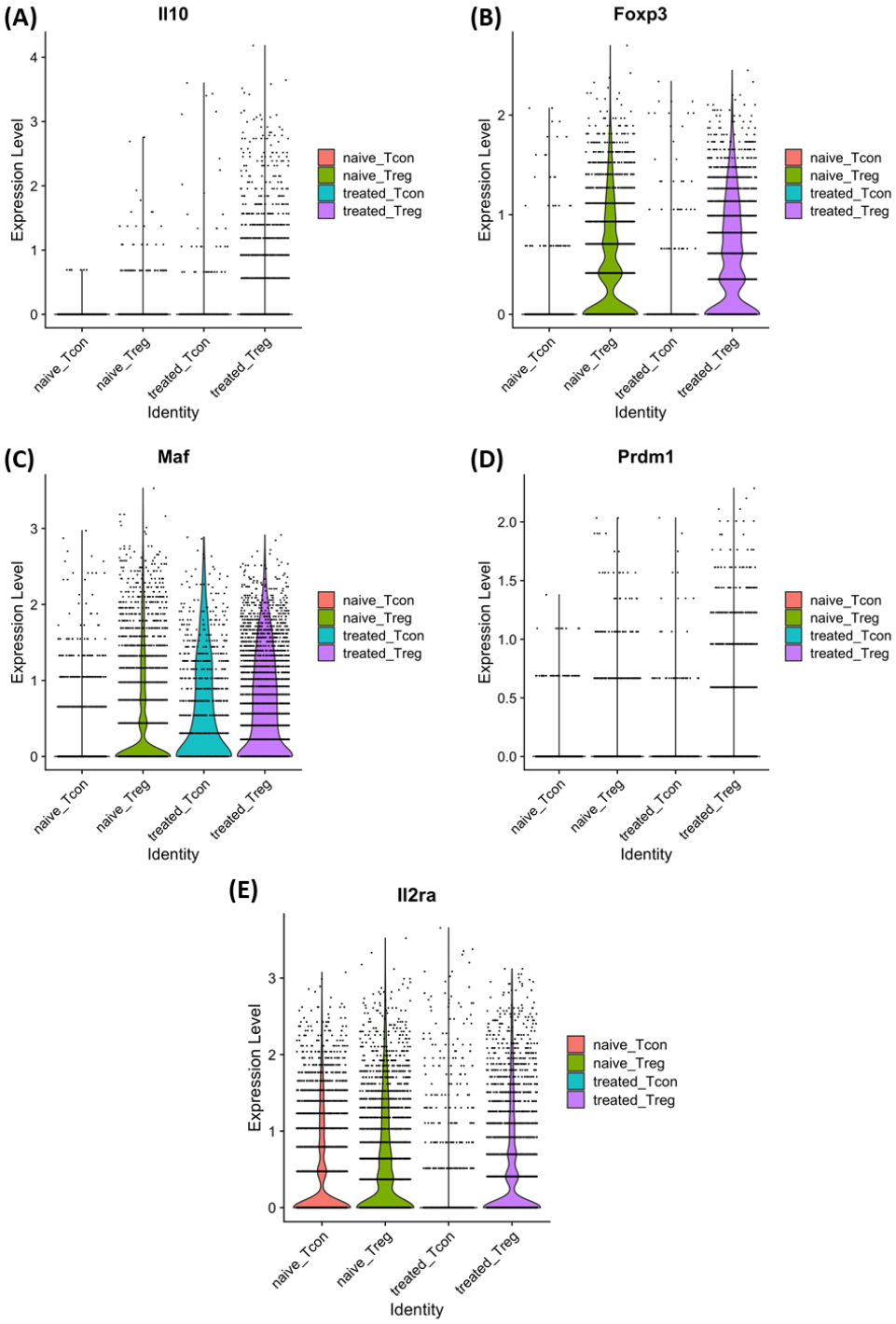



**Figure 5.8 IL-10, c-Maf and Blimp-1 are highly expressed on Tregs following peptide immunotherapy.** *Il10* **(A)**, *Foxp3* **(B)**, *Maf* **(C)**, *Prdm1* (Blimp-1) **(D)** and *Il2ra* (CD25) **(E)** gene expression is shown in each violin plot for all 4 biological samples (Naïve_Tcon, naïve_Treg, treated_Tcon and treated_Treg).

## 5.6 Analysis of differentially expressed genes (DEGs) by bulk and single-cell RNAseq

In addition to the initial genes identified by scRNAseq as described in the previous paragraph, we were keen to expand our study to the global transcriptome of the samples by analysing the differentially expressed genes (DEGs) using both bulk and scRNAseq approaches.

The term 'effector regulatory T cells (eTregs)' is already established in the literature (Ohkura and Sakaguchi, 2011; Cretney et al., 2013). The differentiation of these cells relies on transcription factors, with FoxP3 directly regulating the expression of Blimp-1 and IRF4, which in turn upregulate Blimp-1 expression, a major player for the function of these cells (Ogawa et al., 2018). *Prdm1* was highly upregulated in peptide treated Tregs; however, *Irf4* was not significantly affected by the treatment, indicating the intricate, multiple, and potentially redundant pathways that are involved in the differentiation of these cells.

To begin to tease this apart, we were keen to investigate the wider network of pathways that are involved in the function of eTregs and are also impacted by peptide immunotherapy. To do that, an analysis of differentially expressed genes (DEGs) between naïve versus treated Tregs (Fig. 5.9) or naïve versus treated Tconv (Fig. 5.10) was conducted using the DESeq2 software in R package for bulk RNAseq data or for scRNAseq data the analysis was done in Seurat software using the model MAST. The data are visualised in the form of a volcano plot, with the x axis showing the logarithm of the fold change between treated and untreated groups, and the y axis showing the reverse logarithm of the adjusted p value. The higher the log2FoldChange between samples, the

bigger the difference seen in the expression of the gene of interest, and the higher the value on the y axis, then the more this difference becomes statistically significant. Dots in red show genes that are upregulated in the treated group, while dots in blue show genes that are downregulated in the same group.

In the first comparison between PBS- and 4Y-treated Tregs, we were able to confirm the upregulation of *Il10, Maf,* and *Prdm1* in 4Y-treated Tregs, which was previously shown based on the raw counts in scRNAseq data (paragraph 5.5.1) and establish the statistical significance of this upregulation; the differential expression of *Il10* had the highest statistical significance (higher value in the y axis), followed by *Prdm1* and *maf* (Fig. 5.9A). Another transcription factor, *Nfil3*, was also upregulated in FoxP3$^+$ Tregs following peptide immunotherapy. This is surprising, because it was previously shown that Nfil3$^+$ Tregs exert impaired immunosuppressive activity, because Nfil3 directly binds and negatively regulates the expression of *Foxp3,* which in turn compromises Treg stability (Kim et al., 2019). However, work from our group (Ng et al., 2013) and others (Zhu et al., 2015; Solé and Santamaria, 2021) has shown that Nfil3 is associated with the transcriptional regulation of Tr1 cells and upregulation of IL-10. Therefore, in our setting Nfil3 could play a role in the regulation of IL-10 expression by Tregs, leaving FoxP3 expression unaltered.

Moreover, the genes for co-inhibitory receptors, such as *Lag3* and *Havcr2*, which encode Lag-3 and Tim3, respectively, were upregulated in 4Y-treated Tregs and this is in line with previous data on Tr1 cells in the Tg4 model (Burton et al., 2014). The expression of *Ctla4* and *Tigit* showed a slight increase in the 4Y-treated Tregs; however, this increase was below the cut-off threshold (log2FoldChange < 1) and, therefore, was considered negligible.

Furthermore, genes encoding chemokine receptors, such as *Ccr2* and *Ccr5* were also found to be upregulated in 4Y-treated Tregs, both in the bulk RNAseq data (Fig. 5.9A), as well as in the scRNAseq data (Fig.5.9B), indicating the significance and reproducibility of this observation. These receptors promote cell trafficking and in particular the CCR5-CCL5 axis plays an active role in recruiting T cells into target sites. It has previously been studied in the context of TIL-mediated immune responses in the tumour microenvironment (Aldinucci and Casagrande, 2018; Nagase et al., 2017; Aldinucci et al., 2020). This pathway has also been studied in viral infections and other chronic inflammatory conditions (Zeng et al., 2022); however, its role in the Treg-mediated control of autoimmunity has not been studied extensively.

Interestingly, the expression of the inducible T cell co-stimulator (ICOS) was upregulated in peptide treated Tregs in the bulk RNAseq dataset (Fig. 5.9A). Both in humans and mice, it was shown in $CD4^+$ T cells that the highest levels of ICOS had a positive correlation with the expression of IL-10, demonstrating the central role of ICOS in the differentiation and function of $FoxP3^+$ Tregs (Löhning et al., 2003; Ito et al., 2008). Expression of ICOS is of pivotal importance for Tregs, because when interacting with its ligand ICOS-L, it enables Tregs to survive and suppress more efficiently. In addition, *Cd38* was another upregulated gene in the 4Y-treated group, which has previously been associated with a highly suppressive phenotype amongst Tregs (Feng et al., 2017). Interestingly, expression of epidermal growth factors, *Areg* (amphiregulin) and *Entpd1* (CD39), genes associated with tissue repair were also upregulated in peptide-treated Tregs, highlighting the multifaceted nature of these cells, which are not only involved in immune regulation as previously thought, but may play a role in tissue remodelling and homeostasis (Zhang et al., 2017).

At the same time, genes associated with TCR activation, such as *Nr4a2* and *Nr4a3*, *Ifng* and INF-γ-associated genes, such as *Ift80, Ifi208, Ifit3b* were downregulated in the bulk RNAseq dataset (Fig. 5.9A). *Cd40Ig*, the gene for CD40 ligand, was also downregulated in 4Y-treated Tregs, implying that the CD40-CD40L pathway, involved in the T cell-mediated activation of antigen-presenting cells, is disrupted. *Klf2*, a gene associated with Treg proliferation (Pabbisetty et al., 2014), together with *Lrig* and *Mctp1*, which function on regulatory cells remain obscure, were downregulated in 4Y-treated Tregs with both sequencing methods (Fig. 5.9). Table 5.1 summarises the most significantly upregulated and downregulated genes found in Tregs with both bulk and scRNAseq. Fig. 5.11A shows the inter-section of both sequencing methods using a Venn diagram to illustrate the up- or down-regulated genes.

We were also very keen to study the impact of peptide immunotherapy on 4Y-treated Tconv and compare that to Tregs. Interestingly, *Ctla4, Maf*, were also upregulated to 4Y-treated Tconv in both the bulk RNAseq (Fig. 5.10A) and scRNAseq data (Fig. 5.10B), while *Il10* was only upregulated in the bulk RNAseq. *Pdcd1*, a gene encoding the inhibitory receptor PD-1 was also upregulated on 4Y-treated Tconv as shown by both sequencing methods (Fig. 5.10). Surprisingly, genes such as *Nrp1* and *Ikzf2*, which have been strongly associated with FoxP3$^+$ Tregs, were upregulated in this population of 4Y-treated Tconv. This could potentially be due to the fact that there is a small percentage of FoxP3$^+$ cells in this biological group; whether this is because of limitations in the purification or whether the 4Y-treated Tconv cells acquire some Treg-like characteristics following peptide treatment is not clear.

Furthermore, based on the bulk RNAseq results, there is an upregulation of *Ifng* and IFN-γ related genes, such as *Irf1* and immunity related GTPases produced in cells

exposed to IFN-γ, *Irgm1* and *Irgm2,* activation-related genes, i.e., *Nr4a3* and *Il2* and genes of the tumour necrosis factor receptor superfamily, *Tnfrsf4* (OX40), *Tnfrsf8, Tnfrsf9* (4-1BB) (Fig. 5.10A). Expression of genes associated with Th17 cytokines, such as *Il17a, Il17f,* and *Il21* was also increased in 4Y-treated Tconv, as well as *Cxcl9, Cxcl10* and *Cxcl11,* which together with their receptor CXCR3 form an axis implicated in immune migration, differentiation and activation (Tokunaga et al., 2018).

Taken together, the overall transcriptional profile of the 4Y-treated Tconv group indicates that this is a quite heterogeneous and diverse population of cells that has been highly activated and even though it possesses some effector genes, there are also some other genes that are linked to their regulatory potential, making the classification of these cells quite challenging. Because most of the genes that were upregulated in the 4Y-treated group are associate with T cell activation, it is hard to discriminate whether this effect is due to tolerance induction or the stimulation prior to RNA analysis. Therefore, it will be useful to include a resting population of PBS- and 4Y-treated Tregs and Tconv, alongside the *in vitro*-stimulated ones, to be able to draw more conclusive results.

However, these controls were included in previous work from our lab that aimed to assess the impact of tolerance induction on the transcriptional profile of total CD4tol cells from the Tg4 model (Bevington et al., 2020) providing some insight on the background levels of gene expression at the steady state. Due to limitations in the experimental design (i.e., mice availability and cost of sequencing), we were able to examine only 4 biological samples and we were keen to compare 4Y-treated Tregs and Tconv alongside their PBS counterparts.

Most of the genes that were identified by the bulk RNAseq were also confirmed by scRNAseq (Fig. 5.10B) and table 5.2 summarises the most significant upregulated and downregulated genes found in 4Y-treated Tconv with both bulk and scRNAseq. Finally, fig. 5.13B shows the inter-section of both sequencing methods using a Venn diagram to illustrate the up- or down-regulated genes.

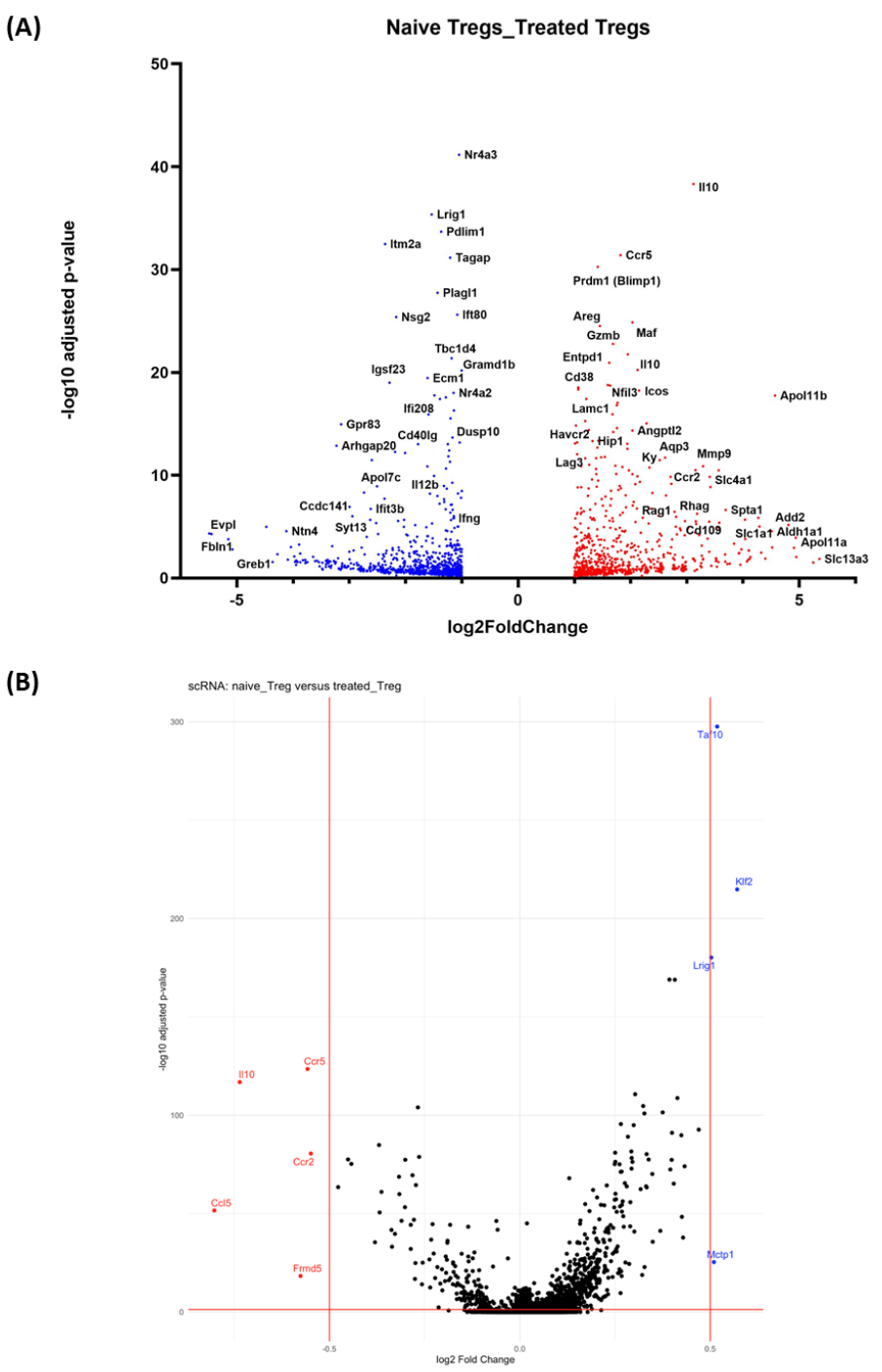



**Fig. 5.9: Peptide immunotherapy induces the upregulation of tolerance-associated genes in FoxP3+ Tregs with a concomitant downregulation of effector genes.** Three days after peptide treatment, spleens were harvested and FoxP3$^{+}$ Tregs were isolated based on CD25 expression as described previously. Cells were stimulated *in vitro*, and total RNA was extracted and used for bulk RNA sequencing **(A)**, or cells were used for single-cell RNA sequencing **(B)**. For the bulk RNA sequencing, differential expression analysis was performed in R using DESeq2 software. Each comparison includes a volcano plot and the default average log2 fold change filter was set to 1. For the scRNA-seq analysis, the differential expression testing was performed with Seurat v4.1.1 with the model MAST. To be considered for differential expression the gene needed to be present in 10% of the cell for the comparison. The default average log2 fold change filter was set to 0.5.

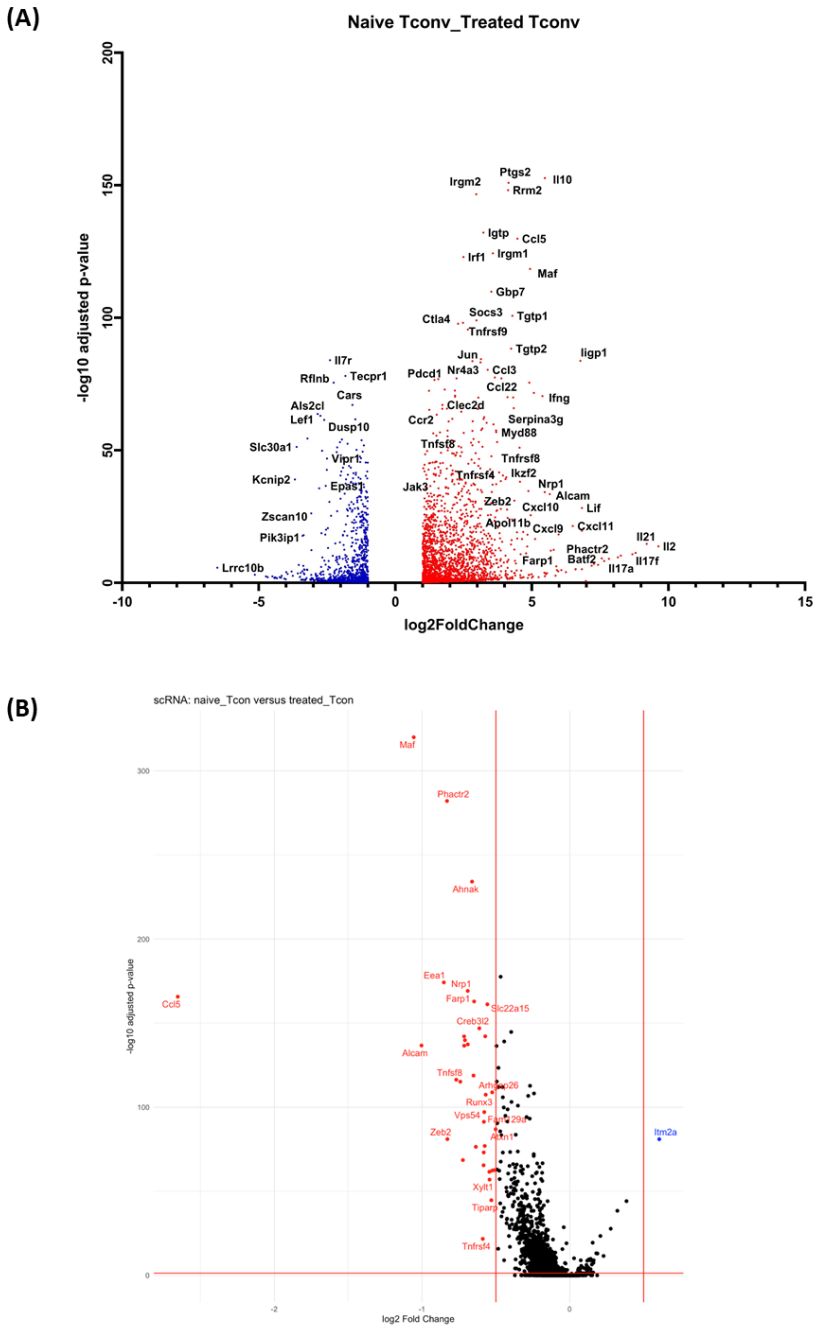



**Fig. 5.10: Peptide treatment has an impact on 4Y-treated Tconv cells by inducing some tolerance-associated genes that are also found in 4Y-treated Tregs.** Three days after peptide treatment, spleens were harvested and FoxP3$^{+}$ Tregs were isolated based on CD25 expression. The Treg-depleted fraction (CD25$^{-}$) from peptide-treated mice (treated Tconv) served as the 4Y-treated Tconv group and the Treg-depleted fraction from naïve mice served as PBS-treated T conv control. Both groups were stimulated *in vitro*, and total RNA was extracted and used for bulk RNA sequencing **(A)**, or cells were used for single-cell RNA sequencing **(B)**. For the bulk RNA sequencing, differential expression analysis was performed in R using DESeq2 software. Each comparison includes a volcano plot and the default average log2 fold change filter was set to 1. For the scRNA-seq analysis, the differential expression testing was performed with Seurat v4.1.1 with the model MAST. To be considered for differential expression the gene needed to be present in 10% of the cell for the comparison. The default average log2 fold change filter was set to 0.5.

| Category | Gene | Bulk log2Fold Change | Bulk adjusted p value | Single cell (sc) log2Fold Change | Single cell (sc) adjusted p value |
|---|---|---|---|---|---|
| bulk up/ sc up | **Ccr2** | 2.7033446894542 | 2.98564E-08 | 0.548678944 | 2.63686E-81 |
| bulk up/ sc up | **Il10** | 2.62341963013484 | 3.62157E-11 | 0.735483523 | 1.2811E-117 |
| bulk up/ sc up | **Ccr5** | 1.80288923334093 | 1.07667E-25 | 0.557310003 | 2.9408E-124 |
| bulk up/ sc up | **Ccl5** | 0.857600303314105 | 0.017722114 | 0.802024344 | 2.39183E-52 |
| bulk down/ sc down | **Klf2** | -0.740126047 | 8.10433E-21 | -0.570761592 | 1.441E-215 |
| bulk down/ sc down | **Mctp1** | -1.109709506 | 0.019715533 | -0.509561383 | 3.93174E-26 |
| bulk down/ sc down | **Lrig1** | -1.523480364 | 1.27925E-30 | -0.502725922 | 6.2228E-181 |

**Table 5.1: Summary of differentially expressed genes between PBS-treated and 4Y-treated Tregs.** A combined analysis of bulk RNA-seq and single-cell RNA-seq was performed by intersecting differential expression testing comparison results. There were 4 genes that were significantly upregulated and 3 genes that were significantly downregulated in 4Y-treated Tregs compared to PBS-treated Tregs with both methods.

| Category | Gene | Bulk log2Fold Change | Bulk adjusted p value | Single cell (sc) log2Fold Change | Single cell (sc) adjusted p value |
|---|---|---|---|---|---|
| bulk up/ sc up | **Maf** | 2.407069788 | 6.23084E-21 | 1.056415495 | 1.056415E-495 |
| bulk up/ sc up | **Ctla4** | 1.380506617 | 8.87711E-17 | 0.709801475 | 2.709801E-475 |
| bulk up/ sc up | **Pdcd1** | 2.161495838 | 1.01631E-36 | 0.525597333 | 3.525597E-333 |
| bulk up/ sc up | **Runx2** | 0.528308603 | 0.005213019 | 0.741076688 | 5.741076E-688 |
| bulk up/ sc up | **Ikzf2** | 1.091026423 | 1.72468E-19 | 0.71488544 | 3.71488E-544 |
| bulk up/ sc up | **Nrp1** | 2.128222135 | 1.5932E-14 | 0.690977757 | 7.1632E-171 |
| bulk up/ sc up | **Tnfrsf4** | 2.216325936 | 2.29841E-37 | 0.589001004 | 2.03213E-22 |
| bulk up/ sc up | **Tnfrsf8** | 1.601420216 | 1.59719E-20 | 0.768700941 | 4.4089E-117 |
| bulk down/ sc down | **Itm2a** | -0.822850961 | 0.000487642 | 0.605624702 | 1.0172E-81 |

**Table 5.2: Summary of differentially expressed genes between PBS-treated and 4Y-treated Tconv.** A combined analysis of bulk RNA-seq and single-cell RNA-seq was performed by intersecting differential expression testing comparison results. There were 8 genes that were significantly upregulated and 1 gene that were significantly downregulated in 4Y-treated Tconv compared to PBS-treated Tconv with both methods.

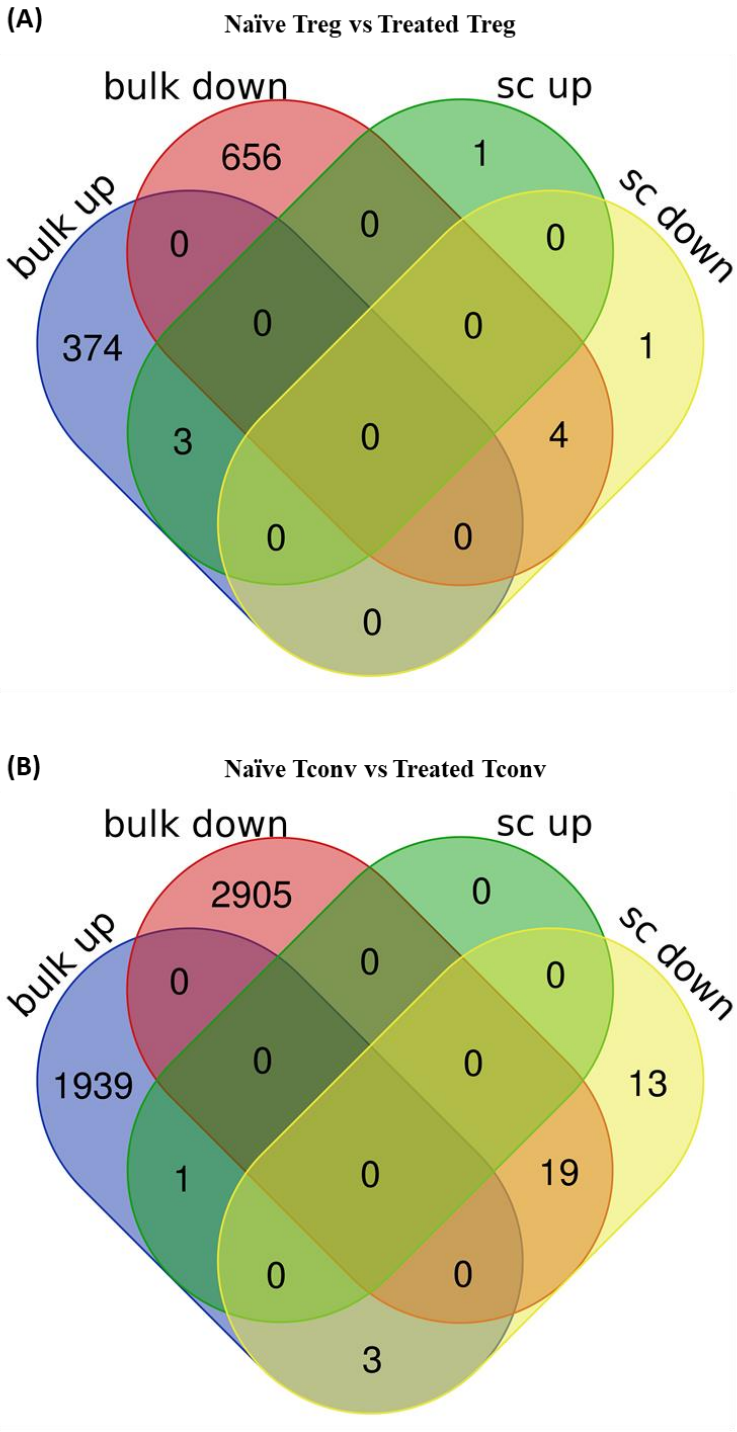



**Fig. 5.11: Combined bulk and scRNA-seq data.** A combined analysis of bulk RNA-seq and single-cell RNA-seq was performed by intersecting differential expression testing comparison results. To be considered for analysis a transcript needed to have a p-value < 0.05 and log2 fold change < -0.5 or > 0.5. Transcripts passing these filters were separated into a down-regulated and up-regulated list for the bulk data and single-cell data separately. This generated 4 lists that were intersected together. The intersection is shown visually as a Venn diagram.

## 5.7 Correlation of IL-10 with other genes associated with immune tolerance using scRNAseq

From the previous data, it was clear that bulk RNAseq was able to provide a more in-depth analysis, since more gene targets were revealed with this method compared to scRNAseq, which was used primarily for validation at a single cell level. However, the advantage of scRNAseq data set was the fact that it allows the analysis of the transcriptional profile of a selected population of cells, i.e., IL-10$^{+}$ cells. Therefore, it enables the targeted evaluation of a selected group of cells and in that way, it circumvents potential issues with the purity of the samples tested.

To be able to correlate IL-10 with other tolerance associated genes in Tregs, two approaches were followed for the analysis of the scRNAseq data. Firstly, IL-10$^{+}$ cells across the 4 biological samples were pooled together and differentially expressed genes between IL-10$^{+}$ and IL-10$^{-}$ cell populations was analysed, regardless of FoxP3 expression (Fig. 5.12A). Interestingly, in the IL-10$^{+}$ group of cells, there was an upregulation of genes also found to be upregulated in 4Y-treated Tregs, such as *Maf, Ccr2, Ccr5, Ccl5, Ctla4,* and *Icos* amongst others and this is consistent with previous findings on IL-10$^{+}$ Tr1 cells in the Tg4 model (Burton et al., 2014; Bevington et al., 2020).

Furthermore, we also analysed the differentially expressed genes found exclusively in IL-10$^{+}$ cells between PBS- and 4Y-treated Tregs (Fig. 5.12B). As expected, the genes that were upregulated in the IL-10$^{+}$ population of 4Y-treated Tregs (Fig. 5.12B) were overlapping with the ones found in the total population of 4Y-treated Tregs (Fig. 5.9B), with the key upregulated genes being *Il10, Ccr2, Ccr5*, while the downregulated ones being *Klf2* and *Taf10,* whose association with Treg biology has not been established yet.

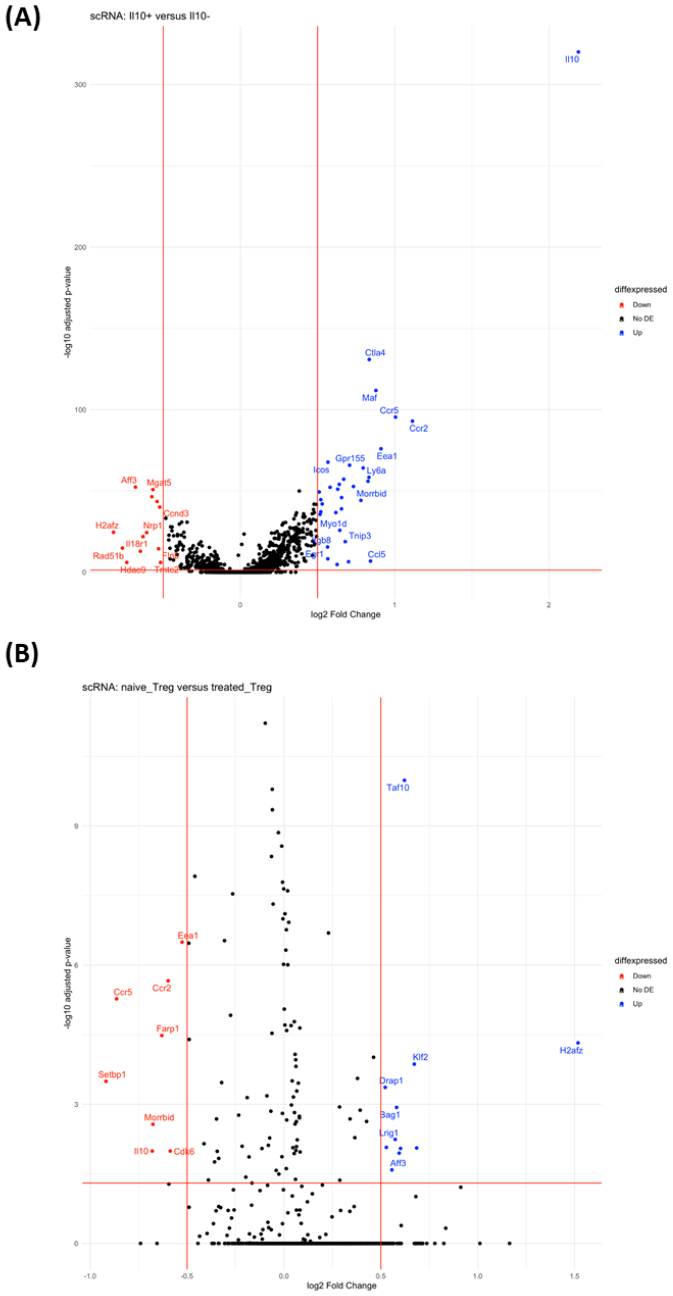



**Fig. 5.12: IL-10 expression is associated with upregulation of other regulatory genes such as CTLA-4, Maf, Icos, Ccr2 and Ccr5 on FoxP3$^+$ Tregs.** Il10$^+$ cells were defined as having expression > 0 and Il10$^-$ cells as having an expression value of 0. Differential expression testing was performed with Seurat v4.1.1 with the model MAST. For a gene to be considered for differential expression testing it needed to present in at least 10% of the cells across the comparison. IL-10$^+$ and IL-10$^-$ cells were pooled together from all samples and differentially expressed genes were analysed and visualised with a volcano plot **(A)**. Genes upregulated in the IL-10+ group are presented in blue, while genes upregulated in the IL-10- group are shown in red. The default average log2 fold change filter was set to 0.5. **(B)** IL-10+ cells were pooled together and differentially expressed genes were analysed. Genes upregulated in naïve Tregs are shown in blue and genes upregulated in treated Tregs are shown in red.

Another advantage of scRNAseq over bulk RNAseq, is the ability to study the co-expression of selected target genes in the chosen populations of cells. This is a very useful tool, since it enables us to draw some associations between the genes that are affected at the same time by peptide treatment, and therefore may be part of the same pathway of regulatory genes that govern the function either 4Y-treated Tregs (Fig. 5.13) or 4Y-treated Tconv (Fig. 5.14). Cells expressing one or the other marker are visualised in the UMAP with a single-coloured dot (either pink or green), while cells that express both markers are displayed as white dots.

Surprisingly, it appears that there is very low level of co-expression at the RNA level between FoxP3 and IL-10 in Tregs both before (Fig. 5.13A, i) and after peptide treatment (Fig. 5.13B, i); contrary to what has been previously shown with flow cytometry data, where approximately 30% of total $CD4^+$ T cells from 4Y-treated Tregs expressed both FoxP3 and IL-10. This can be due to the fact that this percentage of double-positive cells is not high enough to be detected with the scRNAseq analysis. Notably, there was some degree of co-expression between *Maf* and *Il10* in 4Y-treated (Fig. 5.13B, ii), but not PBS-treated (Fig.5.13A, ii) Tregs. The strongest correlation was seen between *Foxp3* and *Maf* (Fig. 5.13, iii) and *Foxp3* with *Prdm1* (Fig. 5.13, iv) in 4Y-treated Tregs, while *Prdm1* was not co-expressed with *Il10* as much in the same biological group (Fig. 5.13, v). Therefore, expression of *Maf* correlated both with *Foxp3* and less so with *Il10*, and similar pattern was also true for *Prdm1*.

For the 4Y-treated Tconv, again, there were barely any cells co-expressing *Foxp3* and *Il10*; however, the strongest correlation was observed between *Maf* and either *Il10* (Fig. 5.14, ii) or *Foxp3* (Fig. 5.14, ii).

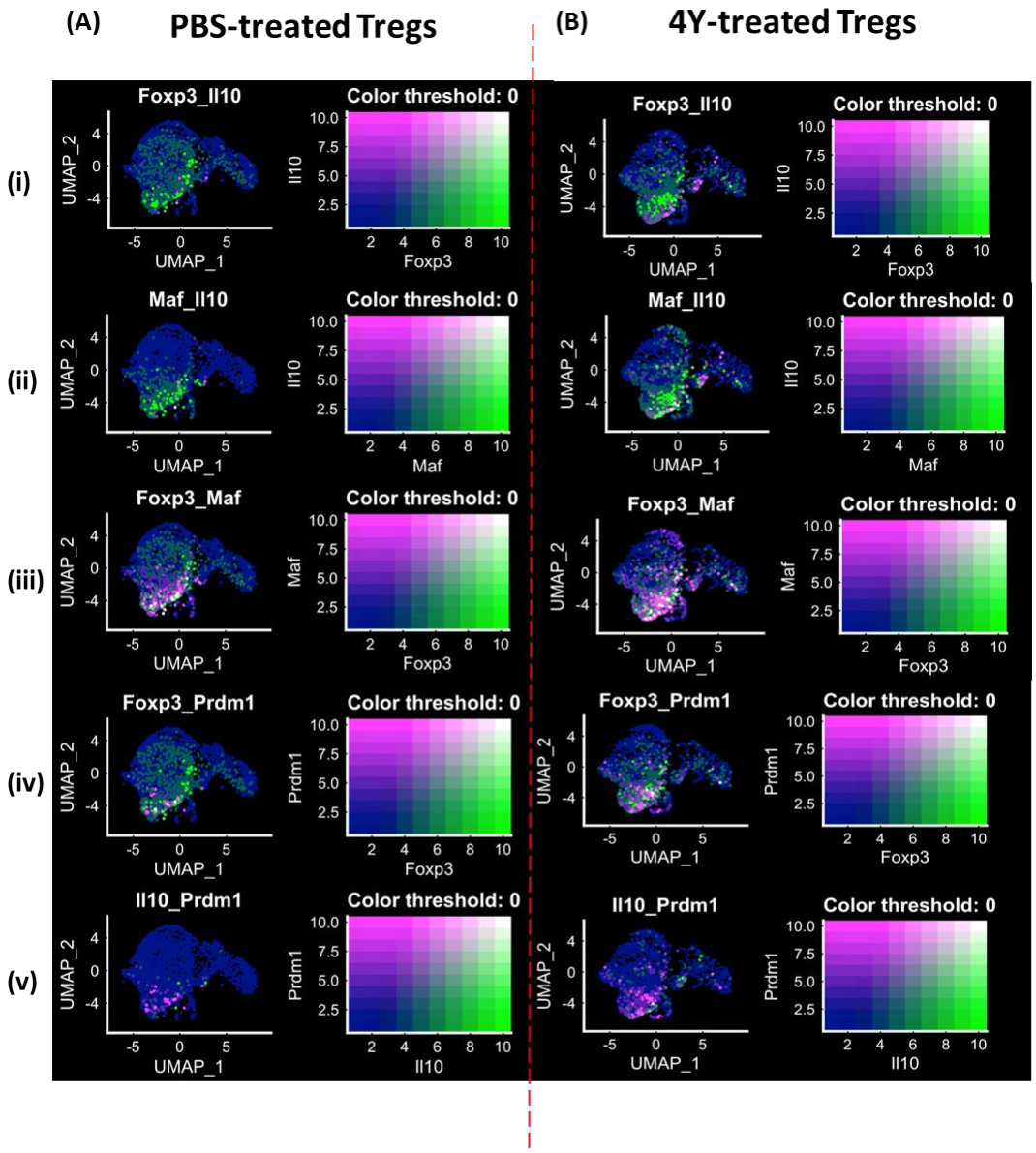



**Figure 5.13 Co-expression plots of chosen target genes in PBS- and 4Y-treated Tregs** UMAP plots showing the co-expression of 2 selected genes. The co-expression plots are shown for selected genes in either PBS-treated **(A)** or 4Y-treated **(B)** Tregs and the group of genes studied in parallel are Foxp3_Il10 (i), Maf_Il10 (ii), Foxp3_Maf (iii), Foxp3_Prdm1 (iv) and Il10_Prdm1 (v).

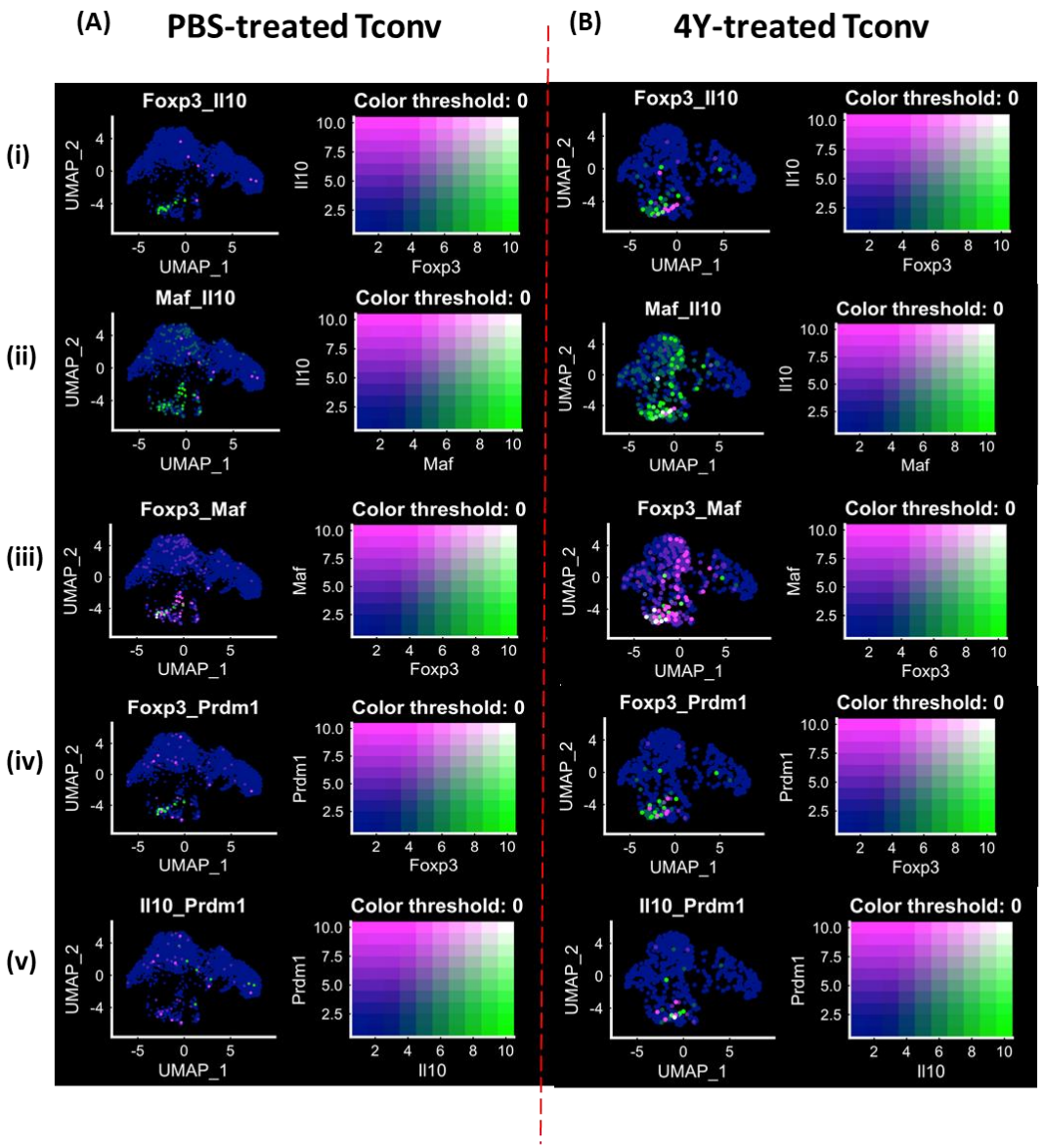



**Figure 5.14 Co-expression plots of chosen target genes in naïve and treated T conventional cells.** UMAP plots showing the co-expression of 2 selected genes. The co-expression plots are shown for selected genes in either PBS-treated **(A)** or 4Y-treated **(B)** Tconv and the group of genes studied in parallel are Foxp3_Il10 (i), Maf_Il10 (ii), Foxp3_Maf (iii), Foxp3_Prdm1 (iv) and Il10_Prdm1 (v).

## 5.8 Validation of selected DEGs by RT-PCR

Despite the QC methods applied in the RNA sequencing data, there is still a small chance of getting some artifacts with these methods. Real-time PCR (RT-PCR) is still considered the gold standard for gene expression analysis, particularly when the copy number of the template is low. Therefore, even though RNA sequencing provides a great tool for analysing a wide array of genes in one go to be able to narrow down the research interest, RT-PCR provides a fast, reliable, and affordable way to validate sequencing results using a different methodology. The results are presented as ΔΔCT, which calculates the relative fold change in gene expression of samples, and it was normalised to the chosen reference gene, GAPDH that was used as an endogenous control.

As expected, the IL-10-related genes, *Prdm1, Nfil3* and *Maf* were upregulated predominantly in 4Y-treated Tregs and less so in 4Y-treated Tconv as compared to their PBS counterparts (Fig. 5.15A). Expression of *Il10* was significantly upregulated in 4Y-treated Tregs or Tconv compared to their PBS-treated counterparts (Fig. 5.18B, middle); while *Ifng* was upregulated predominately in 4Y-treated Tconv and less so in 4Y-treated Tregs (Fig. 5.15B, left). This is not surprising since these cells come from a Th1-skewed model, and they can produce IFN-γ upon TCR stimulation (Gabrysova et al., 2009). Notably, *Il2* was only found in 4Y-treated Tconv, but not FoxP3$^{+}$ Tregs, either treated or untreated (Fig. 5.15B, right). This is consistent with the literature, since it has been demonstrated that even though Tregs have abundant expression of the interleukin 2 receptor α-chain (IL-2Rα; CD25), and they can respond to IL-2 produced by Tconv, they are unable to produce IL-2 themselves (Chinen et al., 2016).

Finally, the genes encoding the co-inhibitory receptors, *Ctla4, Tigit, Lag3*, were all upregulated both in Tregs and Tconv following peptide treatment (Fig. 5.15C).

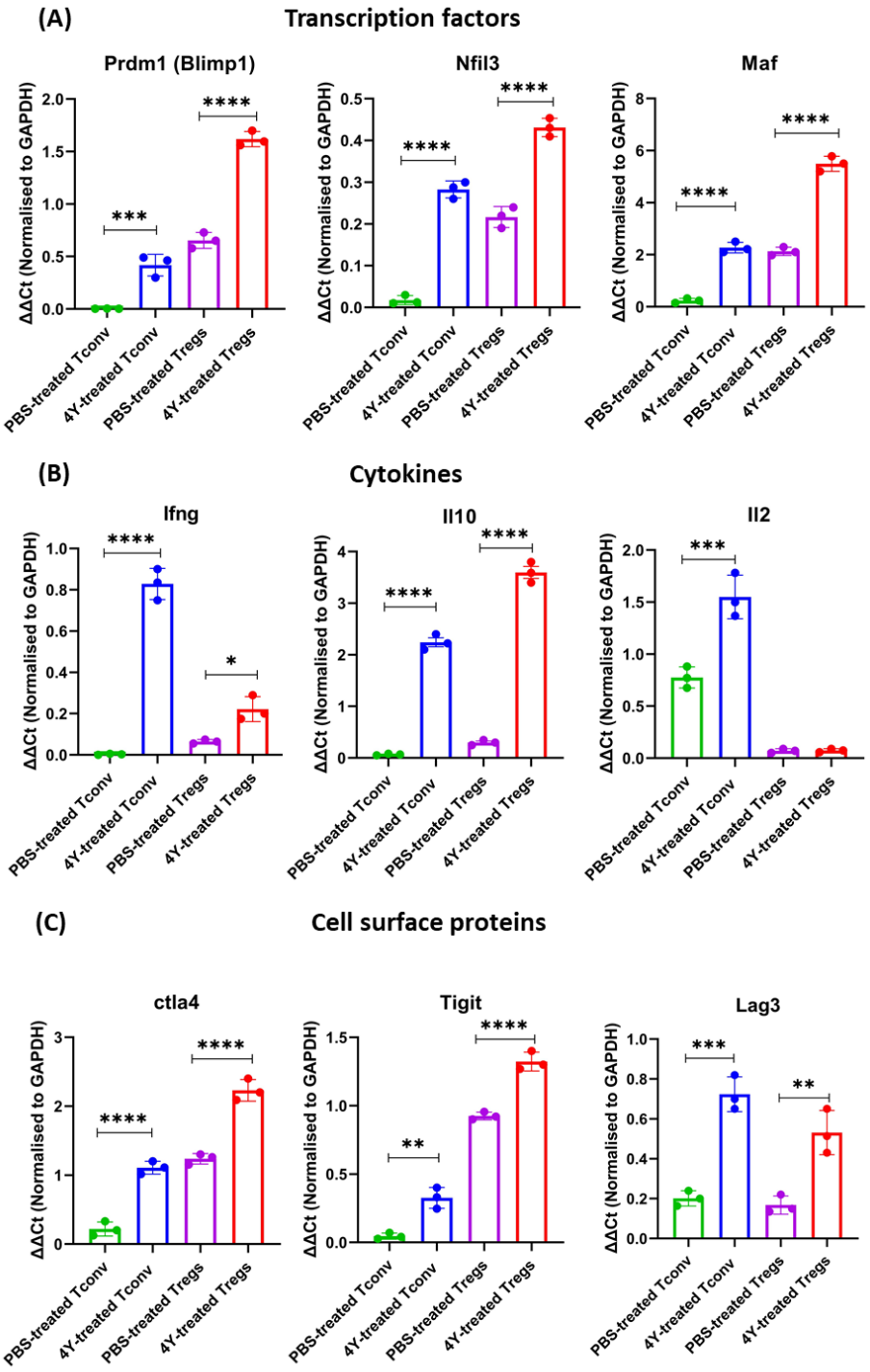



**Fig. 5.15: Expression of genes associated with the differentiation and function of both Tconv and Tregs following tolerance induction.** Tg4 mice were treated with 6 subcutaneous doses of $MBP_{Ac1-9}$ [4Y] as described previously. Spleens were harvested 3 days after the final treatment, and cells were purified based on CD25 expression using magnetic beads to create 4 groups: i) 4Y-treated Tregs ii) PBS-treated Tregs iii) 4Y-treated Tconv and iv) PBS-treated Tconv. Cells from all 4 groups were stimulated *in vitro,* total RNA was extracted and reverse transcribed and expression levels of transcription factors (A), cytokines (B) and cell surface proteins (C) were determined by quantitative real-time PCR after normalisation to the housekeeping gene, GAPDH. Results show the relative expression of the gene of interest from three and are collated from two repeat experiments. The statistical significance between groups was assessed by one-way ANOVA with Tukey's multiple comparisons test.

## 5.9 Demethylation analysis of FoxP3 CNS2 region

Epigenetic changes in the DNA can play a critical role on Treg cell stability. Upregulation of FoxP3 that determines Treg lineage, depends on complete demethylation of the Treg cell-specific demethylated region (TSDR), also known as CNS2, a CpG-rich region in the *Foxp3* locus (Floess et al., 2007). Poor demethylation of the CNS2 region can result in reduced transcription of the *Foxp3* gene, that, in turn, leads to loss of Treg stability and function (Ohkura et al., 2012; Polansky et al., 2008).

To assess Treg stability following peptide immunotherapy, we aimed to investigate the methylation status in TSDR by bisulfite sequencing according to the protocol developed by Arai and colleagues in Shimon Sakaguchi's lab (Arai et al., 2022). Briefly, spleens from Tg4 mice were harvested three days after the final dose and Tregs were isolated as described previously in this chapter ($CD25^+$ vs $CD25^-$ fraction from treated and untreated mice), giving rise to the 4 biological groups tested: 4Y-treated Tregs, PBS-treated Tregs, 4Y-treated Tconv, PBS-treated Tconv. Cells were stimulated *in vitro* and subsequently placed into the indicated lysis buffer to be able to disrupt the cell membrane and extract the DNA. Samples were kept at -80$^o$C until shipped to Osaka University for the bisulfite sequencing experiment.

The FoxP3 CNS2 region was amplified by PCR, cloned, and sequenced. The results show that the demethylation of the FoxP3 CNS2 region was approximately 50% in Tregs (either PBS- or 4Y-treated). This observation was a bit surprising since it has been previously established that 80-90% of Tregs are demethylated. There are two possible explanations for this discrepancy; either the Treg sample may contain cells other than Tregs, since the purity obtained was less than 100%, or this can be due to the fact that some of the Tg4 mice used for this experiment were females. In female cells, X-

chromosome inactivation controls the activation status on X chromosomes, both structurally and functionally (Loda et al., 2022; Bacher et al., 2006). *Foxp3* is on the X chromosome, and regulated by the same mechanism; therefore, in this analysis, the demethylation rate is around 50% because of the inactivated X chromosome. For this type of analysis, male mice are preferred, but when this is not possible, it may be better to examine methylation of other genes such as *Ctla4*, *Ikzf2* (Helios), and *Ikzf4* (Eos).

Despite the limitations, we were still able to draw some conclusions regarding the impact of peptide immunotherapy on the demethylation status of the FoxP3 CNS2 region. Interestingly, it appears that 4Y-treated Tregs have similar % demethylation to PBS-treated Tregs (Fig. 5.16A, i and ii). Furthermore, the levels of demethylation in the 4Y-treated and PBS-treated Tconv were very similar to each other, but significantly lower compared to 4Y-treated and PBS-treated Tregs (Fig. 5.16B, i and ii). This is not surprising since demethylation of the CNS2 region is a hallmark of $FoxP3^+$ Tregs.

This is expected, since Tconv do not normally express Foxp3, therefore the % demethylation should be <10%. In our samples, there were some impurities in the Tconv populations that could account for the higher percentage of demethylation; however, it remains clear that peptide treatment did not affect the demethylation, hence the stability of Tregs. Therefore, whether the differences seen in terms of the suppressive capacity of these cells is due to other signalling processes, post-transcriptional or other type of epigenetic modifications remains to be determined.

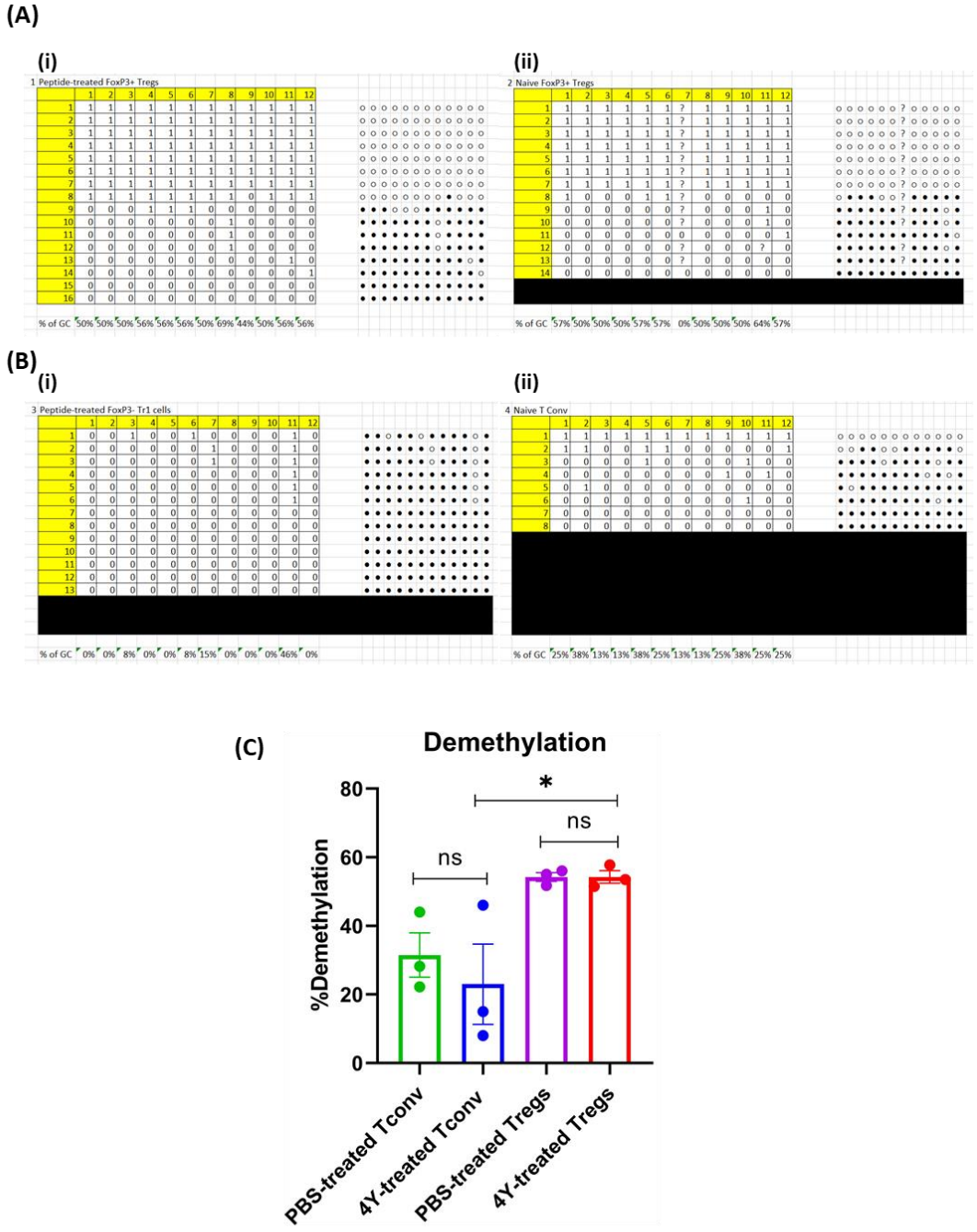



**Fig. 5.16: Demethylation status of FoxP3 CNS2 region.** The vertical axis of the tables shows the clones obtained and the horizontal axis shows the methylation position in the Foxp3 CNS2 region. 16 clones were analysed; clones for which no results were obtained are blacked out. This table is represented by black (methylated CpGs) and white (demethylated CpGs) circles in the figure on the right. If a mutation is included and methylation cannot be determined, it is marked with a question mark (?). The average % demethylation across the 16 clones was calculated per mouse tested. **(A)** Representative table and summary dotplots of methylated or unmethylated clones in 4Y-treated (i) or PBS-treated (ii) Tregs coming from one mouse. **(B)** Representative table and summary dotplots of methylated or unmethylated clones in 4Y-treated (i) or PBS-treated (ii) Tconv from one mouse. **(C)** Summary bar graphs display individual and mean average values of % demethylation of 3 mice of per group (±SEM). Statistical significance was calculated by one-way ANOVA with Tukey's multiple comparison test.

## 5.10 Discussion

In this chapter, a comprehensive gene expression profiling analysis combined with flow cytometric characterisation of different regulatory T cell populations was presented. It is very clear from these data that peptide treatment has an impact on FoxP3$^{+}$ Tregs by inducing them to upregulate certain genes associated with tolerance with concomitant downregulation of effector genes; therefore, this transcriptional re-programming essentially licenses Tregs to acquire a highly tolerogenic phenotype, as shown in Chapter 4.

Although previously thought to be a relatively homogeneous population, it has become increasingly accepted that Tregs are comprised of multiple subsets with unique functions. Inherent **heterogeneity** in seemingly pure Treg populations requires a single cell expression analysis in addition to bulk RNAseq approaches to be able to define the target populations more precisely before analysing their transcriptional signatures. Although bulk RNAseq aims to identify differences between sample conditions at the population level, scRNAseq allows the identification of differences between cell types at a single cell level. The complementary data generated from both sequencing methods has demonstrated that peptide immunotherapy gives rise to a population of regulatory T cells that has the transcriptional signature of **effector** and potentially **memory Tregs,** driven by the expression of IL-10, Blimp-1, ICOS, c-Maf, TIGIT, CTLA-4 amongst others. These markers have been well established as markers of eTregs (Miragaia et al., 2019).

The idea that there is a population of suppressor cells that could have an important role in ‘remembering’ the self-antigen they encountered and maintain long-lived tolerance was first introduced by Loblay and colleagues more than 4 decades ago (Loblay et al., 1978), but the lack of tools to define this cell population at that time hampered the

progress that could have been made in the field. In recent years, Rosenblum and colleagues have shown that upon expression of self-antigens in peripheral tissues, thymus-derived regulatory T cells become activated, proliferate and can differentiate into more potent suppressors which can orchestrate the resolution of organ-specific autoimmune or inflammatory responses.

Following the resolution of the immune response, activated Tregs can persist and continue to reside in the target tissue, where they are readily available to attenuate secondary autoimmune reactions upon re-encounter with the autoantigen that initially primed them. In this way, tissues that have undergone autoimmune inflammatory reactions develop 'regulatory memory' conferred by Tregs (Rosenblum et al., 2011). Gratz and colleagues have shown that these memory Tregs are dependent on IL-7 and not IL-2 for their maintenance in peripheral tissues (Gratz et al., 2013), unlike resting Tregs that are highly dependent on IL-2 for survival and effector Tregs that primarily rely on ICOS signalling (Smigiel et al., 2014). Our results show that 4Y-treated Tregs upregulate ICOS, indicating that this is a population of effector Tregs; however, it will be interesting to investigate their dependence on IL-7 to examine the potential of these cells to obtain a more memory-like phenotype.

Furthermore, memory Tregs have several characteristics of effector memory T conv cells, including survival in the absence of TCR stimulation, residence in non-lymphoid tissues, expression of markers indicative of prior activation, and enhanced functional activity upon antigen re-exposure (Akbar et al., 2007). They can migrate to antigen-expressing tissues where they stably reside (**tissue-resident memory Tregs**) or recirculate between blood and non-lymphoid tissues (**effector memory Tregs**). A recent publication from Brull and colleagues has proposed some markers to distinguish between

naïve, effector and memory Tregs; however, there is an extensive overlap between them, making the characterisation of these cells quite challenging (Estrada Brull et al., 2022).

In our data set, 4Y-treated Tregs have high expression of CTLA-4 and chemotactic molecules such as Ccr2 and Ccr5, which are indicative of an active, effector phenotype; however, they do not express CD44 or CD103 that are strongly linked to effector and memory Tregs (Liston and Gray, 2014; van der Veeken et al., 2016). This highlights that the current understanding of eTreg biology is rudimentary compared with that of effector T conv cells primarily due to the lack of lineage-specific markers. The identification of these markers in the future will pave the way for the precise phenotypic characterisation of Tregs that derive from peptide treatment.

Furthermore, it is becoming increasingly clear that tissues play a major role in regulating the immune responses that occur within them in an attempt to mitigate damage caused by inflammation and preserve organ function. It has been proposed that amphiregulin$^{+}$ Tregs may play a key role in **tissue repair** and maintenance of immune homeostasis in peripheral organs by elaborating mediators acting on parenchymal cells (Arpaia et al., 2015). Intriguingly, Tregs from peptide treated Tg4 mice upregulated the expression of *Areg*, the gene that encodes amphiregulin, which promotes repair under inflammatory conditions and organ injury (Estrada Brull et al., 2022; Berasain and Avila, 2014). Notably, expression of *Ccr5*, another significantly upregulated gene on 4Y-treated Tregs, has been associated with Treg recruitment as knock out mice show impaired Treg infiltration as well as adverse remodelling and cardiac deterioration after myocardial infarction (Dobaczewski et al., 2010). This striking observation highlights that peptide treatment gives rise to Tregs that are not only able to supress inflammatory response but

can also be involved in the subsequent restoration of immune homeostasis and tissue repair.

It has been established in the literature that persistent exposure to antigen can result in **T cell exhaustion**, a state of functional hypo responsiveness best characterised in the context of chronic viral infection (Wherry and Kurachi, 2015). Therefore, someone could argue that the cells that are generated via the dose escalation protocol are exhausted, since they also express high levels of **inhibitory receptors**, a common feature of exhausted T cells. However, it was clearly shown that these cells are highly functional and responsive upon antigen encounter; hence, they exert an effector phenotype and fall under the general characteristic of eTregs, based on their transcriptional profile and suppressive potential.

Finally, it has been hypothesised that this state of increased suppressive capacity seen in eTregs is reversible depending on environmental signals, otherwise it would lead to undesired, generalised immunosuppression. There is still an unmet need for identification of markers to determine lineage-defining indicators of **cell fate/identity** versus those that reflect a **transient cell state** influenced by local inflammatory cues – a task plaguing also the more extensively studied field of CD8 memory T cells (Chang et al., 2014). It remains to be determined whether peptide treatment has a permanent, imprinting effect on Tregs making them acquire a highly tolerogenic phenotype, or whether this effect is reversible, and stability of this lineage depends on environmental cues together with continuous TCR stimulation.

Concluding statement

The data presented in this chapter demonstrate that repeated exposure to tolerogenic antigen stimulation expands the population of IL-10$^{+}$ cells by giving rise not

only to Tr1 cells, which have been studied extensively in the past, but also to **effector/memory Tregs** that upregulate tolerance-related genes, such as *Il10, Maf, Prdm1* and importantly, are potent mediators of bystander suppression. IL-10 has been strongly linked to the expression of inhibitory receptors on Tregs, in line with what was previously shown on Tr1 cells (Burton et al., 2014). Demethylation of FoxP3 CNS2 locus remains unaltered by this treatment, but other epigenetic changes have yet to be determined.

This work paves the way for identifying and harnessing the network of regulatory pathways that serve to limit tissue inflammation and are of pivotal importance for controlling autoimmune reactions and preserving end-organ function. The suppressive phenotype of these eTregs, together with their potential capacity to mediate long-term, peripheral tolerance as memory Tregs, make them attractive targets for therapeutic intervention in a variety of clinical areas, such as autoimmunity and transplantation, where the balance between immunity and tolerance requires more tight regulation.

# CHAPTER 6:

# GENERAL DISCUSSION

Even though the concept of antigen-specific desensitisation has been known for over a century, the mechanism of action is still not fully understood (Noon, 1911). Weiner and colleagues first described the phenomenon of bystander suppression in 1991 demonstrating that oral administration of antigen can give rise to $CD8^+$ T cells, which once they get activated via their TCR, hence in an antigen-specific manner, they can then exhibit their suppressive effect in an antigen-independent manner (Miller et al., 1991). This observation was shown both *in vitro* and *in vivo* in the EAE model, highlighting the potential of 'antigen-driven bystander suppression', to downregulate a T cell-driven autoimmune inflammatory response in a physiological environment.

A few years later, data from our lab using the (B10.PL x SJL) F1 murine model supported the hypothesis that intranasal administration of antigen can control EAE and the degree of T cell tolerance mediated by $CD4^+$ T cells was dependent on the myelin antigen, with different epitopes ($MBP_{Ac1-9}$, $MBP_{89-101}$, and $PLP_{139-151}$), exhibiting different suppressive potential (Anderton and Wraith, 1998). In more recent years, Santamaria and colleagues showed that administration of nanoparticles (NP) coated with epitopes that are relevant to disease and bound to major histocompatibility complex II (pMHC II) molecules can generate antigen-specific $CD4^+$ Tr1 cells that can ameliorate autoimmune responses in murine models regardless of the genetic background (Clemente-Casares et al., 2016). These Tr1 cells are capable of blunting both their cognate autoantigen as well as other disease-associated antigens; therefore, the ability of these cells to respond to disease-relevant and irrelevant NP-pMHC II therapies demonstrates the potential capacity of these cells for bystander suppression (Singha et al., 2017).

However, despite the evidence describing bystander suppression in the last 30 years summarised in figure 6.1, there remains the need for a better understanding of the

mechanism of action of the different regulatory T cells underpinning this phenomenon especially in the context of autoimmunity.

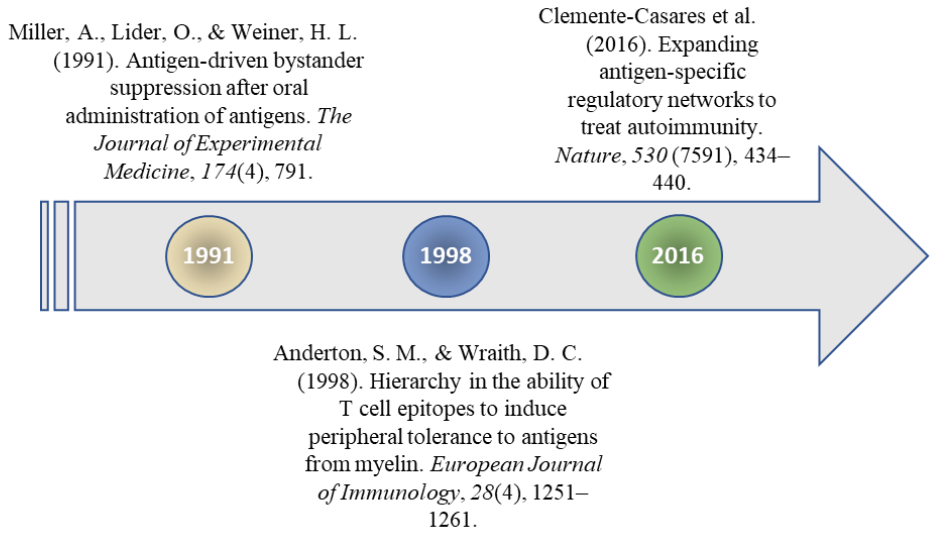



**Fig. 6.1 : Timeline of major breakthroughs in the field of antigen-driven bystander suppression.** Bystander suppression was first described in autoimmune disease by Weiner and colleagues in 1991 following oral administration of the antigen. A few years later, data generated from the Wraith lab revealed a certain degree of hierarchy in the capacity of different myelin epitopes to induce peripheral tolerance using the Tg4 model described in this thesis. In more recent years, Santamaria and colleagues introduced a new approach using nanoparticles coated with disease-associated epitopes bound to MHC II molecules to induce Tr1 cells with immunomodulatory potential.

In this thesis, chapter 4 aimed to provide some insight into the **functionality** of the different regulatory T cells that arise from antigen-specific immunotherapy, with a particular focus on their ability to mediate bystander suppression. Following tolerance induction, there was a clear expansion of IL-10$^{+}$ cells, both FoxP3$^{+}$ Tregs and FoxP3$^{-}$ Tr1 cells in line with previous work from the Wraith lab (Gabryšová et al., 2009; Anderton and Wraith, 1998; Burkhart et al., 1999; Gabryšová and Wraith, 2010). However, the impact of tolerance induction had been studied mainly in the context of Tr1 cells in the past since these cells greatly outnumber FoxP3$^{+}$ Tregs in the Tg4 model. The work presented herein provides a novel understanding on the hierarchy amongst regulatory T cell populations to mediate bystander suppression, with peptide treated FoxP3$^{+}$ Tregs being the most potent cells. This finding was quite significant, since it illustrates, for the first time, that **peptide immunotherapy can license FoxP3$^{+}$ Tregs to acquire an effector phenotype and mediate bystander suppression *in vitro***. Importantly, these findings were recapitulated in an *in vivo* environment, demonstrating the **physiological relevance** of this observation.

Furthermore, it was shown that inducing tolerance to recipient (Tg4 x C57BL/6) F1 mice established a tolerogenic environment that prevented the proliferation and activation of newly transferred 2D2 responder cells. The tolerance induction witnessed in this system was more profound compared to the induction of bystander suppression of 2D2 cells that was mediated by the adoptive co-transfer of CD4tol cells *in vivo*. We speculate that this was due to the fact that in the first case, the regulatory T cells massively outnumber the responders, whereas in the latter there is a 1:1 ratio of responders to putative suppressors. This observation indicates that applying peptide-based immunotherapies to patients with autoimmune conditions could induce an antigen-

specific tolerogenic environment in an easier, more straightforward, and much more affordable way compared to adoptive T cell transfers, since it may prove difficult to transfer enough regulatory T cells to have an impact.

Treg-based therapies has become quite popular in recent years with a few clinical trials showing promising results in the field of liver (Levitsky et al., 2009) and kidney transplantation (Roemhild et al., 2020; Sawitzki et al., 2020), as well as autoimmune diseases (Bluestone et al., 2015; Dong et al., 2021); however, the high cost and the challenges arising from their manufacture, administration, stability, trafficking and durability impose significant limitations when considering this therapeutic option (Raffin et al., 2019). Further research on the optimal **delivery system** and **dosing strategy** used in antigen-specific immunotherapies will bring this approach into wider clinical use for the treatment of autoimmune diseases.

Historically, in certain autoimmune conditions, such as multiple sclerosis (MS), T cells appeared to be the driving force in the pathogenesis of the diseases however, recent evidence support the active contribution of B cells in the establishment and progression of relapsing-remitting MS (RRMS) through autoantibody responses driven by antigen recognition and via cross regulation of T cells (Roach and Cross, 2021). In particular, proinflammatory B cells found in MS patients regulate the polarisation of T cells towards a proinflammatory phenotype through secretion of cytokines, such as IL-6, IL-12, TNF-α and GM-CSF (Piccio et al., 2010). **B cell depletion therapies** utilise monoclonal antibodies against anti-CD20, a surface marker expressed by B cells, to convert B cells from proinflammatory to regulatory **(Bregs)**. Three major anti-CD20 antibodies have been developed for the treatment of MS: rituximab, ocrelizumab and ofatumumab (Florou et al., 2020). All three of these drugs showed encouraging results in clinical trials for

RRMS with reduced disease progression and radiographic findings as evidenced by magnetic resonance imaging (MRI) results (Hawker et al., 2009; Kappos et al., 2011; Sorensen et al., 2014), demonstrating the therapeutic potential of this approach; however, they have yet to be evaluated in other forms of MS.

In a similar approach, **monoclonal antibodies against CD3** have been developed for the treatment of type I diabetes (T1D), an autoimmune disease in which the dysfunction of β cells of the pancreas leads to reduced insulin production (Ke et al., 2021). These antibodies can either deplete the targeted cell population, with potential side effects deriving from the compromised protective adaptive immunity, or modulate the function of T effector cells to regain their regulatory capacity (Skyler, 2013). Results from a clinical trial showed that patients with new-onset T1D treated with teplizumab, an anti-CD3 monoclonal antibody, had reduced decline in C-peptide levels even after 2 years of disease onset, and decreased frequency of IFN-γ-producing, Th1-like T cells highlighting the efficacy of this immunotherapeutic approach (Herold et al., 2013). It would be interesting to develop a therapeutic regime that would combine monoclonal antibodies against T or B cells, together with tolerogenic peptides. As demonstrated in this thesis, peptide treatment establishes a tolerogenic phenotype by inducing potent regulatory T cells and also by modulating DCs; therefore, harnessing its potential to develop robust **combinatorial therapies** with monoclonal antibodies against CD3, CD20 or both could provide long-lasting protection and potentially establish a novel, more robust and efficacious therapeutic approach for the treatment of autoimmune diseases.

Furthermore, initial *in vitro* data using the linked peptide versus separate $MOG_{35-55}$ and $MBP_{Ac1-9}$ peptides demonstrated an increased potency of linked suppression versus *bona fide* bystander suppression and the importance of relevant epitopes being expressed

in a close physiological context (i.e., on the same APC), for suppression to occur. As observed in EAE, tolerance towards $PLP_{139-151}$, was sufficient to control T cell responses to not only PLP but also MBP by bystander effects that were sufficient to control disease development (Anderton and Wraith, 1998). These autoantigens are myelin sheath proteins; hence, they are expressed within the same tissue. Therefore, antigen-specific immunotherapies are more effective if the target antigens are expressed in close proximity in a physiological environment and therefore are more permissible to bystander suppression.

It could be argued that the Tg4 model, a **TCR transgenic mouse**, is artificial, hence raising doubts regarding the general applicability of peptide immunotherapy to humans. In non-transgenic mice, the TCR diversity is far greater and not every antigen can be presented in the thymus at sufficient levels to induce the selection of adequate numbers of T cells specific for each antigen. Therefore, TCR transgenic models can be a powerful tool to study antigen-specific immune responses since the frequency of antigen-specific cells is sufficiently high to measure the effect of antigen administration directly. Unpublished data from our lab has also shown that tolerance induction gives rise to a population of IL-$10^+$ cells in **(B10.PL x C57BL/6) F1 non-transgenic mice**. These cells showed a similar phenotype to $CD4^+$ T cells from the Tg4 mouse (correlation of increased IL-10 expression with co-inhibitory receptors); however, the absolute numbers of IL-$10^+$ cells in the F1 mice was much lower compared to the Tg4, because in this mouse there is a smaller percentage of antigen-specific ($V\beta8^+$) T cells being tolerised against 4Y peptide, compared to the high percentage of $V\beta8^+$ cells found in the Tg4 mouse (approximately 95% of total CD4).

Therefore, the F1 mouse could be used as a **proof of concept** for the applicability of tolerance induction in a non-transgenic setting, but the limitations in terms of cell numbers renders the mechanistic study of these regulatory T cells challenging. Hence, in order to circumvent this, the Tg4 transgenic mouse was preferred as a model to further shed light on the mechanism of action of peptide-induced regulatory T cells. Importantly, it is worth noting that this approach showed promising results in a recent phase 1 study in Graves' disease (Pearce et al., 2019) and both phase 1 and 2 trials in multiple sclerosis (Chataway et al., 2018), further reinforcing the therapeutic potential of this approach.

Furthermore, chapter 5 presented data demonstrating that peptide treatment modifies the FoxP3$^{+}$ Treg transcriptome in a co-ordinated manner, resulting in a distinct phenotype characterised by the expression of specific transcription factors, negative co-stimulatory molecules, and cytokines. We have followed a cross-disciplinary approach incorporating elements from both experimental and computational biology to provide a **transcriptome-wide analysis of Treg gene expression** associated with effective antigen-specific immunotherapy. Notably, in 4Y-treated Tregs there were marked changes associated with the repression of transcripts relating to the development of an inflammatory immune response and induction of transcripts that are critical for the orchestration of regulatory processes. The transcriptional reprogramming seen among FoxP3$^{+}$ Tregs is reminiscent of the impact of tolerance induction on the transcriptional signature expressed by Tr1 cells (Burton et al., 2014).

Surprisingly, despite the previously reported association between TIGIT and both FoxP3$^{-}$ Tr1 and FoxP3$^{+}$ Tregs (Burton et al., 2014; Kurtulus et al., 2015), it was not possible to establish a role for this co-inhibitory receptor in the generation, stability and function of these cells as presented in the functional *in vitro* assays (Chapter 3) and also

in the RNA sequencing data (Chapter 5), where Tim-3 and Lag-3 were upregulated in 4Y-treated Tregs, but not TIGIT. The literature around the role of TIGIT in autoimmunity remains **controversial**. In the case of rheumatoid arthritis (RA), there are some studies showing a negative correlation between TIGIT activity and disease progression (Zhao et al., 2016), while other groups demonstrate exactly the opposite, claiming that TIGIT overexpression is linked to $CD4^+$ T cell exhaustion and subsequent inability of cells to control disease progression (Greisen et al., 2017). Notably, the frequencies of TIGIT-expressing $CD4^+$ and $CD8^+$ T cells were increased in patients with primary Sjögren's syndrome (pSS) compared to healthy controls and were linked to pSS disease activity (Deng et al., 2020) and similarly, in systemic lupus erythematosus (SLE) the frequency of $CD3^+CD4^+TIGIT^+$ T cells was higher compared to $CD3^+CD4^+TIGIT^-$ T cells (Luo et al., 2017). Therefore, TIGIT can act both as a positive and a negative prognostic marker and it varies across autoimmune diseases or even across studies focusing on the same disease.

In addition to the differential role in different disease setting, TIGIT also demonstrates distinct functions in different cell types. Even though there is evidence showing that the expression of TIGIT on Tregs correlates with lineage stability and superior suppressive capacity against Th1 and Th17 immune responses (Joller et al., 2014; Fuhrman et al., 2015), recent data showed increased expression of TIGIT on Tregs of RA patients, but no correlation between TIGIT and disease activity (Yang et al., 2019). Conversely, Bregs were capable of mitigating autoimmune diseases and preventing allograft rejection via immunosuppressive cytokines and immunoregulatory pathways that involved IL-10 and TIGIT (Cherukuri et al., 2021). Finally, consistent with its inhibitory characteristics, the percentage of $TIGIT^+$ NK cells were decreased in SLE

patients compared to healthy controls and the frequency of these cells was inversely related to the IFN-γ-producing capacity of NK cells in both groups (Wang et al., 2015). Intriguingly, patients with active SLE had significantly lower frequencies of $TIGIT^+$ NK cells compared to those with inactive disease highlighting that the expression of TIGIT correlated negatively with the progression and severity of SLE (Luo et al., 2018).

Joller and colleagues demonstrated that TIGIT can have a direct impact on attenuating TCR signals independent of APCs by using agonistic anti-TIGIT mAbs (Joller et al., 2011). This observation highlighted the potential role of TIGIT in the maintenance of peripheral tolerance and the control of autoimmune responses; however, the function of TIGIT may play a different role in different tissues or cell types and even at different stages of disease progression; therefore, this level of functional complexity can often lead to inconclusive results since TIGIT is studied in different contexts and using different murine models. Despite the conflicting results in the literature, it was clearly and consistently demonstrated in this thesis that TIGIT does not play a role in the development or function of different regulatory $CD4^+$ T cell population in the Tg4 mouse, a Th1-skewed model. Arguably, TIGIT can have a more profound effect in different disease settings, cell types (i.e., $CD8^+$ T cells or NK cells) or even species, since data from pre-clinical mouse models do not always reflect the human studies.

It has been suggested in the literature that $CD4^+$ T conv cells and Tregs undergo two distinct differentiation pathways that run in parallel to ensure the **balance between immunity and tolerance** (Fig. 6.1). During antigen-specific activation in secondary lymphoid organs, activated 'effector' T cells (both Tconv and Tregs) are generated. In particular, upon encounter with infectious agents, naïve Tconv cells become activated and mount a protective immune response to clear the invading pathogen and restore tissue

homeostasis. These activated **effector Tconv** can then, in turn, give rise to either **central memory Tconv** that reside in secondary lymphoid organs, or **effector memory Tconv** and **tissue-resident memory Tconv** that circulate in the periphery (Sallusto et al., 2004; Roberts et al., 2005). On the other hand, repeated exposure to self-antigens can give rise to activated, effector Tregs which can subsequently differentiate to effector memory Tregs in the periphery. It is currently unknown whether Tregs found in non-lymphoid tissues consist of tissue-resident memory cells or effector memory cells or both and it is also not fully understood whether central memory Tregs are generated during this process (Rosenblum et al., 2011, 2016; Gratz et al., 2013).

The data presented in this thesis contributes to this newly emerging field of Treg differentiation by demonstrating that antigen-specific immunotherapy can give rise to activated effector and potentially effector memory Tregs that can successfully mediate bystander suppression, modulate the maturation of dendritic cells via IL-10 secretion and could potentially be involved in tissue homeostasis, since it was shown that they upregulate amphiregulin and CD39, previously associated with tissue regeneration (Zhang et al., 2017). Further characterisation of the heterogeneity found within the regulatory T cell populations will pave the way towards better understanding the phenotype and function of these cells both in the steady-state and in disease settings.

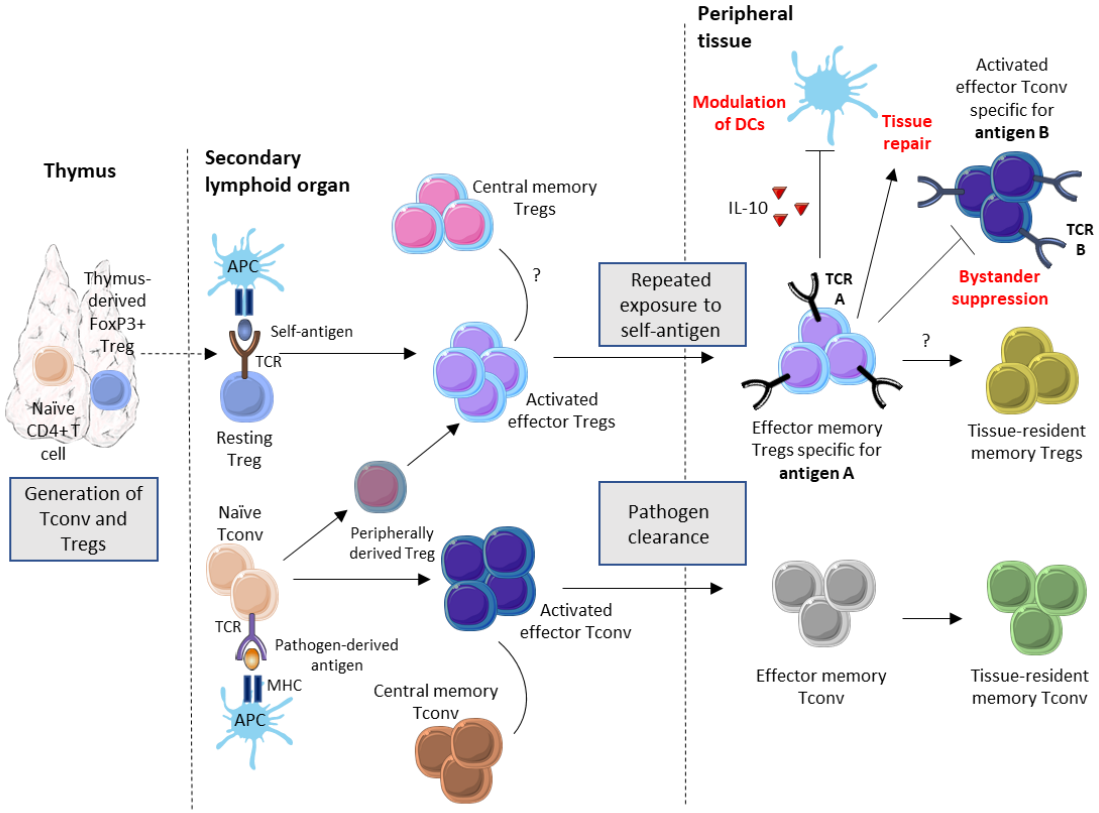



**Fig. 6.2 : Life cycle of regulatory and conventional CD4⁺ T cells.** Naïve conventional CD4⁺ T cells and regulatory T cells (Tregs) are generated in the thymus. Upon antigen-specific activation in secondary lymphoid organs, these populations give rise to conventional effector Tconv cells and 'effector' Tregs. Effector Tregs can arise from both thymus-derived and peripherally-derived Tregs. Central memory T cells are generated from a subset of activated conventional effector T cells and remain in secondary lymphoid organs. It is currently unknown whether central memory Tregs are generated. Effector memory cells are generated from a subset of both Tconv cells and Tregs. These cells migrate to antigen-expressing peripheral tissues where they stably reside (as tissue-resident memory T cells) or where they recirculate between blood and non-lymphoid tissues (as effector memory T cells). It is currently unknow whether the memory Treg populations that are found in peripheral tissues comprise tissue-resident memory Tregs, effector memory Tregs or both. Data arising from this thesis demonstrate that effector Tregs can mediate bystander suppression, inhibit maturation of dendritic cells in an IL-10-dependent manner, and be involved in tissue repair.

Figure adjusted from: Rosenblum, M. D., Way, S. S., & Abbas, A. K. (2016). Regulatory T cell memory. *Nature Reviews Immunology*, *16*(2), 90–101.

## 6.1 Future directions

- *In vitro* bystander suppression

Chapter 4 has introduced an *in vitro* system to study the mechanisms underpinning bystander suppression. Additional modifications of the system with the use of blocking/agonistic antibodies or knock-out mice will allow the assessment of suppressive cytokines (IL-10 and TGF-β), as well as co-inhibitory receptors (CTLA-4, PD-1, TIM-3, LAG-3,) in the ability of $MBP_{Ac1-9}$-specific T cells to suppress $MOG_{35-55}$-specific 2D2 T cells. Each of these co-inhibitory molecules could play a role in mediating cell contact-dependent bystander suppression (Anderson et al., 2016). Chapter 3 provided enough evidence on the role of TIGIT in immune regulation mediated by $CD4^+$ T cells; therefore, it will be interesting to investigate other co-inhibitory receptors either alone or in conjunction, to elucidate the different pathways that play a role in bystander suppression.

We have previously shown that peptide immunotherapy induces suppression of immune responses in clinical trials of therapy in ongoing disease, demonstrating that 4 peptides from MBP can suppress ongoing MS (Streeter et al., 2015). This implies that bystander suppressive mechanisms might be at play in that setting. Therefore, to test this hypothesis, it would be interesting to examine the capacity of regulatory T cells to suppress antigen-experienced (i.e., Th1 differentiated), effector 2D2 T cells to test whether bystander suppression can also regulate ongoing immune responses, in addition to naïve responses. Also, all the *in vitro* suppression assays were done with the separate $MBP_{Ac1-9}$ and $MOG_{35-55}$ peptides, so it would be interesting to repeat some of the bystander suppression assays using the linked peptide and compare the levels of suppression observed.

- Confocal imaging of peptide loaded (B10.PL x C57BL/6) F1 APCs with Tg4 regulatory T cells and 2D2 responder cells

It was shown with transwell assays that cell contact was required for CD4tol cells to mediate bystander suppression. We hypothesised that when both $MBP_{Ac1-9}$ and $MOG_{35-55}$ are presented on the same APC, responder and suppressor come in contact during antigen presentation. It will be intriguing to visualise the clustering of T cells around a central APC and compare the stimulation with the linked versus separate peptides.

- *In vivo* bystander suppression

In the adoptive co-transfers described in chapter 4, the population of putative suppressors that was used constituted total $CD4^+$ T cells from tolerised Tg4 mice and it was shown that they can mediate bystander suppression. It will be interesting to further build on that observation and co-transfer either tolerised $FoxP3^+$ Tregs or $FoxP3^-IL\text{-}10^+$ Tr1 cells together with 2D2 responder cells and test which one of the two populations is responsible for bystander suppression *in vivo*.

- Generation of a FoxP3/IL-10 double reporter mouse on Tg4 background and cell sorting of the cell populations

One of the main limitations of this study was the purity of the samples tested, since the purity of the enriched Treg population was approximately 85% using a positive selection kit. At the time of this study, there was only an IL-10 reporter available in the lab, while there was also a FoxP3 reporter in the past that was discontinued due to the impairment of FoxP3 induction on naïve peripheral Tregs because of the transgene (Verhagen et al., 2013a). The 'cleanest' way to study both Tregs and Tr1 cells in the same biological system would be to create a double reporter mouse for FoxP3 and IL-10 on the

Tg4 background. In this way, the isolation of pure FoxP3$^+$ Tregs and FoxP3$^-$IL-10$^+$ Tr1 cells would be possible.

For the isolation of FoxP3$^+$ Tregs, a cell sorting approach could be also used instead of an isolation kit to be able to utilise more surface markers for a more precise identification of these cells; however, we reasoned that the shear stress of the sorting and the long duration of the process would affect the cell viability and compromise the final yield of cell numbers. It was quite challenging to isolate adequate numbers of Tregs for the experiments, ofter having to combine spleens from sex- and age-matched Tg4 mice to achieve the desired number. Therefore, due to the practicalities arising from mice availability, we decided to move forward with enriching the cell populations with a positive selection kit, which resulted in satisfactory purity for what we wanted to study.

- Whole genome DNA methylation analysis

Chapter 5 covered the transcriptional profiling of the different regulatory populations. We were keen to take this a step forward and study the impact of peptide immunotherapy on the whole genome by studying the methylation status of the loci of genes that were found to be differentially expressed in our RNAseq datasets. The results from the methylation of the CNS2 region showed no effect of peptide immunotherapy on the FoxP3 genetic region, which was not surprising, since PBS- and 4Y-treated Tregs has similar levels of FoxP3 expression by flow cytometry analysis. However, we hypothesise that the regions of DEGs would display an altered epigenetic landscape associated with chromatin accessibility.

# REFERENCES


Abbas, A.K., Benoist, C., Bluestone, J.A., et al. (2013) Regulatory T cells: recommendations to simplify the nomenclature. *Nature Immunology*, 14 (4): 307–308.

Ahmadzadeh, M., Johnson, L.A., Heemskerk, B., et al. (2009) Tumor antigen-specific CD8 T cells infiltrating the tumor express high levels of PD-1 and are functionally impaired. *Blood*, 114 (8): 1537–1544.

Akbar, A.N., Vukmanovic-Stejic, M., Taams, L.S., et al. (2007) The dynamic co-evolution of memory and regulatory CD4+ T cells in the periphery. *Nature Reviews Immunology*, 7 (3): 231–237.

Akkaya, B., Oya, Y., Akkaya, M., et al. (2019) T regulatory cells mediate specific suppression by depleting peptide-MHC II from dendritic cells. *Nature Immunology*, 20 (2): 218–231.

Aldinucci, D., Borghese, C. and Casagrande, N. (2020) The CCL5/CCR5 Axis in Cancer Progression. *Cancers*, 12 (7): 1–30.

Aldinucci, D. and Casagrande, N. (2018) Inhibition of the CCL5/CCR5 Axis against the Progression of Gastric Cancer. *International Journal of Molecular Sciences*, 19 (5): 1477.

Ali, M.A., Liu, Y.F., Arif, S., et al. (2017) Metabolic and immune effects of immunotherapy with proinsulin peptide in human new-onset type 1 diabetes. *Science Translational Medicine*, 9 (402).

Allison, J.P. and Havran, W.L. (1991) The immunobiology of T cells with invariant gamma delta antigen receptors. *Annual Review of Immunology*, 9 (1): 679–705.

Allison, J.P. and Krummel, M.F. (1995) The Yin and Yang of T cell costimulation. *Science*, 270 (5238): 932–933.

Anderson, A.C., Joller, N. and Kuchroo, V.K. (2016a) Lag-3, Tim-3, and TIGIT: Co-inhibitory Receptors with Specialized Functions in Immune Regulation. *Immunity*, 44 (5): 989–1004.

Anderson, G., Owen, J.J.T., Moore, N.C., et al. (1994) Thymic epithelial cells provide unique signals for positive selection of CD4+CD8+ thymocytes in vitro. *The Journal of Experimental Medicine*, 179 (6): 2027–2031.

Anderson, G. and Takahama, Y. (2012) Thymic epithelial cells: working class heroes for T cell development and repertoire selection. *Trends in Immunology*, 33 (6): 256–263.

Anderson, P.O., Sundstedt, A., Yazici, Z., et al. (2005) IL-2 Overcomes the Unresponsiveness but Fails to Reverse the Regulatory Function of Antigen-Induced T Regulatory Cells. *The Journal of Immunology*, 174 (1): 310–319.

Andersson, J., Tran, D.Q., Pesu, M., et al. (2008) CD4 + FoxP3 + regulatory T cells confer infectious tolerance in a TGF-dependent manner. *Journal of Experimental Medicine*, 205 (9): 1975–1981.

Anderton, S.M., Viner, N.J., Matharu, P., et al. (2002) Influence of a dominant cryptic

epitope on autoimmune T cell tolerance. *Nature Immunology*, 3 (2): 175–181.

Anderton, S.M. and Wraith, D.C. (1998) Hierarchy in the ability of T cell epitopes to induce peripheral tolerance to antigens from myelin. *European Journal of Immunology*, 28 (4): 1251–1261.

Anderton, S.M. and Wraith, D.C. (2002) Selection and fine-tuning of the autoimmune T-cell repertoire. *Nature Reviews Immunology*, 2 (7): 487–498.

Apetoh, L., Quintana, F.J., Pot, C., et al. (2010) The aryl hydrocarbon receptor interacts with c-Maf to promote the differentiation of type 1 regulatory T cells induced by IL-27. *Nature Immunology*, 11 (9): 854–861.

Appelberg, R. (2007) Neutrophils and intracellular pathogens: beyond phagocytosis and killing. *Trends in Microbiology*, 15 (2): 87–92.

Arai, M., Fukuda, A., Morimoto, R., et al. (2022) Protocol to evaluate cell lineage stability of mouse natural and induced regulatory T cells using bisulfite sequencing. *STAR Protocols*, 3 (4): 101694.

Aran, D., Looney, A.P., Liu, L., et al. (2019) Reference-based analysis of lung single-cell sequencing reveals a transitional profibrotic macrophage. *Nature Immunology*, 20 (2): 163–172.

Arpaia, N., Green, J.A., Moltedo, B., et al. (2015) A Distinct Function of Regulatory T Cells in Tissue Protection. *Cell*, 162 (5): 1078–1089.

Arstila, T.P., Casrouge, A., Baron, V., et al. (1999) A direct estimate of the human alphabeta T cell receptor diversity. *Science*, 286 (5441): 958–961.

Ashouri, J.F. and Weiss, A. (2017) Endogenous Nur77 is a specific indicator of antigen receptor signaling in human T and B cells. *Journal of Immunology*, 198 (2): 657.

Bacher, C.P., Guggiari, M., Brors, B., et al. (2006) Transient colocalization of X-inactivation centres accompanies the initiation of X inactivation. *Nature Cell Biology*, 8 (3): 293–299.

Bannard, O., Kraman, M. and Fearon, D.T. (2009) Secondary replicative function of CD8+ T cells that had developed an effector phenotype. *Science*, 323 (5913): 505–509.

Banta, K.L., Xu, X., Chitre, A.S., et al. (2022) Mechanistic convergence of the TIGIT and PD-1 inhibitory pathways necessitates co-blockade to optimize anti-tumor CD8+ T cell responses. *Immunity*, 55 (3): 512–526.

Barrat, F.J., Cua, D.J., Boonstra, A., et al. (2002) In Vitro Generation of Interleukin 10–producing Regulatory CD4+ T Cells Is Induced by Immunosuppressive Drugs and Inhibited by T Helper Type 1 (Th1)– and Th2-inducing Cytokines. *The Journal of Experimental Medicine*, 195 (5): 603.

Barzaghi, F., Passerini, L., Gambineri, E., et al. (2012) Demethylation analysis of the FOXP3 locus shows quantitative defects of regulatory T cells in IPEX-like syndrome. *Journal of Autoimmunity*, 38 (1): 49–58.

Bashoura, K.T., Gondarenko, A., Chen, H., et al. (2014) CD28 and CD3 have

complementary roles in T-cell traction forces. *Proceedings of the National Academy of Sciences of the United States of America*, 111 (6): 2241–2246.

Bassing, C.H., Swat, W. and Alt, F.W. (2002) The mechanism and regulation of chromosomal V(D)J recombination. *Cell*, 109.

Bell, G.M., Anderson, A.E., Diboll, J., et al. (2017) Autologous tolerogenic dendritic cells for rheumatoid and inflammatory arthritis. *Annals of the Rheumatic Diseases*, 76 (1): 227–234.

Benham, H., Nel, H.J., Law, S.C., et al. (2015) Citrullinated peptide dendritic cell immunotherapy in HLA risk genotype-positive rheumatoid arthritis patients. *Science Translational Medicine*, 7 (290).

Berasain, C. and Avila, M.A. (2014) Amphiregulin. *Seminars in Cell & Developmental Biology*, 28: 31–41.

Bettelli, E., Pagany, M., Weiner, H.L., et al. (2003) Myelin oligodendrocyte glycoprotein-specific T cell receptor transgenic mice develop spontaneous autoimmune optic neuritis. *Journal of Experimental Medicine*, 197 (9): 1073–1081.

Bevington, S.L., Ng, S.T.H., Britton, G.J., et al. (2020) Chromatin Priming Renders T Cell Tolerance- Associated Genes Sensitive to Activation below the Signaling Threshold for Immune Response Genes. *Cell Reports*, 31 (10): 107748.

Bhattacharyya, S., Sen, P., Wallet, M., et al. (2004) Immunoregulation of dendritic cells by IL-10 is mediated through suppression of the PI3K/Akt pathway and of IκB kinase activity. *Blood*, 104 (4): 1100–1109.

Bluestone, J.A., Buckner, J.H., Fitch, M., et al. (2015) Type 1 diabetes immunotherapy using polyclonal regulatory T cells. *Science Translational Medicine*, 7 (315).

Blum, J.S., Wearsch, P.A. and Cresswell, P. (2013) Pathways of antigen processing. *Annual Review of Immunology*, 31: 443–473.

Borsellino, G., Kleinewietfeld, M., Mitri, D. Di, et al. (2007) Expression of ectonucleotidase CD39 by Foxp3 ♂ Treg cells : hydrolysis of extracellular ATP and immune suppression. *Blood*, 110 (4): 1225–1232.

Brockmann, L., Gagliani, N., Steglich, B., et al. (2017) IL-10 Receptor Signaling is essential for TR1 cell function in vivo. *Journal of Immunology*, 198 (3): 1130.

Brockmann, L., Soukou, S., Steglich, B., et al. (2018) Molecular and functional heterogeneity of IL-10-producing CD4+ T cells. *Nature Communications*, 9 (1): 1–14.

Brodin, P. and Davis, M.M. (2017) Human immune system variation. *Nature Reviews Immunology*, 17 (1): 21–29.

Brubaker, S.W., Bonham, K.S., Zanoni, I., et al. (2015) Innate immune pattern recognition: a cell biological perspective. *Annual Review of Immunology*, 33: 257–290.

Bullock, W.W., Katz, D.H. and Benacerraf, B. (1975) Induction of T-lymphocyte responses to a small molecular weight antigen. II. specific tolerance induced in azebenzenearsonate (ABA)-specific T cells in Guniea pigs by administration of low doses

of an ABA conjugate of chloroacetyl tyrosine in incomplete F. *The Journal of Experimental Medicine*, 142 (2): 261–274.

Burkhart, C., Liu, G.Y., Anderton, S.M., et al. (1999) Peptide-induced T cell regulation of experimental autoimmune encephalomyelitis: a role for IL-10. *International Immunology*, 11 (10): 1625–1634.

Burnet, F.M. (1959) *The clonal selection theory of acquired immunity*.

Burns, J., Rosenzweig, A., Zweiman, B., et al. (1983) Isolation of myelin basic protein-reactive T-cell lines from normal human blood. *Cellular Immunology*, 81 (2): 435–440.

Burton, B.R., Britton, G.J., Fang, H., et al. (2014) Sequential transcriptional changes dictate safe and effective antigen-specific immunotherapy. *Nature Communications*, 5: 1–13.

Campbell, J.D., Buckland, K.F., McMillan, S.J., et al. (2009) Peptide immunotherapy in allergic asthma generates IL-10-dependent immunological tolerance associated with linked epitope suppression. *The Journal of Experimental Medicine*, 206 (7): 1535–1547.

Cao, X., Cai, S.F., Fehniger, T.A., et al. (2007) Granzyme B and perforin are important for regulatory T cell-mediated suppression of tumor clearance. *Immunity*, 27 (4): 635–646.

Carambia, A., Freund, B., Schwinge, D., et al. (2015) Nanoparticle-based autoantigen delivery to Treg-inducing liver sinusoidal endothelial cells enables control of autoimmunity in mice. *Journal of Hepatology*, 62 (6): 1349–1356.

Castriconi, R., Dondero, A., Corrias, M.V., et al. (2004) Natural killer cell-mediated killing of freshly isolated neuroblastoma cells: critical role of DNAX accessory molecule-1-poliovirus receptor interaction. *Cancer Research*, 64 (24): 9180–9184.

Ceredig, R. and Rolink, T. (2002) A positive look at double-negative thymocytes. *Nature Reviews Immunology*, 2 (11): 888–897.

Chan, L.S., Vanderlugt, C.J., Hashimoto, T., et al. (1998) Epitope Spreading: Lessons From Autoimmune Skin Diseases. *Journal of Investigative Dermatology*, 110 (2): 103–109.

Chang, J.T., Wherry, E.J. and Goldrath, A.W. (2014) Molecular regulation of effector and memory T cell differentiation. *Nature Immunology*, 15 (12): 1104–1115.

Chang, X., Gao, J.X., Jiang, Q., et al. (2005) The Scurfy mutation of FoxP3 in the thymus stroma leads to defective thymopoiesis. *The Journal of Experimental Medicine*, 202 (8): 1141.

Chataway, J., Martin, K., Barrell, K., et al. (2018) Effects of ATX-MS-1467 immunotherapy over 16 weeks in relapsing multiple sclerosis. *Neurology*, 90 (11).

Chaudhary, B. and Elkord, E. (2016) Regulatory T Cells in the Tumor Microenvironment and Cancer Progression: Role and Therapeutic Targeting. *Vaccines*, 4 (3).

Chaudhry, A. and Rudensky, A.Y. (2013) Control of inflammation by integration of environmental cues by regulatory T cells. *The Journal of Clinical Investigation*, 123 (3):

939–944.

Chauvin, J.M., Pagliano, O., Fourcade, J., et al. (2015) TIGIT and PD-1 impair tumor antigen-specific $CD8^+$ T cells in melanoma patients. *The Journal of Clinical Investigation*, 125 (5): 2046–2058.

Chen, L. and Flies, D.B. (2013) Molecular mechanisms of T cell co-stimulation and co-inhibition. *Nature Reviews Immunology*, 13 (4): 227–242.

Chen, W.J., Jin, W., Hardegen, N., et al. (2003) Conversion of peripheral CD4+CD25- naive T cells to CD4+CD25+ regulatory T cells by TGF-beta induction of transcription factor Foxp3. *The Journal of Experimental Medicine*, 198 (12): 1875–1886.

Chen, X., Lu, P.H., Liu, L., et al. (2016) TIGIT negatively regulates inflammation by altering macrophage phenotype. *Immunobiology*, 221 (1): 48–55.

Chen, Y., Kuchroo, V.K., Inobe, J.I., et al. (1994) Regulatory T cell clones induced by oral tolerance: suppression of autoimmune encephalomyelitis. *Science*, 265 (5176): 1237–1240.

Cherukuri, A., Mohib, K. and Rothstein, D.M. (2021) Regulatory B cells: TIM-1, transplant tolerance, and rejection. *Immunological Reviews*, 299 (1): 31–44.

Chihara, N., Madi, A., Karwacz, K., et al. (2016) Differentiation and Characterization of Tr1 Cells. *Current protocols in immunology*, 113.

Chihara, N., Madi, A., Kondo, T., et al. (2018) Induction and transcriptional regulation of the co-inhibitory gene module in T cells. *Nature*, 558 (7710): 454–459.

Chinen, T., Kannan, A.K., Levine, A.G., et al. (2016) An essential role for the IL-2 receptor in Treg cell function. *Nature Immunology*, 17 (11): 1322–1333.

Clemente-Casares, X., Blanco, J., Ambalavanan, P., et al. (2016) Expanding antigen-specific regulatory networks to treat autoimmunity. *Nature*, 530 (7591): 434–440.

Collison, L.W., Workman, C.J., Kuo, T.T., et al. (2008) The inhibitory cytokine IL-35 contributes to regulatory T-cell function. *Nature Letters*, 450.

Cooper, M.D. and Alder, M.N. (2006) The evolution of adaptive immune systems. *Cell*, 124 (4): 815–822.

Cowan, J.E., Parnell, S.M., Nakamura, K., et al. (2013) The thymic medulla is required for Foxp3+ regulatory but not conventional CD4+ thymocyte development. *The Journal of Experimental Medicine*, 210 (4): 675–681.

Cretney, E., Kallies, A. and Nutt, S.L. (2013) Differentiation and function of Foxp3 + effector regulatory T cells. *Trends in Immunology*, 34 (2): 74–80.

Cretney, E., Xin, A., Shi, W., et al. (2011) The transcription factors Blimp-1 and IRF4 jointly control the differentiation and function of effector regulatory T cells. *Nature Immunology*, 12 (4): 304–312.

Cusick, M.F., Libbey, J.E. and Fujinami, R.S. (2012) Molecular Mimicry as a Mechanism of Autoimmune Disease. *Clinical Reviews in Allergy & Immunology*, 42 (1): 102.

Cutolo, M., Sulli, A., Capellino, S., et al. (2004) Sex hormones influence on the immune system: Basic and clinical aspects in autoimmunity. *Lupus*, 13 (9): 635–638.

Dai, S., Zeng, H., Liu, Z., et al. (2021) Intratumoral CXCL13+CD8+T cell infiltration determines poor clinical outcomes and immunoevasive contexture in patients with clear cell renal cell carcinoma. *Journal for Immunotherapy of Cancer*, 9 (2).

Delves, P.J. and Roitt, I.M. (2000) The immune system. First of two parts Mackay, I.R. and Rosen, F.S. (eds.). *The New England Journal of Medicine*, 343 (1): 37–49.

Deng, C., Chen, Y., Li, W., et al. (2020) Alteration of CD226/TIGIT immune checkpoint on T cells in the pathogenesis of primary Sjögren's syndrome. *Journal of Autoimmunity*, 113.

Dengjel, J., Schoor, O., Fischer, R., et al. (2005) Autophagy promotes MHC class II presentation of peptides from intracellular source proteins. *Proceedings of the National Academy of Sciences of the United States of America*, 102 (22): 7922–7927.

Derbinski, J., Schulte, A., Kyewski, B., et al. (2001) Promiscuous gene expression in medullary thymic epithelial cells mirrors the peripheral self. *Nature Immunology*, 2 (11): 2915–2922.

Dias, S., D'Amico, A., Cretney, E., et al. (2017) Effector Regulatory T Cell Differentiation and Immune Homeostasis Depend on the Transcription Factor Myb. *Immunity*, 46 (1): 78–91.

Dixon, K.O., Schorer, M., Nevin, J., et al. (2018) Functional Anti-TIGIT Antibodies Regulate Development of Autoimmunity and Antitumor Immunity. *The Journal of Immunology*, 200 (8): 3000–3007.

Dobaczewski, M., Xia, Y., Bujak, M., et al. (2010) CCR5 signaling suppresses inflammation and reduces adverse remodeling of the infarcted heart, mediating recruitment of regulatory T cells. *The American Journal of Pathology*, 176 (5): 2177–2187.

Dong, S., Hiam-Galvez, K.J., Mowery, C.T., et al. (2021) The effect of low-dose IL-2 and Treg adoptive cell therapy in patients with type 1 diabetes. *JCI insight*, 6 (18).

Dougall, W.C., Kurtulus, S., Smyth, M.J., et al. (2017) TIGIT and CD96: new checkpoint receptor targets for cancer immunotherapy. *Immunological Reviews*, 276 (1): 112–120.

Ean -F Rançois, J. and Ach, B. (2002) The effect of infections on susceptibility to autoimmune and allergic diseases. *The New England Journal of Medicine*, 347 (12): 911–920.

Ellis, A.K., Frankish, C.W., O'Hehir, R.E., et al. (2017) Treatment with grass allergen peptides improves symptoms of grass pollen-induced allergic rhinoconjunctivitis. *The Journal of Allergy and Clinical Immunology*, 140 (2): 486–496.

Esensten, J.H., Helou, Y.A., Chopra, G., et al. (2016) CD28 Costimulation: From Mechanism to Therapy. *Immunity*, 44 (5): 973–988.

Estrada Brull, A., Panetti, C. and Joller, N. (2022) Moving to the Outskirts: Interplay Between Regulatory T Cells and Peripheral Tissues. *Frontiers in Immunology*, 13.

Fathman, C.G. and Lineberry, N.B. (2007) Molecular mechanisms of CD4+ T-cell anergy. *Nature Reviews Immunology*, 7 (8): 599–609.

Feng, X., Zhang, L., Acharya, C., et al. (2017) Targeting CD38 suppresses induction and function of T regulatory cells to mitigate immunosuppression in multiple myeloma. *Clinical Cancer Research*, 23 (15): 4290.

Fife, B.T. and Bluestone, J.A. (2008) Control of peripheral T-cell tolerance and autoimmunity via the CTLA-4 and PD-1 pathways. *Immunological Reviews*, 224 (1): 166–182.

Finak, G., McDavid, A., Yajima, M., et al. (2015) MAST: A flexible statistical framework for assessing transcriptional changes and characterizing heterogeneity in single-cell RNA sequencing data. *Genome Biology*, 16 (1): 1–13.

Fischer, S. and Deindl, E. (2022) State of the Art of Innate Immunity—An Overview. *Cells*, 11 (17): 2705.

Flajnik, M.F. and Kasahara, M. (2001) Comparative genomics of the MHC: glimpses into the evolution of the adaptive immune system. *Immunity*, 15 (3): 351–362.

Flajnik, M.F. and Kasahara, M. (2010) Origin and evolution of the adaptive immune system: genetic events and selective pressures. *Nature Reviews Genetics*, 11 (1): 47–59.

Floess, S., Freyer, J., Siewert, C., et al. (2007) Epigenetic control of the foxp3 locus in regulatory T cells. *PLoS biology*, 5 (2): 0169–0178. Available at: https://pubmed.ncbi.nlm.nih.gov/17298177/ (Accessed: 28 November 2022).

Florou, D., Katsara, M., Feehan, J., et al. (2020) Anti-CD20 Agents for Multiple Sclerosis: Spotlight on Ocrelizumab and Ofatumumab. *Brain Sciences*, 10 (10): 1–13.

Fontenot, J.D., Dooley, J.L., Farr, A.G., et al. (2005) Developmental regulation of Foxp3 expression during ontogeny. *The Journal of Experimental Medicine*, 202 (7): 901–906.

Fontenot, J.D., Gavin, M.A. and Rudensky, A.Y. (2003) Foxp3 programs the development and function of CD4 + CD25 + regulatory T cells. *Nature Publishing Group*, 4 (4).

Förster, R., Davalos-Misslitz, A.C. and Rot, A. (2008) CCR7 and its ligands: balancing immunity and tolerance. *Nature Reviews Immunology*, 8 (5): 362–371.

Friedline, R.H., Brown, D.S., Nguyen, H., et al. (2009) CD4+ regulatory T cells require CTLA-4 for the maintenance of systemic tolerance. *The Journal of Experimental Medicine*, 206 (2): 421.

Fuertes Marraco, S.A., Neubert, N.J., Verdeil, G., et al. (2015) Inhibitory Receptors Beyond T Cell Exhaustion. *Frontiers in Immunology*, 6.

Fuhrman, C.A., Yeh, W.-I., Seay, H.R., et al. (2015) Divergent Phenotypes of Human Regulatory T Cells Expressing the Receptors TIGIT and CD226. *The Journal of Immunology*, 195 (1): 145–155.

Fujinami, R.S., Oldstone, M.B.A., Wroblewska, Z., et al. (1983) Molecular mimicry in virus infection: crossreaction of measles virus phosphoprotein or of herpes simplex virus

protein with human intermediate filaments. *Proceedings of the National Academy of Sciences of the United States of America*, 80 (8): 2346–2350.

Fuschiotti, P., Pasqual, N., Hierle, V., et al. (2007) Analysis of the TCR α-chain rearrangement profile in human T lymphocytes. *Molecular Immunology*, 44 (13): 3380–3388.

Gabryšová, L., Alvarez-Martinez, M., Luisier, R., et al. (2018) c-Maf controls immune responses by regulating disease-specific gene networks and repressing IL-2 in CD4+ T cells. *Nature Immunology*, 19 (5): 497.

Gabrysova, L., Nicolson, K.S., Streeter, H.B., et al. (2009) Negative feedback control of the autoimmune response through antigen-induced differentiation of IL-10–secreting Th1 cells. *Journal of Experimental Medicine*, 206 (8): 1755–1767.

Gabryšová, L., Nicolson, K.S., Streeter, H.B., et al. (2009) Negative feedback control of the autoimmune response through antigen-induced differentiation of IL-10-secreting Th1 cells. *Journal of Experimental Medicine*, 206 (8): 1755–1767.

Gabryšová, L. and Wraith, D.C. (2010) Antigenic strength controls the generation of antigen-specific IL-10-secreting T regulatory cells. *European Journal of Immunology*, 40 (5): 1386–1395.

Gagliani, N., Magnani, C.F., Huber, S., et al. (2013) Coexpression of CD49b and LAG-3 identifies human and mouse T regulatory type 1 cells. *Nature Medicine*, 19 (6): 739–746.

Gasteiger, G. and Rudensky, A.Y. (2014) Interactions between innate and adaptive lymphocytes. *Nature Reviews Immunology*, 14 (9): 631–639.

Ge, S.X., Son, E.W. and Yao, R. (2018) iDEP: An integrated web application for differential expression and pathway analysis of RNA-Seq data. *BMC Bioinformatics*, 19 (1): 1–24.

Ge, Z., Peppelenbosch, M.P., Sprengers, D., et al. (2021) TIGIT, the Next Step Towards Successful Combination Immune Checkpoint Therapy in Cancer. *Frontiers in Immunology*, 12.

Germain, R.N. (2002) T cell development and the CD4-CD8 lineage decision. *Nature Reviews Immunology*, 2 (5): 309–322.

Goel, G., King, T., Daveson, A.J., et al. (2017) Epitope-specific immunotherapy targeting CD4-positive T cells in coeliac disease: two randomised, double-blind, placebo-controlled phase 1 studies. *The Lancet. Gastroenterology & hepatology*, 2 (7): 479–493.

Goldman, K.P., Park, C.S., Kim, M., et al. (2005) Thymic cortical epithelium induces self tolerance. *European Journal of Immunology*, 35 (3): 709–717.

Goodnow, C.C., Sprent, J., Barbara, B.F., et al. (2005) Cellular and genetic mechanisms of self tolerance and autoimmunity. *Nature*, 435 (7042): 590–597.

Gratz, I.K., Rosenblum, M.D. and Abbas, A.K. (2013) The life of regulatory T cells. *Annals of the New York Academy of Sciences*, 1283 (1): 8–12.

Greisen, S.R., Yan, Y., Hansen, A.S., et al. (2017) Extracellular vesicles transfer the receptor programmed death-1 in rheumatoid arthritis. *Frontiers in Immunology*, 8 (JUL).

Grimm, J.B., English, B.P., Chen, J., et al. (2015) A general method to improve fluorophores for live-cell and single-molecule microscopy. *Nature Methods*, 12 (3): 244–250.

Groux, H., O'Garra, A., Bigler, M., et al. (1997) A CD4+ T-cell subset inhibits antigen-specific T-cell responses and prevents colitis. *Nature*, 389 (6652): 737–742.

Hajiasghar-Sharbaf, R., Asgarian-Omran, H., Valadan, R., et al. (2021) CD8+ T-cells Co-expressing PD-1 and TIGIT Are Highly Frequent in Chronic Lymphocytic Leukemia. *Iranian Journal of Allergy, Asthma, and Immunology*, 20 (6): 751–763.

Hao, Y., Hao, S., Andersen-Nissen, E., et al. (2021) Integrated analysis of multimodal single-cell data. *Cell*, 184 (13): 3573-3587.e29.

Harada, Y., Harada, Y., Elly, C., et al. (2010) Transcription factors Foxo3a and Foxo1 couple the E3 ligase Cbl-b to the induction of Foxp3 expression in induced regulatory T cells. *The Journal of Experimental Medicine*, 207 (7): 1381.

Harjunpää, H. and Guillerey, C. (2019) TIGIT as an emerging immune checkpoint. *Clinical and Experimental Immunology*, pp. 0–2.

Harrington, L.E., Hatton, R.D., Mangan, P.R., et al. (2005) Interleukin 17-producing CD4+ effector T cells develop via a lineage distinct from the T helper type 1 and 2 lineages. *Nature Immunology*, 6 (11): 1123–1132.

Harry, R.A., Anderson, A.E., Isaacs, J.D., et al. (2010) Generation and characterisation of therapeutic tolerogenic dendritic cells for rheumatoid arthritis. *Annals of the Rheumatic Diseases*, 69 (11): 2042–2050.

Hawker, K., O'Connor, P., Freedman, M.S., et al. (2009) Rituximab in patients with primary progressive multiple sclerosis: results of a randomized double-blind placebo-controlled multicenter trial. *Annals of Neurology*, 66 (4): 460–471.

Hayatsu, N., Miyao, T., Tachibana, M., et al. (2017) Analyses of a Mutant Foxp3 Allele Reveal BATF as a Critical Transcription Factor in the Differentiation and Accumulation of Tissue Regulatory T Cells. *Immunity*, 47 (2): 268–283.

Heath, V.L., Moore, N.C., Parnell, S.M., et al. (1998) Intrathymic expression of genes involved in organ specific autoimmune disease. *Journal of Autoimmunity*, 11 (4): 309–318.

Herold, K.C., Gitelman, S.E., Ehlers, M.R., et al. (2013) Teplizumab (Anti-CD3 mAb) Treatment Preserves C-Peptide Responses in Patients With New-Onset Type 1 Diabetes in a Randomized Controlled TrialMetabolic and Immunologic Features at Baseline Identify a Subgroup of Responders. *Diabetes*, 62 (11): 3766–3774.

Heufler, C., Koch, F., Stanzl, U., et al. (1996) Interleukin-12 is produced by dendritic cells and mediates T helper 1 development as well as interferon-gamma production by T helper 1 cells. *European Journal of Immunology*, 26 (3): 659–668.

Heymann, F., Peusquens, J., Ludwig-Portugall, I., et al. (2015) Liver Inflammation

Abrogates Immunological Tolerance Induced by Kupffer Cells. *Hepatology*, 62 (1): 279–291.

Höfer, T., Krichevsky, O. and Altan-Bonnet, G. (2012) Competition for IL-2 between Regulatory and Effector T Cells to Chisel Immune Responses. *Frontiers in Immunology*, 3.

Holder, K.A. and Grant, M.D. (2020) TIGIT Blockade: A Multipronged Approach to Target the HIV Reservoir. *Frontiers in Cellular and Infection Microbiology*, 10: 175.

Homann, D., Holz, A., Bot, A., et al. (1999) Autoreactive CD4+ T cells protect from autoimmune diabetes via bystander suppression using the IL-4/Stat6 pathway. *Immunity*, 11 (4): 463–472.

Hori, S. (2014) Lineage stability and phenotypic plasticity of $Foxp3^{+}$ regulatory T cells. *Immunological Reviews*, 259 (1): 159–172.

Hori, S., Nomura, T. and Sakaguchi, S. (2003) Control of Regulatory T Cell Development by the Transcription Factor Foxp3. *Science*, 299: 1057–1062.

Hoyne, G.F., Dallman, M.J. and Lamb, J.R. (1999) Linked Suppression in Peripheral T Cell Tolerance to the House Dust Mite Derived Allergen Der p 1. *International Archives of Allergy and Immunology*, 118 (2–4): 122–124.

Hoyne, G.F., O'hehir, R.E., Wraith, D.C., et al. (1993) Inhibition of T cell and antibody responses to house dust mite allergen by inhalation of the dominant T cell epitope in naive and sensitized mice. *The Journal of Experimental Medicine*, 178 (5): 1783–1788.

Hsieh, C.S., Lee, H.M. and Lio, C.W.J. (2012) Selection of regulatory T cells in the thymus. *Nature Reviews Immunology*, 12 (3): 157–167.

Huang, W. and August, A. (2015) The signaling symphony: T cell receptor tunes cytokine-mediated T cell differentiation. *Journal of Leukocyte Biology*, 97 (3): 477–485.

Hung, A.L., Maxwell, R., Theodros, D., et al. (2018) TIGIT and PD-1 dual checkpoint blockade enhances antitumor immunity and survival in GBM. *Oncoimmunology*, 7 (8).

Hwang, B., Lee, J.H. and Bang, D. (2018) Single-cell RNA sequencing technologies and bioinformatics pipelines. *Experimental & Molecular Medicine*, 50 (8): 1–14.

Hwang, J.R., Byeon, Y., Kim, D., et al. (2020) Recent insights of T cell receptor-mediated signaling pathways for T cell activation and development. *Experimental & Molecular Medicine*, 52 (5): 750–761.

Inglesfield, S., Cosway, E.J., Jenkinson, W.E., et al. (2019) Rethinking Thymic Tolerance: Lessons from Mice. *Trends in Immunology*, 40 (4): 279–291.

Ito, T., Hanabuchi, S., Wang, Y.H., et al. (2008) Two functional subsets of FOXP3+ regulatory T cells in human thymus and periphery. *Immunity*, 28 (6): 870–880.

Ivanov, I.I., McKenzie, B.S., Zhou, L., et al. (2006) The orphan nuclear receptor RORgammat directs the differentiation program of proinflammatory IL-17+ T helper cells. *Cell*, 126 (6): 1121–1133.

Iwasaki, A. and Medzhitov, R. (2010) Regulation of adaptive immunity by the innate

immune system. *Science*, 327 (5963): 291–295.

Iwasaki, Y., Fujio, K., Okamura, T., et al. (2013) Egr-2 transcription factor is required for Blimp-1- mediated IL-10 production in IL-27-stimulated CD4 + T cells. *European Journal of Immunology*, 43: 1063–1073.

Jacobson, D.L., Gange, S.J., Rose, N.R., et al. (1997) Epidemiology and estimated population burden of selected autoimmune diseases in the United States. *Clinical Immunology and Immunopathology*, 84 (3): 223–243.

Jansson, L., Vrolix, K., Jahraus, A., et al. (2018) Immunotherapy With Apitopes Blocks the Immune Response to TSH Receptor in HLA-DR Transgenic Mice. *Endocrinology*, 159 (9): 3446–3457.

Johnston, R.J., Comps-Agrar, L., Hackney, J., et al. (2014) The immunoreceptor TIGIT regulates antitumor and antiviral CD8(+) T cell effector function. *Cancer Cell*, 26 (6): 923–937.

Joller, N., Hafler, J.P., Brynedal, B., et al. (2011) Cutting edge: TIGIT has T cell-intrinsic inhibitory functions. *Journal of Immunology*, 186 (3): 1338–1342.

Joller, N. and Kuchroo, V.K. (2017) Tim-3, Lag-3, and TIGIT. *Curr Top Microbiol Immunol*, 410: 127–156.

Joller, N., Lozano, E., Burkett, P.R., et al. (2014) Treg cells expressing the co-inhibitory molecule TIGIT selectively inhibit pro-inflammatory Th1 and Th17 cell responses. *Immunity*, 40 (4): 569.

Jollife, I.T. and Cadima, J. (2016) Principal component analysis: a review and recent developments. *Philosophical Transactions of the Royal Society A: Mathematical, Physical and Engineering Sciences*, 374 (2065).

Josefowicz, S.Z., Lu, L.F. and Rudensky, A.Y. (2012) Regulatory T cells: mechanisms of differentiation and function. *Annual Review of Immunology*, 30: 531–564.

Josefsson, S.E., Huse, K., Kolstad, A., et al. (2018) T Cells Expressing Checkpoint Receptor TIGIT Are Enriched in Follicular Lymphoma Tumors and Characterized by Reversible Suppression of T-cell Receptor Signaling. *Clinical Cancer Research*, 24 (4): 870–881.

Jung, D. and Alt, F.W. (2004) Unraveling V(D)J Recombination: Insights into Gene Regulation. *Cell*, 116 (2): 299–311.

Kaiko, G.E., Horvat, J.C., Beagley, K.W., et al. (2008) Immunological decision-making: how does the immune system decide to mount a helper T-cell response? *Immunology*, 123 (3): 326–338.

Kane, L.P., Andres, P.G., Howland, K.C., et al. (2001) Akt provides the CD28 costimulatory signal for up-regulation of IL-2 and IFN-gamma but not TH2 cytokines. *Nature Immunology*, 2 (1): 37–44.

Kappler, J.W., Roehm, N. and Marrack, P. (1987) T cell tolerance by clonal elimination in the thymus. *Cell*, 49 (2): 273–280.

Kappos, L., Li, D., Calabresi, P.A., et al. (2011) Ocrelizumab in relapsing-remitting multiple sclerosis: a phase 2, randomised, placebo-controlled, multicentre trial. *Lancet*, 378 (9805): 1779–1787.

Ke, Q., Kroger, C.J., Clark, M., et al. (2021) Evolving Antibody Therapies for the Treatment of Type 1 Diabetes. *Frontiers in Immunology*, 11: 3949.

Kendal, A.R. and Waldmann, H. (2010) Infectious tolerance: therapeutic potential. *Current opinion in Immunology*, 22 (5): 560–565.

Keşmir, C., Borghans, J.A.M. and de Boer, R.J. (2000) Diversity of Human αβ T Cell Receptors. *Science*, 288 (5469): 1135–1135.

Khattri, R., Cox, T., Yasayko, S., et al. (2003) An essential role for Scurfin in CD4 + CD25 + T regulatory cells. *Nature Immunology*, 4 (4): 337–342.

Kim, H.S., Sohn, H., Jang, S.W., et al. (2019) The transcription factor NFIL3 controls regulatory T-cell function and stability. *Experimental & Molecular Medicine*, 51 (7).

Klein, L., Hinterberger, M., Wirnsberger, G., et al. (2009) Antigen presentation in the thymus for positive selection and central tolerance induction. *Nature Reviews Immunology*, 9 (12): 833–844. Available at: http://dx.doi.org/10.1038/nri2669.

Klein, L., Robey, E.A. and Hsieh, C.S. (2019) Central CD4+ T cell tolerance: deletion versus regulatory T cell differentiation. *Nature Reviews Immunology*, 19 (1): 7–18. Available at: https://pubmed.ncbi.nlm.nih.gov/30420705/ (Accessed: 8 October 2022).

Klunk, J., Vilgalys, T.P., Demeure, C.E., et al. (2022) Evolution of immune genes is associated with the Black Death. *Nature*, pp. 1–8.

Koch, M.A., Tucker-heard, G., Perdue, N.R., et al. (2009) The transcription factor T-bet controls regulatory T cell homeostasis and function during type 1 inflammation. *Nature immunology*, 10 (6).

Koizumi, S. ichi, Sasaki, D., Hsieh, T.H., et al. (2018) JunB regulates homeostasis and suppressive functions of effector regulatory T cells. *Nature Communications*, 9 (1): 1–14.

Krummel, M.F. and Allison, J.P. (1995) CD28 and CTLA-4 have opposing effects on the response of T cells to stimulation. *The Journal of Experimental Medicine*, 182 (2): 459–465.

Kunicki, M.A., Amaya Hernandez, L.C., Davis, K.L., et al. (2018) Identity and Diversity of Human Peripheral Th and T Regulatory Cells Defined by Single-Cell Mass Cytometry. *Journal of iImmunology*, 200 (1): 336–346.

Kurd, N. and Robey, E.A. (2016) T cell selection in the thymus: a spatial and temporal perspective. *Immunological Reviews*, 271 (1): 114.

Kurtulus, S., Sakuishi, K., Ngiow, S.F., et al. (2015) TIGIT predominantly regulates the immune response via regulatory T cells. *Journal of Clinical Investigation*, 125 (11): 4053–4062.

Kwon, H., Jun, H.-S., Khil, L.-Y., et al. (2004) Role of CTLA-4 in the activation of single-

and double-positive thymocytes. *Journal of Immunology*, 173 (11): 6645–6653.

Lerner, A., Jeremias, P. and Matthias, T. (2015) The World Incidence and Prevalence of Autoimmune Diseases is Increasing. *International Journal of Celiac Disease*, 3 (4): 151–155.

Levine, A.G., Arvey, A., Jin, W., et al. (2014) Continuous requirement for the TCR in regulatory T cell function. *Nature Immunology*, 15 (11): 1070–1078.

Levine, A.G., Mendoza, A., Hemmers, S., et al. (2017) Stability and function of regulatory T cells. *Nature Publishing Group*.

Levings, B.M.K., Sangregorio, R. and Roncarolo, M. (2001) Human CD25+CD4+ T Regulatory Cells Suppress Naive and Memory T Cell Proliferation and Can Be Expanded In Vitro without Loss of Function. *Journal of Experimental Medicine*, 193 (11): 1295–1301.

Levitsky, J., Miller, J., Wang, E., et al. (2009) Immunoregulatory profiles in liver transplant recipients on different immunosuppressive agents. *Human Immunology*, 70 (3): 146–150.

Li, M.O. and Rudensky, A.Y. (2016) T cell receptor signalling in the control of regulatory T cell differentiation and function. *Nature Reviews Immunology*, 16 (4): 220–233.

Li, W., Deng, C., Yang, H., et al. (2021) Expansion of circulating peripheral TIGIT+CD226+ CD4 T cells with enhanced effector functions in dermatomyositis. *Arthritis Research and Therapy*, 23 (1): 1–12.

Li, X. and Zheng, Y. (2015) Regulatory T cell identity: formation and maintenance. *Trends in Immunology*, 36 (6): 344–353.

Linsley, P.S., Brady, W., Urnes, M., et al. (1991) CTLA-4 is a second receptor for the B cell activation antigen B7. *The Journal of Experimental Medicine*, 174 (3): 561–569.

Lio, C.W.J. and Hsieh, C.S. (2008) A two-step process for thymic regulatory T cell development. *Immunity*, 28 (1): 100–111.

Lissy, N.A., Van Dyk, L.F., Becker-Hapak, M., et al. (1998) TCR antigen-induced cell death occurs from a late G1 phase cell cycle check point. *Immunity*, 8 (1): 57–65.

Liston, A. and Gray, D.H.D. (2014) Homeostatic control of regulatory T cell diversity. *Nature Reviews Immunology*, 14 (3): 154–165.

Liston, A. and Piccirillo, C.A. (2013) Developmental plasticity of murine and human Foxp3(+) regulatory T cells. *Advances in Immunology*, 119: 85–106.

Liu, G.Y., Fairchild, P.J., Smith, R.M., et al. (1995) Low avidity recognition of self-antigen by T cells permits escape from central tolerance. *Immunity*, 3 (4): 407–415.

Liu, G.Y. and Wraith, D.C. (1995) Affinity for class II MHC determines the extent to which soluble peptides tolerize autoreactive T cells in naive and primed adult mice—implications for autoimmunity. *International Immunology*, 7 (8): 1255–1263.

Liu, S., Zhang, H., Li, M., et al. (2013) Recruitment of Grb2 and SHIP1 by the ITT-like motif of TIGIT suppresses granule polarization and cytotoxicity of NK cells. *Cell Death*

*and Differentiation*, 20 (3): 456–464.

Liu, X., Li, M., Wang, X., et al. (2019) PD-1+ TIGIT+ CD8+ T cells are associated with pathogenesis and progression of patients with hepatitis B virus-related hepatocellular carcinoma. *Cancer Immunology, Immunotherapy*, 68 (12): 2041–2054.

Loblay, R.H., Pritchard-Briscoe, H. and Basten, A. (1978) Suppressor T-cell memory. *Nature*, 272 (5654): 620–622.

Loda, A., Collombet, S. and Heard, E. (2022) Gene regulation in time and space during X-chromosome inactivation. *Nature Reviews Molecular Cell Biology*, 23 (4): 231–249.

Löhning, M., Hutloff, A., Kallinich, T., et al. (2003) Expression of ICOS in vivo defines CD4+ effector T cells with high inflammatory potential and a strong bias for secretion of interleukin 10. *The Journal of Experimental Medicine*, 197 (2): 181–193.

Love, M.I., Huber, W. and Anders, S. (2014) Moderated estimation of fold change and dispersion for RNA-seq data with DESeq2. *Genome Biology*, 15 (12): 1–21.

Lozano, E., Dominguez-Villar, M., Kuchroo, V., et al. (2012) The TIGIT/CD226 axis regulates human T cell function. *Journal of Immunology*, 188 (8): 3869.

Lucca, L.E., Axisa, P.P., Singer, E.R., et al. (2019) TIGIT signaling restores suppressor function of Th1 Tregs. *JCI Insight*, 4 (3).

Lucca, L.E. and Dominguez-Villar, M. (2020) Modulation of regulatory T cell function and stability by co-inhibitory receptors. *Nature Reviews Immunology*, 20 (11): 680–693.

Luo, C.T., Liao, W., Dadi, S., et al. (2016) Graded Foxo1 activity in Treg cells differentiates tumour immunity from spontaneous autoimmunity. *Nature*, 529 (7587): 532–536.

Luo, Q., Li, X., Fu, B., et al. (2018) Decreased expression of TIGIT in NK cells correlates negatively with disease activity in systemic lupus erythematosus. *International Journal of Clinical and Experimental Pathology*, 11 (5): 2408.

Luo, Q., Ye, J., Zeng, L., et al. (2017) Elevated expression of TIGIT on CD3+CD4+ T cells correlates with disease activity in systemic lupus erythematosus. *Allergy, Asthma and Clinical Immunology*, 13 (1): 1–12.

MacLeod, C.M., Gopie, N., Hourihan, K.L., et al. (2010) The production effect: delineation of a phenomenon. *Journal of Experimental Psychology*, 36 (3): 671–685.

Malek, T.R. and Castro, I. (2010) Interleukin-2 Receptor Signaling: At the Interface between Tolerance and Immunity. *Immunity*, 33 (2): 153.

Mantovani, A. and Garlanda, C. (2023) Humoral Innate Immunity and Acute-Phase Proteins. *The New England Journal of Medicine*, 388 (5): 439–452.

Marrack, P., Scott-Browne, J.P., Dai, S., et al. (2008) Evolutionarily Conserved Amino Acids That Control TCR-MHC Interaction. *Annual Review of Immunology*, 26: 171–203.

Martin, E., Capini, C., Duggan, E., et al. (2007) Antigen-specific suppression of established arthritis in mice by dendritic cells deficient in NF-kappaB. *Arthritis and Rheumatism*, 56 (7): 2255–2266.

Masson, D., Jarry, A., Baury, B., et al. (2001) Overexpression of the CD155 gene in human colorectal carcinoma. *Gut*, 49 (2): 236–240.

Matzinger, P. and Guerder, S. (1989) Does T-cell tolerance require a dedicated antigen-presenting cell? *Nature*, 338 (6210): 74–76.

Maynard, C.L., Harrington, L.E., Janowski, K.M., et al. (2007) Regulatory T cells expressing interleukin 10 develop from Foxp3+ and Foxp3− precursor cells in the absence of interleukin 10. *Nature Immunology*, 8 (9): 931–941.

Mazza, G., Ponsford, M., Lowrey, P., et al. (2002) Diversity and dynamics of the T-cell response to MBP in DR2+ve individuals. *Clinical and Experimental Immunology*, 128 (3): 538.

Metzler, B., Anderton, S.M., Manickasingham, S.P., et al. (2000) Kinetics of peptide uptake and tissue distribution following a single intranasal dose of peptide. *Immunological Investigations*, 29 (1): 61–70.

Metzler, B. and Wraith, D.C. (1993) Inhibition of experimental autoimmune encephalomyelitis by inhalation but not oral administration of the encephalitogenic peptide: influence of MHC binding affinity. *International Immunology*, 5 (9): 1159–1165.

Miller, A., Lider, O., Al-Sabbagh, A., et al. (1992) Suppression of experimental autoimmune encephalomyelitis by oral administration of myelin basic protein. V. Hierarchy of suppression by myelin basic protein from different species. *Journal of Neuroimmunology*, 39 (3): 243–250.

Miller, A., Lider, O. and Weiner, H.L. (1991) Antigen-driven bystander suppression after oral administration of antigens. *The Journal of Experimental Medicine*, 174 (4): 791–798.

Miller, C., Ragheb, J.A. and Schwartz, R.H. (1999) Anergy and Cytokine-Mediated Suppression as Distinct Superantigen-Induced Tolerance Mechanisms in Vivo. *The Journal of Experimental Medicine*, 190 (1): 53.

Miragaia, R.J., Gomes, T., Chomka, A., et al. (2019) Single-Cell Transcriptomics of Regulatory T Cells Reveals Trajectories of Tissue Adaptation. *Immunity*, 50 (2): 493–504.

Moldaver, D. and Larché, M. (2011) Immunotherapy with peptides. *Allergy*, 66 (6): 784–791.

Moran, A.E., Holzapfel, K.L., Xing, Y., et al. (2011) T cell receptor signal strength in Treg and iNKT cell development demonstrated by a novel fluorescent reporter mouse. *The Journal of Experimental Medicine*, 208 (6): 1279–1289.

Mosser, D.M. and Zhang, X. (2008) Interleukin-10: new perspectives on an old cytokine. *Immunological Reviews*, 226 (1): 205.

Nagai, K. (2020) Co-inhibitory Receptor Signaling in T-Cell-Mediated Autoimmune Glomerulonephritis. *Frontiers in Medicine*, 7: 706.

Nagase, H., Takeoka, T., Urakawa, S., et al. (2017) ICOS+ Foxp3+ TILs in gastric cancer are prognostic markers and effector regulatory T cells associated with Helicobacter pylori. *International Journal of Cancer*, 140 (3): 686–695.

Nakatsukasa, H., Oda, M., Yin, J., et al. (2019) Loss of TET proteins in regulatory T cells promotes abnormal proliferation, Foxp3 destabilization and IL-17 expression. *International Immunology*, 31 (5): 335–347.

Navarro, S., Lazzari, A., Kanda, A., et al. (2014) Bystander immunotherapy as a strategy to control allergen-driven airway inflammation. *Mucosal Immunology*, 8 (4): 841–851.

Negishi, N., Sato, T., Yamashita-Kanemaru, Y., et al. (2018) CD155-Transducing Signaling through TIGIT Plays an Important Role in Transmission of Tolerant State and Suppression Capacity. *ImmunoHorizons*, 2 (10): 338–348.

Ng, T.H.S., Britton, G.J., Hill, E. V., et al. (2013) Regulation of adaptive immunity; the role of interleukin-10. *Frontiers in Immunology*, 4.

Nicolson, K.S., O'Neill, E.J., Sundstedt, A., et al. (2006) Antigen-Induced IL-10 + Regulatory T Cells Are Independent of CD25 + Regulatory Cells for Their Growth, Differentiation, and Function. *The Journal of Immunology*, 176 (9): 5329–5337.

Nicolson, K.S., Streeter, H.B., Verhagen, J., et al. (2009) Negative feedback control of the autoimmune response through antigen-induced differentiation of IL-10–secreting Th1 cells. *Journal of Experimental Medicine*, 206 (8): 1755–1767.

Niu, J., Maurice-Dror, C., Lee, D.H., et al. (2022) First-in-human phase 1 study of the anti-TIGIT antibody vibostolimab as monotherapy or with pembrolizumab for advanced solid tumors, including non-small-cell lung cancer. *Annals of Oncology*, 33 (2): 169–180.

Noguchi, Y., Maeda, A., Lo, P.C., et al. (2019) Human TIGIT on porcine aortic endothelial cells suppresses xenogeneic macrophage-mediated cytotoxicity. *Immunobiology*, 224 (5): 605–613.

Noon, L. (1911) Prophylactic Inoculation against Hay Fever. *The Lancet*, 4 (4): 1572–1573.

O'Neill, E.J., Day, M.J. and Wraith, D.C. (2006) IL-10 is essential for disease protection following intranasal peptide administration in the C57BL/6 model of EAE. *Journal of Neuroimmunology*, 178 (1–2): 1–8.

O'Neill, L.A.J., Golenbock, D. and Bowie, A.G. (2013) The history of Toll-like receptors - redefining innate immunity. *Nature Reviews Immunology*, 13 (6): 453–460.

Obata, Y., Furusawa, Y., Endo, T.A., et al. (2014) The epigenetic regulator Uhrf1 facilitates the proliferation and maturation of colonic regulatory T cells. *Nature Immunology*, 15 (6): 571–579.

Ogawa, C., Bankoti, R., Ogawa, C., et al. (2018) Blimp-1 Functions as a Molecular Switch to Prevent Inflammatory Activity in Foxp3 + ROR g t + Regulatory T Report Blimp-1 Functions as a Molecular Switch to Prevent Inflammatory Activity in Foxp3 + ROR g t + Regulatory T Cells. *Cell Reports*, 25: 19–28.

Ohkura, N., Hamaguchi, M., Morikawa, H., et al. (2012) T cell receptor stimulation-induced epigenetic changes and Foxp3 expression are independent and complementary events required for Treg cell development. *Immunity*, 37 (5): 785–799.

Ohkura, N. and Sakaguchi, S. (2011) Maturation of effector regulatory T cells. *Nature*

*Immunology*, 12 (4): 283–284.

Ohnmacht, C., Park, J., Cording, S., et al. (2015) The microbiota regulates type 2 immunity through ROR γ t T cells. *Sciencexpress Reports*, (July): 1–9.

Okada, H., Kuhn, C., Feillet, H., et al. (2010) The 'hygiene hypothesis' for autoimmune and allergic diseases: an update. *Clinical and Experimental Immunology*, 160 (1): 1.

Owen, D.L., Sjaastad, L.E. and Farrar, M.A. (2019) Regulatory T Cell Development in the Thymus. *The Journal of Immunology*, 203 (8): 2031–2041.

Pabbisetty, S.K., Rabacal, W., Maseda, D., et al. (2014) KLF2 is a rate-limiting transcription factor that can be targeted to enhance regulatory T-cell production. *Proceedings of the National Academy of Sciences of the United States of America*, 111 (26): 9579–9584.

Pacheco, Y., Acosta-Ampudia, Y., Monsalve, D.M., et al. (2019) Bystander activation and autoimmunity. *Journal of Autoimmunity*, 103.

Pagès, F., Ragueneau, M., Rottapel, R., et al. (1994) Binding of phosphatidylinositol-3-OH kinase to CD28 is required for T-cell signalling. *Nature*, 369 (6478): 327–329.

Pandiyan, P., Zheng, L., Ishihara, S., et al. (2007) CD4 + CD25 + Foxp3 + regulatory T cells induce cytokine deprivation – mediated apoptosis of effector CD4 + T cells. *Nature immunology*, 8 (12): 1353–1362.

Parkin, J. and Cohen, B. (2001) An overview of the immune system. *Lancet*, 357 (9270): 1777–1789.

Patel, D., Couroux, P., Hickey, P., et al. (2013) Fel d 1-derived peptide antigen desensitization shows a persistent treatment effect 1 year after the start of dosing: A randomized, placebo-controlled study. *Journal of Allergy and Clinical Immunology*, 131 (1).

Patterson, S.J., Han, J.M., Garcia, R., et al. (2011) Cutting edge: PHLPP regulates the development, function, and molecular signaling pathways of regulatory T cells. *Journal of Immunology*, 186 (10): 5533–5537.

Pauken, K.E. and Wherry, E.J. (2014) TIGIT and CD226: Tipping the Balance between Costimulatory and Coinhibitory Molecules to Augment the Cancer Immunotherapy Toolkit. *Cancer Cell*, 26 (6): 785–787.

Pearce, S.H.S., Dayan, C., Wraith, D.C., et al. (2019) Antigen-Specific Immunotherapy with Thyrotropin Receptor Peptides in Graves' Hyperthyroidism: A Phase I Study. *Thyroid*, 29 (7): 1003–1011.

Peggs, K.S., Quezada, S.A. and Allison, J.P. (2009) Cancer immunotherapy: co-stimulatory agonists and co-inhibitory antagonists. *Clinical and Experimental Immunology*, 157 (1): 9.

Perona-Wright, G., Anderton, S.M., Howie, S.E.M., et al. (2007) IL-10 permits transient activation of dendritic cells to tolerize T cells and protect from central nervous system autoimmune disease. *International Immunology*, 19 (9): 1123–1134.

Perry, J.S.A., Lio, C.W.J., Kau, A.L., et al. (2014) Distinct contributions of Aire and antigen-presenting-cell subsets to the generation of self-tolerance in the thymus. *Immunity*, 41 (3): 414–426.

Piccio, L., Naismith, R.T., Trinkaus, K., et al. (2010) Changes in B and T lymphocytes and chemokines with rituximab treatment in multiple sclerosis. *Archives of neurology*, 67 (6): 707. doi:10.1001/ARCHNEUROL.2010.99.

Piccirillo, C.A., Letterio, J.J., Thornton, A.M., et al. (2002) CD4+CD25+ Regulatory T Cells Can Mediate Suppressor Function in the Absence of Transforming Growth Factor b 1 Production and Responsiveness. *Journal of Experimental Medicine*, 196 (2): 237–245.

Polansky, J.K., Kretschmer, K., Freyer, J., et al. (2008) DNA methylation controls Foxp3 gene expression. *European Journal of Immunology*, 38 (6): 1654–1663.

Ponsford, M., Mazza, G., Coad, J., et al. (2001) Differential responses of CD45+ve T-cell subsets to MBP in multiple sclerosis. *Clinical and Experimental Immunology*, 124 (2): 315.

Pribyl, T.M., Campagnoni, C.W., Kampf, K., et al. (1993) The human myelin basic protein gene is included within a 179-kilobase transcription unit: expression in the immune and central nervous systems. *Proceedings of the National Academy of Sciences of the United States of America*, 90 (22): 10695–10699.

Qin, S., Cobbold, S.P., Pope, H., et al. (1993) "Infectious" Transplantation Tolerance. *Science*, 259 (5097): 974–977.

Qin, S., Xu, L., Yi, M., et al. (2019) Novel immune checkpoint targets: moving beyond PD-1 and CTLA-4. *Molecular Cancer*, 18 (1): 1–14.

Qu, H.Q., Bradfield, J.P., Grant, S.F.A., et al. (2009) Remapping the type I diabetes association of the CTLA4 locus. *Genes and Immunity*, 10.

Qureshi, O.S., Zheng, Y., Nakamura, K., et al. (2011) Trans-Endocytosis of CD80 and CD86: A Molecular Basis for the Cell-Extrinsic Function of CTLA-4. *Science*, pp. 600–604.

Raffin, C., Vo, L.T. and Bluestone, J.A. (2019) Treg cell-based therapies: challenges and perspectives. *Nature Reviews Immunology 2019 20:3*, 20 (3): 158–172. doi:10.1038/s41577-019-0232-6.

Ramagopal, U.A., Liu, W., Garrett-Thomson, S.C., et al. (2017) Structural basis for cancer immunotherapy by the first-in-class checkpoint inhibitor ipilimumab. *Proceedings of the National Academy of Sciences of the United States of America*, 114 (21): 4223–4232.

Raphael, I., Kumar, R., McCarl, L.H., et al. (2021) TIGIT and PD-1 Immune Checkpoint Pathways Are Associated With Patient Outcome and Anti-Tumor Immunity in Glioblastoma. *Frontiers in Immunology*, 12.

Read, S., Greenwald, R., Izcue, A., et al. (2006) Blockade of CTLA-4 on CD4+CD25+ regulatory T cells abrogates their function in vivo. *Journal of Immunology*, 177 (7): 4376–4383.

Riley, J.L. and June, C.H. (2005) The CD28 family: A T-cell rheostat for therapeutic control of T-cell activation. *Blood*, 105 (1): 13–21.

Roach, C.A. and Cross, A.H. (2021) Anti-CD20 B Cell Treatment for Relapsing Multiple Sclerosis. *Frontiers in Neurology*, 11: 1936.

Roberts, A.D., Ely, K.H. and Woodland, D.L. (2005) Differential contributions of central and effector memory T cells to recall responses. *The Journal of Experimental Medicine*, 202 (1): 123.

Roche, P.A. and Furuta, K. (2015) The ins and outs of MHC class II-mediated antigen processing and presentation. *Nature Reviews Immunology*, 15 (4): 203–216.

Roemhild, A., Otto, N.M., Moll, G., et al. (2020) Regulatory T cells for minimising immune suppression in kidney transplantation: phase I/IIa clinical trial. *BMJ*, 371.

Roncarolo, M.G., Gregori, S., Bacchetta, R., et al. (2014) Tr1 cells and the counter-regulation of immunity: natural mechanisms and therapeutic applications. *Current topics in microbiology and immunology*, 380: 39–68.

Rosenblum, M.D., Gratz, I.K., Paw, J.S., et al. (2011) Response to self antigen imprints regulatory memory in tissues. *Nature*, 480 (7378): 538–542.

Rosenblum, M.D., Way, S.S. and Abbas, A.K. (2016) Regulatory T cell memory. *Nature Reviews Immunology*, 16 (2): 90–101.

Rubtsov, Y.P., Rasmussen, J.P., Chi, E.Y., et al. (2008) Regulatory T cell-derived interleukin-10 limits inflammation at environmental interfaces. *Immunity*, 28 (4): 546–558.

Rutz, S., Noubade, R., Eidenschenk, C., et al. (2011) Transcription factor c-Maf mediates the TGF-β-dependent suppression of IL-22 production in T(H)17 cells. *Nature Immunology*, 12 (12): 1238–1245.

Sabatos-Peyton, C.A., Verhagen, J. and Wraith, D.C. (2010) Antigen-specific immunotherapy of autoimmune and allergic diseases. *Current Opinion in Immunology*, 22 (5): 609–615.

Sakaguchi, S. (1995) Immunologic Self-Tolerance Maintained by activated T cells expressing IL-2 receptor α-chain (CD25). *The Journal of Immunology*.

Sakaguchi, S. (2000) Regulatory T cells: key controllers of immunologic self-tolerance. *Cell*, 101 (5): 455–458.

Sallusto, F., Geginat, J. and Lanzavecchia, A. (2004) Central memory and effector memory T cell subsets: function, generation, and maintenance. *Annual Review of Immunology*, 22: 745–763.

Sanchez-Correa, B., Valhondo, I., Hassouneh, F., et al. (2019) DNAM-1 and the TIGIT/PVRIG/TACTILE axis: Novel immune checkpoints for natural killer cell-based cancer immunotherapy. *Cancers*, 11 (6): 1–15.

Sansom, D.M. (2000) CD28, CTLA-4 and their ligands: who does what and to whom? *Immunology*, 101 (2): 169.

Sawitzki, B., Harden, P.N., Reinke, P., et al. (2020) Regulatory cell therapy in kidney transplantation (The ONE Study): a harmonised design and analysis of seven non-randomised, single-arm, phase 1/2A trials. *Lancet*, 395 (10237): 1627–1639.

Schietinger, A. and Greenberg, P.D. (2014) Tolerance and Exhaustion: Defining Mechanisms of T cell Dysfunction. *Trends in Immunology*, 35 (2): 51.

Schnell, A., Bod, L., Madi, A., et al. (2020) The yin and yang of co-inhibitory receptors: toward anti-tumor immunity without autoimmunity. *Cell Research*, 30 (4): 285–299.

Schorer, M., Rakebrandt, N., Lambert, K., et al. (2020) TIGIT limits immune pathology during viral infections. *Nature Communications*, 11 (1): 1–14.

Schroeder, A., Mueller, O., Stocker, S., et al. (2006) The RIN: An RNA integrity number for assigning integrity values to RNA measurements. *BMC Molecular Biology*, 7 (1): 1–14.

Schuijs, M.J., Hammad, H. and Lambrecht, B.N. (2019) Professional and "Amateur" Antigen Presenting Cells In Type 2 Immunity. *Trends in Immunology*, 40 (1): 22.

Schwartz, R.H. (1990) Culture Model for Lymphocyte Clonal Anergy. *Science*, (7).

Sefik, E., Geva-zatorsky, N., Oh, S., et al. (2016) Individual intestinal symbionts induce a distinct population of RORγ+ regulatory T cells. *Science*, 349 (6251): 993–997.

Selby, M.J., Engelhardt, J.J., Quigley, M., et al. (2013) Anti-CTLA-4 antibodies of IgG2a isotype enhance antitumor activity through reduction of intratumoral regulatory T cells. *Cancer Immunology Research*, 1 (1): 32–42.

Sharma, S. and Raghavan, S.C. (2016) Nonhomologous DNA End Joining. *Encyclopedia of Cell Biology*, 1: 451–455.

Shepard, E.R., Wegner, A., Hill, E. V., et al. (2021) The Mechanism of Action of Antigen Processing Independent T Cell Epitopes Designed for Immunotherapy of Autoimmune Diseases. *Frontiers in Immunology*, 12 (April): 1–14.

Shevach, E.M. (2002) CD4+ CD25+ suppressor T cells: more questions than answers. *Nature Reviews Immunology*, 2 (6): 389–400.

Shevach, E.M. (2006) From vanilla to 28 flavors: multiple varieties of T regulatory cells. *Immunity*, 25 (2): 195–201.

Shevach, E.M. (2009) Mechanisms of Foxp3 + T Regulatory Cell-Mediated Suppression. *Immunity*, 30 (5): 636–645.

Shevach, E.M. and Thornton, A.M. (2015) tTregs, pTregs, and iTregs: Similarities and Differences Ethan. *Immunological Reviews*, 259 (1): 88–102.

Simpson, T.R., Li, F., Montalvo-Ortiz, W., et al. (2013) Fc-dependent depletion of tumor-infiltrating regulatory T cells co-defines the efficacy of anti-CTLA-4 therapy against melanoma. *The Journal of Experimental Medicine*, 210 (9): 1695–1710.

Singha, S., Shao, K., Yang, Y., et al. (2017) Peptide-MHC-based nanomedicines for autoimmunity function as T-cell receptor microclustering devices. *Nature nanotechnology*, 12 (7): 701–710.

Skyler, J.S. (2013) The Compelling Case for Anti-CD3 in Type 1 Diabetes. *Diabetes*, 62 (11): 3656–3657.

Smigiel, K.S., Richards, E., Srivastava, S., et al. (2014) CCR7 provides localized access to IL-2 and defines homeostatically distinct regulatory T cell subsets. *Journal of Experimental Medicine*, 211 (1): 121–136. doi:10.1084/.20131142.

Solé, P. and Santamaria, P. (2021) Re-Programming Autoreactive T Cells Into T-Regulatory Type 1 Cells for the Treatment of Autoimmunity. *Frontiers in Immunology*, 12: 2712.

Song, Y.W., Im, C.H., Park, J.H., et al. (2011) T-cell immunoglobulin and mucin domain 3 genetic polymorphisms are associated with rheumatoid arthritis independent of a shared epitope status. *Human Immunology*, 72 (8): 652–655.

Soond, D.R., Slack, E.C.M., Garden, O.A., et al. (2012) Does the PI3K pathway promote or antagonize regulatory T cell development and function? *Frontiers in Immunology*, 3.

Sorensen, P.S., Lisby, S., Grove, R., et al. (2014) Safety and efficacy of ofatumumab in relapsing-remitting multiple sclerosis: a phase 2 study. *Neurology*, 82 (7): 573–581.

St-Pierre, C., Trofimov, A., Brochu, S., et al. (2015) Differential Features of AIRE-Induced and AIRE-Independent Promiscuous Gene Expression in Thymic Epithelial Cells. *Journal of Immunology*, 195 (2): 498–506.

Stamm, H., Wellbrock, J. and Fiedler, W. (2018) Interaction of PVR/PVRL2 with TIGIT/DNAM-1 as a novel immune checkpoint axis and therapeutic target in cancer. *Mammalian Genome*, 29 (11–12): 694–702.

Stanietsky, Noa; Tihana, L. (2014) Mouse TIGIT inhibits NK-cell cytotoxicity upon interaction with PVR. *European Journal of Immunology*, 43 (8): 1–21.

Steinman, R.M., Hawiger, D. and Nussenzweig, M.C. (2003) Tolerogenic dendritic cells. *Annual Review of Immunology*, 21: 685–711.

Stephens, G.L., Andersson, J. and Shevach, E.M. (2007) Distinct subsets of FoxP3+ regulatory T cells participate in the control of immune responses. *Journal of Immunology*, 178 (11): 6901–6911.

Streeter, H.B., Rigden, R., Martin, K.F., et al. (2015) Preclinical development and first-in-human study of ATX-MS-1467 for immunotherapy of MS. *Neurology, Neuroimmunology & Neuroinflammation*, 2 (3).

Sun, Y., Luo, J., Chen, Y., et al. (2020) Combined evaluation of the expression status of CD155 and TIGIT plays an important role in the prognosis of LUAD (lung adenocarcinoma). *International Immunopharmacology*, 80.

Sundstedt, A., Höiden, I., Rosendahl, A., et al. (1997) Immunoregulatory role of IL-10 during superantigen-induced hyporesponsiveness in vivo. *The Journal of Immunology*, 158 (1).

Sundstedt, A., Neill, E.J.O., Nicolson, K.S., et al. (2003) Role for IL-10 in Suppression Mediated by Peptide-Induced Regulatory T Cells In Vivo. *The Journal of Immunology*, 170: 1240–1248.

Szabo, S.J., Kim, S.T., Costa, G.L., et al. (2000) A novel transcription factor, T-bet, directs Th1 lineage commitment. *Cell*, 100 (6): 655–669.

Tahara-Hanaoka, S., Shibuya, K., Kai, H., et al. (2006) Tumor rejection by the poliovirus receptor family ligands of the DNAM-1 (CD226) receptor. *Blood*, 107 (4): 1491–1496.

Tahara-Hanaoka, S., Shibuya, K., Onoda, Y., et al. (2004) Functional characterization of DNAM-1 (CD226) interaction with its ligands PVR (CD155) and nectin-2 (PRR-2/CD112). *International Immunology*, 16 (4): 533–538.

Tai, X., Cowan, M., Feigenbaum, L., et al. (2005) CD28 costimulation of developing thymocytes induces Foxp3 expression and regulatory T cell differentiation independently of interleukin 2. *Nature Immunology*, 6 (2): 152–162.

Tai, X., Erman, B., Alag, A., et al. (2013) Foxp3 transcription factor is proapoptotic and lethal to developing regulatory T cells unless counterbalanced by cytokine survival signals. *Immunity*, 38 (6): 1116–1128.

Takaba, H. and Takayanagi, H. (2017) The Mechanisms of T Cell Selection in the Thymus. *Trends in Immunology*, 38 (11): 805–816.

Takada, K. and Takahama, Y. (2015) Positive-selection-inducing self-peptides displayed by cortical thymic epithelial cells. *Advances in Immunology*, 125 (1): 87–110.

Takahashi, T., Kuniyasu, Y., Toda, M., et al. (1998) Immunologic self-tolerance maintained by suppressive T cells : induction of autoimmune disease by breaking their anergic / suppressive state. *International Immunology*, 10 (12): 1969–1980.

Taylor, A., Verhagen, J., Akkoç, T., et al. (2009) IL-10 suppresses CD2-mediated T cell activation via SHP-1. *Molecular Immunology*, 46 (4): 622–629.

Thaventhiran, T. (2013) T Cell Co-inhibitory Receptors-Functions and Signalling Mechanisms. *Journal of Clinical & Cellular Immunology*, 01 (S12).

Thornton, A.M., Lu, J., Korty, P.E., et al. (2019) Helios+ and Helios− Treg subpopulations are phenotypically and functionally distinct and express dissimilar TCR repertoires. *European Journal of Immunology*, 49 (3): 398.

Thornton, A.M. and Shevach, E.M. (1998) *CD4+CD25+ Immunoregulatory T cells suppress poluclonal T cell activation in vitro by inhibiting interleukin 2 production*., 188 (2).

Thornton, A.M. and Shevach, E.M. (2000) Suppressor Effector Function of CD4 + CD25 + Immunoregulatory T Cells Is Antigen Nonspecific. *The Journal of Immunology*, 164: 183–190.

Thornton, C.A. and Morgan, G. (2009) Innate and adaptive immune pathways to tolerance. *Nestle Nutrition Workshop Series: Pediatric Program*, 64: 45–61. doi:10.1159/000235782.

Thrower, S.L., James, L., Hall, W., et al. (2009) Proinsulin peptide immunotherapy in type 1 diabetes: report of a first-in-man Phase I safety study. *Clinical and Experimental Immunology*, 155 (2): 156–165.

Tivol, E.A., Borriello, F., Schweitzer, A.N., et al. (1995) Loss of CTLA-4 leads to massive lymphoproliferation and fatal multiorgan tissue destruction, revealing a critical negative regulatory role of CTLA-4. *Immunity*, 3 (5): 541–547.

Tokunaga, R., Zhang, W., Naseem, M., et al. (2018) CXCL9, CXCL10, CXCL11/CXCR3 axis for immune activation - a target for novel cancer therapy. *Cancer treatment reviews*, 63: 40.

Turley, D.M. and Miller, S.D. (2007) Peripheral tolerance induction using ethylenecarbodiimide-fixed APCs uses both direct and indirect mechanisms of antigen presentation for prevention of experimental autoimmune encephalomyelitis. *Journal of Immunology*, 178 (4): 2212–2220.

Turvey, S.E. and Broide, D.H. (2010) Innate immunity. *The Journal of Allergy and Clinical Immunology*, 125.

Umeshappa, C.S., Mbongue, J., Singha, S., et al. (2020) Ubiquitous antigen-specific T regulatory type 1 cells variably suppress hepatic and extrahepatic autoimmunity. *The Journal of Clinical Investigation*, 130 (4): 1823.

Umeshappa, C.S., Singha, S., Blanco, J., et al. (2019) Suppression of a broad spectrum of liver autoimmune pathologies by single peptide-MHC-based nanomedicines. *Nature Communications*, 10 (1): 1–17.

Vardjan, N., Gabrijel, M., Potokar, M., et al. (2012) IFN-γ-induced increase in the mobility of MHC class II compartments in astrocytes depends on intermediate filaments. *Journal of Neuroinflammation*, 9 (1): 1–13.

Vasanthakumar, A., Moro, K., Xin, A., et al. (2015) The transcriptional regulators IRF4, BATF and IL-33 orchestrate development and maintenance of adipose tissue-resident regulatory T cells. *Nature Immunology*, 16 (3): 276–285.

van der Veeken, J., Gonzalez, A.J., Cho, H., et al. (2016) Memory of Inflammation in Regulatory T Cells. *Cell*, 166 (4): 977–990.

Verhagen, J., Burton, B.R., Britton, G.J., et al. (2013a) Modification of the FoxP3 transcription factor principally affects inducible T regulatory cells in a model of experimental autoimmune encephalomyelitis. *PloS one*, 8 (4).

Verhagen, J., Gabryšová, L., Minaee, S., et al. (2009) Enhanced selection of FoxP3+ T-regulatory cells protects CTLA-4-deficient mice from CNS autoimmune disease. *Proceedings of the National Academy of Sciences of the United States of America*, 106 (9): 3306–3311.

Verhagen, J., Genolet, R., Britton, G.J., et al. (2013b) CTLA-4 controls the thymic development of both conventional and regulatory T cells through modulation of the TCR repertoire. *Proceedings of the National Academy of Sciences of the United States of America*, 110 (3).

Vieira, P.L., Christensen, J.R., Minaee, S., et al. (2004) IL-10-Secreting Regulatory T Cells Do Not Express Foxp3 but Have Comparable Regulatory Function to Naturally Occurring CD4 + CD25 + Regulatory T Cells. *The Journal of Immunology*, 172 (10): 5986–5993.

Vyas, J.M., Van Der Veen, A.G. and Ploegh, H.L. (2008) The known unknowns of antigen processing and presentation. *Nature Reviews Immunology*, 8 (8): 607–618.

Walczak, A., Siger, M., Ciach, A., et al. (2013) Transdermal application of myelin peptides in multiple sclerosis treatment. *JAMA neurology*, 70 (9): 1105–1109.

Walunas, T.L., Bakker, C.Y. and Bluestone, J.A. (1996) CTLA-4 ligation blocks CD28-dependent T cell activation. *The Journal of Experimental Medicine*, 183 (6): 2541–2550.

Wang, F., Hou, H., Wu, S., et al. (2015) TIGIT expression levels on human NK cells correlate with functional heterogeneity among healthy individuals. *European Journal of Immunology*, 45 (10): 2886–2897.

Wang, F.F., Wang, Y., Wang, L., et al. (2018) TIGIT expression levels on CD4+ T cells are correlated with disease severity in patients with psoriasis. *Clinical and Experimental Dermatology*, 43 (6): 675–682.

Wang, M., Ji, B., Wang, J., et al. (2014) Tim-3 polymorphism downregulates gene expression and is involved in the susceptibility to ankylosing spondylitis. *DNA and Cell Biology*, 33 (10): 723–728.

Ward-Kavanagh, L.K., Lin, W.W., Šedý, J.R., et al. (2016) The TNF Receptor Superfamily in Co-stimulating and Co-inhibitory Responses. *Immunity*, 44 (5): 1005–1019.

Warnock, M.G. and Goodacre, J.A. (1997) Cryptic T cell epitopes and their role in the pathogenesis of autoimmune diseases. *British Journal of Rheumatology*, 36: 1144–1150.

Waterhouse, P., Penninger, J.M., Timms, E., et al. (1995) Lymphoproliferative disorders with early lethality in mice deficient in Ctla-4. *Science*, 270 (5238): 985–988.

Wei, X., Zhang, J., Gu, Q., et al. (2017) Reciprocal Expression of IL-35 and IL-10 Defines Two Distinct Effector Treg Subsets that Are Required for Maintenance of Immune Tolerance. *Cell reports*, 21 (7): 1853–1869.

Weiss, J.M., Bilate, A.M., Gobert, M., et al. (2012) Neuropilin 1 is expressed on thymus-derived natural regulatory T cells, but not mucosa-generated induced Foxp3+ T reg cells. *The Journal of Experimental Medicine*, 209 (10): 1723–1742.

Wherry, E.J. and Kurachi, M. (2015) Molecular and cellular insights into T cell exhaustion. *Nature Reviews Immunology*, 15 (8): 486–499.

White, A.M. and Wraith, D.C. (2016) Tr1-like T cells - An enigmatic regulatory t cell lineage. *Frontiers in Immunology*, 7: 1–7.

Wilkinson, R.W., Anderson, G., Owen, J.J., et al. (1995) Positive selection of thymocytes involves sustained interactions with the thymic microenvironment. *Journal of Immunology*, 155 (11): 5234–40.

Williams, J.A., Zhang, J., Jeon, H., et al. (2014) Thymic medullary epithelium and thymocyte self tolerance require cooperation between CD28-CD80/86 and CD40-CD40L costimulatory pathways. *Journal of Immunology*, 192 (2): 630.

Wing, J.B. and Sakaguchi, S. (2012) Multiple treg suppressive modules and their

adaptability. *Frontiers in Immunology*, 3.

Wing, K., Onishi, Y., Prieto-martin, P., et al. (2008) CTLA-4 Control over Foxp3 + Regulatory T Cell Function. *Science*, 322: 271–276.

Wohlfert, E.A., Grainger, J.R., Bouladoux, N., et al. (2011) GATA3 controls Foxp3 + regulatory T cell fate during inflammation in mice. *Journal of Clinical Investigation*, 121 (11): 4503–4515.

Wraith, D. (2016) Autoimmunity: Antigen-specific immunotherapy. *Nature*, 530 (7591): 422–423.

Wraith, D.C. (2018) Designing antigens for the prevention and treatment of autoimmune diseases. *Current Opinion in Chemical Engineering*, 19: 35–42.

Wraith, D.C., Smilek, D.E. and Webb, S. (1992) MHC-binding peptides for immunotherapy of experimental autoimmune disease. *Journal of Autoimmunity*, pp. 103–113.

Wu, L. and Shortman, K. (2005) Heterogeneity of thymic dendritic cells. *Seminars in Immunology*, 17 (4): 304–312.

Xiao, Y., Chen, P., Luo, C., et al. (2021) Discovery of a novel anti PD-L1 X TIGIT bispecific antibody for the treatment of solid tumors. *Cancer treatment and research communications*, 29.

Xu, J., Yang, Y., Qiu, G., et al. (2009) c-Maf regulates IL-10 expression during Th17 polarization. *Journal of Immunology*, 182 (10): 6226–6236.

Yadav, M., Louvet, C., Davini, D., et al. (2012) Neuropilin-1 distinguishes natural and inducible regulatory T cells among regulatory T cell subsets in vivo. *The Journal of Experimental Medicine*, 209 (10): 1713–1722.

Yang, M., Liu, Y., Mo, B., et al. (2019) Helios but not CD226, TIGIT and Foxp3 is a Potential Marker for CD4+ Treg Cells in Patients with Rheumatoid Arthritis. *Cellular physiology and biochemistry : international journal of experimental cellular physiology, biochemistry, and pharmacology*, 52 (5): 1178–1192.

Yasuma-Mitobe, K. and Matsuoka, M. (2018) The roles of coinhibitory receptors in pathogenesis of human retroviral infections. *Frontiers in Immunology*, 9 (NOV): 2755.

Yu, X., Harden, K., Gonzalez, L.C., et al. (2008) The surface protein TIGIT suppresses T cell activation by promoting the generation of mature immunoregulatory dendritic cells. *Nature Immunology*, 10 (1): 48–57.

Yue, C., Gao, S., Li, S., et al. (2022) TIGIT as a Promising Therapeutic Target in Autoimmune Diseases. *Frontiers in Immunology*, 13.

Yue, X., Lio, C.W.J., Samaniego-Castruita, D., et al. (2019) Loss of TET2 and TET3 in regulatory T cells unleashes effector function. *Nature Communications*, 10 (1): 1–14.

Zeng, Z., Lan, T., Wei, Y., et al. (2022) CCL5/CCR5 axis in human diseases and related treatments. *Genes & Diseases*, 9 (1): 12.

Zhang, C., Li, L., Feng, K., et al. (2017) “Repair” Treg Cells in Tissue Injury. *Cellular*

*Physiology and Biochemistry*, 43 (6): 2155–2169.

Zhang, D., Hu, W., Xie, J., et al. (2018a) TIGIT-Fc alleviates acute graft-versus-host disease by suppressing CTL activation via promoting the generation of immunoregulatory dendritic cells. *Biochimica et biophysica acta. Molecular basis of disease*, 1864: 3085–3098.

Zhang, J., Markovic-Plese, S., Lacet, B., et al. (1994) Increased frequency of interleukin 2-responsive T cells specific for myelin basic protein and proteolipid protein in peripheral blood and cerebrospinal fluid of patients with multiple sclerosis. *The Journal of Experimental Medicine*, 179 (3): 973–984.

Zhang, Q., Bi, J., Zheng, X., et al. (2018b) Blockade of the checkpoint receptor TIGIT prevents NK cell exhaustion and elicits potent anti-tumor immunity. *Nature Immunology*, 19 (7): 723–732.

Zhang, Q. and Vignali, D.A.A. (2016) Co-stimulatory and co-inhibitory pathways in autoimmunity. *Immunity*, 44 (5): 1034.

Zhang, Y., Garcia Ibanez, L. and Toellner, K.-M. (2016) Regulation of germinal center B-cell differentiation. *Immunological Reviews*, 270 (1): 8–19.

Zhao, W., Dong, Y., Wu, C., et al. (2016) TIGIT overexpression diminishes the function of CD4 T cells and ameliorates the severity of rheumatoid arthritis in mouse models. *Experimental Cell Research*, 340 (1): 132–138.

Zheng, G.X.Y., Terry, J.M., Belgrader, P., et al. (2017) Massively parallel digital transcriptional profiling of single cells. *Nature Communications*, 8.

Zheng, W.P. and Flavell, R.A. (1997) The transcription factor GATA-3 is necessary and sufficient for Th2 cytokine gene expression in CD4 T cells. *Cell*, 89 (4): 587–596.

Zhu, C., Sakuishi, K., Xiao, S., et al. (2015) An IL-27/NFIL3 signaling axis drives Tim-3 and IL-10 expression and T cell dysfunction. *Nature Communications*, 6: 6072.

Zhu, J. and Paul, W.E. (2008) CD4 T cells: fates, functions, and faults. *Blood*, 112 (5): 1557–1569.

Zhu, J. and Paul, W.E. (2010) Peripheral CD4+ T-cell differentiation regulated by networks of cytokines and transcription factors. *Immunological Reviews*, 238 (1): 247–262.

Zhu, J., Yamane, H. and Paul, W.E. (2012) Differentiation of Effector CD4 T cell populations. *Annual Review of Immunology*, (1): 445–489.

Zikherman, J. and Au-Yeung, B. (2015) The role of T cell receptor signaling thresholds in guiding T cell fate decisions. *Current opinion in immunology*, 33: 43–48.

Zimmer, R., Scherbarth, H.R., Rillo, O.L., et al. (2013) Lupuzor/P140 peptide in patients with systemic lupus erythematosus: a randomised, double-blind, placebo-controlled phase IIb clinical trial. *Annals of the rheumatic diseases*, 72 (11): 1830–1835.

Zong, L., Peng, H., Sun, C., et al. (2019) Breakdown of adaptive immunotolerance induces hepatocellular carcinoma in HBsAg-tg mice. *Nature Communications*, 10 (1).